I. The land-atmosphere water flux across plant, ecosystem, global and social scales
II. GIS and spatial analysis for environmental justice and wildlife

by

Joshua Benjamin Fisher

B.S. (University of California, Berkeley) 2001

A dissertation submitted in partial satisfaction of the

requirements for the degree of

Doctor of Philosophy
in

Environmental Science, Policy and Management

in the

GRADUATE DIVISION

of the

UNIVERSITY OF CALIFORNIA, BERKELEY

Committee in charge:

Professor Dennis D. Baldocchi, Co-Chair
Professor Gregory S. Biging, Co-Chair
Professor Todd E. Dawson
Professor Louise P. Fortmann

Spring 2006

The dissertation of Joshua Benjamin Fisher is approved:

Co-Chair Date

Co-Chair Date

Date

Date

University of California, Berkeley

Spring 2006

I. The land-atmosphere water flux across plant, ecosystem, global and social scales
II. GIS and spatial analysis for environmental justice and wildlife

© 2006

by

Joshua Benjamin Fisher

Abstract

I. The land-atmosphere water flux across plant, ecosystem, global and social scales
II. GIS and spatial analysis for environmental justice and wildlife

by

Joshua Benjamin Fisher

Doctor of Philosophy in Environmental Science, Policy and Management

University of California, Berkeley

Professor Dennis D. Baldocchi, Co-Chair

Professor Gregory S. Biging, Co-Chair

I. Evapotranspiration is a major component of the terrestrial water balance, and is central to the processes and models of global circulation and climate change, ecosystem carbon cycling, floods, droughts and irrigation. Over the entire land surface of the globe, approximately two-thirds of rainfall returns to the atmosphere as evapotranspiration, making evapotranspiration the largest single component of the hydrological cycle. Two main problems exist, however, of which the solutions are the objectives of this thesis: 1) evapotranspiration is very difficult to measure and predict, especially at synoptic spatial scales; 2) the processes that control evapotranspiration are weighted inconsistently across spatial scales. My methodology includes a combination of sap flow for transpiration in individual trees and shrubs, modeling as applied to eddy covariance measurements for ecosystems, remote sensing for the land-atmosphere flux over continents and the globe, and intellectual property rights and common property resources theories for data sharing. I found that nocturnal transpiration occurs in many species, which violates many long-held leaf-scale assumptions about daytime-dependency of photosynthesis-transpiration

coupling; simple models tend to better predict ecosystem evapotranspiration measurements than do more theoretically accurate, but complex models, which are subject to greater sources of uncertainty; evapotranspiration can be estimated accurately using only remote sensing and a simple model of evapotranspiration with sophisticated ecophysiological constraints; and, that payment is always required in data sharing, but that the currency and value of payment in academia are associated with publication, authorship and acknowledgment. This thesis contributes to advancement in the science, understanding, and prediction of a major component in the water budget.

II. Spatial point patterns tend not to be random, but functions of larger processes that control behaviors and locations of people, institutions and wildlife. It is the goal here to identify and quantify the scales and dimensions at which clusters occur, and link these results to policy and management decisions that control these scales. Through internships at the U.S. Environmental Protection Agency and NASA Ames Research Center, I applied this methodology to projects on environmental justice and wildlife management. The environmental justice aspect focuses on West Oakland, California, where a low-income, high-minority community was situated among a dense distribution of point source air toxics polluters. The wildlife management aspect focuses on the threatened burrowing owl (*Athene cunicularia*), which was managed with conservation areas of varying sizes set aside on federal land. Both parts shared the same methods—a combination of geographic information systems (GIS), first-order intensity distributions, and second-order Ripley's K analysis; the West Oakland project included air modeling. At West Oakland, I quantified a disproportionate clustering of point source polluters,

identified the potential exposure from the most dangerous polluter, and addressed the issue of non-point source air toxics. At NASA Ames, I identified the scale and timing of owl clusters, and the spatial pattern response to conservation areas of matching versus disaggregate scales. The policy implications of my environmental justice results were that the major West Oakland point source polluter was shut down. The management implications of my burrowing owl analysis were informed decisions on conservation area sizes.

Dr. Dennis D. Baldocchi Dissertation Co-Chair	Dr. Gregory S. Biging Dissertation Co-Chair

Table of Contents

List of Figures ii

List of Tables v

Preface vi

Acknowledgments x

I. The land-atmosphere water flux across plant, ecosystem, global and social scales

Chapter 1 – What the towers don't see at night: Nocturnal sap flow in trees and shrubs at two AmeriFlux sites in California 1

Chapter 2 – Evapotranspiration models compared on a Sierra Nevada forest ecosystem 32

Chapter 3 – Global estimates of the land-atmosphere water flux: A remote sensing driven, flux site-validated ecophysiological model of evapotranspiration 65

Chapter 4 – Data producers and data users: Misuse, mistrust, and the advancement of science 106

II. GIS and spatial analysis for environmental justice and wildlife

Chapter 5 – Scales of environmental justice: Combining GIS and spatial analysis for air toxics in West Oakland, California 156

Chapter 6 – Use of GIS and spatial analysis to assess wildlife management measures: A burrowing owl example 189

III. Appendices

A Instructions for Building Sap Flow Sensors 209

B Datalogger Code for Sap Flow Measurement 215

C Equations for Processing and Calculation of Sap Flow Data 222

D MATLAB Code for Evapotranspiration Model with Remote Sensing Data ... 224

List of Figures

***Chapter 1* – What the towers don't see at night: Nocturnal sap flow in trees and shrubs at two AmeriFlux sites in California**

Fig. 1. (A) Blodgett Forest, a *P. ponderosa* plantation, is located in the Sierra Nevada mountains and Tonzi Ranch, an oak-savanna, in the lower foothills of the Sierrra Nevada mountains of California. (B) Distribution of *P. ponderosa* and *Q. douglasii* in California based on the GAP analysis (Scott et al. 1993). … 6

Fig. 2. Soil moisture at 50 cm depth during 2005. ……... 8

Fig. 3. Daytime and nighttime averages during 2005 for (A) *Q. douglasii*, (B) *P. ponderosa*, and (C) *A. manzanita* and *C. cordulatus*. ……..... 12

Fig. 4. (A) Vapor pressure deficit for 2005 at the oak-savanna site. (B) Daily averaged nighttime *VPD* and sap flow for *Q. douglasii*. (C) Linear regression of the data in Fig. 3B. (D) Linear regression for daily averaged nighttime *VPD* and sap flow for 2005 at the Sierra Nevada site for *P. ponderosa*. ……. 14

Fig. 5. (A) *VPD* versus T_a follows an exponential curve. (B) As T_a increases at the Sierra Nevada site, nighttime sap flow increases much more rapidly. The exponential relationship holds for nighttime sap flow versus T_a during the summer at the (C) Sierra Nevada site, but not the (D) oak-savanna site. ……. 15

Fig. 6. Five-day period for sap flow and solar radiation (A) late in the year when *VPD* and T_a are low so only refilling occurs and (B) and in the middle of the summer when water loss (diagonal stripes) follows refilling period. ……. 17

Fig. 7. (A) Daytime averaged sap flow and *LE* from eddy covariance at the Sierra Nevada site. (B) Linear regression of the data in Fig. 7A. ……... 19

Fig. 8. (A) Daytime averaged *LE* for above-canopy and below-canopy towers at the oak-savanna site. (B) The difference between the above- and below-canopy towers equals the *LE* from only the trees, which is compared to the sap flow from a 16 cm (DBH) tree. (C) The correlation between eddy covariance and sap flow is reduced due to the temporal lag as seen in Fig. 8B. ……... 20

Fig. 9. (A) Nighttime averaged sap flow compared with nighttime averaged *LE* from eddy covariance at the Sierra Nevada site. (B) Nighttime averaged sap flow compared with nighttime averaged *LE* from the difference between the above- and below-canopy eddy covariance towers at the oak-savanna site. (C) Measured nighttime transpiration was much larger for sap flow than for eddy covariance at both sites. (D) The number of nights with valid measurements was larger for sap flow as compared with eddy covariance. …… 22

***Chapter 2* – Evapotranspiration models compared on a Sierra Nevada forest ecosystem**

Fig. 1. Potential *LE* without soil moisture function for (a) 1997 and (b) 1998. … 47

Fig. 2. Simulated versus measured (actual) *LE* during (a) 1997 and (b) 1998. … 48

Fig. 3. Simulated versus measured *LE* during (a) 1997 and (b) 1998. …….. 49

***Chapter 3* – Global estimates of the land-atmosphere water flux: A remote sensing driven, flux site-validated ecophysiological model of evapotranspiration**

Fig. 1. The 16 FLUXNET sites used in the validation spanned across N. America, S. America, Europe, Asia, and Australia. …….. 74

Fig. 2. Predicted evapotranspiration (*LE*) versus observed evapotranspiration at 16 FLUXNET sites for 2000-2003 with 1:1 line. ……. 81

Fig. 3. Overprediction of the original Priestley-Taylor (1972) method, and improvement to the *LE* prediction from our model. ……. 81

Fig 4. Month-to-month variation in evapotranspiration for 1994. ……... 83

Fig 5. Soil evaporation (LE_s) and canopy transpiration (LE_c) for 1994. …….. 84

Fig 6. Year-to-year change in evapotranspiration. ……... 85

Fig. 7. Continental averages of total *LE* for each year (mm). …….. 87

Fig. 8. ISLSCP-II precipitation with our *LE* and calculated runoff. …… 89

Fig. 9. Net radiation (R_n) as the average across latitudinal bands. We used the ISLSCP-II at 1 degree as a comparison with other published estimates. ……. 90

Fig. 10. Evaporative Fraction (EF) as the average across latitudinal bands. We show EF for year 1986 as a comparison with other published values. ……. 90

Fig. 11. Annual total *LE* as the average across latitudinal bands. We include our R_n from ISLSCP-II as a reference. …….. 91

Fig. 12. Monthly total *LE* as the average across latitudinal bands. …….. 92

Fig. 13. Method of Moments global output based on variability within ISLSCP-II input parameters. ……... 94

Chapter 4 **– Data producers and data users: Misuse, mistrust, and the advancement of science**

Fig. 1. The proportion of design principles present in cases. 142

Chapter 5 **– Scales of environmental justice: Combining GIS and spatial analysis for air toxics in West Oakland, California**

Fig. 1 (a) TRI (1999) facilities in the San Francisco Bay Area. (b) Intensity distribution of points per grid cell in longitude by latitude. (c) Ripley's K test. 169

Fig. 2 (a) TRI (1999) facilities in Alameda County. (b) Intensity distribution. (c) Ripley's K test. …….. 171

Fig. 3 (a) TRI (1999) facilities in the City of Oakland. (b) Intensity distribution. (c) Ripley's K test. …… 172

Fig. 4. Broad race distribution map based on racial majority for each block in West Oakland. ……... 173

Fig. 5. Median household income by block group (frequency) in US Dollars. … 174

Fig. 6 (a) and (b) Extent of Red Star Yeast emissions based on BAAQMD's Health Risk Screening Analysis on population density per square mile. (c) Total number of people potentially affected by Red Star Yeast emissions. ……... 175

Fig. 7 (a) Gasoline stations within 1.5-mile radius of West Oakland center. (b) Alternative driving route around the high population density. ……. 177

Chapter 6 **– Use of GIS and spatial analysis to assess wildlife management measures: A burrowing owl example**

Fig. 1. Distribution of all burrowing owls observed from 1998-2004 at NASA Ames Research Center, California. ……... 198

Fig. 2. Number of burrowing owls sited per month. The durations of the two mows in 2004 are indicated in between the two sets of vertical lines. 199

Fig. 3. Mean nearest neighbor distances by month for 2003 and 2004. …….. 200

Fig. 4. First-order intensity distribution for all active burrows during 2004. ….. 201

Fig. 5. Ripley's K plot for August 2003, April 2004 and August 2004. …….. 202

Fig. 6. Cluster change over time based on the difference of the Ripley's K plot and the upper confidence interval for each month. ……... 203

List of Tables

***Chapter 1* – What the towers don't see at night: Nocturnal sap flow in trees and shrubs at two AmeriFlux sites in California**

Table 1. Correlation coefficients for nighttime sap flow predictors (*VPD*, *Ta*, and wind speed) versus nighttime sap flow for *Q. douglasii* and *P. ponderosa*. 16

***Chapter 2* – Evapotranspiration models compared on a Sierra Nevada forest ecosystem**

Table 1. Comparison of the increasing complexity of the models in terms of number of parameters required. ……..... 42

Table 2. Measured values of the Priestley-Taylor coefficient, α, as tabled by Flint and Childs (1991) and appended with their and our values. ……..... 51

***Chapter 3* – Global estimates of the land-atmosphere water flux: A remote sensing driven, flux site-validated ecophysiological model of evapotranspiration**

Table 1. AmeriFlux sites used for model validation. Additional site information can be found at http://public.ornl.gov/ameriflux/ ……. 73

Table 2. Model parameters and equations. R_n is net radiation ($W \cdot m^{-2}$), G is ground heat flux ($W \cdot m^{-2}$), T is air temperature (°C), RH is relative humidity ($0<RH<1$), VPD is saturation vapor pressure deficit (kPa), Δ is slope of saturation-to-vapor pressure curve ($kPa \cdot °C^{-1}$), γ is the psychrometric constant (~0.066 $kPa \cdot °C^{-1}$), s is desorptivity of the soil (~4 $mm \cdot day^{-0.5}$), and T_{avg}, RH_{avg} and VPD_{avg} are mean monthly values of T, RH and VPD, respectively. …….. 77

Table 3. Cross-correlations between ISLSCP-II global input parameters. …….. 92

***Chapter 4* – Data producers and data users: Misuse, mistrust, and the advancement of science**

Table 1. Design principles for successful data sharing (from Ostrom 1991). ….. 125

Table 2. Summary of interviewee statements rights, ownership and patents/copyrights. …… 130

Table 3. Ostrom's design principles applied to 17 data sharing cases. …… 143

Preface

Environmental Science, Policy and Management. This is the name of my department, a description of this Doctor of Philosophy, and three distinct disciplines with one unifying theme. As the debate rages on about definitions of and distinctions between interdisciplinarity and multidisciplinarity, students are pushed towards a combination of the two by disciplinary teachers, yet pulled into a single discipline by warnings and caution that success and quality can be achieved only with a single-focus thesis.

How can I develop a quality dissertation that achieves success across multiple disciplines? Section 1 of this thesis, "The land-atmosphere flux across plant, ecosystem, global and social scales," is a combination of biophysical and social science with policy and management implications. Section 2, "GIS and spatial analysis for environmental justice and wildlife," focuses on policy and management with a scientific foundation.

I began in the field at the plant level (Chapter 1) with methods in field ecology and biometeorology. The aim here was to understand what was happening on the ground and to be exposed to environmental variation that is best learned with one's hands rather than from a book. I built sap flow sensors by hand that would extend my senses inside the plant to detect water uptake and temporal patterns. As I began to compile my sap flow data, a new hot topic emerged—is there transpiration at night? There should not be, if transpiration is perfectly coupled with photosynthesis, which would occur only in the presence of light for most plant types. Yet, new light was being shed on those of us working in the dark—what we once thought were outliers were beginning to emerge as an undeniable pattern, particularly with increasing refinement of measurement detection.

Hence, the first chapter, “What the towers don’t see at night: Nocturnal sap flow in trees and shrubs at two AmeriFlux sites in California,” is dedicated to this topic.

Next, I shifted to an analysis of models that must be parameterized by these field data. We cannot build sap flow sensors or eddy covariance towers everywhere, so we must predict evapotranspiration based on its covariates. The problem, however, is that some of those covariates are easy to measure and some quite difficult. Further, some of those covariates explain much more of the variance in evapotranspiration than do others. What is the “best” model? A theoretically perfect model might explain every single drop of water as it moves throughout the hydrologic cycle, controlled by every unit of energy and the movement and properties of molecules and quarks. A practically perfect model would require one easy-to-measure parameter that predicts evapotranspiration reasonably well. The former is constrained by available data, which turn into error-prone approximations and assumptions that propagate through the model. The latter might work well in general, but generates large errors at specific sites. Thus, the “best” model is likely somewhere between those two extremes, run by a few parameters that explain most of the variance in most settings. Chapter 2, “Evapotranspiration models compared on a Sierra Nevada forest ecosystem,” evaluates a range of simple to complex models.

Scale is a critical issue in these models: how on earth can we go from plant and ecosystem measurements to regional and global estimates? What was difficult to measure on the ground for the models in Chapter 2 becomes impossible to measure from space or from satellites that give us global pictures. We can, however, measure some things from space that are critical to the global land-atmosphere water flux. First and foremost is net radiation—we know how much is coming in from the sun, and with

albedo, atmospheric corrections and other processing steps we can get a good estimate of this parameter. Second, we know surface temperature and from this we can derive air temperature and vapor pressure. Third, we know how much land the vegetation covers so we can partition between soil evaporation and canopy transpiration; we also know how green the vegetation is and its seasonal variation as related to moisture and temperature. Finally, from our work at previously described scales, we know how the vegetation and earth responds and reacts to each of these parameters with respect to evapotranspiration. In Chapter 3, "Global estimates of the land-atmosphere water flux: A remote sensing driven, flux site-validated ecophysiological model of evapotranspiration," I integrate knowledge from the first two chapters with remote sensing and GIS to develop a new model and estimates of the global land-atmosphere water flux.

"If I have seen further," Isaac Newton wrote, "it is by standing on the shoulders of giants." Global questions require global data, but no one individual can collect and analyze that much data alone. Collaborations and building on the work of others is essential. Nonetheless, misuse or mistrust by collaborating parties can stymie scientific advancement. The question then is: Why does data sharing lead to conflict in some cases, but not in others? I approach this question with a combination of two theories. First, much research has been done already on shared natural resources such as fisheries, forests and water within a common property theory framework. Second, intellectual property rights theory addresses non-physical property such as ideas, knowledge and data. In Chapter 4, "Data producers and data users: Misuse, mistrust, and the advancement of science," I combine common property and intellectual property rights theories to data sharing among the FLUXNET and remote sensing data communities.

Science? Check. Policy and Management? As part of my graduate career, I decided not to limit myself within the bubble of my university, but to gain experience in other types of institutions. I spent two summers at the U.S. Environmental Protection Agency (EPA), Region 9 Air Division, and one at NASA Ames Research Center, Office of Safety, Environmental and Mission Assurance. My primary advisor at UC Berkeley left the university in my second year as a graduate student, and I switched into a lab with more of a GIS focus and a professor who taught spatial statistics. I applied my developing skills in GIS and spatial analysis to projects at the EPA and NASA.

In Chapter 5, "Scales of environmental justice: Combining GIS and spatial analysis for air toxics in West Oakland, California," I included a direct human health element to environmental degradation. In an interdisciplinary vein, I brought a methodology from ecology into the environmental justice realm to help quantify the somewhat qualitative notions of injustice and disproportionate burden. The US EPA used this analysis in conjunction with other analyses to affect policy and shut down the most harmful polluter in West Oakland. In Chapter 6, "Use of GIS and spatial analysis to assess wildlife management measures: A burrowing owl example," I use these exact same methods on a completely different problem. Instead of looking for harmful clusters of polluters, NASA was looking for clusters of threatened burrowing owls so that they could set aside managed conservation areas that matched the size of those clusters.

And, this is how I tied Science, Policy and Management together with a unifying environmental theme. Enjoy the read! I enjoyed the ride.

Acknowledgments

My parents, Dennis Fisher and Angelia Leung, are a large part of who I am and what kind of work I produce. My father taught me to think scientifically, and my mother taught me to think creatively. The back-and-forth flying between the two environmental opposites of Anchorage (dad) and Los Angeles (mom), staring out the window for hours as the scenery changed, lead to my interest in environmental sciences and remote sensing.

Troy Schulze was a key role model for me in high school because he was finding success in and enjoying a subject (environmental studies) that interested me, and he was in a stage in his life (college) that was to be my next stage. Hap Palmer provided me with environmental conscientiousness, health concern, and a humorous life outlook. My sister, Claralyse Palmer, is an inspiration to me because I want to inspire her. I hope to make the rest of my family proud as well: Leung's—Maria, Galen, Richard, Bob, Jack, Bambuda, Satva, Wu-li, Molly, Kip and Kimery; Fisher's—Morris, Edna, Fred and Grace; Palmer's—Kelly, Wes, Dan, Megan, Kayla, Penny, Jan, Larry, Judy and all of the exponentially growing number of kids and spouses. When I entered UC Berkeley as an undergraduate, my Uncles Galen and Richard offered me a piece of advice that has stuck with me to today. They said, "Don't worry about who had higher SAT's or high school GPA's coming in. Right now, everyone is smart so it's an even slate. Those who succeed are those who work the hardest." I have taken that advice to heart.

Terry DeBiase, who was a graduate student while I was a sophomore undergrad, was my next key role model. Terry welcomed me into his lab and spent many hours working with me as I participated in the lab's research and developed my own senior

thesis. Terry inspired me not only to continue with my research, but also to help other students as much and more than he helped me.

For development of my research skills and knowledge, I am grateful to my primary graduate advisors: Ye Qi, Greg Biging, Dennis Baldocchi, Maggi Kelly, Louise Fortmann and Todd Dawson. Allen Goldstein, Peng Gong, Jeff Romm, Dara O'Rourke, and David Winickoff also have provided me with invaluable advice on my research. Ming Xu, Jianwu Tang, Mark Henderson, Jun-Hak Lee, Alan Di Vittorio, Luis Ibañez, Tim Robards, Ian Tullis, Jorge Kuriel, Ted Hehn, Karin Tuxen, Qinghua Guo, Desheng Liu, Laurent Misson, Rich Brenner, Vanessa Boukili, Qian Yu, Qi Chen, Richard Battrick, Russell Tonzi, Lynne Trulio, Dave Guiliano, Catherine Brown, Richard Grow and John Kennedy all contributed to my graduate career. My next key role model was Kevin Tu, who was a post-doc in the Dawson lab. Together we produced papers, posters and talks that we presented across the world. I am grateful to my funding sources, all of which are acknowledged following each chapter, but in particular to NASA Headquarters under the Earth System Science Fellowship Grant NGT5-30473.

My best friend, Aaron Stein, has provided continuity and a witness to my life. Before the music plays me off, I need to mention a few more life-long friends: Todd Kohn, Dryw Jones, Matt Jacoby, Wes Nurss, Becky Handlin, Laura Highcove, Tandra Ghose and Rahul Thakar. Finally, last but far from least, Carmel Levitan, the main love of my life, who inspires me, pushes me, teaches me and will be me with me through it all, I thank you. Oh, and who can forget, my chubby bunnies Petey Wheaty Wheaty, Cordelia Amelia Bedelia Deetz, and Cleo B—the ultimate stress relieving diversions.

To all, I thank you.

Chapter 1

What the towers don't see at night: Nocturnal sap flow in trees and shrubs at two AmeriFlux sites in California

Abstract At the leaf scale a long held assumption is that stomata open to take up CO_2 for photosynthesis in the presence of light and stomata close at night, causing both photosynthesis and transpiration are assumed to go to zero. Energy balance models and evapotranspiration equations often rely on net radiation as an upper bound, and some models reduce evapotranspiration to zero at night when there is no solar radiation. Emerging research is showing, however, that nocturnal transpiration can occur throughout the night in a variety of vegetation types and biomes. At the ecosystem scale, eddy covariance measurements have provided extensive data on latent heat flux for a multitude of ecosystem types globally. Nighttime eddy covariance measurements, however, generally are unreliable due to low turbulence. If nighttime water loss occurs significantly, then these eddy flux towers may be missing some key information on latent heat flux because some proportion is occurring at night. We installed and measured rates of sap flow using the heat ratio method (Burgess et al. 2001) at two AmeriFlux (part of FLUXNET) sites in California, USA. The heat ratio method is able to measure and quantify low rates of sap flow, including zero and negative (i.e., hydraulic lift) rates, unlike the widely used Granier method (Granier 1985), which requires an assumed zero sap flow to calibrate the measurements. We measured sap flow in five *Pinus ponderosa* trees, three *Arctostaphylos manzanita* and two *Ceanothus cordulatus* shrubs in the Sierra

Nevada Mountains; and, five *Quercus douglasii* trees at an oak-savanna in the Central Valley of California. Nocturnal sap flow was observed in all species measured; significant nighttime water loss was observed in both species of trees. Vapor pressure deficit and air temperature were strong indicators of nighttime transpiration; the influence of wind speed on nighttime transpiration was insignificant at our sites. We differentiated refilling from water loss from data from 2005, and calculated the percentage of nighttime transpiration underestimated in the eddy covariance measurements at both sites. These data contribute to the emerging literature on nighttime transpiration for multiple species in two ecosystems at eddy flux sites.

Introduction

Energy balance models rely on closure from the equation $R_n = LE + H + G + S$, where net radiation (R_n) is partitioned into evapotranspiration (LE), sensible heat (H), ground (G) and canopy (S) storage. They generally reduce LE to zero when R_n goes to zero (and negative at night), though nighttime LE can be induced by large downward H on wet surfaces in an inverted nighttime temperature profile (Monteith 1957; Baldocchi 1992). Without large nighttime H and wet surfaces, however, LE is minimal. Most LE equations rely heavily on R_n, which generally accounts for the bulk of variability in LE (Penman 1948; Monteith 1965; Priestley and Taylor 1972; Shuttleworth and Wallace 1985; Fisher et al. 2005). The widely-used Priestley-Taylor (1972) model, for instance, is calculated as $LE = 1.26*R_n*\Delta/(\Delta+\gamma)$, where Δ is the rate of change of vapor pressure with temperature, and γ is the psychrometric constant. As R_n goes to zero, the assumption is that there should be no LE for the Priestley-Taylor calculation. This assumption has been

generally accepted because at the leaf scale stomata open during the day to take up CO_2 for photosynthesis in the presence of light, and stomata close at night. Subsequently, both photosynthesis and transpiration go to zero as radiation diminishes. Nonetheless, a number of studies have shown nighttime conductance, accounting for 5-30% of daily water loss, based on gas exchange measurements (Rawson and Clarke 1988; Winner et al. 1989; Matyssek et al. 1995; Assaf and Zieslin 1996; Donovan et al. 1999; Snyder et al. 2003).

The eddy covariance method, which is based on micrometeorological theory and the covariance between vertical wind velocity and scalar concentration fluctuations (Baldocchi et al. 1988; Desjardins 1991), allows for measurement of water, carbon and energy exchange between the biosphere and atmosphere on relatively large spatial scales (1-5 km^2) at high frequency (10 Hz, averaged to 30 min). Flux measurements can be in error at night, however, when wind turbulence is light and intermittent (Goulden et al. 1996; Cienciala et al. 1998; Lee 1998; Cienciala and Lindroth 1999; Kellomaki and Wang 2000; Baldocchi 2003; Turnipseed et al. 2003). Poor estimates and lack of energy balance closure at night under stable stratifications are the result of drainage flows near the ground and below the sensors resulting in underestimates, and short-term venting at sunrise as convective turbulence resumes resulting in overestimates (Leuning and King 1992; Grace et al. 1996; Moncrieff et al. 1996; Lindroth et al. 1998; Sun et al. 1998; Yi et al. 2000). Although the sources and sinks for *LE*, *H* and CO_2 differ, eddy covariance measurement error generally may be underestimated by up to 12% at night (Soegaard et al. 2000; Berger et al. 2001). A comprehensive evaluation of energy balance closure at 22 sites in FLUXNET—a global network of over 200 eddy covariance towers (Wofsy et

al. 1993; Schmid 1994; Baldocchi et al. 2001)—showed a mean imbalance of 20% that was greatest during nocturnal periods (Wilson et al. 2002).

Given the possibility of nocturnal transpiration, and the measurement problems associated with nighttime eddy covariance and limitations with gas exchange measurements, we rely on the measurement of sap flow for individual plants via heat transfer—a direct method of transpiration measurement that does not alter the surrounding environment of the plant—which has been developing for nearly a century (Huber 1932; Marshall 1958; Cermak et al. 1973; Cohen et al. 1981; Granier 1985; Swanson 1994; Smith and Allen 1996). Further, sap flow measurements exclude soil evaporation unlike those for eddy covariance. Generally, a sap flow set contains a heater, an upstream temperature sensor and a downstream temperature sensor inserted into the xylem; sap velocity is calculated from the difference in temperatures due to the traveling heat in the sap. Until recently, there has been no reliable method to measure and quantify low rates of sap flow, including zero and negative (i.e., hydraulic lift) rates—the widely used Granier method (Granier 1985), for example, requires an assumed zero sap flow to calibrate the measurements. It is exactly these low rates of sap flow that are critical to nocturnal transpiration measurements, however. Thus, observations of nocturnal transpiration with the continuous heat Granier method have been limited (Köstner et al. 1998; Oren et al. 2001). A variation of the Granier method, the compensation heat pulse method (Edwards et al. 1996), has allowed for additional observations of nocturnal transpiration (Green et al. 1989; Benyon 1999; Song et al. 1999). Recently, Burgess et al. (2001) developed an improved heat pulse method—the heat ratio method—to measure sap flow, including low and reverse rates, which makes this method well-suited for

nighttime transpiration measurements. This method corrects for physical and thermal errors due to the sensors, including wound effects, and improves on the measurement range and resolution. Since its development, the heat ratio method has been used widely for sap flow measurement and hydraulic redistribution (Kurpius et al. 2003; Bleby et al. 2004; Bucci et al. 2004; Burgess and Dawson 2004; Hultine et al. 2004; Williams et al. 2004; Oliveira et al. 2005).

We used the heat ratio method at two FLUXNET sites (AmeriFlux) to measure sap flow in five ponderosa pine (*Pinus ponderosa* Doug. E. Laws) trees, three manzanita shrubs (*Arctostaphylos manzanita* Parry) and two ceanothus (*Ceanothus cordulatus* Kellogg) shrubs in the Sierra Nevada Mountains; and, five Blue oak (*Quercus douglasii*) trees at an oak-savanna in the Central Valley of California. Given that R_n is negative at night, it cannot drive *LE*, we follow the Penman-Monteith model (Monteith 1965) and recent sap flow research (Hogg and Hurdle 1997; Benyon 1999; Oren et al. 2001) to test (H_0) nocturnal transpiration against possible driving forces of vapor pressure deficit (*VPD*), wind speed and air temperature (T_a). We analyze the differentiation between xylem refilling versus water loss, and the sap flow signal associated with each. Finally, we determine the percentage of nighttime transpiration missing in the eddy covariance measurements at our sites and compare these errors to reported errors in the literature.

Materials and Methods

Study Sites

Data were gathered during year 2005 at Blodgett Forest Research Station (38.895250ºN, 120.632800ºW, 1315 m) in the Sierra Nevada mountains and Tonzi Ranch (38.419200ºN,

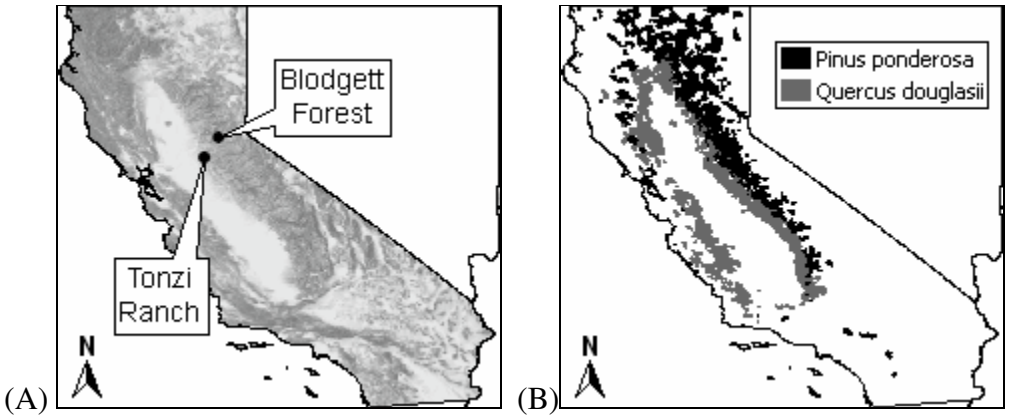

Figure 1. (A) Blodgett Forest, a *P. ponderosa* plantation, is located in the Sierra Nevada mountains and Tonzi Ranch, an oak-savanna, in the lower foothills of the Sierrra Nevada mountains of California, USA (points overlaid on digital elevation model). (B) Distribution of *P. ponderosa* and *Q. douglasii* in California based on the GAP analysis (Scott et al. 1993).

120.950300ºW, 177 m) in the lower foothills of the Sierra Nevada mountains of California, USA (Figures 1A and 1B). The Blodgett Forest study site (Goldstein et al. 2000), owned and managed for commercial purposes by Sierra Pacific Industries, was planted in 1990 at 1275 trees/ha and is dominated by *Pinus ponderosa* P. & C. Lawson with occasional other tree species. The major understory shrubs are *Arctostaphylos manzanita* Parry and *Ceanothus cordulatus* Kellogg (Xu et al. 2001). Shrubs were cut during spring 1999 and the plantation was thinned in May 2000 (Misson et al. 2005; Tang et al. 2005). Tree density was 510 trees/ha in spring 2003, and shrubs were fast developing in the large gaps between tree crowns of the open stand. In spring 2003, total one sided leaf area index (LAI) was 2.49, comprised of 72% *P. ponderosa* in the overstory, and 28% understory shrubs (*A. manzanita* 22% and *C. cordulatus* 6%). Mean tree diameter at breast height (DBH) was 12.0 cm, mean tree height was 4.7 m (mean shrub height was 1.0 m), and basal area was 9.6 $m^2 \cdot ha^{-1}$. The site is characterized by a Mediterranean climate, with warm dry summers and cold wet winters. Since 1998,

annual precipitation has averaged 1290 mm primarily between September and May, and almost no rain in the summer. Daily temperature averaged ranged from 14–27ºC during summers and 0–9ºC during winters. The soil is 60% sand, 29% loam and 11% clay (fine-loamy, mixed, mesic, ultic haploxeralf in the Cohasset series) with pH 5.5 ± 0.3 whose parent material was andesitic lahar (Goldstein et al. 2000).

The Tonzi Ranch study site is an oak-grass savanna consisting of scattered blue oak trees (*Quercus douglasii*), with occasional gray pine trees (*Pinus sabiniana*), and grazed grassland (*Brachypodium distachyon, Hypochaeris glabra, Bromus madritensis,* and *Cynosurus echinatus*) (Kiang 2002). A demographic survey on stand structure of the oak woodland was conducted using a multi-return laser altimeter system; the survey, which extended for a kilometer area centered on the meteorological tower, found mean tree height was 9.41 m ± 4.33 m, mean trunk height was 1.75m ± 1.35 m, mean crown radius was 3.18 m ± 1.54 m and mean basal area was 0.074 m^2 ± 0.0839 m^2 (Chen et al. in press). The trees covered 40% of the landscape (Tang and Baldocchi 2005) and leafed out at the end of March, reaching a maximum LAI for this heterogeneous canopy of 0.706 ± 0.408 as determined by a combination of remote sensing information (CASI, IKONOS, LiDAR) and allometric relationships. This new LAI is slightly greater than our previously published estimate of 0.6 that was derived from a 200 m transect using a LICOR-2000 (Kiang 2002). The grass grows from November to May, and reaches a maximum LAI of around 1 $m^2 \cdot m^{-2}$. The climate is also Mediterranean with a mean annual temperature of 16.3ºC and precipitation of 560 mm. The soil is Auburn extremely rocky silt loam (Lithic haploxerepts) composed of 43% sand, 43% silt and 13% clay. Soil moisture, as measured at both the Sierra Nevada and oak-savanna sites with time

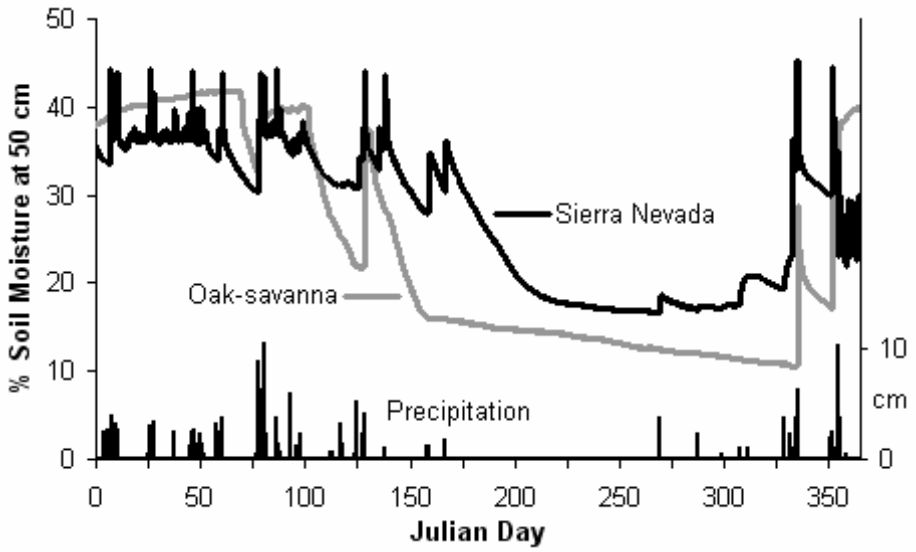

Figure 2. Soil moisture at 50 cm depth during 2005 at the oak-savanna site and Sierra Nevada site. The timing of precipitation is generally the same for both sites so we show data for only the oak-savanna site. Precipitation reached a maximum of 14.2 cm at the Sierra Nevada site and 10.4 cm at the oak-savanna site. The Sierra Nevada site, at an elevation that receives snow, retains moisture longer into the summer though still experiences prolonged summer drought as controlled by the Mediterranean climate.

domain reflectometry (TDR) at 50 cm depth peaks at 35-40% in the winters and drops to 15-20% in the summers (Figure 2).

Sap Flow

Sap flow probe sets were designed following the heat ratio method (Burgess et al. 2001; Burgess and Dawson 2004). We built thermocouple temperature probes with copper-constantan wire (36G) inside a flexible micro-capillary filled with silicone heat transfer compound inserted into a capped steel hypodermic needle. Two thermocouple junctions 1.5 cm apart were soldered to allow for temperature readings at two radial depths (4.0 and 2.5 cm) into the xylem. We built heater probes with coiled nichrome wire (36G, 85 $\Omega \cdot m^{-1}$) inside a flexible mico-capillary inserted into a capped steel hypodermic needle.

Both the thermocouple and heater needle bases were encased in waterproof epoxy resin; needle lengths were 4.5 cm, with 4.0 cm extruding from the epoxy base.

Probes were connected to centrally placed AM416 multiplexers attached to CR10X dataloggers (Campbell Scientific Inc., Logan, UT, USA) with cables ranging from 7 to 17 m depending on the distance from the tree or shrub to the multiplexer. Data were logged every 30 min. We attached a temperature thermistor to each multiplexer for a reference temperature. To control the heat pulse, we built heater relays each with a double pole double throw relay, transistor, resistor and diodes. All materials were powered by deep cycle marine batteries; a 5-W solar panel was used at the oak-savanna site for supplemental battery recharge.

Sap flow sensors were installed in each tree at breast height and in each shrub at the base. We stripped the outer bark to ensure xylem contact, and used a steel drill guide to maintain equidistance (1 cm) between each probe. The sap flow sensors were encased in protective and reflective insulation. Over the course of the year, six heaters burned out and two thermocouples failed; we monitored them regularly so repairs were expedited and data loss minimized. Random data spikes were corrected with a standard deviation threshold calculation. We recorded measurements on a half-hourly time step to align with the eddy flux half-hourly measurements. We calculated heat pulse velocity following Marshall (1958) and converted to sap flow with corrections for probe misalignment, wounding and thermal diffusivity following Burgess et al. (2001). A constant thermal diffusivity of heat through woody tissue was assumed for each species, though it varies with wood water content. We report heat pulse velocities for ease of comparison; volumetric flow rates can be calculated as scaled from plant size.

At the Sierra Nevada site, we conducted a forest inventory and selected five *P. ponderosa*, three *A. manzanita* and two *C. cordulatus* shrubs throughout the eddy flux footprint representative of the stand DBH and height structure. DBH for the five trees were 18, 20, 21, 24 and 24 cm. Individual LAI (or foliage area index) of the shrubs ranged from 1–3 (LAI-2000, LICOR, Lincoln, NE). At the oak-savanna site, we selected five *Q. douglasii* trees as determined from the sampling scheme of Kiang (2002). DBH for the five trees were 16, 18, 22, 23 and 37 cm. Sap flow was measured from the beginning of spring 2005 through winter 2006.

Eddy Covariance

Ongoing eddy covariance flux measurements at the Sierra Nevada and oak-savanna sites have been described extensively (Goldstein et al. 2000; Baldocchi et al. 2004; Misson et al. 2005). Meteorological measurements included in this analysis were R_n, VPD, T_a, wind speed, precipitation and soil moisture at 50 cm depth. Micrometeorological instruments were attached to towers 12.5 m from the ground for the Sierra Nevada site, and 23 m (overstory) and 2 m (understory) for the oak-savanna site. We measured wind velocity and air temperature at 10 Hz with three-dimensional sonic anemometers (ATI Electronics Inc., Boulder, CO for Blodgett; Windmaster Pro, Gill Instruments, Lymington, UK for Tonzi). Water vapor mixing ratios were measured with infrared gas analyzers (model 6262 for Blodgett, 7500 for Tonzi, LICOR, Lincoln, NE). The output of the water vapor channel was referenced to a dew point hygrometer (LI-610, LICOR, Lincoln, NE) at the oak-savanna site. We used the eddy covariance method to measure fluxes of water and carbon dioxide between the biosphere and atmosphere (Goldstein et al. 2000; Baldocchi

et al. 2004). This method quantifies vertical fluxes of scalars from the covariance between vertical wind velocity and scalar fluctuations averaged over 30-min periods, which matched the temporal resolution of the sap flow dataloggers (Shuttleworth et al. 1984; Baldocchi et al. 1988; Wofsy et al. 1993). Data were processed and analyzed in Microsoft's *Excel*, SAS Institute's *JMP IN*, and ESRI's *ArcGIS 9*.0.

Results

Daytime and nighttime average sap flow rises into the summer and decreases into the winter for both *Q. douglasii* (Figure 3A) and *P. ponderosa* (Figure 3B). Data shown are for the 16 cm DBH *Q. douglasii* tree and 20 cm DBH *P. ponderosa* tree, though the annual pattern is similar for the other size classes. A polynomial fit is overlaid for visualization of the general pattern. Note for comparison that the starting date of the sap flow measurements is 16 days earlier for the *P. ponderosa* than the *Q. douglasii*. Although both daytime and nighttime sap flow peak in the summer, they do so at different times where daytime sap flow peaks earlier than does nighttime sap flow. Daytime and nighttime sap flow show the most separation during summer, but converge near zero in the winter. Daytime sap flow peaks earliest for *Q. douglasii* around days 160-170, and nighttime sap flow peaks around days 210-220. For *P. ponderosa*, daytime sap flow peaks around days 190-200, and nighttime sap flow peaks around days 210-220 (same as for *Q. douglasii*). For the *A. manzanita* and *C. cordulatus* shrubs, daytime sap flow follows that of the overstory trees with peaks around days 190-200 (*A. manzanita*) and 200-210 (*C. cordulatus*), but the nighttime sap flow shows a different pattern from the trees by staying close to zero in the summer and increasing in the winter (Figure 3C).

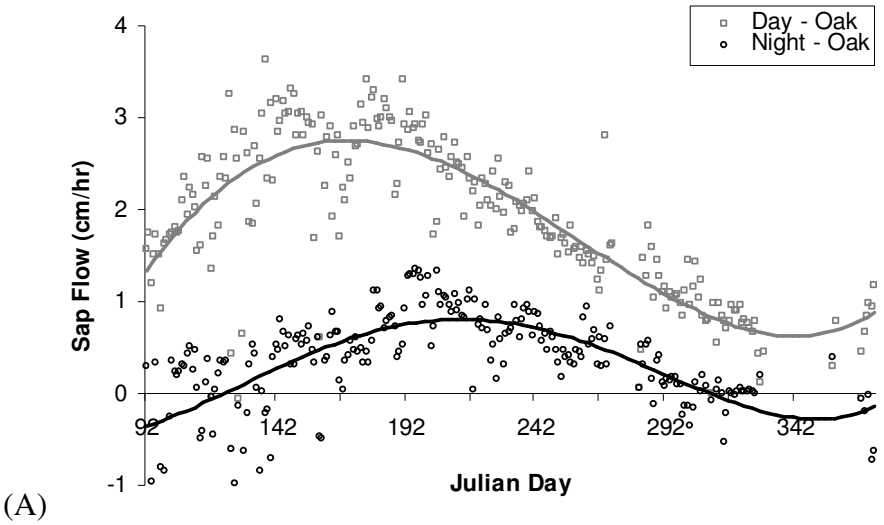

(A)

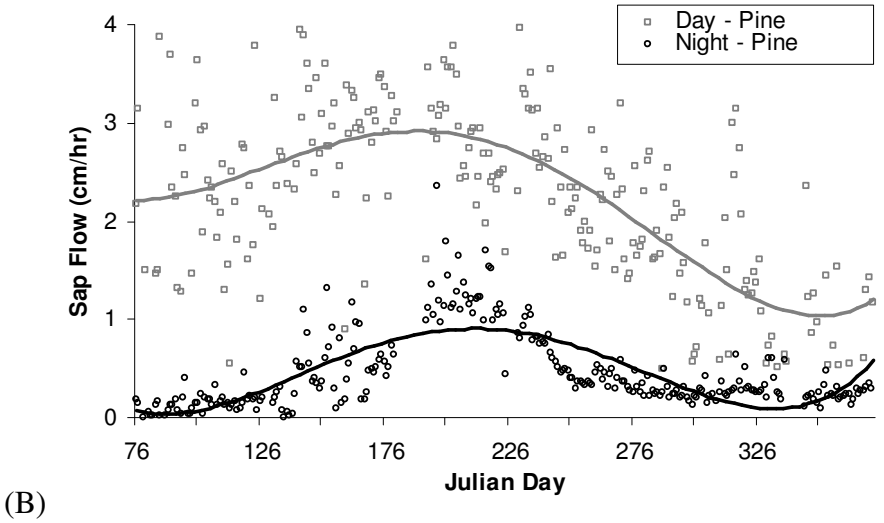

(B)

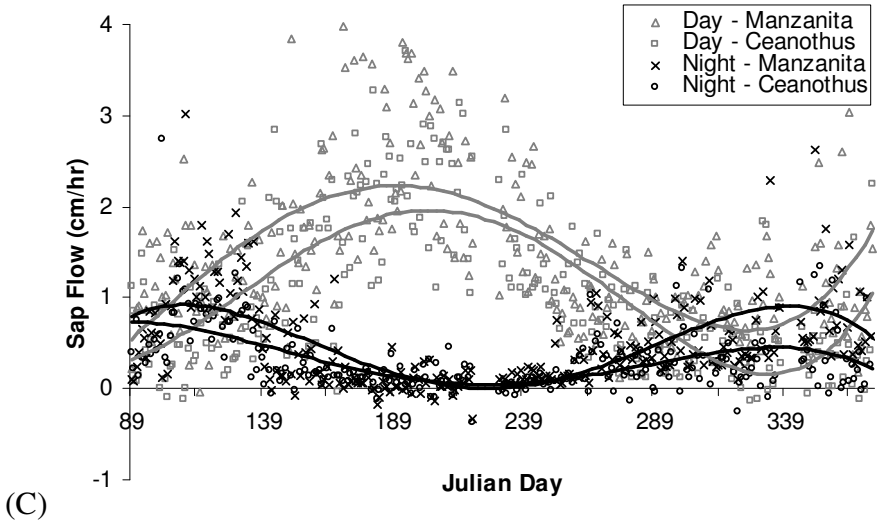

(C)

Figure 3. Daytime and nighttime averages during 2005 for (A) *Q. douglasii*, (B) *P. ponderosa*, and (C) *A. manzanita* and *C. cordulatus*.

Any summer water loss at night for the shrubs is relatively insignificant as compared with daytime transpiration. All species exhibited small amounts of negative sap flow associated with settling or root efflux as described elsewhere (Burgess et al. 2000; Burgess et al. 2000).

For plants that have exhibited nocturnal transpiration, *VPD* has been shown to be a primary driving force (Hogg and Hurdle 1997; Benyon 1999; Oren et al. 2001) and physiological theory grounds these observations (Monteith 1965). *VPD* will not be influential, however, if it goes to zero every night. Both of our sites are very dry so *VPD* remained positive throughout the night, particularly in the summer (Figure 4A). Nighttime averaged *VPD* corresponds closely with nighttime averaged sap flow at both sites (Figure 4B). Linear regression fits (Figures 4C and 4D) showed good and similar agreements for both *Q. douglasii* (r^2=0.79, p<0.0001, RMSE=0.18) and *P. ponderosa* (r^2=0.71, p<0.0001, RMSE=0.17). For *P. ponderosa*, the slope of the regression is steeper and the fit less than that for *Q. douglasii* due to the vertical asymptote of negative sap flow rates at low *VPD*. For four days in the summer when our sites received some chance precipitation (Figure 2), nighttime sap flow decoupled from *VPD*, which dropped during those moist events yet nighttime sap flow increased.

The Penman-Monteith (1965) equation also includes T_a (in saturation vapor pressure and its slope against T_a) as a driver for *LE*. T_a and *VPD* are tightly correlated exponentially at both of our sites (Figure 5A). At the Sierra Nevada site, as nighttime T_a increased into the summer, nighttime sap flow increased much more rapidly (Figure 5B). The linear regression fit (r^2=0.70, p<0.0001, RMSE=0.24) is similar to that with *VPD* for *P. ponderosa* (Figure 5C), though an exponential curve improves that fit slightly

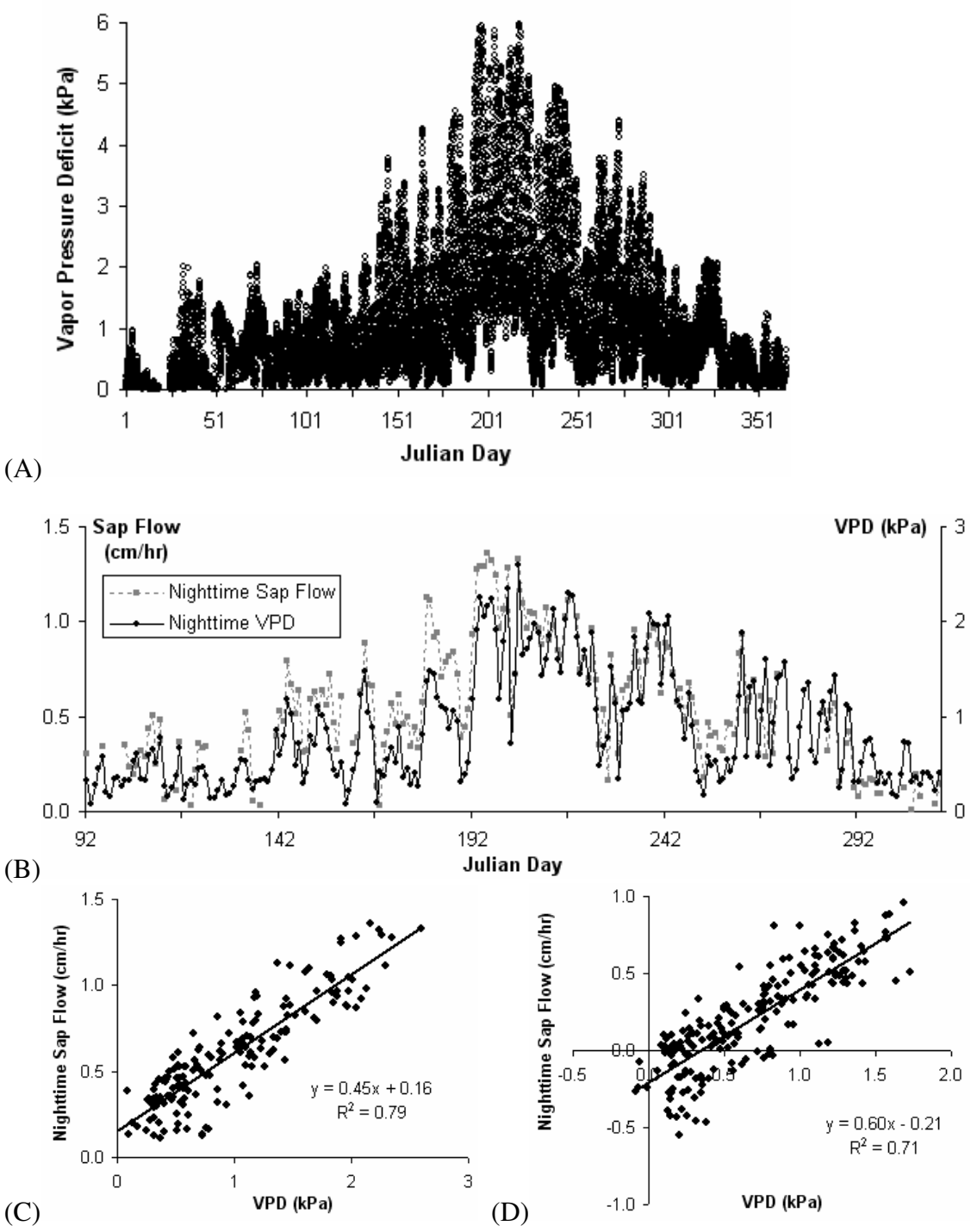

Figure 4. (A) Vapor pressure deficit (*VPD*) climatology for 2005 at the oak-savanna site. (B) Daily averaged nighttime *VPD* and sap flow for a *Q. douglasii* (16 cm DBH) tree. (C) Linear regression of the data in Figure 3B. (D) Linear regression for daily averaged nighttime *VPD* and sap flow for 2005 at the Sierra Nevada site for a *P. ponderosa* (18 cm DBH) tree.

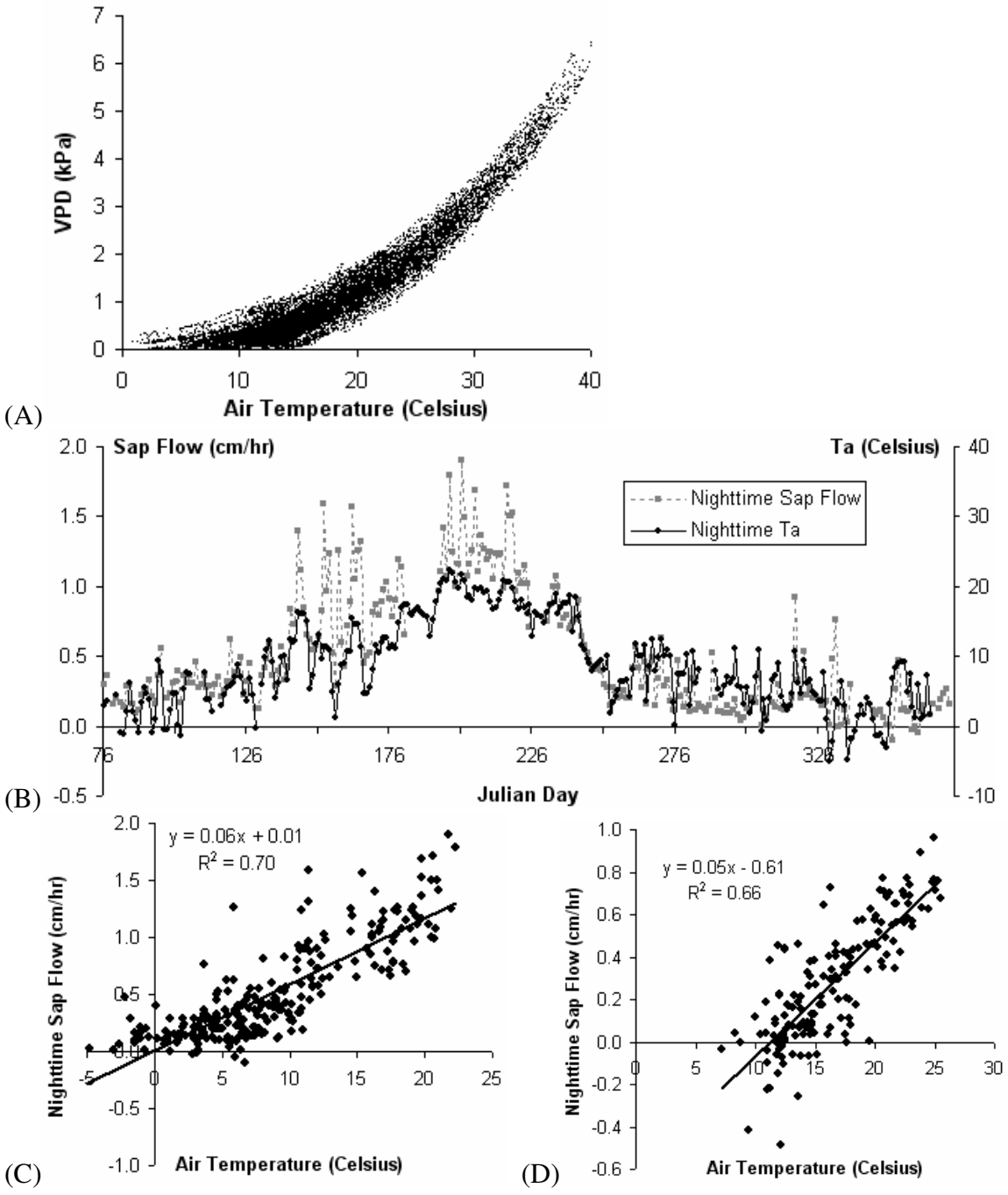

Figure 5. (A) Vapor pressure deficit (*VPD*) versus air temperature (T_a) follows an exponential curve for 2005 at both sites; data shown here are for the oak-savanna site. (B) As T_a increases at the Sierra Nevada site, nighttime sap flow (20 cm DBH) increases much more rapidly. The exponential relationship holds for nighttime sap flow versus T_a during the summer at the (C) Sierra Nevada site, but not the (D) oak-savanna site (16 cm DBH).

	VPD	*Ta*	Wind speed
Q. douglasii	0.79	0.70	0.01
P. ponderosa	0.71	0.66	0.03

Table 1. Correlation coefficients for nighttime sap flow predictors (*VPD*, *Ta*, and wind speed) versus nighttime sap flow for *Q. douglasii* and *P. ponderosa*.

(r^2=0.72). The linear regression fit for *Q. douglasii* (r^2=0.66, p<0.0001, RMSE=0.25) is reduced from that for *VPD*, however (Figure 5D). The slopes of the linear regression between sap flow and T_a for both species are equivalent (m=0.06 for *P. ponderosa*, and m=0.05 for *Q. douglasii*). A multiple regression of T_a and *VPD* (which are auto-correlated and not expected to improve fits) against nighttime sap flow yields a slight improvement for *P. ponderosa* (r^2=0.80, p<0.0001, RMSE=0.15), but not for *Q. douglasii* (r^2=0.75, p<0.0001, RMSE=0.17), which was better predicted by *VPD* alone. Wind speed was a poor predictor (insignificant correlations) for nighttime transpiration at both sites (Table 1).

To differentiate nighttime xylem refilling (alleviation of xylem pressure from daytime-decreased water potentials) from water loss (actual transpiration or conductance), we assessed the pattern of nocturnal sap flow during two periods: 1) when the nighttime driving force, *VPD*, was minimized (due to moist, cold air—generally during the winter), and 2) when the nighttime driving force was maximized (generally during the summer). Under the first condition, any sap flow occurring at night should be limited to refilling (no loss). The diurnal pattern of sap flow is marked by a rise soon after solar radiation becomes positive, declining with decreasing solar radiation in the evening and tailing off to zero within a couple of hours after sunset (Figure 6A). Under the second condition, when *VPD* remains positive and high throughout the night, nocturnal sap flow follows the same slope and temporal pattern following sunset as in

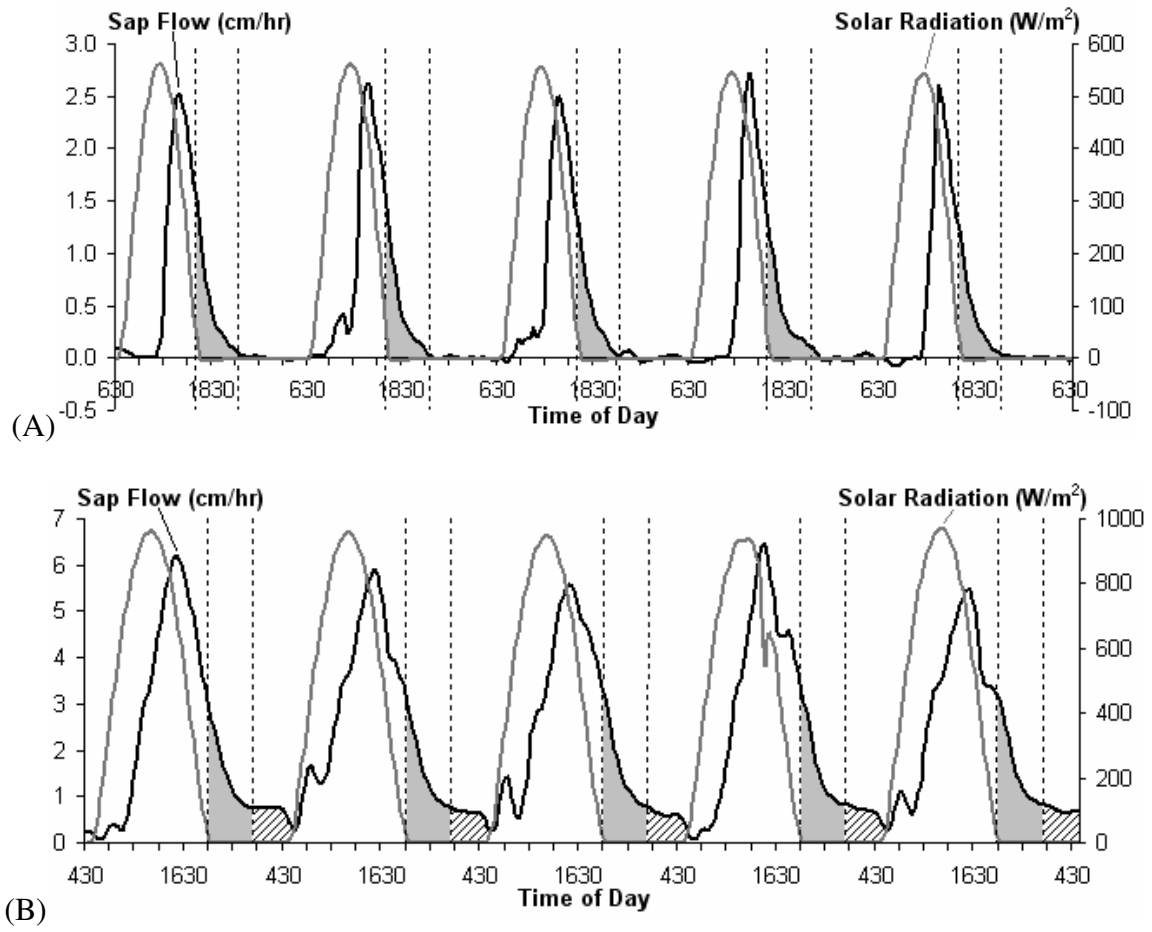

Figure 6. Five-day period for sap flow and solar radiation for a *Q. douglasii* (16 cm DBH) tree (A) late in the year when *VPD* and T_a are low so only refilling occurs (shaded ~3 hour periods between dashed vertical lines) and (B) and in the middle of the summer when water loss (diagonal stripes) follows refilling period. The diurnal pattern of *VPD* and T_a match the diurnal pattern of sap flow.

Figure 6A, but remains positive throughout the night as well (Figure 6B). The integral of sap flow from the end of the refilling period to sunrise marks the amount of nighttime water loss. Refilling constitutes 80% and water loss 20% of the integral of nocturnal sap flow in Figure 6B. At sunrise, when *VPD* and T_a drop briefly in the inversion, sap flow also drops to zero before ramping back up in the typical diurnal pattern. Also evident in Figures 6A and 6B is a small peak then dip right after sunrise. This sub-peak represents the depletion of stored water rather than soil moisture for transpiration (Tatarinov and

Cermak 1999; Steppe and Lemeur 2004). The subsequent replenishment of this source is evident by the steeper slope in sap flow following the sub-peak. The sub-peak is not always evident in the sap flow measurements, however, depending on how fast the trees are able to replenish the storage.

After differentiating nocturnal refilling from water loss, our next step was to link nighttime transpiration from the sap flow measurements to measurements of *LE* from eddy covariance at the towers. First, to assess this link during reliable measurement periods, we evaluated daytime sap flow with daytime *LE*. At the Sierra Nevada site, daytime averaged sap flow follows daytime averaged *LE* throughout the year, though with scatter due to the disconnect between individual tree response and the average response of all trees in the footprint (Figures 7A and 7B). The fit between sap flow and *LE* was similar for every tree at this site (r^2=0.62, p<0.0001, RMSE=0.51). At the oak-savanna site, where the life cycle of the grassland contributes to ecosystem *LE* in this open canopy, we separated the two sources of *LE* with an above-canopy eddy flux tower and a below-canopy eddy flux tower (Figure 8A). The grasses and near-surface soil dry out and stop contributing significantly to overall *LE* before day 200, but tree transpiration continues for another 50 days. The sap flow measurements, however, indicate a lag to eddy covariance whereby the trees continue to transpire at high rates much further into the summer, finally reducing to near zero around day 340 (Figure 8B). Furthermore, the fit between daytime sap flow and daytime *LE* is poor (r^2=0.44, p<0.0001, RMSE=0.55), although a logarithmic relationship improves the fit (r^2=0.54) for the data shown and for the other *Q. douglasii* trees. A logarithmic fit indicates that trees tap a deeper source of soil moisture and thus continue to transpire further into the given very high rates of *LE* as

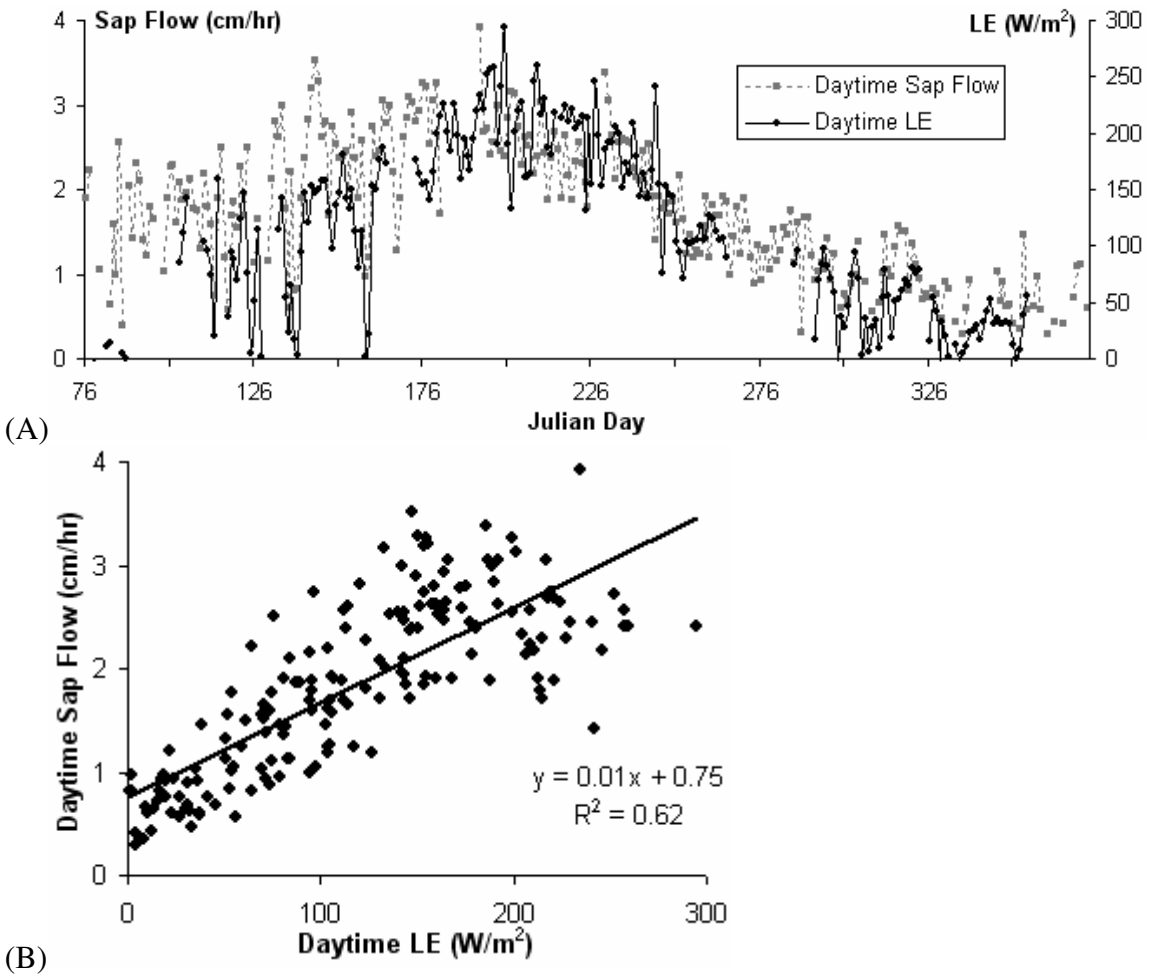

Figure 7. (A) Daytime averaged sap flow (20 cm DBH) and *LE* from eddy covariance at the Sierra Nevada site. (B) Linear regression of the data in Figure 7A.

measured by eddy covariance, the sap flow measurements are not recording such high rates and may reach a daytime average cap of 4 cm/hr (individual measurements at 30-min reached 10 cm/hr). Stand structure is much more heterogeneous at the oak-savanna site than at the Sierra Nevada site (which is a relatively uniform plantation). Nonetheless, the objective here is not to scale up individual tree sap flow measurements to footprint measurements, but to assess whether or not daytime sap flow follows daytime eddy covariance *LE*, which it does albeit with scatter at both sites and time lag at the oak-savanna site, for relative comparison with nighttime measurements.

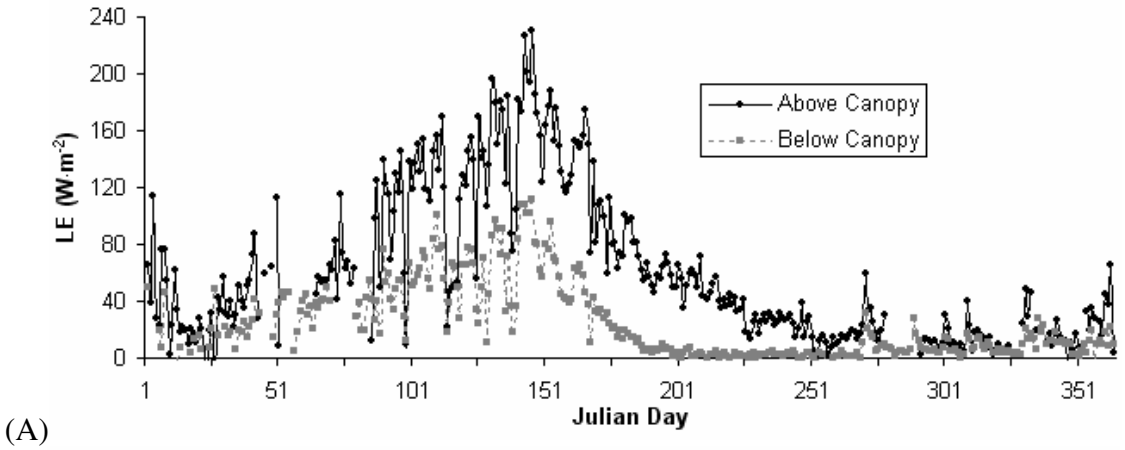

(A)

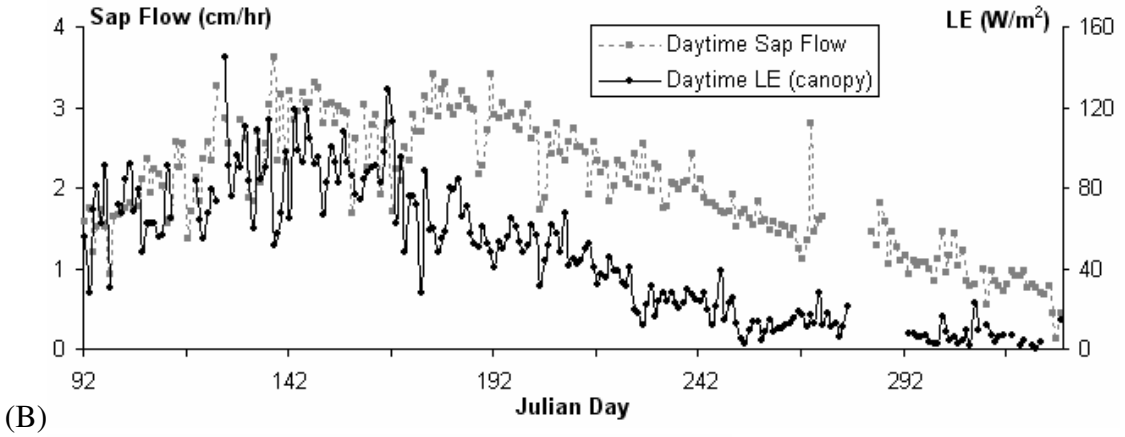

(B)

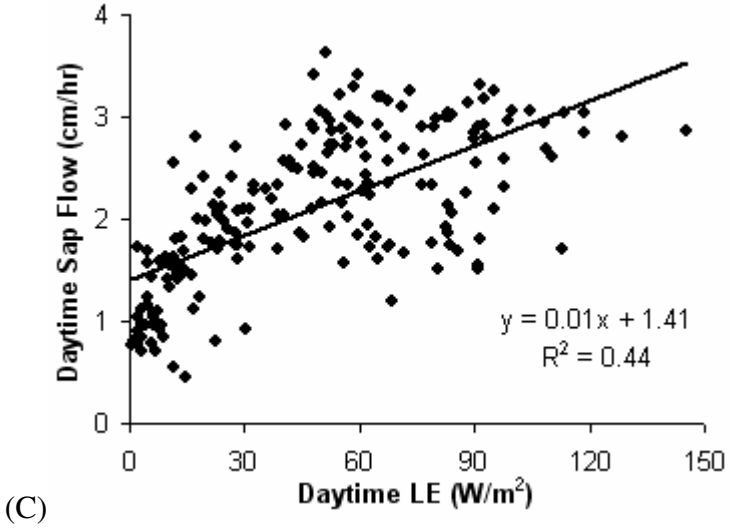

(C)

Figure 8. (A) Daytime averaged *LE* for above-canopy and below-canopy towers at the oak-savanna site. (B) The difference between the above- and below-canopy towers equals the *LE* from only the trees, which is compared to the sap flow from a 16 cm (DBH) tree. (C) The correlation between eddy covariance and sap flow is reduced due to the temporal lag as seen in Figure 8B.

Given the approximation of daytime sap flow to daytime eddy covariance *LE*, our next analysis compared nighttime sap flow to nighttime eddy covariance *LE*. As would be expected from the introduction of nighttime eddy covariance measurements, these measurements did not correspond well to nighttime sap flow. At the Sierra Nevada site, the summer nighttime transpiration was significantly underestimated (Figure 9A). At the oak-savanna site, nighttime *LE* sometimes matched nighttime sap flow, but for the most part underestimated nighttime transpiration as well (Figure 9B). Nighttime sap flow as a percent of daily total was 18% versus 6% for eddy covariance at the oak-savanna site, and 21% (sap flow) versus 1% (eddy covariance) at the Sierra Nevada site (Figure 9C). The number of nights with valid measurements was also greater for sap flow than for eddy covariance—185 versus 153 at the oak-savanna site, and 241 versus 208 at the Sierra Nevada site during our measurement period for 2005 (Figure 9D). The number of days with valid measurements were equivalent for sap flow and eddy covariance at the oak-savanna site (Figure 8B), though for the Sierra Nevada site sap flow maintained higher reliability due in large part to a 3-week eddy covariance gap around day 276 (Figure 7A). For valid data, nighttime eddy covariance measurements depend on adequate wind speed and equipment reliability, whereas nighttime sap flow measurements depend only on equipment reliability.

Discussion

There were many peculiarities in the shrub sap flow data that are difficult to explain. During the day the sap flow values were very sporadic, jumpy and inconsistent, due to a sunlight/sunfleck and diffuse light exposure-response from shading by the adjacent trees

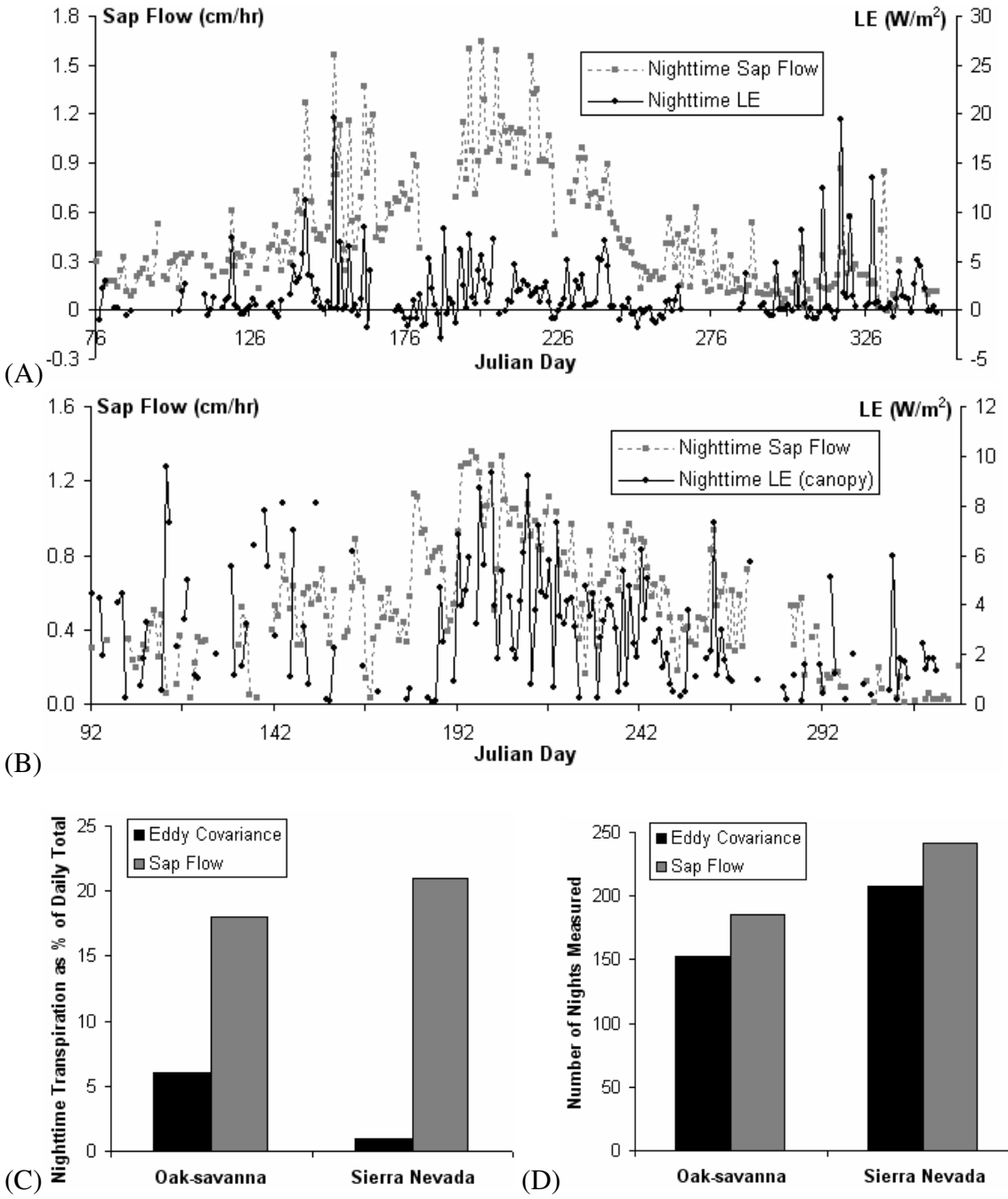

Figure 9. (A) Nighttime averaged sap flow for the same tree as in Figure 7 compared with nighttime averaged *LE* from eddy covariance at the Sierra Nevada site. (B) Nighttime averaged sap flow for the same tree as in Figure 8 compared with nighttime averaged *LE* from the difference between the above- and below-canopy eddy covariance towers at the oak-savanna site. (C) Measured nighttime transpiration was much larger for sap flow than for eddy covariance at both sites. (D) The number of nights with valid measurements was larger for sap flow as compared with eddy covariance.

(Norman et al. 1971; Abrams and Mostoller 1995). During the night, however, the sap flow measurements were very stable, although there was movement in the data in response to refilling, redistribution of water and nutrients, or leaky stomata coupled with an atmospheric driver. Unfortunately, we could not determine the causes for this response, though the nighttime sap flow was minimal so that any nighttime loss may be insignificant. Figure 3C shows an unusual nighttime response over the course of the year, whereby an inverse of the tree nighttime sap flow response is exhibited with relatively high nighttime sap flow during the winter and low nighttime sap flow during the summer. Snow covers many of the shrubs in the winter so it is assumed that the shrubs are inactive during this period. Daytime sap flow measurements during the winter tended to be zero or missing, but nighttime sap flow measurements were stable with some movement. During the summer, daytime sap flow resembles the pattern of that for the trees, but nighttime sap flow is close to zero. The shrubs likely are exposed and limited to a different source of soil moisture—possibly more shallow—than are the trees, though we did dig up some shrubs and found that they send down a tap root in addition to the fine shallow roots. The shallow soils are very dry during the summer, however (Figure 2). Thus, it is likely that the shrubs are very well-adapted to drought conditions and will not lose any water at night unless moisture conditions are high (Hinckley et al. 1983; Condit et al. 1995; Reynolds et al. 1999).

Nighttime transpiration was well-coupled (low Ω) with *VPD* except for sporadic rain events during the water-limited summer, and was not well-coupled with wind speed (McNaughton and Jarvis 1991). There was a strong response with T_a as well, though with *VPD* and T_a so well-correlated it is difficult to separate the two influences.

Although nighttime T_a reached >30ºC, it is unlikely that nighttime transpiration was a regulated response to cool the leaves (Montero et al. 2001). Wind was not well-coupled (high Ω) with sap flow because our sites were very dry (hence, low Ω with *VPD*). Wind will be more coupled with transpiration in a humid environment, where it can act as a physical mechanism to break up the stable boundary layer above the leaf and canopy, and to remove recently transpired water vapor and replace the air immediately above the leaf with dry air (Meinzer et al. 1995). *VPD* is a well-known driver of transpiration due to the water potential gradient and the ability of dry air to pull in water from a source of higher water potential (Monteith 1965). In a moist environment, however, *VPD* may not be as well-coupled to sap flow as it is at our sites. At the root, however, soil moisture is perhaps the most important input at our sites, without which no transpiration could occur regardless of values for *VPD*, T_a, or any other driver. Sap flow was minimized when soil moisture was at its lowest—at 10.5% around day 330 for the oak-savanna site and at 16.8% around day 260 for the Sierra Nevada site (Figure 2).

One of the key questions in nocturnal sap flow is how to differentiate between refilling and actual water loss. Nighttime refilling occurs because leaf water potential declines during daytime transpiration so at night the water potential gradient between soil and plant drives this nocturnal sap flow (Burgess and Dawson 2004). Refilling, in other words, is the alleviation of built-up xylem pressure. Three general drivers control the slope of the diurnal sap flow curve: 1) the stomata are wide open to allow for maximum photosynthesis and subsequent water loss, 2) the stomata close, but sap flow continues to satisfy refilling and water potential gradients, and 3) the stomata are partially open due to imperfect closure (van Hove et al. 1992), which allows sap flow to continue at a

decreased, but positive rate. The three phases or slopes can be seen in Figure 6B. During the day, there are a few distinct sub-slopes to the first phase—the depletion of stored water, the subsequent replenishment of that water the slope of which depends on how quickly the stored water was depleted, and the continuation of sap flow as dictated by solar radiation. As soon as solar radiation goes to zero, the negative slope of sap flow shifts to less negative during the refilling phase, which can be seen in both Figures 6A and 6B. The refilling phase is marked by the narrow period between the dashed vertical lines from when solar radiation goes to zero until the slope of the decline shifts to a steady, near-zero slope. Water loss from nighttime transpiration is the period of sap flow following the refilling phase until solar radiation becomes positive.

Gas exchange measurements have shown nighttime transpiration to be 5-30% of daily water loss (Rawson and Clarke 1988; Winner et al. 1989; Matyssek et al. 1995; Assaf and Zieslin 1996; Donovan et al. 1999; Snyder et al. 2003), and nighttime eddy covariance errors have been reported to be around 12-20% (Soegaard et al. 2000; Berger et al. 2001; Wilson et al. 2002). We report nighttime transpiration as a percent of daily water loss at 18% (oak-savanna site) and 21% (Sierra Nevada site) from sap flow—well within the range of published values from gas exchange (5-30%). The nighttime eddy covariance *LE* as a percent of daily water loss was 12% underestimated (oak-savanna site) and 20% underestimated (Sierra Nevada site) relative to sap flow measurements—also right within the range of published error (12-20%). Much of the eddy covariance error analysis has been focused on CO_2 with the assumption that *LE* errors match, and we confirm those assumptions at our sites. The relative ranges of our measurements show congruence with the literature and provide amounts of transpiration on a 30 min interval.

We recommend *VPD* as a proxy with which to estimate and gap-fill uncertain nighttime eddy covariance measurements at our sites and other sites with similar climatology and vegetation.

In an effort to quantify nocturnal transpiration at our sites we relied on a number of measurement and analytical methods. To measure sap flow, we used the heat ratio method, which was especially useful for low flow rates that are critical to nighttime measurements. We found that nocturnal sap flow was present in the two species of trees (*P. ponderosa* and *Q. douglasii*) and two species of shrubs (*A. manzanita* and *C. cordulata*) studied, though significant nighttime water loss was present only in the trees. In testing possible nighttime drivers, *VPD*, T_a and wind speed, we found at our sites that *VPD* did not go to zero every day and was strongly coupled with nighttime sap flow (r^2=0.79 and 0.71 at the oak-savanna and Sierra Nevada sites, respectively), T_a was also associated with nighttime sap flow but auto-correlated with *VPD*, and wind speed was insignificant with nighttime sap flow. Because *VPD* was so well-coupled with nighttime sap flow, we were able to assess nocturnal sap flow when *VPD* was low and high to determine patterns of refilling versus water loss. Individual sap flow measurements generally followed daytime eddy covariance *LE* measurements for large-scale footprints, but diverge considerably at night. Finally, we were able to quantify the amount of water loss underestimated from nighttime eddy covariance, or what the "towers don't see at night." We suggest that new models of evapotranspiration, water balance, net primary productivity and climate change reflect this proportion of nighttime *LE*.

Acknowledgments

The authors thank G. Biging, V. Boukili, R. Brenner, S. Burgess, A. DiVittorio, T. Hehn, J. Kuriel, J. Lee, B. Leung, C. Levitan, S. Ma, M. McKay, R. Oliveira, S. Rambeau, K. Simonin, R. Tonzi and K. Tu for assistance and support in this work. J. Fisher was supported by NASA Headquarters under the Earth System Science Fellowship Grant NGT5-30473, and by Faculty Research Grants from the University of California, Berkeley. Measurements at both Tonzi Ranch and Blodgett Forest were supported in part by the Office of Science, Biological and Environmental Research Program (BER), U.S. Department of Energy, and through the Western Regional Center of the National Institute for Global Environmental Change (NIGEC) under Cooperative Agreement No. DE-FCO2-03ER63613. Additional support at Tonzi Ranch was made possible by DOE/TCP and WESTGEC. Additional support at Blodgett Forest was made possible by grants from the Kearney Foundation of Soil Science and the University of California Agricultural Experiment Station. Financial support does not constitute an endorsement of the views expressed in this article/report.

References

Abrams, M.D. and S.A. Mostoller 1995. Gas-exchange, leaf structure and nitrogen in contrasting successional tree species growing in open and understory sites during a drought. Tree Physiology. 15:361-370.

Assaf, G. and N. Zieslin 1996. Night water consumption by rose plants. Journal of Horticultural Science. 71:673-678.

Baldocchi, D. 1992. A lagrangian random-walk model for simulating water vapor, CO2 and sensible heat flux densities and scalar profiles over and within a soybean canopy. Boundary Layer Meteorology. 61:113-144.

Baldocchi, D., E. Falge, L.H. Gu, R.J. Olson, D. Hollinger, S.W. Running, P.M. Anthoni, C. Bernhofer, K. Davis, R. Evans, J. Fuentes, A. Goldstein, G. Katul, B.E. Law, X.H. Lee, Y. Malhi, T. Meyers, W. Munger, W. Oechel, K.T.P. U, K. Pilegaard, H.P. Schmid, R. Valentini, S. Verma, T. Vesala, K. Wilson and S.C. Wofsy 2001.

FLUXNET: A new tool to study the temporal and spatial variability of ecosystem-scale carbon dioxide, water vapor, and energy flux densities. Bulletin of the American Meteorological Society. 82:2415-2434.

Baldocchi, D., B. Hicks and T. Meyers 1988. Measuring biosphere-atmosphere exchanges of biologically related gases with micrometeorological methods. Ecology. 69:1331.

Baldocchi, D.D. 2003. Assessing the eddy covariance technique for evaluating carbon dioxide exchange rates of ecosystems: past, present and future. Global Change Biology. 9:479-492.

Baldocchi, D.D., L.K. Xu and N. Kiang 2004. How plant functional-type, weather, seasonal drought, and soil physical properties alter water and energy fluxes of an oak–grass savanna and an annual grassland. Agricultural and Forest Meteorology. 123:13-39.

Benyon, R.G. 1999. Nighttime water use in an irrigated Eucalyptus grandis plantation. Tree Physiology. 19:853-859.

Berger, B.W., K.J. Davis, C.X. Yi, P.S. Bakwin and C.L. Zhao 2001. Long-term carbon dioxide fluxes from a very tall tower in a northern forest: Flux measurement methodology. Journal of Atmospheric and Oceanic Technology. 18:529-542.

Bleby, T.M., S.S.O. Burgess and M.A. Adams 2004. A validation, comparison and error analysis of two heat-pulse methods for measuring sap flow in Eucalyptus marginata saplings. Functional Plant Biology. 31:645-658.

Bucci, S.J., F.G. Scholz, G. Goldstein, F.C. Meinzer, J.A. Hinojosa, W.A. Hoffman and A.C. Franco 2004. Processes preventing nocturnal equilibration between leaf and soil water potential in tropical savanna woody species. Tree Physiology. 24:1119-1127.

Burgess, S.S.O., M.A. Adams and T.M. Bleby 2000a. Measurement of sap flow in roots of woody plants: a commentary. Tree Physiology. 20:909-913.

Burgess, S.S.O., M.A. Adams, N.C. Turner, C.R. Beverly, C.K. Ong, A.A.H. Khan and T.M. Bleby 2001. An improved heat pulse method to measure low and reverse rates of sap flow in woody plants. Tree Physiology. 21:589-598.

Burgess, S.S.O. and T.E. Dawson 2004. The contribution of fog to the water relations of *Sequoia sempervirens* (D. Don): foliar uptake and prevention of dehydration. Plant, Cell and Environment. 27:1023-1034.

Burgess, S.S.O., J.S. Pate, M.A. Adams and T.E. Dawson 2000b. Seasonal water acquisition and redistribution in the Australian woody phreatophyte, *Banksia prionotes*. Annals of Botany. 85:215-224.

Cermak, J., M. Deml and M. Penka 1973. New method of sap flow-rate determination in trees. Biologia Plantarum. 15:171-178.

Chen, Q., D.D. Baldocchi and P. Gong in press. Isolating individual trees in a savanna woodland using small footprint LiDAR data. Photogrammetric Engineering and Remote Sensing

Cienciala, E. and A. Lindroth 1999. Analysis of carbon and water fluxes from the NOPEX boreal forest: comment. Journal of Hydrology. 218:92-94.

Cienciala, E., S.W. Running, A. Lindroth, A. Grelle and M.G. Ryan 1998. Analysis of carbon and water fluxes from the NOPEX boreal forest: comparison of

measurements with FOREST-BGC simulations. Journal of Hydrology. 212-213:62-78.

Cohen, Y., M. Fuchs and G.C. Green 1981. Improvement of the heat pulse method for determining sap flow in trees. Plant, Cell and Environment. 4:391-397.

Condit, R., S.P. Hubbell and R.B. Foster 1995. Mortality-rates of 205 neotropical tree and shrub species and the impact of a severe drought. Ecological Monographs. 65:419-439.

Desjardins, R.L. 1991. Review of techniques to measure CO2 flux densities from surface and airborne sensors. *In* Advances in Bioclimatology. Springer, Berlin, pp. 2-23.

Donovan, L.A., D.J. Grise, J.B. West, R.A. Pappert, N.N. Alder and J.H. Richards 1999. Predawn disequilibrium between plant and soil water potentials in two cold-desert shrubs. Oecologia. 120:209-217.

Edwards, W.R.N., P. Becker and J. Cermák 1996. A unified nomenclature for sap flow measurements. Tree Physiology. 17:537-543.

Fisher, J.B., T.A. Debiase, Y. Qi, M. Xu and A.H. Goldstein 2005. Evapotranspiration models compared on a Sierra Nevada forest ecosystem. Environmental Modelling & Software. 20:783-796.

Goldstein, A.H., N.E. Hultman, J.M. Fracheboud, M.R. Bauer, J.A. Panek, M. Xu, Y. Qi, A.B. Guenther and W. Baugh 2000. Effects of climate variability on the carbon dioxide, water, and sensible heat fluxes above a ponderosa pine plantation in the Sierra Nevada (CA). Agricultural and Forest Meteorology. 101:113-129.

Goulden, M.L., J.W. Munger, S.M. Fan, B.C. Daube and S.C. Wofsy 1996. Measurements of carbon sequestration by long-term eddy covariance: methods and a critical evaluation of accuracy. Global Change Biology. 2:169-182.

Grace, J., Y. Malhi, J. Lloyd, J. McIntyre, A.C. Miranda, P. Meir and H.S. Miranda 1996. The use of eddy covariance to infer the net carbon dioxide uptake of Brazilian rain forest. Global Change Biology. 2:209-217.

Granier, A. 1985. A new method of sap flow measurement in tree stems. Annales des Sciences Forestieres. 42:193-200.

Green, S.R., K.G. McNaughton and B.E. Clothier 1989. Observations of night-time water-use in kiwifruit vines and apple-trees. Agricultural and Forest Meteorology. 48:251-261.

Hinckley, T.M., F. Duhme, A.R. Hinckley and H. Richter 1983. Drought relations of shrub species - assessment of the mechanisms of drought resistance. Oecologia. 59:344-350.

Hogg, E.H. and P.A. Hurdle 1997. Sap flow in trembling aspen: implications for stomatal responses to vapour pressure deficit. Tree Physiology. 17:501-509.

Huber, B. 1932. Einige Grundfragen des Wärmehaushalts der Pflanzen. I. Die Ursache der hohen Sukkulenten-Temperaturen. Ber Dtsch Bot Ges. 50:68-76.

Hultine, K.R., R.L. Scott, W.L. Cable, D.C. Goodrich and D.G. Williams 2004. Hydraulic redistribution by a dominant, warm-desert phreatophyte: seasonal patterns and response to precipitation pulses. Functional Ecology. 18:530-538.

Kellomaki, S. and K.Y. Wang 2000. Short-term environmental controls on carbon dioxide flux in a boreal coniferous forest: model computation compared with measurements by eddy covariance. Ecological Modelling. 128:63-88.

Kiang, N. 2002a. Savannas and seasonal drought: The landscape-leaf connection through optimal stomatal control. *In* Environmental Science, Policy and Management. University of California, Berkeley, Berkeley, CA, p. 303.

Kiang, N. 2002b. Stomatal control under drought: a function of landscape optimization. *In* Department of Environmental Science, Policy and Management. University of California, Berkeley, Berkeley.

Köstner, B., E.M. Falge, M. Alsheimer, R. Geyer and J.D. Tenhunen 1998. Estimating tree canopy water use via xylem sapflow in an old Norway spruce forest and a comparison with simulation-based canopy transpiration estimates. Annales des Sciences Forestieres. 55:125-139.

Kurpius, M.R., J.A. Panek, N.T. Nikolov, M. McKay and A.H. Goldstein 2003. Partitioning of water flux in a Sierra Nevada ponderosa pine plantation. Agricultural and Forest Meteorology. 117:173-192.

Lee, X.H. 1998. On micrometeorological observations of surface-air exchange over tall vegetation. Agricultural and Forest Meteorology. 91:39-49.

Leuning, R. and K.M. King 1992. Comparison of eddy-covariance measurements of CO_2 fluxes by open-path and closed-path CO_2 analysers. Boundary-Layer Meteorology. 59:297-311.

Lindroth, A., A. Grelle and A.S. Moren 1998. Long-term measurements of boreal forest carbon balance reveal large temperature sensitivity. Global Change Biology. 4:443-450.

Marshall, D.C. 1958. Measurement of sap flow in conifers by heat transport. Plant Physiology. 33:385-396.

Matyssek, R., M.S. Gunthardtgoerg, S. Maurer and T. Keller 1995. Nighttime exposure to ozone reduces whole-plant production in Betula-pendula. Tree Physiology. 15:159-165.

McNaughton, K.G. and P.G. Jarvis 1991. Effects of spatial scale on stomatal control of transpiration. Agricultural and Forest Meteorology. 54:279-302.

Meinzer, F.C., G. Goldstein, P. Jackson, N.M. Holbrook, M.V. Gutierrez and J. Cavelier 1995. Environmental and physiological regulation of transpiration in tropical forest gap species: the influence of boundary-layer and hydraulic-properties. Oecologia. 101:514-522.

Misson, L., J. Tang, M. Xu, M. McKay and A.H. Goldstein 2005. Influences of recovery from clear-cut, climate variability, and thinning on the carbon balance of a young ponderosa pine plantation. Agricultural and Forest Meteorology. 130:207-222.

Moncrieff, J.B., Y. Malhi and R. Leuning 1996. The propagation of errors in long-term measurements of land-atmosphere fluxes of carbon and water. Global Change Biology. 2:231.

Monteith, J.L. 1957. Dew. Quarterly Journal of the Royal Meteorological Society. 83:322-341.

Monteith, J.L. 1965. Evaporation and the environment. Symposium of the Society of Exploratory Biology. 19:205-234.

Montero, J.I., A. Anton, P. Munoz and P. Lorenzo 2001. Transpiration from geranium grown under high temperatures and low humidities in greenhouses. Agricultural and Forest Meteorology. 107:323-332.

Norman, J.M., E.E. Miller and C.B. Tanner 1971. Light intensity and sunfleck-size distributions in plant canopies. Agronomy Journal. 63:743-748.

Oliveira, R.S., T.E. Dawson, S.S.O. Burgess and D.C. Nepstad 2005. Hydraulic redistribution in three Amazonian trees. Oecologia. 145:354-363.

Oren, R., J.S. Sperry, B.E. Ewers, D.E. Pataki, N. Phillips and J.P. Megonigal 2001. Sensitivity of mean canopy stomatal conductance to vapor pressure deficit in a flooded Taxodium distichum L. forest: hydraulic and non-hydraulic effects. Oecologia. 126:21-29.

Penman, H.L. 1948. Natural evaporation from open water, bare soil and grass. *In* Royal Society of London Ser. A, pp. 120-146.

Priestley, C.H.B. and R.J. Taylor 1972. On the assessment of surface heat flux and evaporation using large scale parameters. Monthly Weather Review. 100:81-92.

Rawson, H.M. and J.M. Clarke 1988. Nocturnal transpiration in wheat. Australian Journal of Plant Physiology. 15:397-406.

Reynolds, J.F., R.A. Virginia, P.R. Kemp, A.G. de Soyza and D.C. Tremmel 1999. Impact of drought on desert shrubs: Effects of seasonality and degree of resource island development. Ecological Monographs. 69:69-106.

Schmid, H.P. 1994. Source areas for scalars and scalar fluxes. Boundary Layer Meteorology. 67:293-318.

Scott, J.M., F. Davis, B. Csuti, R. Noss, B. Butterfield, C. Groves, H. Anderson, S. Caicco, F. Derchia, T.C. Edwards, J. Ulliman and R.G. Wright 1993. GAP analysis: a geographic approach to protection of biological diversity. Wildlife Monographs. 123:1-41.

Shuttleworth, W.J., J.H. Gash, C.R. Lloyd, C.J. Moore, J. Roberts, A.O.M. Filho, G. Fisch, V.P.S. Filho, M.N.G. Ribeiro, L.C.B. Molion, L.D.A. Sa, J.C.A. Nobre, O.M.R. Cabral, S.R. Patel and J.C. De Moraes 1984. Eddy correlation measurements of energy partition for Amazonian forest. Quarterly Journal of the Royal Meteorological Society. 110:1143-1162.

Shuttleworth, W.J. and J.S. Wallace 1985. Evaporation from sparse crops-an energy combination theory. Quarterly Journal of the Royal Meteorological Society. 111:839-855.

Smith, D.M. and S.J. Allen 1996. Measurement of sap flow in plant stems. Journal of Experimental Botany. 47:1833-1844.

Snyder, K.A., J.H. Richards and L.A. Donovan 2003. Night-time conductance in C-3 and C-4 species: do plants lose water at night? Journal of Experimental Botany. 54:861-865.

Soegaard, H., C. Nordstroem, T. Friborg, B.U. Hansen, T.R. Christensen and C. Bay 2000. Trace gas exchange in a high-arctic valley 3. Integrating and scaling CO2 fluxes from canopy to landscape using flux data, footprint modeling, and remote sensing. Global Biogeochemical Cycles. 14:725-744.

Song, Y., M.B. Kirkham, J.M. Ham and G.J. Kluitenberg 1999. Dual probe heat pulse technique for measuring soil water content and sunflower water uptake. Soil & Tillage Research. 50:345-348.

Steppe, K. and R. Lemeur 2004. An experimental system for analysis of the dynamic sap-flow characteristics in young trees: results of a beech tree. Functional Plant Biology. 31:83-92.

Sun, J.L., R. Desjardins, L. Mahrt and I. MacPherson 1998. Transport of carbon dioxide, water vapor and ozone by turbulence and local circulations. Journal of Geophysical Research-Atmospheres. 103:25873-25885.

Swanson, R.H. 1994. Significant historical developments in thermal methods for measuring sap flow in trees. Agricultural and Forest Meteorology. 72:113-132.

Tang, J. and D.D. Baldocchi 2005. Spatial–temporal variation in soil respiration in an oak–grass savanna ecosystem in California and its partitioning into autotrophic and heterotrophic components. Biogeochemistry. 73:183-207.

Tang, J., Y. Qi, M. Xu, L. Misson and A.H. Goldstein 2005. Forest thinning and soil respiration in a ponderosa pine plantation in the Sierra Nevada. Tree Physiology. 25:57-66.

Tatarinov, F. and J. Cermak 1999. Daily and seasonal variation of stem radius in oak. Annals of Forest Science. 56:579-590.

Turnipseed, A.A., D.E. Anderson, P.D. Blanken, W.M. Baugh and R.K. Monson 2003. Airflows and turbulent flux measurements in mountainous terrain Part 1. Canopy and local effects. Agricultural and Forest Meteorology. 119:1-21.

van Hove, L.W.A., M.E. Bossen, M.G.J. Mensink and O. van Kooten 1992. Physiological effects of a long term exposure to low concentrations of NH_3, NO_2 and SO_2 on Douglas fir (*Pseudotsuga menziesii*). Physiologia Plantarum. 86:559-567.

Williams, D.G., W. Cable, K. Hultine, J.C.B. Hoedjes, E.A. Yepez, V. Simonneaux, S. Er-Raki, G. Boulet, H.A.R. de Bruin, A. Chehbouni, O.K. Hartogensis and F. Timouk 2004. Evapotranspiration components determined by stable isotope, sap flow and eddy covariance techniques. Agricultural and Forest Meteorology. 125:241-258.

Wilson, K., A. Goldstein, E. Falge, M. Aubinet, D. Baldocchi, P. Berbigier, C. Bernhofer, R. Ceulemans, H. Dolman, C. Field, A. Grelle, A. Ibrom, B.E. Law, A. Kowalski, T. Meyers, J. Moncrieff, R. Monson, W. Oechel, J. Tenhunen, R. Valentini and S. Verma 2002. Energy balance closure at FLUXNET sites. Agricultural and Forest Meteorology. 113:223-243.

Winner, W.E., A.S. Lefohn, I.S. Cotter, C.S. Greitner, J. Nellessen, L.R. McEvoy, R.L. Olson, C.J. Atkinson and L.D. Moore 1989. Plant responses to elevational gradients of O3 exposures in Virginia. Proceedings of the National Academy of Sciences, USA. 86:8828-8832.

Wofsy, S.C., M.L. Goulden, J.W. Munger, S.M. Fan, P.S. Bakwin, B.C. Daube, S.L. Bassow and F.A. Bazzaz 1993. Net exchange of CO_2 in a mid-latitude forest. Science. 260:1314-1317.

Xu, M., T.A. Debiase, Y. Qi, A. Goldstein and Z. Liu 2001. Ecosystem respiration in a young ponderosa pine plantation in the Sierra Nevada Mountains, California. Tree Physiology. 21:309-318.

Yi, C., K.J. Davis, P.S. Bakwin, B.W. Berger and L.C. Marr 2000. Influence of advection on measurements of the net ecosystem-atmosphere exchange of CO2 from a very tall tower. Journal of Geophysical Research. 105:9991-9999.

Chapter 2

Evapotranspiration models compared on a Sierra Nevada forest ecosystem

Abstract Evapotranspiration, a major component in terrestrial water balance and net primary productivity models, is difficult to measure and predict. This study compared five models of potential evapotranspiration (PET) applied to a ponderosa pine forest ecosystem at an AmeriFlux site in Northern California. The AmeriFlux sites are research forests across the United States, Canada, Brazil, and Costa Rica with instruments on towers that measure carbon, water, and energy fluxes into and out of the ecosystems. The evapotranspiration models ranged from simple temperature and solar radiation-driven equations to physically-based combination approaches and included reference surface and surface cover-dependent algorithms. For each evapotranspiration model, results were compared against mean daily latent heat from half-hourly measurements recorded on a tower above the forest canopy. All models calculate potential evapotranspiration (assuming well-watered soils at field capacity), rather than actual evapotranspiration (based on soil moisture limitations), and thus overpredicted values from the dry summer seasons of 1997 and 1998. A soil moisture function was integrated to estimate actual evapotranspiration, resulting in improved accuracy in model simulations. A modified Priestley-Taylor model performed well given its relative simplicity.

Introduction

Over the entire land surface of the globe, rainfall averages around 750 $mm \cdot year^{-1}$, of which some two-thirds is returned to the atmosphere as evapotranspiration, making evapotranspiration the largest single component of the terrestrial hydrological cycle (Baumgartner and Reichel 1975). Carbon dioxide (CO_2)-induced greenhouse warming has accelerated the necessity to understand the hydrologic cycle and climate change (Houghton et al. 1990; GCIP-GEWEX 1993; IGP-BAHC 1993; Watson 1995; Kaczmarek et al. 1996). Evapotranspiration and CO_2 uptake by vegetation are intrinsically coupled, leading to links and feedbacks between land surface and climate that have only begun to be explored (Hutjes et al. 1998; Savabi and Stockle 2001). Forests can strongly influence the global hydrologic and carbon cycles and thus climate (Musselman and Fox 1991). A limited number of canopy-scale eddy covariance studies have shown that drought stress plays a significant role in net ecosystem exchange (e.g., Baldocchi 1997). The development of models describing climate-landscape relationships, such as water and carbon fluxes at ecosystem levels, is a necessary step in understanding and predicting the effects of changes in climate on landscape and on water resources (Kite 1998).

Evapotranspiration model estimates and field measurements vary widely. Differences in the treatment of evapotranspiration are prominent among both climate and terrestrial ecosystem models (Shuttleworth 1991; VEMAP 1995). Evapotranspiration has always been difficult to measure, especially on an ecosystem or watershed spatial scale. Methods have been developed to measure evapotranspiration at the leaf level, the tree level, and the stand level. At the stand level, instruments mounted on a tower above the

canopy are routinely used to measure humidity and wind velocities at high frequency, with water fluxes out of the forest canopy calculated by the eddy covariance method. Since the majority of moisture supplied by precipitation returns to the atmosphere as evapotranspiration, and because evapotranspiration is one of the most difficult processes to evaluate in hydrologic analysis, estimates are generally considered to be a significant source of error in streamflow simulation (Burnash 1995). Nonetheless, effective characterization of the evapotranspiration process is critical for completing the water balance in terrestrial ecosystems, and accurately predicting the effects of global climate and land use change. A process-based understanding of evapotranspiration is needed to quantify likely changes in evapotranspiration due to climate and land surface change (Choudhury and DiGirolamo 1998; Hutjes et al. 1998). Therefore, we find it necessary to evaluate various evapotranspiration methods employed in these modeling efforts.

The current modeling approach for estimating evapotranspiration is to calculate potential evapotranspiration (PET) using methods driven by meteorological data and/or vegetation characteristics, and to scale this estimate down to actual evapotranspiration (AET) based on limitations in available water (i.e., soil moisture) (Stannard 1993; Federer et al. 1996; Vörösmarty et al. 1998). PET has been used to describe the evapotranspiration that would occur given an adequate water supply at all times (Linsley et al. 1958). However, the term PET is somewhat ambiguous, because the upper limit to evapotranspiration is dependent on vegetation type as well as soil water and climatic conditions (Burman and Pochop 1994). The historical development of the PET concept has led to a variety of both PET definitions and methods (Shuttleworth 1991; Federer et al. 1996). Following the nomenclature of Shuttleworth (1991), we examined two types of

PET modeling approaches: reference-surface PET methods and surface-dependent PET methods. Reference-surface evapotranspiration is defined as evapotranspiration that would occur from a land surface specified as a "reference crop" (usually a short, uniform, green plant cover such as alfalfa or grass) under designated weather conditions and soil at field capacity (also termed well-watered soil) (Shuttleworth 1991; Federer et al. 1996). Reference-surface methods generally focus on an empirical relationship between temperature and PET, but neglect vegetation. Surface-dependent evapotranspiration is defined as evapotranspiration that would occur from a specified land surface, and the methods generally include a combination of vegetation and soil characteristics.

Several models for estimating evapotranspiration have been introduced in the literature, and our study includes many of them. Vörösmarty et al., (1998) compared 9 models on all the watersheds of the continental US. Other studies compared PET models at the fetch scale for sparsely vegetated rangeland (Stannard 1993), wildland vegetation in semiarid rangeland (Di 1993), partial canopy/residue-covered fields (Farahani and Ahuja 1996), maize with bare soil (Farahani and Bausch 1995), and barley (Tourula and Heikinheimo 1998). Federer et al. (1996) compared PET models at seven locations, but did not compare the PET estimates with measurements, because the purpose was to inform global modeling efforts on the relative variation between methods. McNaughton and Black (1973) performed energy balance measurements of evapotranspiration in a Douglas fir forest with soil at field capacity, resulting in a PET model used in our study. Few studies have analyzed evapotranspiration dynamics in forest ecosystems not only because of the general focus on agriculture, but also because of the difficulty of obtaining evapotranspiration measurements in forests.

The primary objective of our study is to compare a subset of the PET models used by Vörösmarty et al. (1998), but at a smaller spatial scale with known evapotranspiration in a forest plantation calculated from micrometeorological measurements and eddy covariance methods at our study site. The models include surface-dependent methods developed by Shuttleworth and Wallace (1985), Monteith (1965), Priestley and Taylor (1972), and McNaughton and Black (1973), and a reference-surface method by Penman (1948); the models were chosen because they are commonly used in water balance models (e.g., Willmott et al. 1985a; Arnell and Reynard 1996), terrestrial ecosystem (net primary production) models (e.g., Melillo et al. 1993; Parton et al. 1993; Running and Hunt 1993), hydroinformatics (Naoum and Tsanis 2003), and in remote sensing (Li and Lyons 2002). While scale and water-limitations at our site are important to this study, the critical factor driving our study is the use of ecosystem scale flux data. The flux measurements at the Blodgett Forest site, as part of AmeriFlux and the larger FLUXNET network of towers across the world, measure water, carbon, and energy fluxes as well as meteorological variables above the forest ecosystem canopy (e.g., Goldstein et al. 2000). Although the first modeling and analysis of forest evapotranspiration was done in the 1970s (e.g., Spittlehouse and Black 1979), the flux data from the tower are novel and only recently have researchers used such data to drive larger-scale ecosystem models.

We assess the PET models at this stand-scale using data from a tower at the Blodgett Forest Research Station in California. We analyzed data acquired continuously over two climatically different growing seasons: 1997 was drier than the climatic mean, and 1998 was cooler and wetter than the climatic mean (influenced by El Niño). Evapotranspiration rates (measured evapotranspiration) were derived from eddy

covariance measurements, and environmental variables were measured that are known to influence evapotranspiration rates, such as net radiation, wind speed, air temperature, relative humidity, and soil moisture.

Methods and materials

Site description

Data were gathered during the summers of 1997 and 1998 in the Sierra Nevada mountains at Blodgett Forest Research Station (38°53´42.9´´N, 120°37´57.9´´W, 1315 m), a research forest of the University of California, Berkeley (Goldstein et al. 2000). The forest was planted in 1990 and was dominated by ponderosa pine trees (*Pinus ponderosa* Doug. E. Laws), the most common conifer species in North America. The canopy also included individuals of Douglas fir (*Pseudotsuga menziesii*), white fir (*Abies concolor*), giant sequoia (*Sequoiadendron giganteum*), incense-cedar (*Calocedrus decurrens*) and California black oak (*Quercus kelloggii*). The major understory shrubs were manzanita (*Arctostaphylos* spp.) and *Ceonothus* spp. (Xu, 2001a). In 1997, about 25% of the ground area was covered by shrubs, 30% by conifer trees, 2% by deciduous trees, 7% by forbs, 3% by grass and 3% by stumps. The site is characterized by a Mediterranean climate with an average annual precipitation of 163 cm (180 cm in 1997 and 117 cm in 1998), the majority of which falls between September and May, and almost no rain in the summer. The soil is a fine-loamy, mixed, mesic, ultic haploxeralf in the Cohasset series whose parent material was andesitic lahar (Goldstein et al. 2000).

Measurements

Infrastructure for the canopy scale flux measurements consisted of a 10 m measurement tower (Upright Inc.). From 1 June to 10 September 1997 and from 1 May to 30 October 1998, fluxes of CO_2, H_2O, and sensible heat were measured by the eddy covariance method. Environmental parameters such as wind speed and direction, air temperature and humidity, net and photosynthetically active radiation, soil temperature, soil moisture, soil heat flux, rain, and atmospheric pressure were also monitored. A system to measure the vertical profiles of CO_2 and H_2O was added in 1998. The data acquisition system was separated in two parts: (1) a fast response system which monitored data at high frequency (up to 10 Hz) used to calculate eddy covariance, with raw data stored in 30 min data sets; and (2) a slow response system which monitored environmental parameters and stored 30 min averaged data (Goldstein et al. 2000).

Wind velocity and temperature were measured at 10 Hz with a three-dimensional sonic anemometer (ATI Electronics Inc., Boulder, CO) mounted 5 m above the canopy to obtain an accurate reading of air above the canopy. The height will vary in other ecosystems depending on the vegetation characteristics, but the purpose is to measure representative wind characteristics. CO_2 and H_2O mixing ratios were measured with an infrared gas analyzer (IRGA, LICOR model 6262, Lincoln, NE). Fluxes of CO_2, H_2O, and sensible heat between the forest and the atmosphere were determined by the eddy covariance method (Goldstein et al. 2000). This method quantifies vertical fluxes of scalars between the forest and the atmosphere from the covariance between vertical wind velocity and scalar fluctuations averaged over 30 min periods (e.g., Shuttleworth et al. 1984; Baldocchi et al. 1988; Wofsy et al. 1993; Moncrieff et al. 1996). Environmental

parameters were recorded on a CR10X datalogger (Campbell Scientific Inc., Logan, UT). Soil moisture probes were buried horizontally at 10 and 20 cm depth to record an upper soil moisture profile for the relatively flat and homogenous site. Brandes (1998) has also shown, through principal components analysis, that lateral spatial variability contributes only a small portion (<10 percent) of the total variance of a soil moisture data set, so our point measurements can be extrapolated laterally to the rest of the site. We used the soil moisture measurements at 20 cm because the plantation trees were young and the deepest roots had not extended past roughly a meter, though we acknowledge that moisture content can change throughout the soil profile. The 20 cm measurements represent our best available data at estimating moisture in the rooting zone, and the upper soil layers do not change drastically in composition, though the bedrock depth has not yet been measured. The soil moisture measurements at 10 cm were sensitive to variability in surface conditions. Total (all-sided) LAI was estimated using two techniques that resulted in similar estimates, (1) the LI-2000 (Li-Cor Inc., Lincoln, NE), which calculates LAI from diffuse sunlight measurements made with a "fish eye" (148° conical field-of-view) optical sensor as fully described in Welles and Norman (1991), and (2) an allometric method that scaled up from leaf-level determination using the measured geometry of trees (Xu et al. 2001).

We recognize systematic errors associated with the eddy covariance method. Travel through the sampling tube and instrument response time from sensor separation between wind and scalar measurements cause damping of high frequency fluctuations by the closed-path IRGA and time lags between wind and scalar data (Rissman and Tetzlaff 1994). Further, the sonic anemometer is unreliable in resolving fine-scale eddies in light

winds (Goulden et al. 1996; Moncrieff et al. 1996). Generally, these types of errors result in the underestimation of flux (Leuning and King 1992). The inability of the sonic anemometer to resolve the vertical wind occurs mainly at night as the fluctuations become dominated by small, high frequency eddies (Goulden et al. (1996) use $u^* < 0.17$ m s^{-1} as the threshold for reliable measurements). The inability of the sonic anemometer to resolve fine-scale eddies in light winds (e.g., during night) produced systematic errors in the sensible heat flux to correct the CO_2 and H_2O fluxes. Thus, although daytime turbulence was strong enough to produce reliable measurements, the calmer conditions during night rendered the nighttime flux measurements less reliable (Goldstein et al. 2000). For the purpose of this study, we corrected for outliers (greater than three standard deviations from the mean) and missing data points (via interpolation or backup sensors), and evaluated the evapotranspiration models using daytime (5am – 9pm) averages because nighttime measurements were unreliable. Sample size in 1997 was 87 daytime averages based on 3900 measurements, and sample size in 1998 was 149 daytime averages based on 8700 measurements.

Evapotranspiration models

Five PET models of increasing complexity were tested under two classes of land surface speciation (Shuttleworth 1991; Federer et al. 1996). Reference-surface evapotranspiration is defined as evaporation that would result from a specific land surface, referred to as a "reference crop" (Vörösmarty et al. 1998). Surface-dependent evapotranspiration is defined as the evaporation that would occur from any of a variety of

Parameter	Symbol	Units	PT	MB	Penman	PM	SW
Rate of change of vapor pressure w/ temp.	Δ	$kPa \cdot K^{-1}$	√		√	√	√
Total available energy	A	$W \cdot m^{-2}$	√		√	√	√
Psychrometric constant	γ	$kPa \cdot K^{-1}$	√	√	√	√	√
Air temperature	T_a	ºC	√	√	√	√	√
Specific heat at constant pressure	c_p	$J \cdot kg^{-1} \cdot K^{-1}$		√		√	√
Air density	ρ	$kg \cdot m^{-3}$		√	√	√	√
Vapor pressure deficit	D	kPa		√	√	√	√
Bulk stomatal resistance of the canopy	r_{cs}	$s \cdot m^{-1}$		√		√	√
Wind speed	u	$m \cdot s^{-1}$			√	√	√
Aerodynamic resistance above the canopy	r_{aa}	$s \cdot m^{-1}$				√	√
Bulk boundary layer resistance of the veg	r_{ca}	$s \cdot m^{-1}$					√
Aerodynamic res. for substrate & canopy	r_{sa}	$s \cdot m^{-1}$					√
Surface resistance of the substrate	r_{ss}	$s \cdot m^{-1}$					√
Available soil energy	A_s	$W \cdot m^{-2}$					√

Table 1. Comparison of the increasing complexity of the models in terms of number of parameters required. PT is Priestley-Taylor, MB is McNaughton-Black, PM is Penman-Monteith, and SW is Shuttleworth-Wallace.

designated land surfaces. A summary of the parameters and units used in each method is presented in Table 1.

The Priestley-Taylor model (Priestley and Taylor 1972), the simplest of the five, is defined as:

$$\lambda E = \alpha \Delta A / (\Delta + \gamma)$$

where λE is total potential evapotranspiration (in flux units of W/m^2, for example), Δ is the derivative of saturated vapor pressure versus temperature, A is total available energy (net radiation minus soil heat flux), and γ is the psychrometric constant. Δ and γ are functions of air temperature (all models analyzed here are thus functions of air temperature). Priestley and Taylor (1972) determined an average value of 1.26 for α based on measurements of evapotranspiration from a variety of well-watered vegetated and water surfaces (i.e., PET). To estimate AET, α has been redefined to be a function of soil moisture (Flint and Childs 1991).

The McNaughton-Black model (McNaughton and Black 1973) is defined as follows:

$$\lambda E = c_p \rho D / \gamma r_{cs}$$

where c_p is specific heat at constant pressure, ρ is air density, D is vapor pressure deficit, and r_{cs} is bulk stomatal resistance of the canopy.

The Penman model (Penman 1948) was the first effort to combine both energy and atmospheric vapor transport components to estimate PET and is defined as follows:

$$\lambda E = (\Delta A + 73.64 \rho \gamma (1 + 0.54u) D) / (\Delta + \gamma)$$

where u is wind speed, and 73.64 is 2.6 times the latent heat of vaporization (units converted).

The Penman-Monteith model (Monteith 1965) expanded upon the Penman model:

$$\lambda E = (\Delta A + c_p \rho D / r_{aa}) / (\Delta + \gamma + \gamma (r_{cs} / r_{aa}))$$

where r_{aa} is the aerodynamic resistance above the canopy, and r_{cs} is stomatal resistance of the canopy.

For the Shuttleworth-Wallace model (Shuttleworth and Wallace 1985), λE is separated into evaporation from the soil (λE_s) and transpiration from the canopy (λE_c), which are derived from the Penman-Monteith combination equations:

$$\lambda E_s = (\Delta A_s + \rho c_p D_0 / r_{sa}) / (\Delta + \gamma (1 + r_{ss} / r_{sa}))$$

$$\lambda E_c = (\Delta (A - A_s) + \rho c_p D_0 / r_{ca}) / (\Delta + \gamma (1 + r_{cs} / r_{ca}))$$

where A_s is available soil energy, and D_0 is vapor pressure deficit in the canopy; r_{sa} is the aerodynamic resistance between the substrate and canopy source height, r_{ca} is the boundary layer resistance of the vegetation, and r_{ss} is soil resistance. The aerodynamic resistance above the canopy (r_{aa}) and the aerodynamic resistance between the substrate

and canopy source height (r_{sa}) are functions of leaf area index, eddy diffusivity decay constant, roughness length of the vegetation (function of vegetation height), zero plane displacement (function of vegetation height), a reference height above the canopy where meteorological measurements are available, wind speed, von Karman's constant, and roughness length of the substrate. D_0 is derived from the Ohm's law electrical analog for the vapor pressure and temperature difference between the canopy and the reference height above the canopy where fluxes out of the vegetation are measured. D_0 is a function of the measurable vapor pressure deficit at the reference height, D:

$$D_0 = D + (\Delta A - r_{aa}\lambda E_c(\Delta + \gamma)) / \rho c_p$$

and D can thus be substituted for D_0 into the combination equations. The total evaporation from the crop, λE, for the Shuttleworth-Wallace model is the sum of the Penman-Monteith combination equations with D substituted in for D_0:

$$\lambda E = C_c PM_c + C_s PM_s$$

where PM_c describes evaporation from the closed canopy, and PM_s describes evaporation from the bare substrate. The new Penman-Monteith equations have the form:

$$PM_c = \frac{(\Delta A + (\rho c_p D - \Delta r_{ca} A_s)/(r_{aa} + r_{ca}))}{(\Delta + \gamma(1 + r_{cs}/(r_{aa} + r_{ca}))}$$

$$PM_s = \frac{(\Delta A + (\rho c_p D - \Delta r_{sa}(A - A_s)/(r_{aa} + r_{sa}))}{(\Delta + \gamma(1 + r_{ss}/(r_{aa} + r_{sa}))}$$

The coefficients C_c and C_s are resistance combination equations:

$$C_c = 1 / (1 + R_c R_a/(R_s(R_c + R_a)))$$

$$C_s = 1 / (1 + R_s R_a/(R_c(R_s + R_a)))$$

where

$$R_a = (\Delta + \gamma) r_{aa}$$

$$R_s = (\Delta + \gamma) r_{sa} + \gamma r_{ss}$$

$$R_c = (\Delta + \gamma) r_{ca} + \gamma r_{cs}$$

The evapotranspiration models described above calculate potential evapotranspiration rather than actual evapotranspiration. Potential evapotranspiration is defined as the evapotranspiration flux from the ecosystem under well-watered soil conditions (i.e., soil at or close to, field capacity). We derived actual evapotranspiration from potential evapotranspiration using a simple soil moisture function, $f(\phi)$ (Saxton et al. 1986):

$$\lambda E_{actual} = f(\phi) * \lambda E$$

where λE_{actual} is the actual evapotranspiration and the soil moisture function is a dimensionless variable estimated by a simple linear model:

$$f(\phi) = M / \text{Field capacity}$$

where M is soil volumetric moisture at 20 cm depth (at rooting zone). Field capacity (for which soil water potential is at -10 kPa) for the fine-loamy soil texture at our site was determined as 39% based on Saxton et al. (1986) and compared well to maximum soil moisture observed after rain events. Field capacity can be defined as the percentage of water remaining in a soil two or three days after its having been saturated and after free drainage has practically ceased. Brandes and Wilcox (2000) have shown that simple linear models of the evapotranspiration/soil moisture process are appropriate for hydrologic modeling. Soil moisture models have been developed with increasing complexity to better represent soil physics, such as the module in WATFLOOD that includes permanent wilting point, saturation, and a root fraction to simulate non-linear

features of moisture extraction by vegetation from soil (Soulis et al. 2000); Munro et al. (1998) solve the Richards' equation and the temperature diffusion equation for multi-soil layers. However, we chose the simple, physically-based soil moisture function for three reasons: 1) the data requirements and modeling demands are greatly increased for more complex soil moisture functions; 2) these PET methods are often used in larger spatial scale models where detailed soil physics may not be possible to calculate accurately; and 3) our main goal is to assess the relative accuracy of the PET methods, rather than evaluate the merit of various approaches to modeling soil physics.

Results

Potential versus measured evapotranspiration

For all potential evapotranspiration models, simulated PET compared reasonably well with measured evapotranspiration at the beginning of the summer season (April-May). As the soil moisture decreased through the summer, however, all models tended to overpredict evapotranspiration because the PET models were designed for well-watered soil conditions rather than natural summertime Mediterranean drought conditions (Figure 1). 1997 was drier than 1998, and greater evapotranspiration was observed in 1998. The summer of 1997 was also substantially windier than 1998—this fact influenced the wind-sensitive Penman method, which predicted unrealistically high amounts of evapotranspiration due to the fast winds. In fact, the Penman model predicts an increase of well over 100 $W \cdot m^{-2}$ in evapotranspiration for every 0.5 $m \cdot s^{-1}$ increase in wind speed, holding all other variables constant. The specific increase depends on the values of the fixed variables; VPD in particular effects that increase.

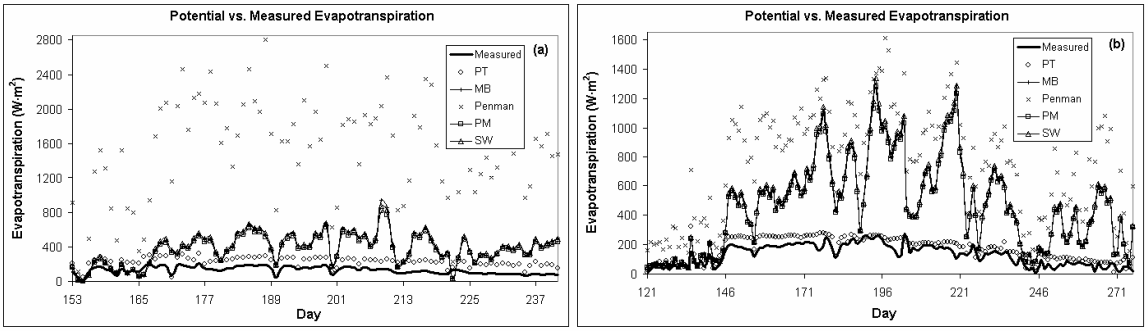

Figure 1. Potential evapotranspiration without soil moisture function for (a) 1997 and (b) 1998. Shuttleworth-Wallace (SW), Penman-Monteith (PM), and McNaughton-Black (MB) all have similar trends and magnitudes, and Priestley-Taylor (PT) comes closest to measured evapotranspiration (Measured ET) in both years with $\alpha = 1.26$. The Penman method was highly sensitive to wind speed in 1997.

PET results from the Shuttleworth-Wallace, Penman-Monteith, and McNaughton-Black models had similar trends and magnitudes; McNaughton-Black tended to give the highest estimates followed by Penman-Monteith and Shuttleworth-Wallace, respectively. Penman-Monteith approximated Shuttleworth-Wallace in the dry season of 1997. The Priestley-Taylor model nearly approximated the measured evapotranspiration in both years, especially in the higher soil moisture year of 1998 when water was not as limiting.

Actual versus measured evapotranspiration

Actual evapotranspiration was derived from potential evapotranspiration for each model by applying the soil moisture function. The actual evapotranspiration estimations provided good approximations of measured evapotranspiration. With the soil moisture function, Shuttleworth-Wallace ($r^2 = 0.46$ in 1997; $r^2 = 0.69$ in 1998), Penman-Monteith ($r^2 = 0.43$ and 0.66), and McNaughton-Black ($r^2 = 0.37$ and 0.62) all performed well with similar trends and magnitudes. Penman-Monteith and McNaughton-Black approximated Shuttleworth-Wallace through both seasons, though McNaughton-Black began to more

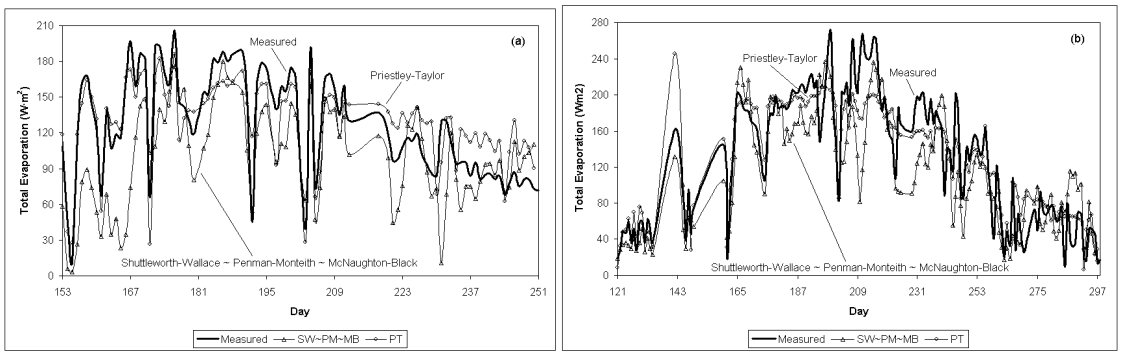

Figure 2. Simulated versus measured evapotranspiration during (a) 1997 and (b) 1998. The soil moisture function is integrated in Shuttleworth-Wallace (SW), Penman-Monteith (PM), and McNaughton-Black (MB). Penman-Monteith and McNaughton-Black excluded due to similarity to SW; while PM approximates SW through both seasons, MB begins to diverge with overprediction late in both seasons as soil moisture decreases. The Priestley-Taylor (PT) graph is shown with $\alpha = 0.73$ in 1997 and 0.94 in 1998. The soil moisture function brought the simulations down to good approximations of measured evapotranspiration. Penman method excluded due to continued overprediction.

severely overpredict AET than the other models did late in both seasons. Priestley-Taylor ($r^2 = 0.73$ and 0.58) significantly underpredicted the measured evapotranspiration with the soil moisture function. Although the Penman simulations were improved, the Penman model still significantly overpredicted measured evapotranspiration. Flint and Childs (1991) state that the assumptions and simplifications used by the Penman model to model the aerodynamic components of evapotranspiration make the Penman model useful only for calculating potential evapotranspiration. The primary modified version of the Penman model, the Penman-Monteith model, allows for calculation of actual evapotranspiration given values for resistances. The soil moisture function performed better across the relatively wet season of 1998 than the dry season of 1997; the models tended to underpredict measured evapotranspiration in 1997 (Figure 2 and 3). In addition, there was smaller scatter, but more sample points, in 1998.

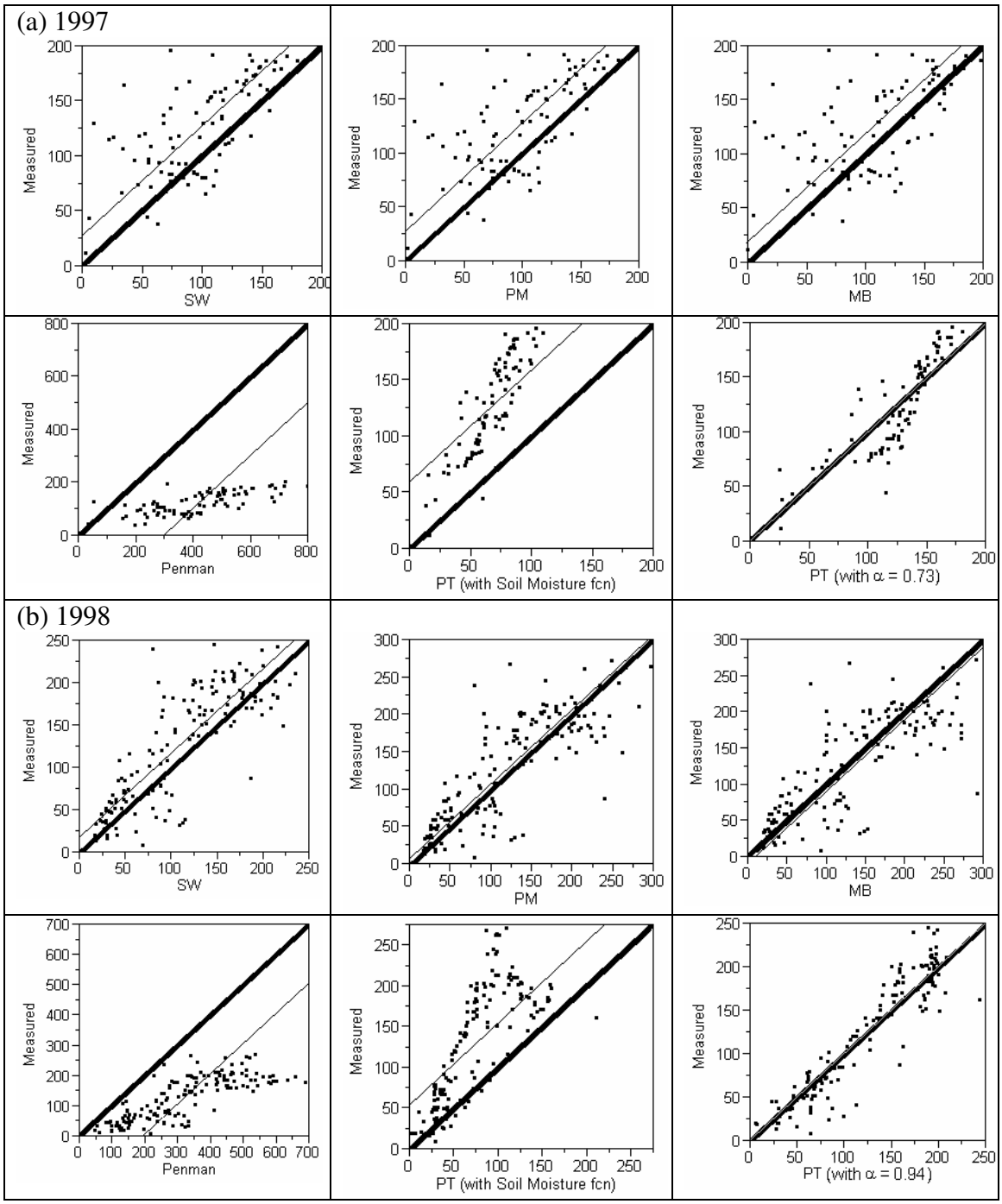

Figure 3. Simulated versus measured evapotranspiration during (a) 1997 and (b) 1998. The soil moisture function is integrated in Shuttleworth-Wallace (SW), Penman-Monteith (PM), McNaughton-Black (MB), Penman, and Priestley-Taylor (PT with Soil Moisture function). The second Priestley-Taylor (PT) graph includes the modified α. The thick diagonal line is the 1:1 line, and the thin diagonal line is the actual difference between the means. Sample size in 1997 was 87 daytime averages based on 3900 measurements, and in 1998 was 149 daytime averages based on 8700 measurements.

Modified α for Priestley-Taylor model

Whether or not use of a soil moisture function is appropriate for the Priestley-Taylor model has been answered, in part, by numerous studies on α. It has become increasingly common to redefine α based on soil moisture, rather than add on a soil moisture function to the original α value of 1.26. Priestley and Taylor originally proposed that α be reduced when soil water content falls below some critical soil moisture value where soil water supply limits evapotranspiration. Spittlehouse and Black (1981) state that the Priestley-Taylor model is in error and no longer appropriate to use if α is fixed. Based on the regression analysis prescribed by Flint and Childs (1991), our redefined α is:

$$\alpha = 0.84M + 0.72$$

where M is soil volumetric moisture of the top 20 cm (rooting zone). The average value for α across both years was 0.87, although that value was slightly lower for the drier 1997 and higher for the wetter 1998. It should be noted that although this equation follows the work of Flint and Childs (1991), the parameters for both this equation and for Flint and Child's redefined α are not physically based and should be looked at critically in comparisons with other models. However, our newly calculated values for α approximate the actual measured values for α at similar sites, as tabled by Flint and Childs (1991); we append our value in Table 2. Determination of α based on either the regressed soil moisture function or measurements done at similar sites resulted in a greatly improved Priestley-Taylor model (r^2 = 0.74 and 0.85). With the new α value, Priestley-Taylor AET estimates were not significantly different from measured

α	Surface conditions	Reference
1.57	Strongly advective conditions	(Jury and Tanner 1975)
1.29	Grass (soil at field capacity)	(Mukammal and Neumann 1977)
1.27	Irrigated ryegrass	(Davies and Allen 1973)
1.26	Saturated surface	(Priestley and Taylor 1972)
1.26	Open-water surface	(Priestley and Taylor 1972)
1.26	Wet meadow	(Stewart and Rouse 1977)
1.18	Wet Douglas-fir forest	(McNaughton and Black 1973)
1.12	Short grass	(De Bruin and Holtslag 1982)
1.05	Douglas-fir forest	(McNaughton and Black 1973)
1.04	Bare soil surface	(Barton 1979)
0.90	Mixed reforestation (water limited)	(Flint and Childs 1991)
0.87	Ponderosa pine (water limited, daytime)	*This study*
0.84	Douglas-fir forest (unthinned)	(Black 1979)
0.80	Douglas-fir forest (thinned)	(Black 1979)
0.73	Douglas-fir forest (daytime)	(Giles et al. 1984)
0.72	Spruce forest (daytime)	(Shuttleworth and Calder 1979)

Table 2. Measured values of the Priestley-Taylor coefficient, α, as tabled by (Flint and Childs 1991) and appended with their and our values.

evapotranspiration across both years. Again, the Priestley-Taylor model performed well despite its relative simplicity.

Discussion

The Shuttleworth-Wallace, Penman-Monteith, and McNaughton-Black models resulted in similar simulations due to the common theoretical basis of their equations—the Penman model. McNaughton-Black, which excludes the radiation budget and any effect from the soil, is a simplification of Penman-Monteith, whereas Shuttleworth-Wallace adds a soil layer to the Penman-Monteith model. The simulations revealed that Penman-Monteith tended to give an intermediate result between these three models. Shuttleworth-Wallace is specifically designed for sparse crops where vegetation is not densely distributed and the soil surface may contribute significantly to total evapotranspiration, which is representative of the Blodgett site. Nonetheless, the

substrate does not significantly contribute to total evapotranspiration because of low soil moisture, particularly in 1997. Thus, the Shuttleworth-Wallace model reduced back to the Penman-Monteith model and gave only slightly better results. In the relatively wet season of 1998, Shuttleworth-Wallace resulted in a more accurate simulation than in 1997 because the increased soil moisture lead to greater soil evaporation. Still, the soil evaporation was not a significant factor at this site and thus the McNaughton-Black model, which neglects the soil as an evaporation source, yielded similar results. Shuttleworth-Wallace has performed well in the literature as well (e.g., Di 1993; Farahani and Bausch 1995; Vörösmarty et al. 1998; Iritz et al. 1999), but the main drawback is the difficulty and extensiveness of the parameter estimation (Farahani and Ahuja 1996). Because our study area is intensively measured as a research site, the parameters for Shuttleworth-Wallace were available for this analysis; other sites or large scale modeling efforts may not be so fortunate.

The upper bound to potential evapotranspiration should be the net radiation (under relatively stable conditions). According to energy balance models, incoming net radiation is partitioned into latent heat, sensible heat, and heat absorbed by the ground—therefore, latent heat, as a fraction of net radiation, should not exceed net radiation. The McNaughton-Black model is not a function of net radation and depends heavily on the accuracy of its other input parameters. An erroneously low stomatal resistance of the canopy (r_{cs}), for instance, can cause the McNaughton-Black model and other PET models that are function of r_{cs} to overpredict evapotranspiration.

For Shuttleworth-Wallace, Penman-Monteith, and McNaughton-Black, we used a constant r_{cs} throughout both seasons derived from the available minimum and maximum

values measured at the site. The models are highly sensitive to r_{cs} and simulated evapotranspiration differed by as much as 26% at the minimum r_{cs} and 20% at the maximum r_{cs}. We evaluated and propagated error in r_{cs}, along with aerodynamic resistance above the canopy (r_{aa}), bulk boundary layer resistance of the vegetation (r_{ca}), aerodynamic resistance for the substrate and canopy (r_{sa}), and surface resistance of the substrate (r_{ss}) in the Shuttleworth-Wallace model via Gaussian error propagation (the final uncertainty for total evapotranspiration is equal to the square root sum of squares of the partial derivative of total uncertainty with respect to each resistance multiplied by the standard deviation of each resistance, respectively):

$$S_{\lambda E} \approx [((\partial \lambda E/\partial r_{ca})(Sr_{ca}))^2 + ((\partial \lambda E/Sr_{cs})(Sr_{cs}))^2 + ((\partial \lambda E/\partial r_{sa})(Sr_{sa}))^2 + ((\partial \lambda E/\partial r_{ss})(Sr_{ss}))^2 + ((\partial \lambda E/\partial r_{aa})(Sr_{aa}))^2]^{0.5}$$

The model is nonlinear, and, for the purposes of the uncertainty analysis, we treated the variables as uncorrelated with one another. Gaussian error propagation is suitable here since it allows for examination of total uncertainty derived from the uncertainties in the parameters of the model. We found that uncertainty in r_{cs} contributes to 53% of the total uncertainty in the Shuttleworth-Wallace model. Based on this finding, much of the overprediction among the PET models may be attributed to uncertainty in r_{cs}. Again, a relatively more complex evapotranspiration model may not be more accurate than a simpler model because the complex model is more difficult to parameterize and results are vulnerable to large error resulting from propagating uncertainty in parameter values.

The success of Priestley-Taylor, given its relative simplicity, shows that this simple model may be preferable to the complex models by Shuttleworth-Wallace,

Penman-Monteith, and McNaughton-Black for a partially-closed canopy under water-limitation. We add to the tabled values of the Priestley-Taylor coefficient, α, for different surface conditions. The data in Table 2 have the potential for playing a crucial role in the integration of the Priestley-Taylor method for estimating AET into larger scale ecosystem models. If most surface conditions have an associated α value under varying water stress conditions, or include α as a function of soil moisture, then it may be possible that ecosystem models could use those values with the method to accurately assess AET given relatively few input parameters.

The soil moisture function plays a key role in deriving actual evapotranspiration from potential evapotranspiration. PET assumes that soil water availability is not the limiting factor for AET (soil is at field capacity) and will thus overpredict evapotranspiration under drier soil conditions. In both years, the PET models performed well at the beginning of the summer season when soil moisture was still high from spring rainfall and residual moisture from snowmelt. But, as soil moisture declined throughout the summer, PET subsequently overpredicted measured evapotranspiration. It is crucial that our study included summertime drought conditions in a Mediterranean environment: it is under these, and similar, conditions that the assumptions of a given PET model can lead to inaccurate results. Analysis of PET models under environmental conditions that they were not initially designed for may be inappropriate. Many ecological models use PET functions on continental and global scales, and are subject to the same overprediction of actual evapotranspiration because of such assumptions (e.g., Running and Coughlan 1988; Raich et al. 1991; Potter et al. 1993; Sellers et al. 1996; Thornton et

al. 1997). Additionally, hydrologic model users at the local catchment scale must be able to handle soil moisture information, or the lack thereof (Wooldridge et al. 2003).

Thus, the relationship between potential and actual evapotranspiration must be addressed in these and future models. Furthermore, these large-scale models would benefit from a simple, but accurate, evapotranspiration component that would be relatively easy to parameterize. Within widely used general circulation models (GCMs) and numerical weather prediction models (NWPs), hydrological components such as evapotranspiration, precipitation and runoff have yet to be estimated with great accuracy. Models of the atmosphere, such as GCMs and NWPs, can be used to predict the impact of changes in the composition of the atmosphere using gas properties and the fundamental equations of energy transfer, mass conservation and atmospheric motion into changes in wind, temperature and moisture content. Despite the rigor of the atmospheric descriptions in such models, the atmosphere/land surface interaction is usually modeled quite crudely (Kite 1998). Most GCMs (e.g., Dickinson and Kennedy 1991; Raich et al. 1991; Sellers et al. 1996) use only a few hydrological parameters lumped over large grid squares, and contain no run-on/runoff transfer between grid squares. Such models generally overestimate precipitation and, as the vertical water balances in each grid square are independent of surrounding squares, they generally underestimate evapotranspiration, leading to an overestimate of water available for runoff (Kite 1998). Information on land surface evapotranspiration is very important in the understanding of climate change. For example, the reduction in evapotranspiration (and the change in surface energy balance) associated with the removal of vegetation in the Sahel has been shown, via GCMs, to produce a reduction in rainfall (e.g., Charney 1975;

Cunnington and Rowntree 1986). Therefore, there is a great need for process-based evapotranspiration models than can characterize different vegetation to allow us to better understand and predict any links between land-use change and climate change (Wallace 1995).

We suggest that the Priestley-Taylor method may be most applicable to models run at large spatial scales because it is easier to parameterize than the widely used Penman-Monteith method, although further research is needed to confirm this suggestion. Furthermore, the models that we analyze here are atmosphere driven evapotranspiration models, which are appropriate for global or regional models since soil moisture information may not be as reliably extrapolated from point measurements as are atmospheric data. The difficulty in extrapolation of point source soil moisture data versus atmospheric data is due to heterogeneity of the soil medium relative to atmospheric mixing and well-understood physical relationships that govern the change in meteorological parameters (e.g., temperature, pressure, relative humidity). Unreliable soil moisture information will introduce a propagation of error in a soil water driven atmosphere exchange model. Nonetheless, as new data sources become increasingly available, especially with remote sensing, these models can and should be modified to allow for integration of the new data. As remotely sensed soil information develops, so too should the models that this information feeds into (Njoku et al. 2003).

Factors not taken into account that may affect the relationship between simulated and actual evapotranspiration include vegetative quality and other environmental variables. For example, ozone deposition, grazing of insects on leaves, the influence of animals such as cows on the environment, and disease are not taken into account when

modeling evapotranspiration. Aside from systematic errors associated with the eddy covariance method, possible bias in the data and models include assumed values for three Shuttleworth-Wallace variables—surface resistance of the substrate, roughness length of bare substrate, and extinction coefficient of the crop for net radiation. We halved, doubled, and multiplied each parameter by a factor of 10 to test for sensitivity; nonetheless, Shuttleworth-Wallace is not highly sensitive to these parameters. Simulated evapotranspiration differed by less than 5% given the changes in these parameters. A major environmental phenomenon influencing the data was the occurrence of an El Niño event before the summer of 1998 that caused the vegetation to grow significantly in 1998; the heterogeneity across seasons allowed for ideal comparisons of the same site under different environmental conditions to see how robust the evapotranspiration models were.

Conclusions

Shuttleworth-Wallace, Penman-Monteith, McNaughton-Black, Priestley-Taylor, and Penman models for estimating evapotranspiration were compared using data from AmeriFlux tower measurements at a ponderosa pine ecosystem. Vörösmarty et al. (1998), in comparing these models on a global scale, found that the Shuttleworth-Wallace method performed best. In our study, Shuttleworth-Wallace, Penman-Monteith, and McNaughton-Black all yielded similar results, although Shuttleworth-Wallace performed slightly better than Penman-Monteith and McNaughton-Black; this similarity was because these models are derived from the Penman model, and because of the insignificant effect of the substrate on evapotranspiration at our site. Priestley-Taylor,

with an appropriately defined □ value, performed remarkably well, especially given its relative simplicity. The Penman model was very sensitive to wind speed in our study. When applying PET models, one must be aware of soil moisture conditions so that potential and actual evapotranspiration are differentiated. Integration of data from all the FLUXNET sites across the globe will be critical in determining the best possible evapotranspiration model to use at global scales for predicting changes in land-surface exchange due to climate change.

Acknowledgements

We wish to thank Matt Orr, Dennis Fisher, and Carmel Levitan for assistance and support in this analysis. This work contributes information to the AmeriFlux and FLUXNET project. The University of California at Berkeley and the University Agriculture Experiment Station funded this study. Joshua Fisher was supported by NASA Headquarters under the Earth System Science Fellowship Grant NGT5-30473. Terry DeBiase was supported by the W.S. Rosecrans and William Siggins Fellowhips.

References

Arnell, N.W. and N.S. Reynard 1996. The effects of climate change due to global warming on river flows in Great Britain. Journal of Hydrology. 183:397-424.

Baldocchi, D. 1997. Measuring and modelling carbon dioxide and water vapour exchange over a temperate broad-leaved forest during the 1995 summer drought. Plant, Cell and Environment. 20:1108-1122.

Baldocchi, D., B. Hicks and T. Meyers 1988. Measuring biosphere-atmosphere exchanges of biologically related gases with micrometeorological methods. Ecology. 69:1331.

Barton, I.J. 1979. A parameterization of the evaporation from nonsaturated surfaces. Journal of Applied Meteorology. 18:43-47.

Baumgartner, A. and E. Reichel 1975. World Water Balance: Mean Annual Global, Continental and Maritime Precipitation, Evaporation and Run-off. Elsevier, Amsterdam.

Black, T.A. 1979. Evapotranspiration from Douglas-fir stands exposed to soil water deficits. Water Resources Research. 15:164-170.

Brandes, D. 1998. A low-dimensional dynamical model of hillslope soil moisture, with application to a semiarid field site. The Pennsylvania State University, Pennsylvania, p. 200.

Brandes, D. and B.P. Wilcox 2000. Evapotranspiration and soil moisture dynamics on a semiarid ponderosa pine hillslope. Journal of the American Water Resources Association. 36:965-974.

Burman, R. and L.O. Pochop 1994. Evaporation, Evapotranspiration and Climatic Data. Elsevier Science B. V., Amsterdam. 600 p.

Burnash, R.J.C. 1995. The NWS River Forecast System - Catchment Modeling. In Computer Models of Watershed Hydrology Ed. V.P. Singh. Water Resources Publications, Highlands Ranch, Colorado, pp. 311- 366.

Charney, J.G. 1975. Dynamics of deserts and drought in the Sahel. Quarterly Journal of the Royal Meteorological Society. 101:193-202.

Choudhury, B.J. and N.E. DiGirolamo 1998. A biophysical process-based estimate of global land surface evaporation using satellite and ancillary data I. Model description and comparison with observations. Journal of Hydrology. 205:164-185.

Cunnington, W.M. and P.R. Rowntree 1986. Simulations of the Saharan atmosphere-dependence on moisture and albedo. Quarterly Journal of the Royal Meteorological Society. 114:373-398.

Davies, J.A. and C.D. Allen 1973. Equilibrium, potential and actual evaporation from cropped surfaces in southern Ontario. Journal of Applied Meteorology. 12:649-657.

De Bruin, H.A.R. and A.A.M. Holtslag 1982. A simple parameterization of the surface fluxes of sensible and latent heat during daytime compared with the Penman-Monteith concept. Journal of Applied Meteorology. 21:1610-1621.

Di, S. 1993. Comparison of Penman-Monteith, Shuttleworth-Wallace, and modified Priestley-Taylor evapotranspiration models for wildland vegetation in semiarid rangeland. Water Resources Research. 29:1379-1392.

Dickinson, R.E. and P.J. Kennedy 1991. Land surface hydrology in a general-circulation model n-global and regional fields needed for validation. Surveys in Geophysics. 12:115-126.

Farahani, H.J. and L.R. Ahuja 1996. Evapotranspiration modeling of partial canopy/residue-covered fields. Transactions of the ASAE. 39:2051-2064.

Farahani, H.J. and W.C. Bausch 1995. Performance of evapotranspiration models for maize - bare soil to closed canopy. Transactions of the ASAE. 38

Federer, C.A., C.J. Vörösmarty and B. Fekete 1996. Intercomparison of methods for calculating potential evaporation in regional and global water balance models. Water Resources Research. 32:2315-2321.

Flint, A.L. and S.W. Childs 1991. Use of the Priestley-Taylor evaporation equation for soil water limited conditions in a small forest clearcut. Agricultural and Forest Meteorology. 56:247-260.

GCIP-GEWEX 1993. Implementation for the GEWEX Continental-Scale International Project (GCIP). In Data Collection and Operational Model Upgrade. IGPO Publ., Washington, DC, USA.

Giles, D.G., T.A. Black and D.L. Spittlehouse 1984. Determination of growing season soil water deficits on a forested slope using water balance analysis. Canadian Journal of Forest Research. 15:107-114.

Goldstein, A.H., N.E. Hultman, J.M. Fracheboud, M.R. Bauer, J.A. Panek, M. Xu, Y. Qi, A.B. Guenther and W. Baugh 2000. Effects of climate variability on the carbon dioxide, water, and sensible heat fluxes above a ponderosa pine plantation in the Sierra Nevada (CA). Agricultural and Forest Meteorology. 101:113-129.

Goulden, M.L., J.W. Munger, S.M. Fan, B.C. Daube and S.C. Wofsy 1996. Measurements of carbon sequestration by long-term eddy covariance: methods and a critical evaluation of accuracy. Global Change Biology. 2:169-182.

Houghton, J.T., G.J. Jenkins and J.J. Ephraums 1990. Climate Change: The IPCC Scientific Assessment. WMO, UNEP, Cambridge University Press, Cambridge, UK.

Hutjes, R.W.A., P. Kabat, S.W. Running, W.J. Shuttleworth, C. Field, B. Bass, M.A.F. da Silva Dias, R. Avissar, A. Becker, M. Claussen, A.J. Dolman, R.A. Feddes, M. Fosberg, Y. Fukushima, J.H.C. Gash, L. Guenni, H. Hoff, P.G. Jarvis, I. Kayane, A.N. Krenke, C. Liu, M. Meybeck, C.A. Nobre, L. Oyebande, A. Pitman, R.A.S. Pielke, M. Raupach, B. Saugier, E.D. Schulze, P.J. Sellers, J.D. Tenhunen, R. Valentini, R.L. Victoria and C.J. Vörösmarty 1998. Biospheric aspects of the hydrological cycle. Journal of Hydrology. 212-213:1-21.

IGP-BAHC 1993. Biospheric Aspects of the Hydrological Cycle (BAHC): The Operational Plan. International Geosphere-Biosphere Programme, Stockholm, Sweden.

Iritz, Z., A. Lindroth, M. Heikinheimo, A. Grelle and E. Kellner 1999. Test of a modified Shuttleworth-Wallace estimate of boreal forest evaporation. Agricultural and Forest Meteorology. 98-99:605-619.

Jury, W.A. and C.B. Tanner 1975. Advection modification of the Priestley and Taylor evapotranspiration formula. Agron. J. 67

Kaczmarek, Z., K.M. Strzepek, L. Somlyódy and V. Priazhinskaya 1996. Water Resources Management in the Face of Climatic/Hydrologic Uncertainties. Kluwer, Hingham, MA, USA.

Kite, G. 1998. Integration of forest ecosystem and climatic models with a hydrologic model. Journal of the American Water Resources Association. 34:743-753.

Leuning, R. and K.M. King 1992. Comparison of eddy-covariance measurements of CO2 fluxes by open-path and closed-path CO2 analysers. Boundary-Layer Meteorology. 59:297-311.

Li, F.Q. and T.J. Lyons 2002. Remote estimation of regional evapotranspiration. Environmental Modelling & Software. 17:61-75.

Linsley, R.K., JR., M.A. Kohler and J.L. Paulhus 1958. Hydrology for Engineers. In Hydrology for Engineers. McGraw-Hill, New York, pp. 151-155.

McNaughton, K.G. and T.A. Black 1973. A study of evapotranspiration from a Douglas Fir forest using the energy balance approach. Water Resources Research. 9:1579-1590.

Melillo, J.M., A.D. McGuire, D.W. Kicklighter, B. Moore, C.J. Vörösmarty and A.L. Schloss 1993. Global climate change and terrestrial net primary production. Nature. 363:234-240.

Moncrieff, J.B., Y. Malhi and R. Leuning 1996. The propagation of errors in long-term measurements of land-atmosphere fluxes of carbon and water. Global Change Biology. 2:231.

Monteith, J.L. 1965. Evaporation and the environment. Symposium of the Society of Exploratory Biology. 19:205-234.

Mukammal, E.I. and H.H. Neumann 1977. Application of the Priestley-Taylor evaporation model to assess the influence of soil moisture on the evaporation from a large weighing lysimter and class A pan. Boundary-Layer Meteorology. 12:243-256.

Munro, R.K., W.F. Lyons, Y. Shao, M.S. Wood, L.M. Hood and L.M. Leslie 1998. Modelling land surface-atmosphere interactions over the Australian continent with an emphasis on the role of soil moisture. Environmental Modelling & Software. 13:333-339.

Musselman, R.C. and D.G. Fox 1991. A review of the role of temperate forests in the global CO2 balance. Journal of Air Waste Management Association. 41:798-807.

Naoum, S. and I.K. Tsanis 2003. Hydroinformatics in evapotranspiration estimation. Environmental Modelling & Software. 18:261-271.

Njoku, E.G., T.J. Jackson, V.L. Lakshmi, T.K. Chan and S.V. Nghiem 2003. Soil moisture retrieval from AMSR-E. IEEE Transactions on Geoscience and Remote Sensing. 41:215-228.

Parton, W.J., J.M.O. Scurlock, D.S. Ojima, T.G. Gilmanov, R.J. Scholes, D.S. Schimel, T. Kirchner, J.-C. Menaut, T.R. Seastedt, E.G. Moya, A. Kamnalrut and J.I. Kinymario 1993. Observations and modeling of biomass and soil organic matter dynamics for the grassland biome worldwide. Global Biogeochemical Cycles. 7:785-809.

Penman, H.L. 1948. Natural evaporation from open water, bare soil and grass. In Royal Society of London Ser. A, pp. 120-146.

Potter, C.S., J.T. Randerson, C.B. Field, P.A. Matson, P.M. Vitousek, H.A. Mooney and S.A. Klooster 1993. Terrestrial ecosystem production: a process based model based on global satellite and surface data. Global Biogeochemical Cycles. 7:811-841.

Priestley, C.H.B. and R.J. Taylor 1972. On the assessment of surface heat flux and evaporation using large scale parameters. Monthly Weather Review. 100:81-92.

Raich, J.W., E.B. Rastetter, J.M. Melillo, D.W. Kicklighter, P.A. Steudler, B.J. Peterson, A.L. Grace, B. Moore III and C.J. Vörösmarty 1991. Potential net primary productivity in South America: Application of a global model. Ecological Applications. 1:399-429.

Rissman, J. and G. Tetzlaff 1994. Application of a spectral correction method for measurements of covariances with fast-response sensors in the atmospheric

boundary layer up to a height of 130 m and testing of the corrections. Boundary-Layer Meteorology. 70:293-305.

Running, S.W. and J.C. Coughlan 1988. A general model of forest ecosystem processes for regional applications I. Hydrologic balance, canopy gas exchange and primary production processes. Ecological Modelling. 42:125-154.

Running, S.W. and E.R. Hunt, Jr. 1993. Generalization of a forest ecosystem process model for other biomes, BIOME-BGC, and an application for global-scale models. In Scaling Processes between Leaf and Landscape Levels Eds. J.R. Ehrlinger and C. Field. Academic Press, San Diego, CA, pp. 141-158.

Savabi, M.R. and C.O. Stockle 2001. Modeling the possible impact of increased CO2 and temperature on soil water balance, crop yield and soil erosion. Environmental Modelling & Software. 16:631-640.

Saxton, K.E., W.J. Rawls, J.S. Romberger and R.I. Papendick 1986. Estimating generalized soil-water characteristics from texture. Soil Science Society of America Journal. 50:1031-1036.

Sellers, P.J., D.A. Randall, G.J. Collatz, J.A. Berry, C.B. Field, D.A. Dazlich, C. Zhang, G.D. Collelo and L. Bounoua 1996. A revised land surface parameterization (SiB2) for atmospheric GCMs. Part I: Model Formulation. Journal of Climate. 9:676-705.

Shuttleworth, W.J. 1991. Evaporation models in hydrology. In Land Surface Evaporation: Measurement and Parameterization Eds. T.J. Schmugge and J.C. André. Springer, New York, USA, pp. 93-120.

Shuttleworth, W.J. and I.R. Calder 1979. Has the Priestley-Taylor equation any relevance to forest evaporation? Journal of Applied Meteorology. 18:639-646.

Shuttleworth, W.J., J.H. Gash, C.R. Lloyd, C.J. Moore, J. Roberts, A.O.M. Filho, G. Fisch, V.P.S. Filho, M.N.G. Ribeiro, L.C.B. Molion, L.D.A. Sa, J.C.A. Nobre, O.M.R. Cabral, S.R. Patel and J.C. De Moraes 1984. Eddy correlation measurements of energy partition for Amazonian forest. Quarterly Journal of the Royal Meteorological Society. 110:1143-1162.

Shuttleworth, W.J. and J.S. Wallace 1985. Evaporation from sparse crops-an energy combination theory. Quarterly Journal of the Royal Meteorological Society. 111:839-855.

Soulis, E.D., K.R. Snelgrove, N. Kouwen, F. Seglenieks and D.L. Verseghy 2000. Towards closing the vertical water balance in Canadian atmospheric models: Coupling of the Land Surface Scheme CLASS with the distributed hydrological model WATFLOOD. Atmosphere-Ocean. 38:251-269.

Spittlehouse, D.L. and T.A. Black 1979. Determination of forest evapotranspiration using Bowen ration and eddy correlation-measurements. Journal of Applied Meteorology. 18:647-653.

Spittlehouse, D.L. and T.A. Black 1981. A growing season water balance model applied to two Douglas-fir stands. Water Resources Research. 17:1651-1656.

Stannard, D.I. 1993. Comparison of Penman-Monteith, Shuttleworth-Wallace, and Modified Priestley-Taylor Evapotranspiration Models for Wildland Vegetation in Semiarid Rangeland. Water Resources Research. 29:1379-1392.

Stewart, R.B. and W.R. Rouse 1977. Substantiation of the Priestley and Taylor parameter alpha=1.26 for potential evaporation in high latitudes. Journal of Applied Meteorology. 16:649-650.

Thornton, P.E., S.W. Running and M.A. White 1997. Generating surfaces of daily meteorological variables over large regions of complex terrain. Journal of Hydrology. 3-4:214-251.

Tourula, T. and M. Heikinheimo 1998. Modeling evapotranspiration from a barley field over the growing season. Agricultural and Forest Meteorology. 91:237-250.

VEMAP, M. 1995. Vegetation/ecosystem modeling and analysis project: comparing biogeography and biogeochemistry models in a continental-scale study of terrestrial ecosystem responses to climate change and CO2 doubling. Global Biogeochemical Cycles. 9:407-437.

Vörösmarty, C.J., C.A. Federer and A.L. Schloss 1998. Potential evaporation functions compared on US watersheds: Possible implications for global-scale water balance and terrestrial ecosystem modeling. Journal of Hydrology. 207:147-169.

Wallace, J.S. 1995. Calculating evaporation: resistance to factors. Agricultural and Forest Meteorology. 73:353-366.

Watson, R.T., Zinyowera, M.C., Moss, R.H. and Dokken, D.J. 1995. Climate Change 1995: Impacts, Adaptations and Mitigation of Climate Change: Scientific-Technical Analyses. Cambridge University Press, Cambridge, UK.

Welles, J.M. and J.M. Norman 1991. Instrument for indirect measurement of canopy architecture. Agronomy Journal. 83:818-825.

Willmott, C.J., C.M. Rowe and Y. Mintz 1985a. Climatology of the terrestrial seasonal water cycle. Journal of Climate. 5:589-606.

Wofsy, S.C., M.L. Goulden, J.W. Munger, S.M. Fan, P.S. Bakwin, B.C. Daube, S.L. Bassow and F.A. Bazzaz 1993. Net exchange of CO2 in a mid-latitude forest. Science. 260:1314-1317.

Wooldridge, S.A., J.D. Kalma and J.P. Walker 2003. Importance of soil moisture measurements for inferring parameters in hydrologic models of low-yielding ephemeral catchments. Environmental Modelling & Software. 18:35-48.

Xu, M., T.A. Debiase, Y. Qi, A. Goldstein and Z. Liu 2001. Ecosystem respiration in a young ponderosa pine plantation in the Sierra Nevada Mountains, California. Tree Physiology. 21:309-318.

Chapter 2 published in:
Fisher, J.B., T.A. DeBiase, Y. Qi, M. Xu, A.H. Goldstein 2005. Evapotranspiration models compared on a Sierra Nevada forest ecosystem. Environmental Modelling & Software. 20:783-796.

Chapter 3

Global estimates of the land-atmosphere water flux: A remote sensing driven, flux site-validated ecophysiological model of evapotranspiration

Abstract Evapotranspiration is a major component of the terrestrial water balance that is tightly coupled to ecosystem carbon cycling, plays a central role in global circulation and climate change models, yet remains difficult to measure and predict at synoptic spatial scales. Numerous models of evapotranspiration have been published that range in data-driven complexity, but global estimates require a model that does not depend on intensive field measurements. The Priestley-Taylor model of potential evapotranspiration is relatively simple, but has proven to be remarkably accurate and theoretically robust. Building on recent advances in ecophysiological theory that allow detection of multiple stresses on plant function using biophysical remote sensing metrics, we developed a bio-meteorological approach for reducing Priestley-Taylor estimates of potential evapotranspiration to actual rates based on constraints imposed by plant stress and soil drought. The model is tested and validated against eddy flux measurements (FLUXNET) in 16 ecosystems from tropical to subalpine environments representing a wide range of plant functional types—grassland, crop, and deciduous broadleaf, evergreen broadleaf, and evergreen needleleaf forests. Five inputs are required, all of which can be potentially determined using remote sensing observations: net radiation (R_n), normalized difference

vegetation index (*NDVI*), soil adjusted vegetation index (*SAVI*), air temperature (T_a), and water vapor pressure (*ea*). Our model is theoretically-based, requires no calibration, tuning or spin-ups, and is applied equally across space and time. Global estimates of evapotranspiration at monthly 1 degree temporal and spatial resolutions during the years 1986-1994 were determined using globally consistent datasets from the International Satellite Land-Surface Climatology Project, Initiative II (ISLSCP-II). ISLSCP-II provides *NDVI* from remote sensing data, R_n from a combination of remote sensing and surface observations, and T_a and *ea* from surface observations. *SAVI* was obtained from the Advanced Very High Resolution Spectroradiometer (AVHRR). The r^2 for all 16 FLUXNET sites across 4 years was 0.93 (RMSE = 21 $W \cdot m^{-2}$). Our model resulted in improved prediction of evapotranspiration across water-limited sites, and was used to show spatial and temporal differences in evapotranspiration across continents and latitudinal bands.

Introduction

Evapotranspiration (*LE*) is a major component in the processes and models of global climate change, water balance, net primary productivity, floods, droughts, and irrigation. The latent heat transported and released by the global water cycle is the principal source of energy that drives the atmospheric circulation and weather disturbances. General circulation models (GCMs) indicate that a rise in global mean temperature due to radiative forcing by increased atmospheric CO_2 could alter water resources significantly for our rapidly growing world population, especially in arid parts of the globe (Myneni et al. 1997). Globally, GCMs tend to overestimate precipitation and underestimate

transpiration from plant water uptake (Henderson-Sellers et al. 1995). Due to the impact of surface hydrological processes on weather and climate, large errors in surface temperature forecasts can be traced to poor handling of *LE* (Kite 1998). *LE* is difficult to measure and predict, however, especially at large spatial scales (Turner 1989). Understanding the variability in water cycle processes requires a spatially detailed analysis of global land surface processes (Running et al. 2000). Closing the water budget worldwide is therefore of utmost importance to water and energy cycle research; the overall goal of which is to deliver reliable estimates of precipitation and *LE* over the whole surface of the earth using a combination of measurements and model estimates (Entekhabi et al. 1999).

The history of global *LE* estimation throughout the past few decades has been marked by a struggle between realistic models that are hindered by complex parameterization and simple models that lack physical realism. The trend has been towards increasing complexity, as opposed to applicability (Federer et al. 1996), yet greater complexity requires detailed input parameters that limit application to regions where the necessary data are available (Kustas and Norman 1996). Before the widespread ecological application of remote sensing data, researchers estimated regional *LE* with interpolated data from thousands of meteorological stations (Baumgartner and Reichel 1975; Budyko 1978; Hare 1980; Morton 1983). One of the oldest and simplest *LE* methods based on temperature developed by Thornthwaite (1948) has been used to generate global patterns in *LE* (Mintz and Walker 1993; Gordon et al. 2005), at times in conjunction with the temperature- and radiation-based model of Priestley and Taylor (1972) (Tateishi and Ahn 1996). In addition, the Penman-Monteith (1965) model has

been used to estimate transpiration in combination with the Priestley-Taylor model for soil evaporation (Choudhury 1997; Choudhury and DiGirolamo 1998; Choudhury et al. 1998). The Penman-Monteith equation is more theoretically accurate than are the Priestley-Taylor or Thornthwaite methods, but requires parameters that are difficult to characterize globally such as aerodynamic resistance, stomatal resistance, and wind speed. Further, such approaches often require estimates of the root zone water availability when plant water stress occurs (Choudhury and DiGirolamo 1998) and precipitation inputs for which there are major uncertainties in global estimates. Despite these limitations, the Penman-Monteith and Priestley-Taylor methods have been shown to have relatively low biases, particularly in comparison to the relatively poor accuracy of the Thornthwaite method (Vörösmarty et al. 1998).

Maurer et al. (2002) derived a substantial dataset of land surface states and fluxes across much of North America from 1950-2000 at a 3-h time step and at 1/8 degree spatial resolution using an engineering-based hydrologic model (Liang et al. 1994; Liang et al. 1996; Liang et al. 2004) forced with surface meteorological data. Their model requires detailed soil information, as does the approach of Federer et al. (2003) who combined the relatively complex Shuttleworth and Wallace (1985) method with a 20-layer soil model. Federer et al. reiterated and expanded what Kustas and Norman (1996) had warned: improvement in estimating *LE* with global water budget models is not likely to result from making the model more complicated. Kergoat et al. (2002) approached global *LE* from a somewhat different perspective using a leaf area index (LAI)-based productivity model, where stomatal conductance of CO_2 was proportional to conductance of water vapor and hence transpiration. Lawrence and Slingo (2004) followed the LAI

approach whereby they based *LE* on stomatal conductance in a photosynthesis model, integrated over canopy LAI. They used a new global dataset from the International Satellite Land Surface Climatology Project (ISLSCP) Initiative II (Los et al. 2000) to drive their model.

Another new global dataset that has emerged for validating remote sensing-driven models is from a global network of eddy covariance towers (FLUXNET) that measure water and energy fluxes over 0.5–5 km^2. Nishida et al. (2003) validated their NOAA/AVHRR-driven model of evaporative fraction across 13 sites in the AmeriFlux network (r^2 = 0.71). Houborg and Soegaard (2004) validated their MODIS/AVHRR-driven model with flux measurements in Denmark (r^2 = 0.58-0.85). Both Nishida et al. and Houborg and Soegaard based their *LE* models on modified Penman-Monteith approaches. In a review of *LE* methods tested against eddy flux data, Fisher et al. (2005) reported in an uncertainty analysis that the complex *LE* models are vulnerable to errors in the input parameters, but also showed the robust success of the simple Priestley-Taylor model. Finally, in a 2005 *PNAS* article, Gordon et al. (2005) assessed global *LE* from a deforestation stand-point. Returning full-circle, unfortunately, Gordon et al. used a modified Thornthwaite (1948) equation in their analysis.

We return to the tradeoff between realism and complexity versus simplicity and applicability. In global modeling, we want the best of both worlds: a simple model that is as accurate as a fully parameterized complex model. We want to drive and validate this model with the newest datasets and control the model with the latest in ecological theory. In addition, we need to quantify the uncertainty in these perpetually uncertain models. Still, as *LE* becomes increasingly important in our changing planet, we seek answers to

the same questions that global *LE* modelers have been asking for decades: what is the global water budget, how is *LE* partitioned between transpiration and evaporation, what are the differences in *LE* across space and time, and where are we seeing the most change?

Here, we address these questions with a model based on ecophysiological theory and tied to the enduring Priestley-Taylor method. The Priestley-Taylor method works very well as a potential *LE* model across most surface conditions under its original form and at $\alpha = 1.26$ (Eichinger et al. 1996). As an actual *LE* model, however, it needs to be constrained by moisture, temperature and soil-canopy partitioning, else it will overpredict actual *LE* in arid areas under water stress (McNaughton and Spriggs 1986). Soil moisture data could connect potential to actual *LE*, but unfortunately these data are largely unavailable and uncertain for most parts of the globe (De Bruin and Stricker 2000). Numerous attempts at adjusting the Priestley-Taylor coefficient have been made to connect potential to actual *LE* (Davies and Allen 1973; McNaughton and Black 1973; Jury and Tanner 1975; Mukammal and Neumann 1977; Stewart and Rouse 1977; Barton 1979; Black 1979; Shuttleworth and Calder 1979; De Bruin and Holtslag 1982; Giles et al. 1984; Flint and Childs 1991; Fisher et al. 2005). We keep α constant at 1.26 so that the Priestley-Taylor equation as a potential *LE* equation remains intact as originally designed and confirmed. The novelty in our approach is to scale-down potential *LE* to actual *LE* based on ecophysiological constraints and soil evaporation partitioning. Our ecophysiological model of the Priestley-Taylor method relies on surface changes as defined by R_n, *NDVI*, *SAVI*, T_a, and *ea*.

R_n, *NDVI*, *SAVI*, T_a, and *ea* can all be acquired solely with remote sensing. Recently, Bisht et al. (2005) developed a method to estimate R_n from solely MODIS. Compared with observed measurements from their study sites, correlation coefficients ranged from 0.85 (daily average) to 0.89 (instantaneous); RMSE's were 60 and 74 $W \cdot m^{-2}$, respectively. Irmak et al. (2003) introduced an equation to measure R_n based on minimum and maximum T_a, incoming solar radiation, and distance between the Earth and sun. They report coefficients of determination across eight validation sites between 0.96 – 0.99. Many studies have compared T_a from satellite sensors to surface measurements across a wide range of land covers (Goetz et al. 1995; Kalluri and Dubayah 1995; Czajkowski et al. 1997; Jin et al. 1997; Prince et al. 1998; Lakshmi and Susskind 2000; Lakshmi et al. 2002). Error in satellite-based T_a has been reported as 4ºC from AVHRR (e.g., Prince et al. 1998; Lakshmi et al. 2002). Vegetation indices such as *NDVI* or *SAVI* are direct products of band calculations. Steven et al. (2003) report *NDVI* and *SAVI* differences for 15 different satellite sensors, including MODIS and AVHRR. Their results showed that the vegetation indices can be interconverted to a precision of 1-2% across all sensors for both vegetation indices. Satellite-based estimates of *ea* have been reported from MODIS and AVHRR (Czajkowski et al. 2002; Motell et al. 2002; Sobrino and El Kharraz 2003). Motell et al. (2002) report a RMSE of 3.8 mm (R = 0.91) for precipitable water vapor satellite estimates based on Dalu (1986) over Hawaii from AVHRR. Czajkowski et al. (2002) showed that near-surface water vapor could be estimated with AVHRR or MODIS with a correlation of 0.36 as compared to BOREAS ground measurements, though they explain the low r^2 values as a result of spatial and temporal mismatches between surface and satellite measurements.

Our primary goals are to develop an ecophysiological-based *LE* model that can potentially be parameterized solely with remote sensing inputs, results in increased accuracy for *LE* prediction, and is robust across a wide range of ecosystems. Our model is theoretically-based, requires no calibration, tuning or spin-ups, and is applied equally across space and time. We validate our model "on the ground" with eddy flux data from 16 FLUXNET sites across tropical to subalpine environments representing a wide range of plant functional types—grassland, crop, and deciduous broadleaf, evergreen broadleaf, and evergreen needleleaf forests. FLUXNET data provide the highest precision and most temporally continuous measurements available with which to scale-up to medium to coarse spatial scale space-based measurements (Kimball et al. 1997). Next, we provide new global estimates of the land-atmosphere water flux as driven by ISLSCP-II global datasets, which are a compilation of datasets from multiple satellite sensors and complementary or supplementary ground data where available; these global estimates can be further improved by higher resolution remote sensing data.

Methods

Data: Validation Sites

We validated the model across a wide range of ecosystems at 16 FLUXNET sites for 2000-2003 (Table 1 and Figure 1) (e.g., Martin et al. 1997; Moncrieff et al. 1997; Hollinger et al. 1999; Goldstein et al. 2000; Granier et al. 2000; Schmid et al. 2000; Flanagan et al. 2002; Monson et al. 2002; Knohl et al. 2003; Xu and Baldocchi 2004; Leuning et al. 2005). These sites represent 6 sub-networks of FLUXNET: AmeriFlux, AsiaFlux, CarboEuroFlux, Fluxnet-Canada, LBA, and OzFlux. For the validation part of

Site	Biome Type	Latitude	Longitude	P.I.
Bondville	Temperate C3/C4 Crop	40° 0' 21.96" N	88° 17' 30.72" W	T. Myers
Griffin	Temperate Evergreen Needleleaf Forest	56° 36' 23.59" N	3° 47' 48.55" W	J. Moncrieff
Hainich	Temperate Deciduous Broadleaf Forest	51° 4' 45.36" N	10° 27' 7.2" E	A. Knohl
Hesse	Temperate Deciduous Broadleaf Forest	48° 40' 27" N	7° 3' 56" E	A. Granier
Howland	Cold-Temperate Evergreen Needleleaf Forest	45° 12' 14.65" N	68° 44' 25" W	D. Hollinger
Mer Bleue	Boreal Wetland	45° 24' 33.84" N	75° 31' 12" W	P. Lafleur
Mize	Subtropical Evergreen Needleleaf Forest	29° 45' 53.28" N	82° 14' 41.34" W	T. Martin
Morgan Monroe	Temperate Deciduous Broadleaf Forest	39° 19' 23.34" N	86° 24' 47.30" W	H. Schmid
Niwot	Sub-Alpine Evergreen Needleleaf Forest	40° 01' 57" N	105° 32' 49" W	R. Monson
NSA-OBS	Boreal Evergreen Needleleaf Forest	55° 52' 46.63" N	98° 28' 50.91" W	S. Wofsy
Takayama	Cold-Temperate Deciduous Broadleaf Forest	36° 08' 46.2N	137° 25' 23.2" E	S. Yamamoto
Tapajos (67m)	Tropical Evergreen Broadleaf Forest	2° 51' 24" S	54° 57' 32" W	S. Wofsy
Tonzi	Mediterranean Savanna	38° 25' 53.76" N	120° 57' 57.54" W	D. Baldocchi
Tumbarumba	Temperate Evergreen Broadleaf Forest	35° 39' 20.6" S	148° 9' 7.5" E	R. Leuning
Walnut River	Temperate C3/C4 Grassland	37° 31' 15" N	96° 51' 18" W	R. Coulter

Table 1. AmeriFlux sites used for model validation. Additional site information can be found at http://public.ornl.gov/ameriflux/

our study, we used *in situ* measurements of R_n, T_a and *ea* obtained from each study site to run the model. *NDVI* and *SAVI* for the sites was determined from the Moderate Resolution Imaging Spectroradiometer (MODIS). The Oak Ridge National Laboratory Distributed Active Archive Center (ORNL DAAC) subsets the full MODIS scenes (1200-km x 1200-km) to 7-km x 7-km areas containing the flux towers. *NDVI* is calculated as $(r_{NIR}-r_{VIS})/(r_{NIR}+r_{VIS})$, and *SAVI* is calculated as $(1.5)(r_{NIR}-r_{VIS})/(r_{NIR}+r_{VIS}+0.5)$ (Huete 1988).

Figure 1. The 16 FLUXNET sites used in the validation spanned across N. America, S. America, Europe, Asia, and Australia.

Our predicted *LE* was compared against the *LE* measured by the eddy covariance method (Baldocchi et al. 1988) at the towers for the respective range of footprints (roughly 0.5-5 km^2). The eddy covariance method quantifies vertical fluxes of scalars between the ecosystem and the atmosphere from the covariance between vertical wind velocity and scalar fluctuations at 10 Hz, and we compute monthly averages to coincide with the global monthly outputs (e.g., Shuttleworth et al. 1984; Baldocchi et al. 1988; Wofsy et al. 1993). We could not validate our model at every FLUXNET site because we were limited by: A) data use permission, B) applicable measurements, and/or C) recent measurements (to correspond to recent satellite remote sensing measurements).

Data: Global Estimates

For global estimates of *LE*, we used input datasets for R_n, *NDVI*, T_a and *ea* from the ISLSCP-II archive (Sellers et al. 1995; Los et al. 2000; Hall et al. 2005). We used precipitation data from ISLSCP-II to calculate runoff from our estimated *LE*. ISLSCP-II data are 1 degree gridded monthly values, which are appropriate for *LE* estimation at the global scale (Federer et al. 1996). ISLSCP, which is one of several projects within the Global Hydrology Project of the Global Energy and Water Cycle Experiment (GEWEX),

is a compilation of data sources from a suite of satellites and aggregation of complementary and supplementary ground measurements.

ISLCP-II used Surface Radiation Budget (SRB) data for R_n for 1986-1995 (Stackhouse et al. 2000), based on meteorological inputs were taken from Goddard Earth Observing System version 1 (GEOS-1) reanalysis data sets (Schubert et al. 1993) from the Data Assimilation Office at NASA Goddard Space Flight Center. Cloud parameters and surface albedos were derived from the International Satellite Cloud Climatology Project data (Pinker and Laszlo 1992; Rossow et al. 1996). Random errors in monthly average SW and LW fluxes are between 10-15 $W \cdot m^{-2}$. R_n in the ISLSCP-II dataset is provided as the 24-hour mean and we therefore corrected for daylength to convert to daytime means. ISLSCP-II provided Fourier-adjusted, sensor and solar zenith angle corrected, interpolated, reconstructed (FASIR) adjusted *NDVI* (Los et al. 2000). T_a, *ea* and precipitation data were from the Climate Research Unit Monthly Climate Data (New et al. 1999; New et al. 2000). These data were interpolated directly from station observations, merged datasets, and from synthetic data estimated using predictive relationships with precipitation and temperature measurements. ISLSCP-II was unable to quantify the errors in T_a, *ea* and precipitation, but previously we report related research on these errors.

Because ISLSCP-II did not provide *SAVI* (Huete 1988), and because MODIS could not provide the temporal history to match with ISLSCP-II, we calculated *SAVI* from AVHRR data. Visible and near-infrared reflectances were obtained from the NOAA/NASA Pathfinder AVHRR dataset (http://disc.sci.gsfc.nasa.gov/landbio/). AVHRR channel 1 (r_{VIS}) records wavelengths from 0.58 – 0.68 micrometers; channel 2

(r_{NIR}) records wavelengths from 0.73 – 1.10 micrometers. The theoretical range of *SAVI* is between 0 and 1, and of *NDVI* between -1 and 1, but the actual measured range from the satellite data ranged from 0 to 0.9 for both indices. A more detailed, comprehensive description of the NOAA series satellites, the AVHRR instrument and data can be found in the NOAA Polar Orbiter Data User's Guide (Kidwell 1991).

Data were processed in MATLAB 6.5, ESRI's ArcGIS 9.1, ImageJ (http://rsb.info.nih.gov/ij/), and Microsoft Excel. AmeriFlux/FLUXNET data can be downloaded at http://daac.ornl.gov/FLUXNET/. ISLSCP-II data can be downloaded at http://islscp2.sesda.com/ISLSCP2_1/html_pages/islscp2_home.html.

Model description

Our model of *LE* is partitioned into canopy evaporation (LE_i), canopy transpiration (LE_c) and soil evaporation (LE_s). The model is driven with five inputs: R_n, *NDVI, SAVI,* T_a, and *ea*. Total evapotranspiration, *LE*, is calculated as the sum of LE_i+LE_c+LE_s. The Priestley-Taylor (1972) equation for potential *LE* based on available energy is used for each component flux, and each is controlled by ecophysiological constraints or conditions to reduce potential *LE* to actual *LE* based on plant physiological status and soil moisture availability (Table 2):

$$LE_i = \left(\frac{f_w}{30}\right) 1.26 \frac{\Delta}{\Delta + \gamma} \left(R_n f_c\right) \quad (1)$$

$$LE_c = \left(1 - f_w\right) f_g f_T 1.26 \frac{\Delta}{\Delta + \gamma} \left(R_n f_c\right) \quad (2)$$

$$LE_s = \left(1 - f_w\right) f_{SM} 1.26 \frac{\Delta}{\Delta + \gamma} \left(R_n \left(1 - f_c\right) - G\right) \quad (3)$$

Parameter	Description	Equation	Reference
LE	Evapotranspiration	$LE_i + LE_c + LE_s$	
LE_i	Interception evaporation	$\left(\frac{f_w}{30}\right)1.26\frac{\Delta}{\Delta+\gamma}\left(R_n f_c\right)$	This study; Priestley and Taylor (1972)
LE_c	Canopy transpiration	$\left(1-f_w\right)f_g f_T 1.26\frac{\Delta}{\Delta+\gamma}\left(R_n f_c\right)$	Norman et al. (1995); This study; Priestley and Taylor (1972)
LE_s	Soil evaporation	$\left(1-f_w\right)f_{SM}\,1.26\frac{\Delta}{\Delta+\gamma}\left(R_n\left(1-f_c\right)-G\right)$	This study; Priestley and Taylor (1972)
f_w	Wet day frequency	$30\left(\frac{s}{2LE_s}\right)^2$	Suleiman and Ritchie (2003)
f_g	Green canopy fraction	$\frac{1.3SAVI}{f_c}$	Gao et al. (2000) and Sellers et al. (1994)
f_c	Fractional total vegetation cover	$NDVI$	Los et al. (2000)
f_T	Plant temperature constraint	$e^{-\left(\frac{T_a-T_{opt}}{T_{opt}}\right)^2}$	June et al. (2004)
f_{SM}	Soil moisture constraint	RH^{VPD}	This study, based on Bouchet (1963)
T_{opt}	Optimum growth temperature	T_a at $\max\{SAVI \cdot T_a \cdot RH^{VPD}\}$	This study, based on Potter et al. (1993)

Table 2. Model parameters and equations. R_n is net radiation (mm), G is ground heat flux (mm), T is air temperature (°C), RH is relative humidity ($0<RH<1$), VPD is saturation vapor pressure deficit (kPa), Δ is slope of saturation-to-vapor pressure curve (kPa·°C^{-1}), γ is the psychrometric constant (~0.066 kPa·°C^{-1}), s is desorptivity of the soil (~4 mm·day$^{-0.5}$), and T_a, RH and VPD are mean monthly values of T_a, RH and VPD, respectively. All f-functions are set to scale between 0 and 1, except f_w, which is in units of month^{-1}.

where Δ is the change in saturation vapor pressure for a change in temperature, and γ is the psychrometric constant. The fractional vegetation cover (f_c), which is approximated as *NDVI* (Townshend and Justice 1986; Los et al. 2000), partitions R_n between the canopy and soil. Soil heat flux (G) should be included in available soil energy ($R_{n,s}$-G), but where G is unavailable R_n may be used alone (Kustas et al. 1993); G is assumed to be close to zero at monthly time steps.

LE_i, which is the evaporation of canopy-intercepted precipitation, is calculated as potential *LE* under wet canopy conditions as determined by time following a rain event. f_w, which is a function of soil moisture and time (Suleiman and Ritchie 2003), determines the conditions under which the system is wet or dry, which set *LE* equal to the potential rate or to the constrained rates.

We calculate two plant physiological limitations to LE_c: green fraction of the canopy that is actively transpiring (f_g) and plant temperature constraint (f_T). f_g is calculated following Gao et al. (2000) as the ratio of fractional green vegetation cover to f_c, where f_g=1.3*SAVI*/f_c. For fractional total vegetation cover *NDVI* is used, but for fractional green vegetation cover we use a ratio of *SAVI* to *NDVI* as described in Sellers et al. (1994). *NDVI* alone can be used to drive f_g, but *SAVI* or the Enhanced Vegetation Index (*EVI*) (Huete et al. 2002) provide soil and atmospheric corrections that lead to a more accurate and robust indication of green vegetation cover; *NDVI* can be contaminated by soil reflectance and atmospheric interference (Gao et al. 2000). The second physiological constraint, f_T was calculated following June et al. (2004) with optimum T_a (T_{opt}) calculated following Potter et al. (1993)'s CASA model as the mean T_a

at the time of peak canopy activity. f_T is an indication of the T_a at which rates of plant growth, photosynthesis and transpiration are highest as determined by peak f_g.

We constrain LE_s by f_{SM}, which is an index of soil drought based on Bouchet (1963) whereby the complementary relationship hypothesis relates surface moisture to the evaporative demand of the atmosphere and allows increased sensitivity during periods of low humidity, RH^{VPD}. Relative humidity (*RH*) and vapor pressure deficit (*VPD*) were calculated from *ea* and the saturation vapor pressure of the air, *es*, based on T_a, but if data are available for *RH* and *VPD*, then *ea* is not needed. Both *RH* and *VPD*, which are functions of each other, are correlated with soil moisture under non-irrigated settings—moist soils will generally have adjacent moist air. We assume that the soil is saturated when the canopy is saturated following a rain event (f_i=0), and thus set LE_c equal to the potential rate and set f_{SM} equal to 1, otherwise LE_c is constrained by the f_{SM} function.

Uncertainty analysis

Uncertainty in the outputs are estimated from the model with the method of moments (Hansen 1982), also known as the boundary element method, the surface integral equation method, and the Galerkin or Galerkin-Petrov method for surface integral equations (Warnick and Chew 2004). The method of moments estimators are obtained from the sample mean and the sample variance of the exceedances (e.g., Madsen et al. 1997). The method of moments is an exact measure of accuracy in comparison with Monte Carlo and other approximate methods that are dependent on the number of simulations run (e.g., Rushdi and Kafrawy 1988). Uncertainty in *LE* is the propagation of

the partial derivatives of the input parameters and their respective co-variances, where x and y are the 5 inputs R_n, *NDVI*, *SAVI*, T_a, and *ea*:

$$s_{LE} = \sqrt{\sum \left(\left(\frac{\partial LE}{\partial x} s_x \right)^2 + 2 r_{xy} \left(\frac{\partial LE}{\partial x} s_x \right) \left(\frac{\partial LE}{\partial y} s_y \right) \right)} \quad (3)$$

We used the method of moments to determine the sensitivity of our model to variation in each of the input parameters. This method is particularly useful when the error in the input data is known, as in the case of flagged anomalous data or uncertainty associated with interpolation/extrapolation or gap filling (e.g., cloud pixels, measurement failure).

Results

AmeriFlux validation

The results for predicted *LE* based on our model versus measured *LE* show good agreement at all 16 FLUXNET sites for 2000-2003 (Figure 2). The r^2 for all sites is 0.93, though the fit varies from site to site; the RMSE is 21 $W \cdot m^{-2}$. Data in Figure 2 are shown as monthly means (to correspond with ISLSCP-II monthly data for the following global analysis). The model accounted for 94% of the variation in cumulative *LE* ($mm \cdot year^{-1}$) with a RMSE of 87 $mm \cdot year^{-1}$, or 16% of the observed mean. The 16 sites represent a wide range of land covers, climates, fluxes and eddy covariance footprints. At one water-limited site that experiences marked summer drought stress, we show how our model matches the measured *LE* in contrast to the overprediction of the original un-constrained Priestley-Taylor method (Figure 3). The original Priestley-Taylor method shows the potential *LE* throughout the hot summer, but with little precipitation and soil moisture the actual *LE* is quite low.

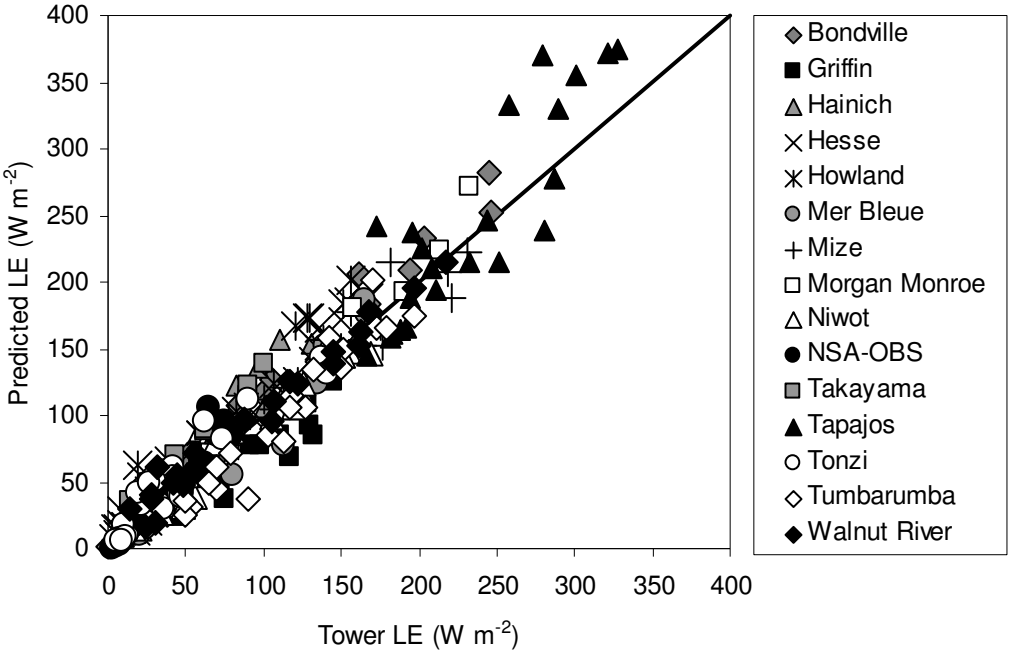

Figure 2. Predicted evapotranspiration (*LE*) versus observed evapotranspiration at 16 FLUXNET sites for 2000-2003 with 1:1 line. The r^2 for all sites for all years is 0.93; the RMSE is 21 W·m^{-2}, which represents 23% of the mean.

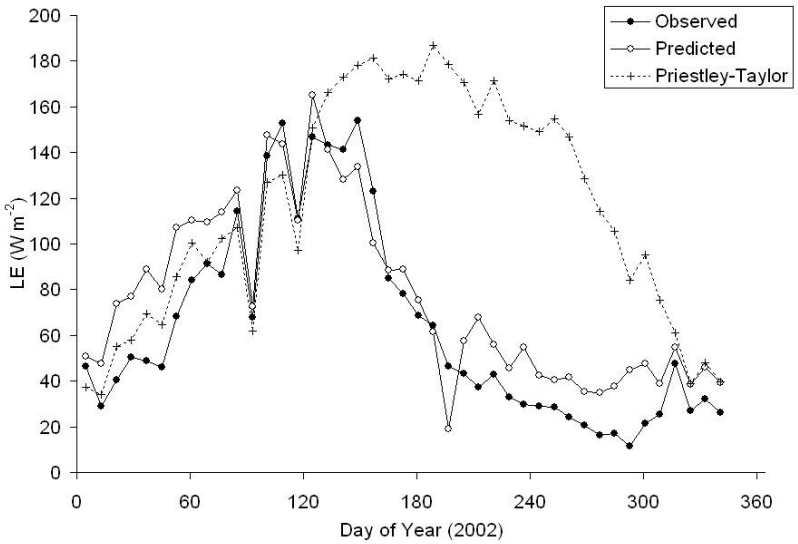

Figure 3. Overprediction of the original Priestley-Taylor (1972) method at a drought-stressed Mediterranean climate site, and improvement to the *LE* prediction from our model.

Global analysis

We assessed the global spatial and temporal patterns of *LE* from 1986-1994 using 1 degree monthly gridded ISLSCP-II input data. The month-to-month pattern for 1994 shows the seasonal shifts (Figure 4). The southern hemispheric tropics remain consistently high throughout the year (~130 $W \cdot m^{-2}$), while the major deserts of northern Africa and Australia remain consistently low (~5 $W \cdot m^{-2}$ and ~20 $W \cdot m^{-2}$, respectively). The major global change on a monthly scale occurs in the high northern latitudes, where *LE* shows high variation with increases into the northern summer while tapering off into the winter. Striping can be seen in the high northern latitudes during the winter due to problematic R_n data (R_n striping in the high southern latitudes was restricted to the Antarctic continent).

Our model partitions *LE* into LE_s and LE_c; the partitioning of *LE* is shown in Figure 5 bi-monthly for 1994. LE_s and LE_c tend to complement or offset each other. In the Amazon LE_s (~25 $W \cdot m^{-2}$) is predicted to be low because of the high canopy cover, and hence high canopy evaporation (~100 $W \cdot m^{-2}$) contribution to *LE*. In the northern latitudes, LE_s becomes activated before LE_c as seen in the March-May figures, though LE_c takes over in the middle of the summer. In the Indian sub-continent LE_s is the major contributor to *LE* due largely to irrigation particularly in the summer, and LE_c is minimal throughout the year here. LE_s and LE_c increase towards the equator into the summer throughout Africa south of the Sahara. LE_s and LE_c are both minimal in the Sahara and Australian Outback deserts.

It may not be surprising that *LE*, LE_s and LE_c exhibit these seasonal patterns throughout the year. But, from year-to-year one might expect little change, especially on

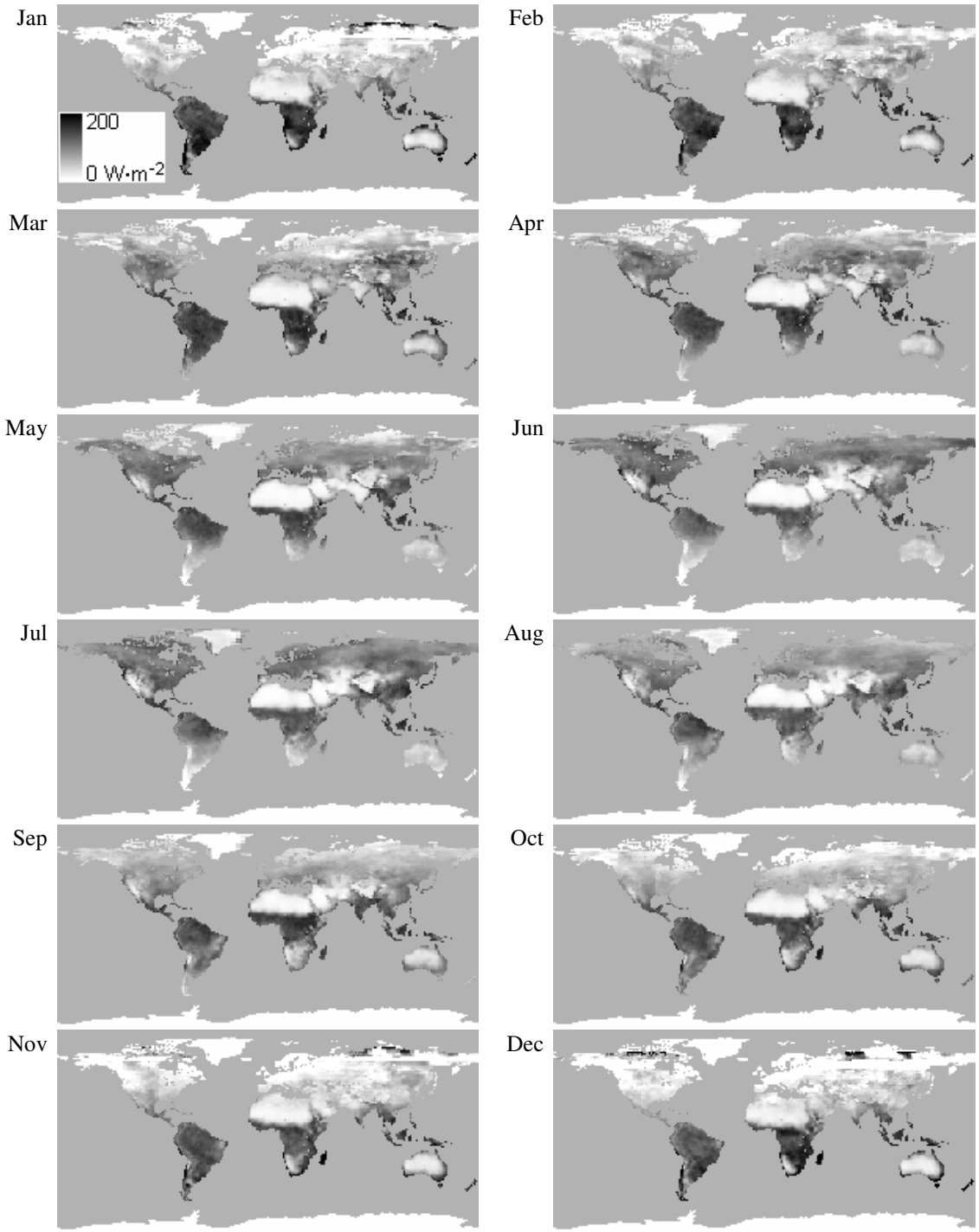

Figure 4. Month-to-month variation in evapotranspiration for 1994. As the seasons progress throughout the year, evapotranspiration in the high northern latitudes increases into the northern summer and tapers off into the winter while the southern hemispheric tropics remain consistent.

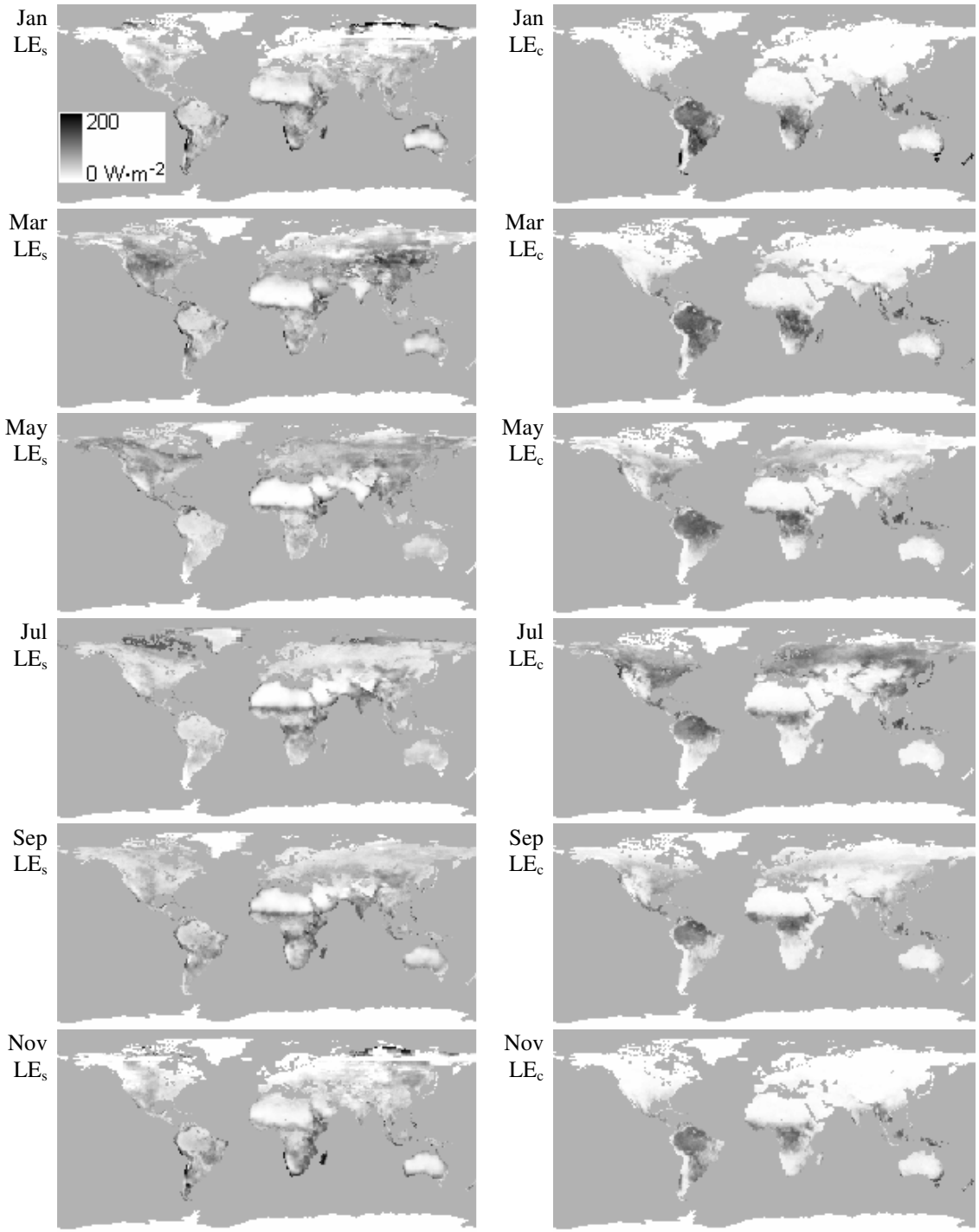

Figure 5. Soil evaporation (LE_s) and canopy transpiration (LE_c) bi-monthly for 1994.

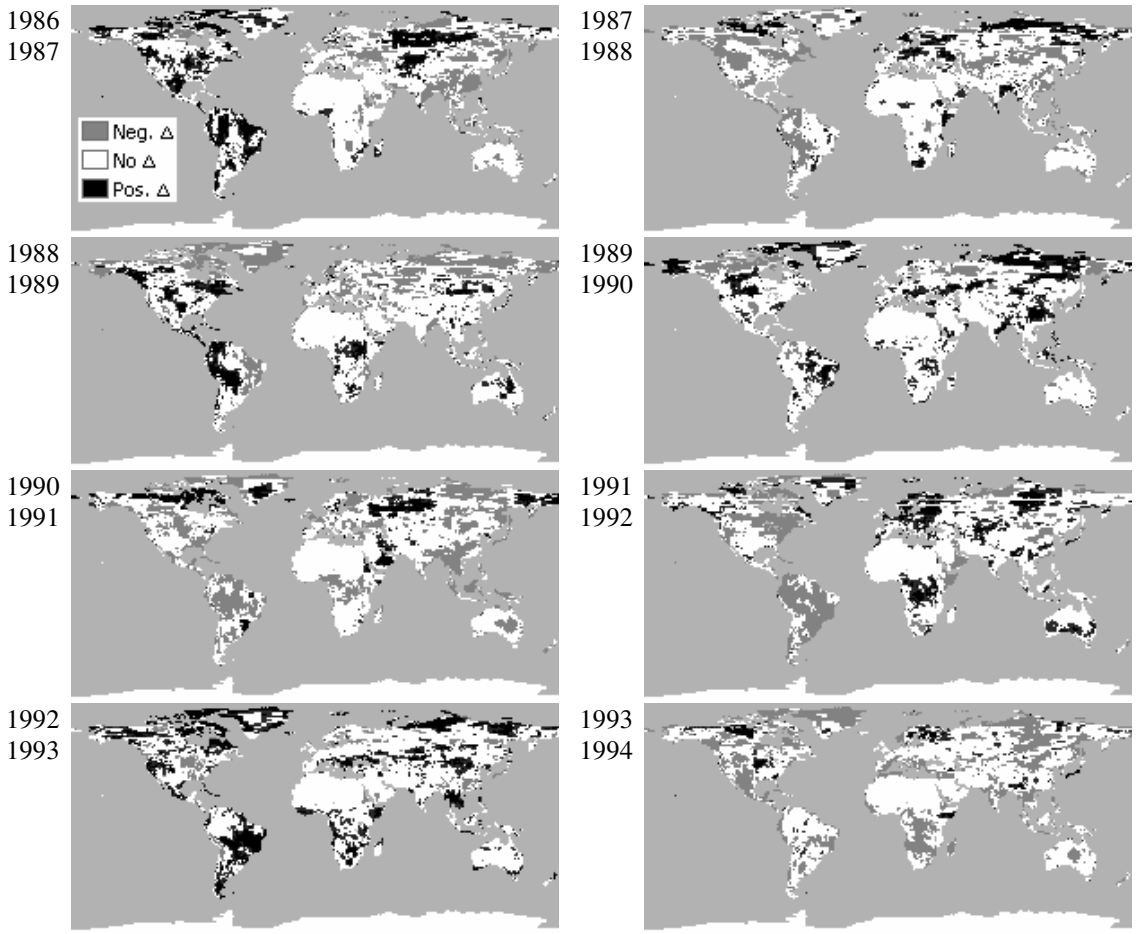

Figure 6. Year-to-year change in evapotranspiration. Gray land areas indicate a negative change between years (<10 $W \cdot m^{-2}$), and black areas indicate an increase in evapotranspiration (>10 $W \cdot m^{-2}$). White areas represent no change, or within two standard deviations around a mean of 0.

an annual average, per pixel basis. We show the year-to-year change in mean annual *LE* from 1986 to 1994 in Figure 6 and report on the major global areas that showed significant increases or decreases in *LE*. From 1986-1987, we see increases in *LE* in pockets of the Amazon, southern North America (Texas/Mexico), the Great Lakes of the U.S. and Canada, northwestern Canada, in parts of the Yukon and northern Alaska, and in central Asia. The major decreases in *LE* occurred in southeastern Asia, eastern India, eastern Europe, and northern China. Increases in *LE* were limited from 1987-1988 to

Europe, northern Russia and Canada, and spots throughout Africa; major decreases in *LE* occurred throughout western South America, western Canada, and across a central belt through Asia. From 1988-1989, a rough switch occurred between those areas that showed significant change from the previous 1987-1988. For instance, decreases from 1987-1988 in western South America and throughout Canada became increases from 1988-1989; additionally, major increases occurred in Australia and central Africa. Decreases in *LE* from 1989-1990 were limited to northern Canada and western Russia; *LE* increased throughout most of Alaska, a large portion of Canada, eastern Brazil, China, eastern India, and northern Russia.

From 1990-1991, major decreases in *LE* occurred throughout much of the world: the Amazon, central North America, central Africa, eastern Australia, Indonesia, southeastern Asia, northern Russia, and Nordic Europe; the largest increases were in eastern Europe and western Russia, with smaller increases in southern Saudia Arabia, northeastern Russia, and northern Canada. Major decreases in *LE* occurred again from 1991-1992, particularly in most of South America and northwestern North America; central Africa, southern Australia, eastern Europe, central Russia, and central Asia showed increases in *LE*. Very few decreases in *LE* occurred from 1992-1993, with only sections in southeast China and near the Great Lakes showing major decreases. Eastern Brazil and Argentina rebounded with an increase in *LE*; *LE* also increased in northwestern U.S., coastal Mexico, southeastern Asia, northern China, parts of northern Russia, and pockets of Africa. From 1993-1994, few major areas of *LE* increase occurred throughout the globe, limited to the Great Lakes, northern Canada, Nordic Europe, a strip in eastern Africa, southern China, and Japan.

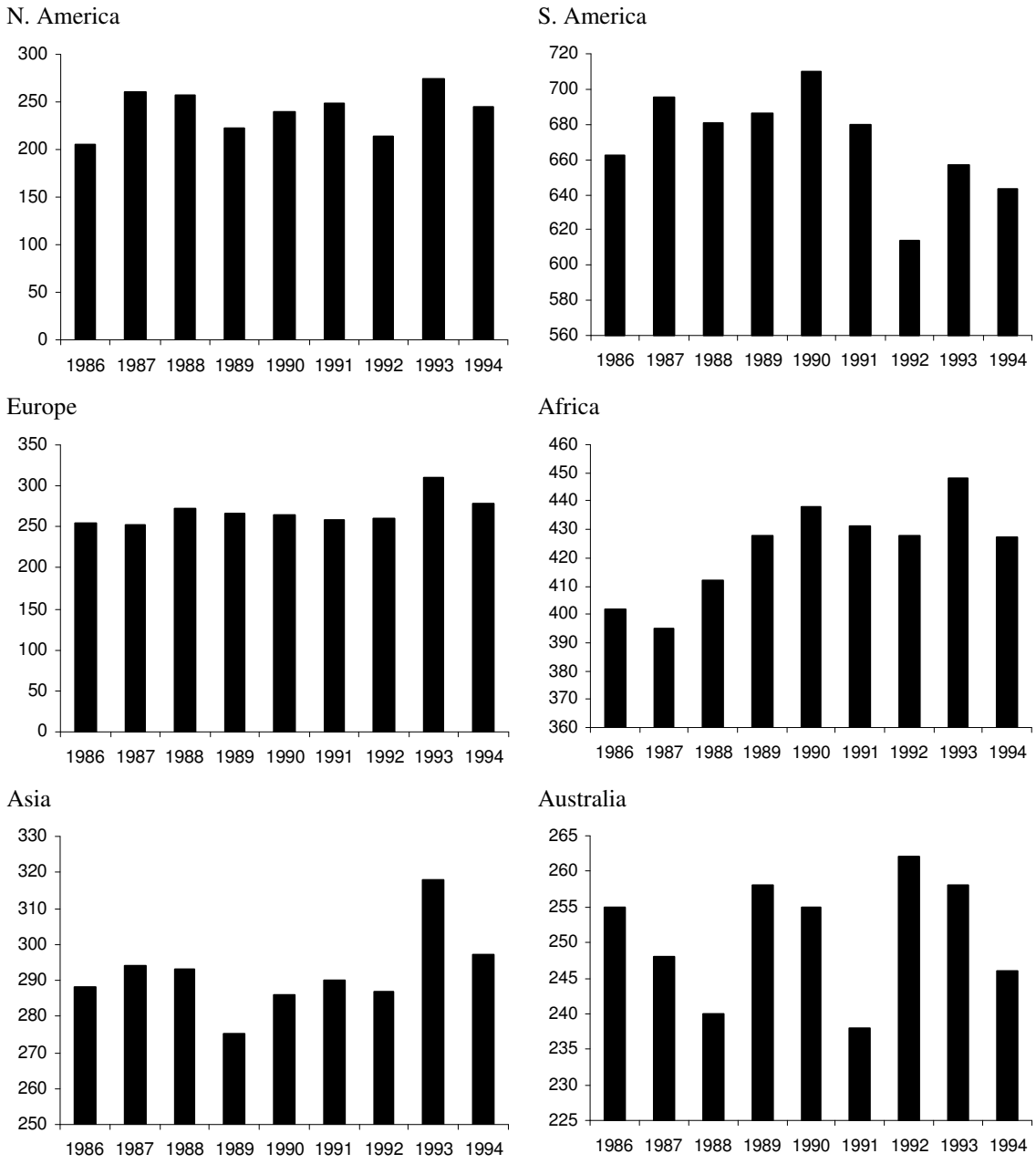

Figure 7. Continental averages (median) of total *LE* for each year (mm). S. America dominates continental *LE*, seconded by Africa. New Zealand is included with Australia.

On an average continental (7-continent model) basis, *LE* for S. America is nearly double that of all other continents, though Africa also shows high rates of *LE* (Figure 7). Medians were selected over means to limit the skew from extremes in pixel *LE*. The northern latitude continents tend to follow the same general temporal trend—generally

stable from 1986-1992 with a peak in 1993 and less so in 1994. The trend for N. America follows that of Europe at r^2=0.36 and Asia at r^2=0.54; Europe and Asia are correlated at r^2=0.62. The southern latitude continents do not correlate well with each other, however. S. America exhibits a sharp drop in 1992 and moderate recovery in 1993 and 1994. Africa had very low rates of *LE* in 1986 and 1987, but returned to stable levels in following years. Australia, which includes New Zealand, shows a repeating 3-year pattern of rise and fall in *LE*.

Runoff is calculated as the difference from our *LE* and ISLSCP-II precipitation (Figure 8). The runoff results are subject to the additional errors associated with the precipitation data; groundwater extraction and human manipulation of watersheds and runoff are not quantified. Across N. America, S. America, and Europe, precipitation is generally partitioned evenly, with *LE* and runoff nearly equal. *LE* rates are much higher across Africa, Asia and Australia, however; runoff for Africa tends to be near zero. Precipitation and *LE* are not correlated with each other from year to year.

As a means of comparison to other global models and estimates of *LE*, we compare our results with Choudhury et al. (1998), Henning (1989), and Budyko (1978). Our R_n from ISLSCP-II was higher across latitudinal bands possibly due to the 1 degree spatial resolution, which may have included high values of overlapping ocean R_n (Figure 9). The high values can be seen particularly around the equator, where the land-to-sea differentiation of R_n is greatest. We show R_n from 1986, though variation across latitudinal bands from year to year tends to be low. Our evaporative fraction (EF) of LE/R_n (1986) is higher as well (Figure 10). Our model tends to predict *LE* closer to the

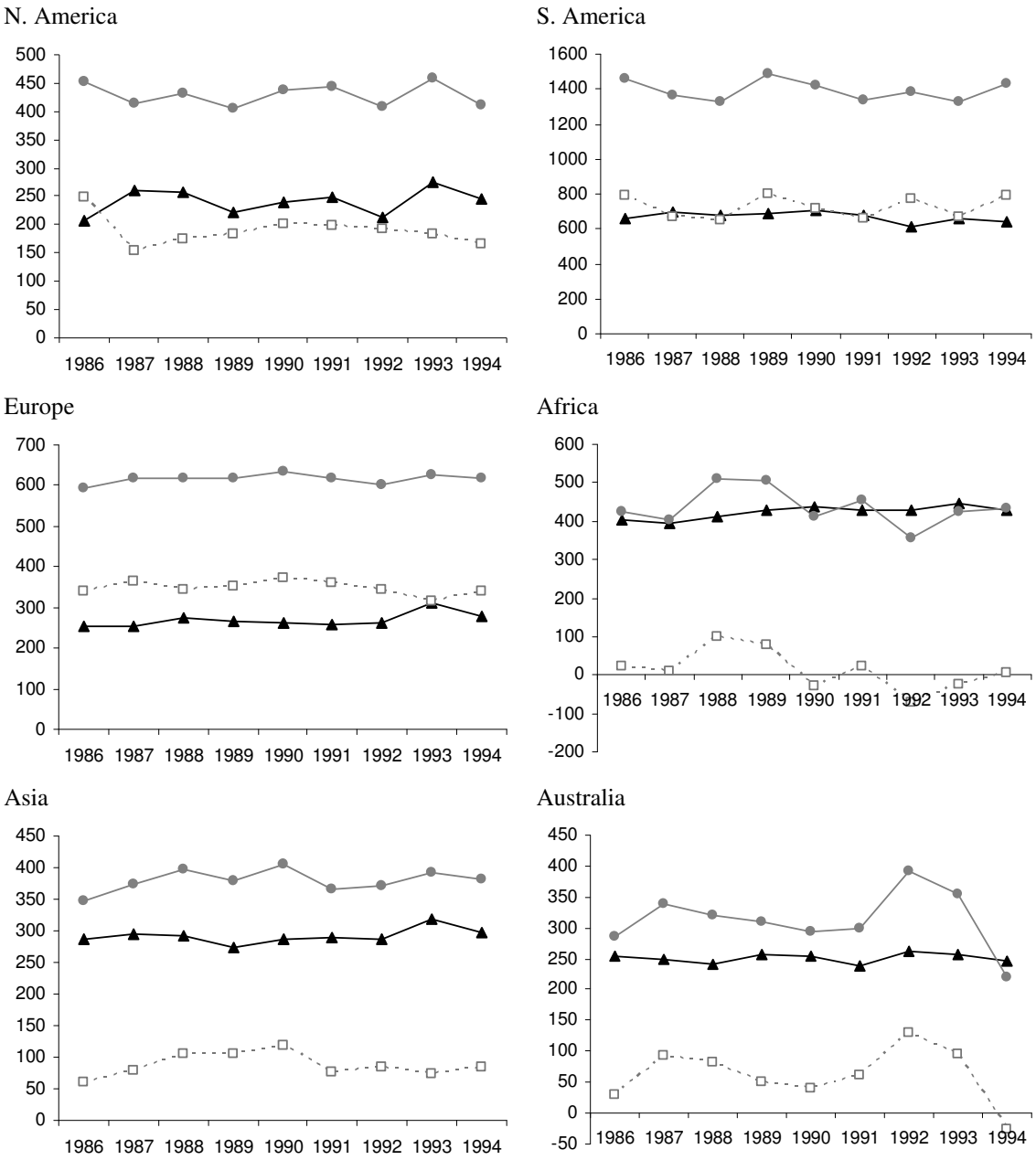

Figure 8. ISLSCP-II precipitation (filled circles, ●) with our *LE* (filled triangles, ▲) and calculated runoff (open squares, □) as a difference (mm). Groundwater extraction is excluded from runoff estimates.

potential rate at the equator and high southern latitudes relative to those previously published values.

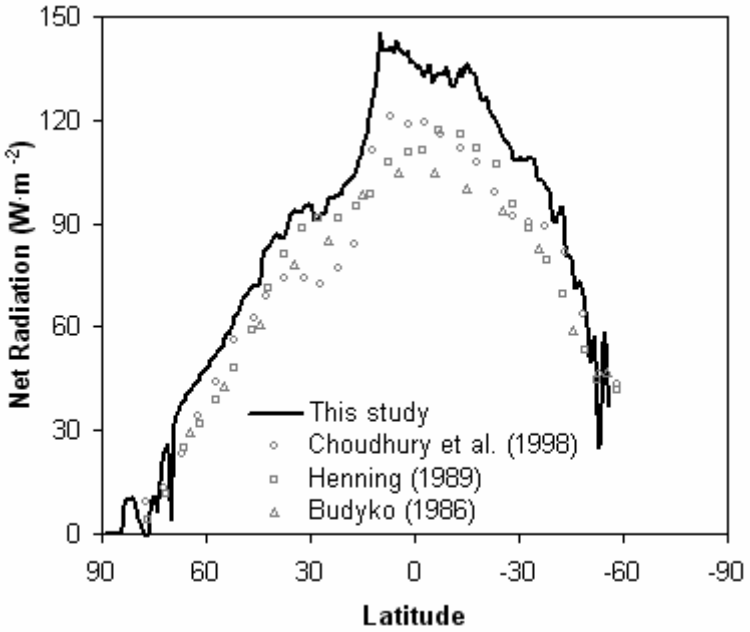

Figure 9. Net radiation (R_n) as the average across latitudinal bands (90ºN to -90ºS). We used the ISLSCP-II at 1 degree as a comparison with other published estimates.

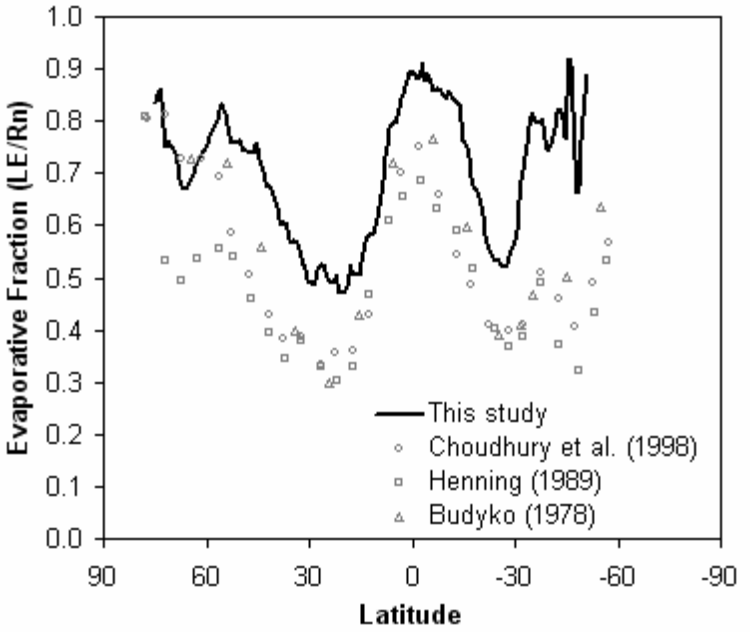

Figure 10. Evaporative Fraction (EF) as the average across latitudinal bands (90ºN to -90ºS). We show EF for year 1986 as a comparison with other published values.

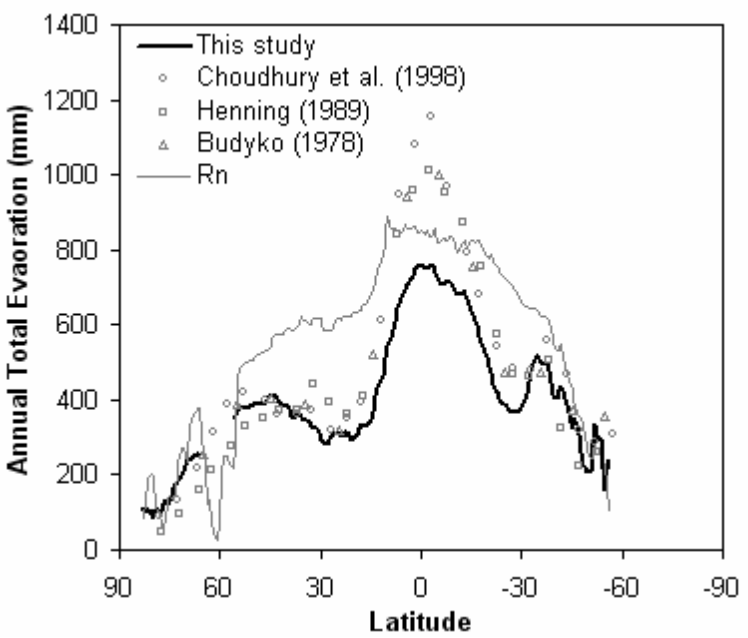

Figure 11. Annual total *LE* as the average across latitudinal bands (90ºN to -90ºS). We include our R_n from ISLSCP-II as a reference.

Annual total *LE* across latitudinal bands follows published values for all latitudes, except around the equator ±10 degrees, where our *LE* is much lower (Figure 11). We include R_n as a reference to show the maximum potential our *LE* could reach. The annual average *LE* per latitudinal band increases as we move south from the Arctic, decreases at the Tropic of Cancer, jumps up around the equator, decreases near the Tropic of Capricorn, increases again 10 degrees further south, then decreases to the Antarctic. The maximum seasonal *LE* at the equator is not necessarily significantly greater than that in the northern and southern hemisphere's annual peaks, but *LE* at the equator is consistently high year-round, unlike the seasonal shifts associated with beyond the tropics (Figure 12). The typical pattern of summer *LE* activity in the northern hemisphere, and opposite pattern for the southern hemisphere can be seen in Figure 12 over the course of the year (1994).

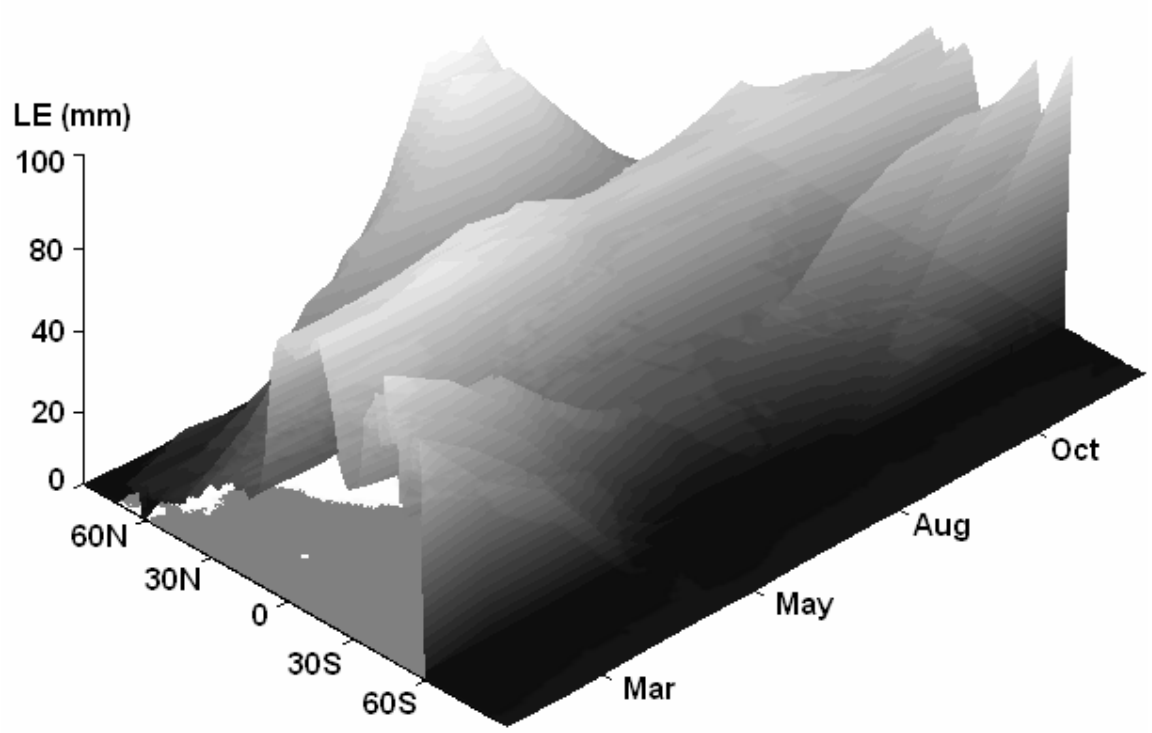

Figure 12. Monthly total *LE* as the average across latitudinal bands across year 1994.

Uncertainty analysis

The certainty of the model outputs result depends largely on the certainty of the input data. To execute the method of moments we first calculated the cross-correlations between the input parameters (Table 3). Associations with *SAVI* were equivalent to those with *NDVI*, so we report uncertainty only in *NDVI*. The cross-correlations were highest among *NDVI* and T_a, *NDVI* and *ea*, and T_a and *ea*. Next, we determined the error within

r^2	*NDVI*	R_n	T_a	*ea*
NDVI		0.03	0.85	0.97
R_n			0.17	0.05
T_a				0.92
ea				

Table 3. Cross-correlations between ISLSCP-II global input parameters for 1993.

each of the four inputs. The uncertainty varies spatially from pixel-to-pixel and region-to-region, and temporally from month-to-month and year-to-year, but we standardized the uncertainty assessment by testing our model by propagating uniform errors of 10% and 25% for each of the four input parameters. At 10% error in the mean of the four inputs, our model is in error at 11.3%. At 25 % error in the mean of the four inputs, our model is in error at 28.3%. The major result of the uncertainty analysis is that our model is heavily dependent on the accuracy of the R_n input data, as error in R_n contributes to the bulk of the model error; *NDVI* is second in total error contribution, followed by minimal error from T_a and *ea*. Errors in T_a and *ea* have minimal influence in our model because we treat these variables in a relative sense for ecophysiological constraints—our model is primarily dependent on the error associated with R_n. Thus, while the uncertainty analysis may suggest a linear dependency of the final error on that in each parameter, the bulk of the error, in fact, is dependent on R_n and to a lesser extent *NDVI*, but not T_a and *ea*.

Specific biomes and climatic areas are more sensitive to uncertainties in some input parameters than others (e.g., Mediterranean sites to T_a). We evaluated the per-pixel variation in the ISLSCP-II input parameters to our model with the Method of Moments to produce a global map of uncertainty in our global *LE* estimates (Figure 13). Lighter areas represent areas of high certainty, whereas darker areas represent areas of high uncertainty. Data shown in Figure 13 are for the average uncertainty for 1994. The largest area of uncertainty results from the high northern latitudinal striping, though spot areas/pixels occur throughout some of the continental edges due generally to missing pixels. Most areas fall within a mid- to low-range of uncertainty.

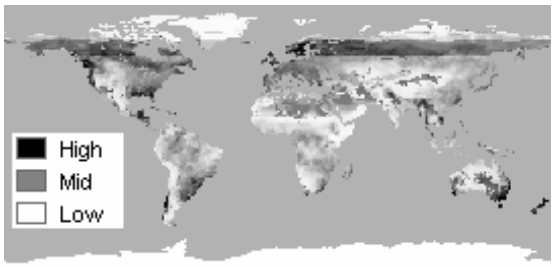

Figure 13. Method of Moments global output based on variability within ISLSCP-II input parameters for 1994. Lighter areas represent low uncertainty and darker areas represent high uncertatinty within the range of *LE* values.

Discussion

Major global climatic perturbations and influences, such as El Niño Southern Oscillation (SOI > 0.5), La Niña (SOI < -0.5), and volcanic eruptions such as Mt. Pinatubo in 1991, have caused alterations in the global water cycle and in the land-atmosphere water flux. In 1992, there were many climatic anomalies linked to the 1991 Mt. Pinatubo eruption (e.g., Hansen et al. 1992)—the second largest volcanic eruption of the century—which may have had an influence on mediating the effects of El Niño for 1992 (Self et al. 1997). The most significant departure from average *LE* inter-annually across our entire dataset occurred in S. America from 1991 to 1992 (Figure 7), where a drop of nearly 70 mm occurred between years due to the Mt. Pinatubo eruption in 1991, which added to any effects from El Niño years in 1991 and 1992. In Australia, however, 1992 marked the year of highest *LE* in our dataset. Although El Niño occurred in 1987, a rise in *LE* across both N. and S. America occurs from 1986 to 1987, corresponding with La Niña in 1988. A drop in *LE* from 1993 to 1994 occurred in both continents, when El Niño also occurred in 1994, but La Niña did not follow in 1995. From 1993-1994, declines in *LE* were evident on every single continent. 1993 marked the highest *LE* rates across N. America, Europe, Africa, and Asia (2nd highest for Australia).

Our partitioning of precipitation into *LE* and runoff generally agrees with previously published values (Gleick 1993; United Nations Environment Programme 2002). For instance, we calculate *LE* as 56% of precipitation in N. America and 48% in S. America, and Gleick/UNEP report it as 55% and 57%, respectively. The largest discrepancies are in our partition for Europe (44%), which underestimates Gleick/UNEP (65%), and our partition for Asia (77%), which overestimates Gleick/UNEP (55%). Our partition for the whole Eurasian continent (56%) is on par with that for Gleick/UNEP (57%), however. Our *LE* tends to be near equal to precipitation for Africa and Australia, and in some years exceeding precipitation, but this is on a continental basis, and Africa and Australia are dominated by the major deserts of the world in terms of area land cover. Hobbins et al. (2001) offer alternative explanations for errors in runoff calculations including groundwater pumping, groundwater flow, surface water diversions, disturbances, hydroclimatological errors, and spatial interpolation of climatic variables.

We are confident in the relative trends and absolute pixel values in the global products from our model, but any estimates smaller (sub-pixel) and larger (continental) contain some caveats. Sub-grid variability is so large that to derive particular site information from the 1 degree pixels could lead to large errors. Continental validation with precipitation and runoff data is also available, but unknown storage-to-*LE* partitioning and upscaling of runoff stream data to 1 degree pixels becomes problematic. ISLSCP-II provides runoff data, but explicitly states that these data are not recommended for model validation because the runoff data are based on a combination of model estimates and discharge measurements. Our next step is to run our model with finer spatial and temporal scale remote sensing data (e.g., global MODIS 1-km^2 data). We also

hesitate to report model estimates for very small spatial scales, such as at the tree or leaf levels. At these scales, parameters that are not included in our model, such as wind speed and resistances, become much more tightly coupled to *LE* (Jarvis and McNaughton 1986; McNaughton and Jarvis 1991). In the northern hemisphere, the continental sums are subject to interference from winter striping. Generally, we assumed values of striping to be close to zero, but these estimates are subject to the accuracy of the assumption. The continental sums for S. America, Africa, and Australia/New Zealand should be accurate, given a few errant pixels; southern hemispheric striping was restricted to Antarctica.

Our calculation for interception and LE_i may be subject to error associated with the monthly time step of the global model. Canopy evaporation occurs on very different temporal scales relative to that for LE_c or LE_s (Leuning et al. 1994). We set the rate of evaporation from intercepted canopy water at equal to potential *LE*, but our determination of precisely when the canopy is wet requires a minimum of 24 hours, and this becomes temporally scaled to monthly assumptions. Thus, it is likely that our calculation of *LE* may be underestimated in areas where LE_i is significant at small time scales.

Two problems are associated with the eddy flux validation: pixel-to-footprint mismatch and eddy flux energy balance closure. First, we used 1-km^2 MODIS *NDVI* pixels for eddy flux footprints that are amorphous polygons and change throughout the day and year. If the vegetation and environmental characteristics within the footprint are representative of the surrounding area in which the MODIS pixels contain, then the pixel-to-footprint match should be adequate. A forested eddy flux site adjacent to a clear cut, for example, would provide *NDVI* problems if both the forest and clear cut were included in the MODIS overlap. Thus, some error in our model estimates for the eddy flux sites

can be attributed to inaccurate *NDVI* estimates for the footprints. Second, our validation is dependent on the accuracy of the eddy flux *LE* measurements, but energy balance closure at these sites is imperfect due to complexity in wind variation, footprint representation, and sampling variability (Wilson et al. 2002). The eddy flux sites generally achieve about 90% closure with 10% of the variation unexplained. Therefore, the best any model could explain would be an r^2 of around 0.90, which is, in fact, generally what our model produces. Still, FLUXNET is the only globally contiguous network of uniform measurements over large areas, high temporal precision, and across a wide variety of hundreds of ecosystems with which to validate models such as ours, particularly with the focus on upscaling from ecosystem to global estimates; furthermore, FLUXNET is well-organized so that access to data remains relatively fluid.

Our model performs well across a wide variety of ecosystems, vegetation types, footprints, and climatic regimes. It is also simple enough so that it can potentially be run solely with remote sensing inputs, and global estimates are easily producible. We have assessed the uncertainty within our model based on the error associated with the input data, and we are confident in the absolute values of *LE* at an ecosystem scale and in the relative trends of *LE* at the global scale. Our model can easily be integrated into larger process models of global climate change, water balance, net primary productivity, floods and droughts, and irrigation. As closing the water budget worldwide is the ultimate objective of water and energy cycle research, we are advancing that much closer to achieving this objective.

Acknowledgments

The authors thank Greg Biging, Todd Dawson, Tandra Ghose, Jun-Hak Lee, and Carmel Levitan for help and assistance with this project. Three anonymous reviewers provided useful comments and insightful suggestions to this manuscript. We thank the many FLUXNET site investigators for allowing us to use their tower eddy flux data for the model validation: R. Coulter, A. Granier, D. Hollinger, A. Knohl, P. Lafleur, R. Leuning, T. Martin, J. Moncrieff, R. Monson, T. Myers, H. Schmid, S. Wofsy, and S. Yamamoto. The authors wish to thank the Distributed Active Archive Center (Code 902.2) at the Goddard Space Flight Center, Greenbelt, MD, 20771, for producing the AVHRR data in their present form and distributing them. The original AVHRR data products were produced under the NOAA/NASA Pathfinder program, by a processing team headed by Ms. Mary James of the Goddard Global Change Data Center; and the science algorithms were established by the AVHRR Land Science Working Group, chaired by Dr. John Townshend of the University of Maryland. Goddard's contributions to these activities were sponsored by NASA's Mission to Planet Earth program. Joshua Fisher was supported by NASA Headquarters under the Earth System Science Fellowship Grant NGT5-30473, and from a University of California, Berkeley Faculty Research Grant.

References

Baldocchi, D., Hicks, B., Meyers, T., 1988. Measuring biosphere-atmosphere exchanges of biologically related gases with micrometeorological methods. Ecology 69, 1331.

Barton, I.J., 1979. A parameterization of the evaporation from nonsaturated surfaces. Journal of Applied Meteorology 18, 43-47.

Baumgartner, A., Reichel, E., 1975. The World of Water balance. Elsevier, New York.

Bisht, G., Venturini, V., Islam, S., Jiang, L., 2005. Estimation of the net radiation using MODIS (Moderate Resolution Imaging Spectroradiometer). Remote Sensing of Environment 97, 52-67.

Black, T.A., 1979. Evapotranspiration from Douglas-fir stands exposed to soil water deficits. Water Resources Research 15 (1), 164-170.

Bouchet, R.J., 1963. Evapotranspiration re´elle evapotranspiration potentielle, signification climatique. Publ. 62, Int. Assoc. Sci. Hydrol., Berkeley, California.

Budyko, M.I., 1978. The heat balance of the Earth. In: J. Gribbin (Ed.), Climatic Change. Cambridge University Press, New York, pp. 85-113.

Choudhury, B.J., 1997. Global pattern of potential evaporation calculated from the Penman-Monteith equation using satellite and assimilated data. Remote Sensing of Environment 61, 64-81.

Choudhury, B.J., DiGirolamo, N.E., 1998. A biophysical process-based estimate of global land surface evaporation using satellite and ancillary data I. Model description and comparison with observations. Journal of Hydrology 205, 164-185.

Choudhury, B.J., DiGirolamo, N.E., Susskind, J., Darnell, W.L., Gupta, S.K., Asrar, G., 1998. A biophysical process-based estimate of global land surface evaporation using satellite and ancillary data II. Regional and global patterns of seasonal and annual variations. Journal of Hydrology 205, 186-204.

Czajkowski, K.P., Goward, S.N., Shirey, D., Walz, A., 2002. Thermal remote sensing of near-surface water vapor. Remote Sensing of Environment 79, 253-265.

Czajkowski, K.P., Mulhern, T., Goward, S., Cihlar, J., Dubayah, R., Prince, S., 1997. Biospheric environmental monitoring at BOREAS using AVHRR observations. Journal of Geophysical Research 102 (D24), 29651-29662.

Dalu, G., 1986. Satellite remote sensing of atmospheric water vapour. International Journal of Remote Sensing 7, 1089-1097.

Davies, J.A., Allen, C.D., 1973. Equilibrium, potential and actual evaporation from cropped surfaces in southern Ontario. Journal of Applied Meteorology 12, 649-657.

De Bruin, H.A.R., Holtslag, A.A.M., 1982. A simple parameterization of the surface fluxes of sensible and latent heat during daytime compared with the Penman-Monteith concept. Journal of Applied Meteorology 21, 1610-1621.

De Bruin, H.A.R., Stricker, J.N.M., 2000. Evaporation of grass under non-restricted soil moisture conditions. Hydrological Sciences Journal 45 (3), 391-406.

Eichinger, W.E., Parlange, M.B., Stricker, H., 1996. On the concept of equilibrium evaporation and the value of the Priestley-Taylor coefficient. Water Resources Research 32 (1), 161-164.

Entekhabi, D., Asrar, G.R., Betts, A.K., Beven, K.J., Bras, R.L., Duffy, C.J., Dunne, T., Koster, R.D., Lettenmaier, D.P., McLaughlin, D.B., Shuttleworth, W.J., van Genuchten, M.T., Wei, M.Y., Wood, E.F., 1999. An agenda for land surface hydrology research and a call for the second international hydrological decade. Bulletin of the American Meteorological Society 80 (10), 2043-2058.

Federer, C.A., Vörösmarty, C., Fekete, B., 2003. Sensitivity of annual evaporation to soil and root properties in two models of contrasting complexity. Journal of Hydrometeorology 4, 1276-1290.

Federer, C.A., Vörösmarty, C.J., Fekete, B., 1996. Intercomparison of methods for calculating potential evaporation in regional and global water balance models. Water Resources Research 32 (7), 2315-2321.

Fisher, J.B., Debiase, T.A., Qi, Y., Xu, M., Goldstein, A.H., 2005. Evapotranspiration models compared on a Sierra Nevada forest ecosystem. Environmental Modelling & Software 20 (6), 783-796.

Flanagan, L.B., Wever, L.A., Carlson, P.J., 2002. Seasonal and interannual variation in carbon dioxide exchange and carbon balance in a northern temperate grassland. Global Change Biology 8 (7), 599-615.

Flint, A.L., Childs, S.W., 1991. Use of the Priestley-Taylor evaporation equation for soil water limited conditions in a small forest clearcut. Agricultural and Forest Meteorology 56, 247-260.

Gao, X., A.R., H., Ni, W.G., Miura, T., 2000. Optical-biophysical relationships of vegetation spectra without background contamination. Remote Sensing of Environment 74 (3), 609-620.

Giles, D.G., Black, T.A., Spittlehouse, D.L., 1984. Determination of growing season soil water deficits on a forested slope using water balance analysis. Canadian Journal of Forest Research 15, 107-114.

Gleick, P.H., 1993. Water in Crisis. Oxford University Press, New York.

Goetz, S.J., Halthore, R., Hall, F.G., Markham, B., 1995. Surface temperature retrieval in a temperature grassland with multi-resolution sensors. Journal of Geophysical Research 100, 25397-25410.

Goldstein, A.H., Hultman, N.E., Fracheboud, J.M., Bauer, M.R., Panek, J.A., Xu, M., Qi, Y., Guenther, A.B., Baugh, W., 2000. Effects of climate variability on the carbon dioxide, water, and sensible heat fluxes above a ponderosa pine plantation in the Sierra Nevada (CA). Agricultural and Forest Meteorology 101, 113-129.

Gordon, L.J., Steffen, W., Jonsson, B.F., Folke, C., Falkenmark, M., Johannessen, A., 2005. Human modification of global water vapor flows from the land surface. Proceedings of the National Academy of Sciences of the United States of America 102 (21), 7612-7617.

Granier, A., Biron, P., Lemoine, D., 2000. Water balance, transpiration and canopy conductance in two beech stands. Agricultural and Forest Meteorology 100 (4), 291-308.

Hall, F.G., Collatz, G.J., Los, S.O., Brown, E., Colstoun, D.E., Landis, D. (Eds.), 2005. ISLSCP Initiative II: DVD/CD-ROM. NASA.

Hansen, J., Lacis, A., Ruedy, R., Sato, M., 1992. Potential climate impact of Mount-Pinatubo eruption. Geophysical Research Letters 19 (2), 215-218.

Hansen, L.P., 1982. Large sample properties of generalized method of moments estimators. Econometrica 50 (4), 1029-1054.

Hare, F.K., 1980. Long-term annual surface heat and water balances over Canada and the United States south of 60 N: Reconciliation of precipitation, run-off and temperature fields. Atmosphere-Ocean 18 (2), 127-153.

Henderson-Sellers, A., Pitman, A.J., Love, P.K., Irannejad, P., Chen, T.H., 1995. The project for intercomparison of land-surface parameterization schemes (PILPS): Phases 2 and 3. Bulletin of the American Meteorological Society 76 (4), 489-503.

Henning, D., 1989. Atlas of the Surface Heat Balance of the Continents, Gebruder Borntraeger, Berlin.

Hobbins, M.T., Ramírez, J.A., Brown, T.C., Claessens, L.H.J.M., 2001. The complementary relationship in estimation of regional evapotranspiration: The

Complementary Relationship Areal Evapotranspiration and Advection-Aridity models. Water Resources Research 37 (5), 1367-1387.
Hollinger, D.Y., Goltz, S.M., Davidson, E.A., Lee, J.T., Tu, K., Valentine, H.T., 1999. Seasonal patterns and environmental control of carbon dioxide and water vapour exchange in an ecotonal boreal forest. Global Change Biology 5 (8), 891-902.
Houborg, R.M., Soegaard, H., 2004. Regional simulation of ecosystem CO2 and water vapor exchange for agricultural land using NOAA AVHRR and Terra MODIS satellite data. Application to Zealand, Denmark. Remote Sensing of Environment 93 (1-2), 150-167.
Huete, A., Didan, K., Miura, T., Rodriguez, E.P., Gao, X., Ferreira, L.G., 2002. Overview of the radiometric and biophysical performance of the MODIS vegetation indices. Remote Sensing of Environment 83 (1-2), 195-213.
Huete, A.R., 1988. A soil-adjusted vegetation index (SAVI). Remote Sensing of Environment 25 (3), 295-309.
Irmak, S., Irmak, A., Jones, J.W., Howell, T.A., Jacobs, J.M., Allen, R.G., Hoogenboom, G., 2003. Predicting daily net radiation using minimum climatological data. Journal of Irrigation and Drainage Engineering 129 (4), 256-269.
Jarvis, P.G., McNaughton, K.G., 1986. Stomatal control of transpiration: scaling up from leaf to region. Advances in Ecological Research 15, 1-49.
Jin, M., Dickinson, R.E., Vogelmann, A.M., 1997. A comparison of CCM2-BATS skin temperature and surface air temperature with satellite and surface observations. Journal of Climate 10, 1505-1524.
June, T., Evans, J.R., Farquhar, G.D., 2004. A simple new equation for the reversible temperature dependence of photosynthetic electron transport: a study on soybean leaf. Functional Plant Biology 31 (3), 275-283.
Jury, W.A., Tanner, C.B., 1975. Advection modification of the Priestley and Taylor evapotranspiration formula. Agron. J. 67 (840-842).
Kalluri, S.N., Dubayah, R.O., 1995. Comparison of atmospheric correction models for thermal bands of the Advanced Very High Resolution Radiometer over FIFE. Journal of Geophysical Research 100 (D12), 25411-25418.
Kergoat, L., Lafont, S., Douville, H., Berthelot, B., Dedieu, G., Planton, S., Royer, J.F., 2002. Impact of doubled CO_2 on global-scale leaf area index and evapotranspiration: Conflicting stomatal conductance and LAI responses. Journal of Geophysical Research 107 (D24), 1-18.
Kidwell, K., 1991. NOAA Polar Orbiter Data User's Guide. NCDC/SDSD., National Climatic Data Center, Washington, DC.
Kimball, J.S., Thornton, P.E., White, M.A., Running, S.W., 1997. Simulating forest productivity and surface-atmosphere carbon exchange in the BOREAS study region. Tree Physiology 17, 589-599.
Kite, G., 1998. Integration of forest ecosystem and climatic models with a hydrologic model. Journal of the American Water Resources Association 34 (4), 743-753.
Knohl, A., Schulze, E.D., Kolle, O., Buchmann, N., 2003. Large carbon uptake by an unmanaged 250-year-old deciduous forest in Central Germany. Agricultural and Forest Meteorology 118 (3-4), 151-167.

Kustas, W.P., Daughtry, C.S.T., Vanoevelen, P.J., 1993. Analytical treatment of the relationships between soil heat flux/net radiation ratio and vegetation indices. Remote Sensing of Environment 46 (3), 319-330.

Kustas, W.P., Norman, J.M., 1996. Use of remote sensing for evapotranspiration monitoring over land surfaces. Hydrological Sciences Journal 41 (4), 495-516.

Lakshmi, V., Small, J., Goetz, S., 2002. Comparison of surface meteorological variables from TOVS and AVHRR. Remote Sensing of Environment 79, 176-188.

Lakshmi, V., Susskind, J., 2000. Comparison of TOVS derived land surface variables with ground observations. Journal of Geophysical Research 105 (D2), 2179-2190.

Lawrence, D.M., Slingo, J.M., 2004. An annual cycle of vegetation in a GCM. Part I: implementation and impact on evaporation. Climate Dynamics 22 (2-3), 87-105.

Leuning, R., Cleugh, H.A., Zegelin, S.J., Hughes, D., 2005. Carbon and water fluxes over a temperate Eucalyptus forest and a tropical wet/dry savanna in Australia: measurements and comparison with MODIS remote sensing estimates. Agricultural and Forest Meteorology 129 (3-4), 151-173.

Leuning, R., Condon, A.G., Dunin, F.X., Zegelin, S., Denmead, O.T., 1994. Rainfall interception and evaporation from soil below a wheat canopy. Agricultural and Forest Meteorology 67 (3-4), 221-238.

Liang, X., Guo, J., Leung, L.R., 2004. Assessment of the effects of spatial resolutions on daily water flux simulations. Journal of Hydrology 298, 287-310.

Liang, X., Lettenmaier, D.P., Wood, E., 1996. One-dimensional statistical dynamic representation of subgrid spatial variability of precipitation in the two-layer variable infiltration capacity model. Journal of Geophysical Research 101 (D16), 21403-21422.

Liang, X., Lettenmaier, D.P., Wood, E., Burges, S.J., 1994. A simple hydrologically based model of land surface water and energy fluxes for general circulation models. Journal of Geophysical Research 99 (D7), 14415-14428.

Los, S.O., Collatz, G.J., Malmstrom, C.M., Pollack, N.H., DeFries, R.S., Bounoua, L., Parris, M.T., Tucker, C.J., Dazlich, D.A., 2000. A global 9-year biophysical land surface dataset from NOAA AVHRR data. Journal of Hydrometeorology 1, 183-199.

Madsen, H., Rasmussen, P.F., Rosbjerg, D., 1997. Comparison of annual maximum series and partial duration series methods for modeling extreme hydrologic events 1. At-site modeling. Water Resources Research 33 (4), 747-757.

Martin, T.A., Brown, K.J., Cermak, J., Ceulemans, R., Kucera, J., Meinzer, F.C., Rombold, J.S., Sprugel, D.G., Hinckley, T.M., 1997. Crown conductance and tree and stand transpiration in a second-growth Abies amabilis forest. Canadian Journal of Forest Research 27 (6), 797-808.

Maurer, E.P., Wood, A.W., Adam, J.C., Lettenmaier, D.P., Nijssen, B., 2002. A long-term hydrologically based dataset of land surface fluxes and states for the conterminous United States. Journal of Climate 15 (22), 3237-3251.

McNaughton, K.G., Black, T.A., 1973. A study of evapotranspiration from a Douglas Fir forest using the energy balance approach. Water Resources Research 9, 1579-1590.

McNaughton, K.G., Jarvis, P.G., 1991. Effects of spatial scale on stomatal control of transpiration. Agricultural and Forest Meteorology 54 (2-4), 279-302.

McNaughton, K.G., Spriggs, T.W., 1986. A mixed-layer model for regional evaporation. Boundary-Layer Meteorology 34 (3), 243-262.

Mintz, Y., Walker, G.K., 1993. Global fields of soil moisture and land surface evapotranspiration dervied from observed precipitation and surface air temperature. Journal of Applied Meteorology 32, 1305-1334.

Moncrieff, J.B., Massheder, J.M., De Bruin, H.A.R., Elbers, J., Friborg, T., Heusinkveld, B., Kabat, P., Scott, S., Soegaard, H., Verhoef, A., 1997. A system to measure surface fluxes of momentum, sensible heat, water vapour and carbon dioxide. Journal of Hydrology 189 (1-4), 589-611.

Monson, R.K., Turnipseed, A.A., Sparks, J.P., Harley, P.C., Scott-Denton, L.E., Sparks, K., Huxman, T.E., 2002. Carbon sequestration in a high-elevation, subalpine forest. Global Change Biology 8 (5), 459-478.

Monteith, J.L., 1965. Evaporation and the environment. Symposium of the Society of Exploratory Biology 19, 205-234.

Morton, F.I., 1983. Operational estimates of areal evapotranspiration and their significance to the science and practice of hydrology. Journal of Hydrology 66, 1-76.

Motell, C., Porter, J., Foster, J., Bevis, M., Businger, S., 2002. Comparison of precipitable water over Hawaii using AVHRR-based split-window techniques, GPS and radiosondes. International Journal of Remote Sensing 23 (11), 2335-2339.

Mukammal, E.I., Neumann, H.H., 1977. Application of the Priestley-Taylor evaporation model to assess the influence of soil moisture on the evaporation from a large weighing lysimter and class A pan. Boundary-Layer Meteorology 12, 243-256.

Myneni, R.B., Keeling, C.D., Tucker, C.J., Asrar, G., Nemani, R.R., 1997. Increased plant growth in the northern high latitudes between 1981-1991. Nature 386, 1380-1393.

New, M., Hulme, M., Jones, P., 1999. Representing twentieth-century space-time climate variability. Part I: Development of a 1961-90 mean monthly terrestrial climatology. Journal of Climate 12, 829-856.

New, M., Hulme, M., Jones, P., 2000. Representing twentieth-century space-time climate variability. Part II: Development of 1901-1996 monthly grids of terrestrial surface climate. Journal of Climate 13 (13), 2217-2238.

Nishida, K., Nemani, R.R., Running, S.W., Glassy, J.M., 2003. An operational remote sensing algorithm of land surface evaporation. Journal of Geophysical Research-Atmospheres 108 (D9), 4270.

Norman, J.M., Kustas, W.P., Humes, K.S., 1995. Source approach for estimating soil and vegetation energy fluxes in observations of directional radiometric surface-temperature. Agricultural and Forest Meteorology 77 (3-4), 263-293.

Pinker, R.T., Laszlo, I., 1992. Modeling surface solar irradiance for satellite applications on a global scale. Journal of Applied Meteorology 31, 194-211.

Potter, C.S., Randerson, J.T., Field, C.B., Matson, P.A., Vitousek, P.M., Mooney, H.A., Klooster, S.A., 1993. Terrestrial ecosystem production: a process based model based on global satellite and surface data. Global Biogeochemical Cycles 7 (4), 811-841.

Priestley, C.H.B., Taylor, R.J., 1972. On the assessment of surface heat flux and evaporation using large scale parameters. Monthly Weather Review 100, 81-92.

Prince, S.D., Goetz, S.J., Dubayah, R.O., Czajkowski, K.P., Thawley, M., 1998. Inference of surface and air temperature, atmospheric precipitable water and vapor pressure deficit using AVHRR satellite observations: validation of algorithms. Journal of Hydrology 212-213, 230-250.

Rossow, W.B., Walker, A.W., Beuschel, D.E., Roiter, M.D., 1996. International Satellite Cloud Climatology Project (ISCCP): Documentation of new cloud data sets. WMO/TD-No. 737, World Meteorological Organization.

Running, S.W., Thornton, P.E., Nemani, R.R., Glassy, J.M., 2000. Global Terrestrial Gross and Net Primary Productivity from the Earth Observing System. In: O.E. Sala, R.B. Jackson, H.A. Mooney and R.W. Howarth (Eds.), Methods in Ecosystem Science. Springer-Verlag New York, Inc., New York, pp. 44-57.

Rushdi, A.M., Kafrawy, K.F., 1988. Uncertainty propagation in fault-tree analyses using an exact method of moments. Microelectronic Reliability 28 (6), 945-965.

Schmid, H.P., Grimmond, C.S.B., Cropley, F., Offerle, B., Su, H.B., 2000. Measurements of CO2 and energy fluxes over a mixed hardwood forest in the mid-western United States. Agricultural and Forest Meteorology 103 (4), 357-374.

Schubert, S., Suarez, M., Park, C.K., Moorthi, S., 1993. GCM simulations of intraseasonal variability in the Pacific North-American region. Journal of the Atmospheric Sciences 50 (13), 1991-2007.

Self, S., Rampino, M.R., Zhao, J., Katz, M.G., 1997. Volcanic aerosol perturbations and strong El Nino events: No general correlation. Geophysical Research Letters 24 (10), 1247-1250.

Sellers, P.J., Los, S.O., Tucker, C.J., Justice, C.O., Dazlich, D.A., Collatz, G.J., Randall, D.A., 1994. A global 1*1 degree NDVI data set for climate studies. Part 2: The generation of global fields of terrestrial biophysical parameters from the NDVI. International Journal of Remote Sensing 15 (17), 3519-3545.

Sellers, P.J., Meeson, B.W., Hall, F.G., Asrar, G., Murphy, R.E., Schiffer, R.A., Bretherton, F.P., Dickinson, R.E., Ellingson, R.G., Field, C.B., Huemmrich, K.F., Justice, C.O., Melack, J.M., Roulet, N.T., Schimel, D.S., Try, P.D., 1995. Remote sensing of the land surface for studies of global change: Models - algorithms - experiments. Remote Sensing of Environment 51 (1), 3-26.

Shuttleworth, W.J., Calder, I.R., 1979. Has the Priestley-Taylor equation any relevance to forest evaporation? Journal of Applied Meteorology 18, 639-646.

Shuttleworth, W.J., Gash, J.H., Lloyd, C.R., Moore, C.J., Roberts, J., Filho, A.O.M., Fisch, G., Filho, V.P.S., Ribeiro, M.N.G., Molion, L.C.B., Sa, L.D.A., Nobre, J.C.A., Cabral, O.M.R., Patel, S.R., De Moraes, J.C., 1984. Eddy correlation measurements of energy partition for Amazonian forest. Quarterly Journal of the Royal Meteorological Society 110, 1143-1162.

Shuttleworth, W.J., Wallace, J.S., 1985. Evaporation from sparse crops-an energy combination theory. Quarterly Journal of the Royal Meteorological Society 111, 839-855.

Sobrino, J.A., El Kharraz, J., 2003. Surface temperature and water vapour retrieval from MODIS data. International Journal of Remote Sensing 24 (24), 5161-5182.

Stackhouse, P.W., Gupta, S.K., Cox, S.J., Chiacchio, M., Mikovitz, J.C., 2000. The WCRP/GEWEX Surface Radiation Budget Project Release 2: An assessment of surface fluxes at 1 degree resolution. In: W.L. Smith and Y.M. Timofeyev (Eds.), IRS 2000: Current Problems in Atmospheric Radiation. International Radiation Symposium, St. Petersburg, Russia, pp. 24-29.

Steven, M.D., Malthus, T.J., Baret, F., Xu, H., Chopping, M.J., 2003. Intercalibration of vegetation indices from different sensors systems. Remote Sensing of Environment 88, 412-422.

Stewart, R.B., Rouse, W.R., 1977. Substantiation of the Priestley and Taylor parameter alpha=1.26 for potential evaporation in high latitudes. Journal of Applied Meteorology 16, 649-650.

Suleiman, A.A., Ritchie, J.T., 2003. Modeling soil water redistribution during second-stage evaporation. Soil Science Society of America Journal 67 (2), 377-386.

Tateishi, R., Ahn, C.H., 1996. Mapping evapotranspiration and water balance for global land surfaces. Journal of Photogrammetry & Remote Sensing 51, 209-215.

Thornthwaite, C.W., 1948. An approach toward a rational classification of climate. Geographical Review 38, 55-94.

Townshend, J.G., Justice, C.O., 1986. Analysis of the dynamics of African vegetation using the normalized difference vegetation index. International Journal of Remote Sensing 7 (11), 1435-1445.

Turner, M.G., 1989. Landscape Ecology: The Effect of Pattern on Process. Annual Review of Ecological Systems 20, 171-197.

United Nations Environment Programme, 2002. The World's Surface Water: Precipitation, Evaporation and Runoff by Region.

Vörösmarty, C.J., Federer, C.A., Schloss, A.L., 1998. Potential evaporation functions compared on US watersheds: Possible implications for global-scale water balance and terrestrial ecosystem modeling. Journal of Hydrology 207, 147-169.

Warnick, K.F., Chew, W.C., 2004. Error analysis of the moment method. IEEE Antennas and Propagation Magazine 46 (6), 38-53.

Wilson, K., Goldstein, A., Falge, E., Aubinet, M., Baldocchi, D., Berbigier, P., Bernhofer, C., Ceulemans, R., Dolman, H., Field, C., Grelle, A., Ibrom, A., Law, B.E., Kowalski, A., Meyers, T., Moncrieff, J., Monson, R., Oechel, W., Tenhunen, J., Valentini, R., Verma, S., 2002. Energy balance closure at FLUXNET sites. Agricultural and Forest Meteorology 113 (1-4), 223-243.

Wofsy, S.C., Goulden, M.L., Munger, J.W., Fan, S.M., Bakwin, P.S., Daube, B.C., Bassow, S.L., Bazzaz, F.A., 1993. Net exchange of CO_2 in a mid-latitude forest. Science 260 (5112), 1314-1317.

Xu, L.K., Baldocchi, D.D., 2004. Seasonal variation in carbon dioxide exchange over a Mediterranean annual grassland in California. Agricultural and Forest Meteorology 123 (1-2), 79-96.

Chapter 4

Data Producers and Data Users: Misuse, Mistrust, and the Advancement of Science

Abstract Although data sharing is an increasingly common practice in contemporary science, there has been no empirical study of the practice of data sharing by scientists. Of particular interest is how scientists self-organize to manage the property issues associated with data sharing. These issues, lying at the intersection of common property theory and intellectual property theory, have been addressed conceptually by Hess and Ostrom (2003). Using their framework and Ostrom's (1990) design principles, we analyze micro-practices around property rights and data sharing, identifying the factors influencing why specific cases of data sharing have led to conflict or successful sharing. The data for this exploratory study are from two data sharing communities in the environmental sciences: FLUXNET—a well-organized network of scientists who measure meteorological fluxes, and the remote sensing data community—a loosely organized group of researchers who work with satellite or aerial imagery. We find that intellectual property law encompasses macro-level legal frameworks that constrain micro level practice, while common property theory illuminates micro-level practice.

Introduction

"If I have seen further," Isaac Newton wrote, "it is by standing upon the shoulders of giants[1]." Today as scientists ask global questions that require global data, collaboration and building on the work of others are still essential to seeing further. The expense and complexity of the data required by researchers working across multiple disciplines at increasingly large spatial scales necessitate the distributed collection and analysis of data since no one individual or institution can collect and analyze that much data. Most of the literature on data sharing focus primarily on technical infrastructure rather than on end-users (Boyle 1996; Kollock and Smith 1996; Huberman and Lukose 1997; Noonan 1998; Lessig 1999; Hess and Ostrom 2003; Frischmann 2005). Our focus is on the property issues that arise when data are shared by data producers and data users. This matter is a practical issue because misuse of data by data users and mistrust by data producers can damage these collaborative links and interfere with scientific advancement. Of particular importance in data sharing arrangements are attribution of credit to data producers (often in the form of co-authorship) and control over the right to publish analysis of a data set as a means of quality control of data analysis. These issues arise in the context of communication among individuals and groups with differing power, politics, and knowledge of rights, rules and regulations regarding data sharing.

The question of property rights in shared data is situated intellectually at the intersection of common property theory and intellectual property theory. Common property theory provides insights into how (often self-organizing) groups of people develop, implement and sustain collective management regimes for resources they use in

[1] Isaac Newton (1642-1727), Letter to Robert Hooke, 5 February 1676, in H. W. Turnbull (ed.) Correspondence of Isaac Newton, vol. 1 (1959) p. 416.

common (Ostrom 1990). Common property theory is typically applied to physically exhaustible natural resources such as pastures, irrigation systems and fish stocks. Intellectual property is an overarching term that encompasses different types of government-granted exclusive powers of control and use over non-exhaustible and intangible goods. These rights cover inventions, creative works, identifying insignia, and some forms of confidential information. They are usually created through statutory law and treaty (Fisher 1999).

Aspects of data sharing appear piecemeal in the literature in each of these theories. Reichman and Samuelson (1997) and Rai (1999) have written on data as a form of intellectual property. Questions of the public domain have been addressed in the intellectual property literature (Hughes 1988; Litman 1990; Posey et al. 1995; May 2000; Drazen 2002) without reference to common property theory. In a conceptual piece on common property theory, Hess and Ostrom (2003) identified properties of data sharing that are similar to common pool resources (hereinafter CPR). But, despite this conceptual signpost, and while common property is clearly relevant to the regimes data-sharing communities create to share and regulate the transfer of data, there has been no published empirical study of data sharing.

We investigate the link of common property and intellectual property theory in the environmental sciences where data sharing is a common practice. The governance of rights to data occurs at three scales: 1) some rights to data are governed by international treaties or national laws; 2) some are affected by policies of the associations or collectives of data producers and users (including formal policies and informal norms) or

the institutions with which they are affiliated; 3) some are the results of negotiations between an individual producer and user. In many cases governance of rights to data may consist of nested property regimes. To complicate matters, data may be treated as a commodity or as a shared resource.

Our research assesses micro-level practices in the governance of property rights issues involved in data sharing. We explore the dynamics of data sharing as applied to CPR theory and the Hess and Ostrom (2003) update. Our analysis treats data as CPR because agents work to produce, use and regulate the use of the resource in data. While the literature in these sciences supports the benefits of data sharing, scientists themselves have given relatively little formal attention to shared data outside of website statements of institutional guidelines. Questions about property abound in the relations between data producers and data users. We are particularly interested in the emergence of rules of data sharing, either in written form or unwritten, formal or informal, by explicit common understanding or nonexistent, and what effect these types of rules may have on conflict. Under what conditions are data shared successfully? We define "successful" as without conflict or irresolvable disagreement, and vice versa for "unsuccessful." The cost of unsuccessful data sharing follows the concept of the "anti-commons," which argues that exclusive rights held by individual users or producers can block advancements in the field as a whole (Heller 1998; Heller and Eisenberg 1998). We examine individual dyadic relationships between data users and data producers as parts of a whole community interested in keeping the flow of data open. Individual outcomes affect the pool of data available to the whole community so we therefore examine how collective decision rules are made. A host of questions arise only some of which we address in this

research. What rights do data producers have over their data? What rights do data users have concerning data analysis, manipulation, distribution, modification, and publication? Do the rights provide enough protection from data misuse or analysis ownership and reward such as monetary, prestige, and publication for the continuation of data production? What are the sanctions against those who bend or break the rules? What is the system under which data access is allowed? Under what conditions are data commoditized or treated as common property? Our hypothesis is that successful data sharing involves rule making—either as explicitly written contracts, codes of conduct or mutual understanding.

We undertook a micro-level empirical study of the behavior of individual data users and producers in two data sharing communities to test the hypothesis that successful data sharing involves rule making—either as explicitly written contracts, codes of conduct or mutual understanding. FLUXNET is a well-organized network of scientists who measure meteorological fluxes (e.g., Key and Schweiger 1998; Baldocchi et al. 2001). The remote sensing data community is a loosely organized group of researchers who work with satellite or aerial imagery (e.g., Singh 1989; Rogers et al. 2002)[2]. Collection and processing of these data are very expensive. Data producers need to expand their labs into the labs of others by guiding others to analyze their data (Latour 1995). This article proceeds in two parts. First we discuss how common property theory and intellectual property theory might be applied to data sharing. Then we present our case study.

[2] For discussion on remote sensing data as CPR, see Lele, S. (2001), "Pixelising the Commons" and "Commonising the Pixel": Boon or bane? *The Common Property Resource Digest*, 58, 1-3.

Common Pool Resources

Empirically, common property theory focuses on common pool resources (CPR). CPR are defined as "a natural or man-made resource system that is sufficiently large as to make it costly (but not impossible) to exclude potential beneficiaries from obtaining benefits from its use" (Ostrom 1990: pg. 30). They refer to a combination of public and private goods whereby the resource is potentially at risk to open-access overconsumption, degradation and depletion, but ownership and maintenance by a community can serve to improve the resource, monitor use, and sanction rule-breaking. Common property theory crosses both disciplinary and theoretical boundaries (McCay and Acheson 1987; Rose 2002). The concept of commons governance that is most accessible to and applicable by practitioners in the biophysical sciences is Elinor Ostrom's (1990) discussion of "design principles" in her classic[3] *Governing the Commons*. Ostrom identified each design principle (clearly defined boundaries, appropriation rules related to local conditions, collective-choice arrangements, monitoring, graduated sanctions, conflict-resolution mechanisms, and minimal recognition of rights to organize) as "an essential element or condition that helps to account for the success of these institutions in sustaining the CPRs and gaining the compliance of generation after generation of appropriators to the rules of use" (Ostrom 1990: pg. 90). The design principles are conditions associated with the success of collective management of natural resources by groups of users. Ostrom (and subsequent work) has shown that the importance of a particular design principle to successful management is highly contingent. The design principles have been used to analyze common property systems such as fisheries (Yandle 2003), forestry (Morrow and Hull 1996; Sekher 2001), and irrigation (Sarker and Itoh 2001) as well as large-scale

[3] Cited over 3,000 times--http://scholar.google.com

resources such as the seas, space and the atmosphere in a "global commons" (Buck 1998). We follow these studies in application of the design principles, but to a different type of resource—the intellectual property resource.

The concept of usufructary rights (e.g., Agarwal 1997; Schroeder 1997)—that is, the right to use something that is the property of another as long as the property is not damaged or destroyed—is key to common property theory (Schlager and Ostrom 1992). The distribution of usufructary rights can lead to highly complex property relations (Fortmann 1988). Different rights holders can have rights to the same resource at different times. They may have rights to different parts of the same resource at the same time. Further, the numbers of right holders may increase over time. With this basic terminology defined, we turn our attention to examining how the design principles could be applied to shared data, a task that is not necessarily straightforward.

Clearly defined boundaries—"Individuals or households who have rights to withdraw resource units from the CPR must be clearly defined, as must the boundaries of the CPR itself"—tend to be physically defined for natural resources though not all natural resources are readily bounded. Ostrom observed that some boundaries were clearly defined, and others were more loosely defined so that a continuum is more likely with information perhaps at one end. The question is how are boundaries defined for information? Spatial proximity or social grouping for natural resources may define the boundaries for who the users are, and similarly for information users with an emphasis on access for global users. This variation indicates that usufruct rights cannot be assumed, but that they should be explicitly stated for clearly defined boundaries. Data use,

including analysis, modification and publication, occurs on an idiosyncratic user-by-user level with local conditions, but must still account for national and international agreements on data use even if these agreements may not be relevant.

Appropriation rules related to local conditions—"Appropriation rules restricting time, place, technology, and/or quantity of resource units are related to local conditions and to provision rules requiring labor, material, and/or money"—must successfully extend outwards when the "local" becomes global. A small community can potentially decide the rules for the best interest of the community, but international agreements and understandings vary worldwide so that there are few universally accepted rules of data appropriation globally. Members of a small community can have collective input into the appropriation rules when they otherwise may not have input as their relative proportion decreases in a global community. Still, a global community may be small enough to retain the same power of collective input. For instance, the community could request identifying information before allowing access to appropriation.

Collective-choice arrangements—"Most individuals affected by the operational rules can participate in modifying the operational rules"—are not so collective when it is not a question of how users use, but the resource producer has disproportionate say on how she wants her data to be used. In traditional property rights issues, Mother Nature (the resource producer) never tells us that she wants to be used—although with degradation she may tell us that she does not want to be used. From a demand and supply standpoint, a community can decide how much resource to expropriate over time based on when the resources may be exhausted. But, no matter what the supply or what data users decide for data appropriation, the data producer has the power to refuse or

delay distribution of the resource—though if the data are of poor quality, then the data producer might be motivated not to share. Resource production and resource distribution or availability are therefore disjoint. Parties affected by the operational rules, including both data producers and data uses, should be able to participate in modifying the operational rules in collective-choice arrangements.

Monitoring—"Monitors, who actively audit CPR conditions and appropriator behavior, are accountable to the appropriators or are the appropriators"—is difficult, again, when the appropriators are global because monitors must watch the flow of information and the change of information in different languages, disciplines, and media. Without physical interaction, the act of access is invisible even when it might be occurring next door. A person could download the data and produce a print copy that never meets the eyes of a monitor. The impact of that hard copy, however, may be limited. Only when that copy is circulated in a journal or manuscript for larger impact will a monitor be able to detect the use of data. At the point where the journal is indexed online through the internet does monitoring become relatively easy, though may be too late. Monitoring by those who actively audit data use activities must be accountable to the appropriators or are appropriators themselves.

Graduated sanctions—"Appropriators who violate operational rules are likely to be assessed graduated sanctions (depending on the seriousness and context of the offense) by other appropriators, by officials accountable to these appropriators, or by both"—must be adapted when the finite nature of the resource is not the resource itself. Again from a demand and supply standpoint, what is at stake here is the limited and valuable credit associated with the resource, not any limitation to the physical bounds of the resource

itself. Given an infinite supply of water, for example, the issue is not how much one takes, but what one does with the water e.g., contaminate it. Data in a digital form are essentially of infinite supply—one could copy a dataset over and over but that would not yield any benefit (and require the cost for more storage). In natural resources the quantity of expropriation is more important in that the misappropriation of one fish out of a thousand, for example, should yield a smaller punishment than for the misappropriation of a thousand fish from the same stock. Graduated sanctions should apply to data use—on one end of the spectrum, one could simply cite a dataset incorrectly, and on the other end of the spectrum, one could take someone's data and sell the data for profit without acknowledging the producer. There are a number of methods by which data producers and data users can break rules, but not all actions have the same intentions or effects. Penalties should be assessed based on gravity of the misuse—minor for an errant citation, more severe for a profit-motivated breach of contract. People who violate rules should be assessed graduated sanctions or penalties appropriate to the violation.

Conflict-resolution mechanisms—"Appropriators and their officials have rapid access to low-cost local arenas to resolve conflicts among appropriators or between appropriators and officials"—need to encompass data users and producers acting at multiple power scales. Universities and institutions across different countries in different political and power regimes may or may not act on the local scale actions of individual data users and producers. The conflict-resolution mechanism of one country or culture may vary or even contradict that of another country or culture. Intellectual property rights may be ill-defined or even unrecognized and international conflicts over these rights can be highly political. Larger institutional or governance rules may not large

influence at all, with local norms or norms of the intellectual epistemic community weighted inconsistently. Conflict-resolution mechanisms or arenas must be in place and accessible to appropriators.

Minimal recognition of rights to organize—"The rights of appropriators to devise their own institutions are not challenged by external governmental authorities"—should be encompassed in a shared intellectual property rights treaty. The recognition of rights, rules, and conflict-resolution mechanisms vary internationally from one country to the next, from culture to culture, and between political administrations. Minimal recognition from outside the community may not even be necessary, however, for the community to uphold and follow its rights. The rights and policies by data sharing institutions to organize must be recognized at a minimum by external governmental authorities

Intellectual Property Rights

The actors in our study are situated in legal, legislative and philosophical contexts with respect to intellectual property rights (IPR). Legally, IPR are embedded in national and international copyright laws, patent laws, trade-secret laws, and court opinions. The legislative Acts that control IPR include Digital Millennium Copyright, Digital Consumer Right to Know, Public Domain Enhancement, Public Access to Science, Consumer Access to Information, Digital Media Consumers Rights, and the Bayh-Dole Act. Both the legal and legislative contexts are rooted in philosophical debates over John Locke's discussions on property, definitions of "bundles of rights", and a notion of the anti-commons in that too many laws, rules and property claims can be detrimental to the purpose of property delineation. IP law protects the public domain, which has been

described as a commons in that some property (intellectual) cannot be privately owned (Litman 1990).

Only recently have researchers explored the idea of IPR in parts of the CPR framework (van Wendel de Joode 2004). We discussed common pool resources as a model by which to base common property theory, and now we introduce IPR as they apply to our research. We address IPR with respect to data with three main questions: What are IPR and IP laws? Why produce IP? Who owns IP? We answer these questions with four concepts: information as property, labor-based rewards, bundle of rights, and the anti-commons.

Data products (e.g., CD's, images, files) are applicable to IPR, although this fit is not perfect as IP tends not to be the product in and of itself, but more the information that makes the product possible (Posey et al. 1995; Reichman and Samuelson 1997; Drazen 2002). Information, however, is ill-defined and can be confused with data and knowledge. Hierarchically, knowledge is the assimilation of information and the understanding of how to use it, information is organized data in context, and data are simple measurements or values (Machlup 1983). The internet has made the dissemination of information and data relatively fast and cheap, but also inconspicuous (U.S. Department of Commerce 1995; Glisson 1996; Smirnoff 1996). Still, many laws serve to protect IPR in "cyberspace" (Lessig 1999). Legal protection is concentrated largely on producers of intellectual content (data producers) rather on access for data users.

IPR are connected with four general types of law that focus primarily on knowledge property and the distinction between what is and is not IP: copyright law,

patent law, trade-secret law, and trademark law[4] (Fisher 1999). Copyright law protects "original forms of expression" such as computer software and data for publication[5]. Digital copyright protection has been argued to be a "virtually perpetual monopoly and limited the scope of fair use rights" due to "dubious" click-through or "shrink wrap" licenses (Bollier 2003). For many of the FLUXNET and remote sensing data portals, click-through licenses are required to gain access to data. Click-through licenses, according to Bollier, are considered questionable because they are not necessarily legally-bound, but data users would be forced to agree to these "licenses" to gain access to the data. In a non-digital sense, users could gain access to the resource without having to agree to the copyright license as long as they did not publish or disseminate the resource. Patent law protects inventions such as the instruments or procedures used to collect data. Trade-secret law protects proprietary information such as the formulas, methods, or strategies that data users employ in analyses and data producers in data production; trade-secret law also provides data producers with a head start to analyze and establish their data, but does not provide legal immunity from direct competition and the limited protection is forfeit once the data are disseminated to the public in print media (Reichman and Samuelson 1997).

Data access has been addressed in U.S. legislative and judicial bodies on copyright, federally funded science, and fair use. In 1998 U.S. Congress passed the "Digital Millennium Copyright Act" (H.R. 2281), which updated the Copyright Act (Title 17 of the U.S. Code) to include digital data (e.g., FLUXNET and remote sensing). The

[4] Trademark law serves to protect identifying words and symbols of goods and services, but is less relevant to data.

[5] Redistributed for-profit publicly available data must include a new and valuable modification or enhancement otherwise the company is liable for copyright infringement.

"Digital Consumer Right to Know Act" (S. 692), required data producers to inform consumers about technological features that would restrict their use of the content (e.g., encryption). This Act is targeted at consumers, but many data users are not necessarily consumers in a strict monetary sense. The "Public Domain Enhancement Act" (H.R. 2601), ensured that abandoned copyrighted works pass into the public domain. A disconnect exists, however, between "passing into the public domain" and the public actually gaining and benefiting from access. The "Public Access to Science Act" (H.R. 2613), aimed to exclude from copyright protection works that resulted from "substantially federally funded scientific research." This Act has been the subject of much debate with some critics arguing that removing copyright protection could hamper academic publishing and negatively affect research funding. The "Consumer Access to Information Act of 2004" (H.R. 3872), failed to allow "fair use" of data comparable to that under copyright law and is partially redundant to database protection under other federal laws, such as the "No Electronic Theft (NET) Act" (American Library Association 2005). The "Digital Media Consumers Rights Act of 2005" (H.R. 1201), focused on "fair use" stemming from the Conference on Fair Use (CONFU) meetings in the late 1990's and from the Fair use doctrine of the Copyright Act (17 U.S.C § 107). "Fair use" is the core of the FLUXNET data sharing policy and many remote sensing data sharing policies.

IP copyright has been disputed in the U.S. courts as well. In the *Feist* opinion on whether or not copyright could be granted to a telephone directory, for instance, the Second Circuit adopted the "sweat of the brow" theory by which copyright could be granted because the directory compiler had labored to collect the data. The Supreme

Court rejected this approach because facts that are "part of the public domain [are] available to every person" and cannot be copyrighted (Feist, 1985). The *Feist* opinion is key to IP in that Intellect can or cannot be considered Property based on a balance between labor to compile the data versus facts that should remain in the public domain.

International copyright law reconciles two or more nations' copyright systems by providing shared conditions for copyright recognition because each country has its own method of recognizing, granting and protecting copyrights. These agreements, however, may require the signatories to alter their domestic laws in order to comply with the terms. The U.S., for example, negotiates international agreements with government entities such as the Office of the U.S. Trade Representative (USTR), the Department of State, the Department of Commerce, and the U.S. Copyright Office. A number of different intergovernmental organizations govern copyright to varying degrees: the first was the Hague Convention of 1899, which covered commercial contracts for copyrighted materials; Free Trade Area of the Americas (FTAA), which focuses on trade, but international copyright law is often implicated; North American Free Trade Agreement (NAFTA), which is developing IP rules; and, the World Intellectual Property Organization (WIPO)[6], one of 16 specialized agencies in the United Nations, which administers 23 treaties on IP to the 179 member nations and works with intergovernmental groups such as the World Trade Organization (WTO) to clarify and define IP enforcement and rights.

[6] The first WIPO treaty on international copyright laws, the Berne Convention, was signed in 1886, but recently improved in 1995 in the TRIPS (Trade Related IPRs) Agreement. In 1996, the WIPO Copyright Treaty updated the copyright provisions of the Berne Convention to include the development of digital commerce.

Our second IPR question, and one of the fundamental questions asked in the rationalist context of IPR is: why would people invest time and money into producing data or analyses when they would reap no monetary reward? As James Boyle (1996) has remarked, "Information is often expensive to create or generate but cheap to copy." Additionally, since the Bayh-Dole Act (1980), universities have been patenting publicly-funded inventions and discoveries. One answer to that question is that monetary reward and profit are not necessarily the motives behind all research and development. But, should data producers and users retain some power over the dissemination of their ideas or products if we are to follow Locke's notion that we own our labor (Locke 1990), which is what most Western notions of property are based on today?

Hughes (1988) justifies the "propertizing" of ideas stemming from Locke with three propositions: labor is required to produce ideas, the commons of knowledge is not devalued by giving property rights over a piece of that commons, and that Locke's non-waste condition is not violated. Although Baird (1983) argued that people "have the right to enjoy the fruits of their labor, even when the labors are intellectual," Hughes pointed out that idea-making may not involve labor since the definition of labor is debatable. Subsequently, the rewards and reasons for rewards for such labor are arguable as valid since the concept of "intellectual labor" itself is arguable as a valid concept. American copyrights and patents, including those from the Constitution, have generally rewarded labor with property for motivation (instrumental proposition of labor theory) as opposed to a moral or ethical imperative to the unpleasantness of labor (normative theory) (Hughes 1988). These rewards, however, have not necessarily been for intellectual labor. Essentially, there are two sides tugging at opposite ends of the motivational rope. On one

side is the answer that monetary reward and profit are not the motives behind all research and development, but that a commitment to science or enjoyment of work may be stronger drivers. On the other side is a fundamental concept on which the U.S. was founded that labor should be rewarded with property. We examine which side is stronger in our cases and the reasons why one side would dictate.

Our final IPR question is: who owns the data produced—the knowledge worker/researcher or the funder (May 2000)? Ownership may best be claimed as parts to a whole, where different rights such as use, dissemination, and publication, are possessed by several agents and agencies. Each right acts as a fraction in a "bundle of rights" (Penner 1996). These rights might include copyrights over ideas, patents over inventions, and dissemination or reproduction of work. The anti-commons, however, suggests that multiple users can block advancements through intentional or inadvertent gridlock; overlapping claims could create a bottleneck, especially when a user needs access to multiple claims to create a single useful product or analysis (Heller 1998; Heller and Eisenberg 1998). Gridlock occurs when the bundle of rights is divided among different people with no clear communication or cooperation. For instance, a *professor* who is supported by a *federal grant*, employed by and uses resources from a *university*, hires *lab techs* for help, and publishes data in a *journal* might give up or be required to share a number of her rights to the work produced; moreover, these same types of agents and agencies may be associated with a *data user* who applies the generated work for additional analyses. Generally, however, these agents and agencies tend to support ownership in the public domain. Another form of gridlock occurs not when there are too many claims, but when conflict arises from personality conflicts. A data producer, for

instance, has the power to exclude or suppress findings due to personal reasons or due to the constraints of multiple claims, both of which can impede analysis on the data in question. To overcome these barriers, norms and unwritten relationships can, but not always, facilitate work and progress (Ostrom 1990; Rai 1999). Hess (2005) postulated that open access for information—meaning "free and unfettered access, without costs or permissions"—does not have negative effects, but instead provides a universal public good. We assess whether or not this proposition holds true in our study, especially where producers of information might restrict information flow if they knew their data were to be shared into an open access system. We inspect how norms and personal relationships affect perceptions of control over pieces to the bundle of rights.

Methods

We compared written institutional policies on ownership and data sharing with the knowledge, perceptions and interpretations of those policies by individuals affected by them. The National Academy of Sciences was among the first national organizations to discuss the benefits of data sharing and ethics with publication policies involving shared data (Fienberg et al. 1985). Other institutions, both professional and governmental, with documented ethical codes and publication policies on data sharing include the American Sociological Association, the American Psychological Association, the National Science Foundation Economics Program, the National Institutes of Health, the National Institute of Justice and the Robert Wood Johnson Foundation (American Psychological Association 1992; Goodman 1996; Bradley et al. 2001; Deck et al. 2001). Our focus was

in the institutions of and researchers associated with the University of California, FLUXNET, and NASA. The analysis was framed in common property and IPR theories.

Data were collected through 17 semi-structured interviews with two primarily data producers, three researchers who both produce and model with shared data equally, and eleven primarily data users consisting of professors, graduate students, one post-doctoral student and one staff researcher. All respondents were researchers in the Department of Environmental Science, Policy and Management at the University of California at Berkeley. Respondents were selected on the basis of their familiarity with both FLUXNET and remotely sensed data, although emphasis on one or the other varied. The respondents included all of the department's FLUXNET and remote sensing faculty and a comprehensive sample of the population of the graduate students working for those faculties.

We asked questions about rights over and ownership of data, analysis, distribution, modification, publication; in addition, we inquired about knowledge of patents, copyrights, and costs. Interviewees were asked if their perceived rights provided enough protection or reward for the continuation of work and data sharing. We requested examples based on personal experiences of data sharing that went smoothly and data sharing that ran into conflict. We coded answers to determine which of Ostrom's (1990) design principles were present in cases with and without conflict. Our analysis differentiates the design principles for successful and unsuccessful common property

Design principle	Application to FLUXNET or Remotely Sensed Data
Clearly defined boundaries	Individuals or research groups who have rights to use FLUXNET and remotely sensed data are explicitly stated.
Appropriation rules related to local conditions	Limits of data use, including analysis, modification and publication, must take into account international agreements.
Collective-choice arrangements	Parties affected by operational rules can participate in modifying the operational rules.
Monitoring	Monitors who actively audit data use activities are accountable to the appropriators or are appropriators themselves.
Graduated sanctions	Data users who violate rules are assessed penalties appropriate to the severity of the violation.
Conflict-resolution mechanisms	Appropriators must have access to local conflict-resolution arenas.
Minimal recognition of rights to organize	The rights and policies by data sharing institutions are not challenged by external governmental authorities.

Table 1. Design principles for successful data sharing (adopted from Ostrom 1990).

data. The design principles[7] are described and operationalized in application to the FLUXNET and remotely sensed data-sharing communities in Table 1.

Results

Institutional Policies

The University of California has a policy on copyright ownership that defines copyright as "the intangible property right granted by Federal statue for an original work fixed in a tangible form of expression" and provides the owner with the following exclusive rights

[7] An eighth design principle, nested enterprises, is not used here because we do not examine the appropriation, provision, monitoring, enforcement, conflict resolution, and governance activities associated with multiple layers within the two communities of interest.

in a work: to reproduce, to prepare derivative works, to distribute by sale or otherwise, to perform publicly, and to display publicly (http://www.ucop.edu/ucophome/uwnews/copyr.html, November 2002). "Sponsored works" and copyrights to "sponsored works" produced by or through the University are owned by the University unless an agreement says otherwise; these works generally include reports and software, but do not include journal articles, lectures, books or other independent copyrighted works. The University generally has a "free-of-cost, nonexclusive, world-wide license" to use and reproduce the copyrighted work for education and research purposes even if an agreement provides for ownership outside of the University.

Although the University of California recognizes copyright for original works in a tangible form of expression, the terms "original" and "tangible form of expression" are both open to interpretation, especially with regards to using other people's data. Institutions and universities realize the academic, legal and economic implications of shared data with respect to copyright and try to make known their respective policies. These policies are often written or summarized on the Web so access is intended to be relatively simple. Whether or not researchers know these policies, know where to find them, or understand the language and ramifications can be revealed in interviews.

The FLUXNET and AmeriFlux (N. & S. American subset of the global FLUXNET) fair-use policy is stated online (http://public.ornl.gov/ameriflux/data-fair-use.shtml, January 2006):

> The AmeriFlux data provided on this site are freely available and were furnished by individual AmeriFlux scientists who encourage their use. Please kindly inform in writing (or e-mail) the appropriate AmeriFlux scientist(s) of how you are using the

> data and of any publication plans. Please acknowledge the data source as a citation or in the acknowledgments if the data are not yet published. If the AmeriFlux Principal Investigators (PIs) feel that they should be acknowledged or offered participation as authors, they will let you know and we assume that an agreement on such matters will be reached before publishing and/or use of the data for publication. If your work directly competes with the PI's analysis they may ask that they have the opportunity to submit a manuscript before you submit one that uses unpublished data. In addition, when publishing please acknowledge the agency that supported the research. Lastly, we kindly request that those publishing papers using AmeriFlux data provide reprints to the PIs providing the data and to the data archive at the Carbon Dioxide Information Analysis Center (CDIAC).

For comparison, the OzFlux (Australian and New Zealand subset of the global FLUXNET) includes a disclaimer and copyright section on their website (http://www.dar.csiro.au/lai/ozflux/disclaimer/index.html, January 2006):

> Disclaimer: You accept all risks and responsibility for losses, damages, costs and other consequences resulting directly or indirectly from using this site and any information or material available from it. To the maximum permitted by law, CSIRO (Commonwealth Scientific and Industrial Research Organisation) excludes all liability to any person arising directly or indirectly from using this site and any information or material available from it.
>
> Copyright: Copyright in the material available at this site is owned by the Commonwealth Scientific and Industrial Research Organisation (CSIRO) and third parties and may only be used in the ways described in this legal notice: you may take temporary copies necessary to browse this site on screen; unless otherwise stated, you may download or print a single copy of CSIRO copyright material for research or personal use; you must not change any of the material or remove any part of any copyright notice.

The FLUXNET and AmeriFlux fair-use policy grants the right to use copyrighted material, regardless of how the Principal Investigators feel the data should be used. The policy requests communication and agreements between data users and the Principal Investigators, which would ideally lead to collective-choice arrangements. Though fair use and first sale doctrines as applied to licensed digital information has been described as precarious (Lessig 1999; National Research Council 2000), the FLUXNET/AmeriFlux policy follows trade secret law in that the producers are granted a head start to analyze and establish their data. The OzFlux statement does not allow for any change of the data, though the definition of "change" is unclear and may vary. For instance, calculating and reporting an average of two values does not change the original data, but does change the reporting of the data. The OzFlux statement includes a section on copyright, which gives the owners certain rights, but the fair use places a limitation on those rights. As a minimum recognition of rights to organize, the data are owned by the Commonwealth Scientific and Industrial Research Organisation. Sanctions and conflict-resolution mechanisms are backed with reference to law, though no laws are explicitly stated.

NASA's Distributed Active Archive Center (DAAC) manages the archival and distribution of NASA data through the Oak Ridge National Laboratory (ORNL). Their data citation policy requests that authors include a bibliographic citation to ORNL DAAC rather than to the individual scientists who provided the data (http://www-eosdis.ornl.gov/policies_intro.shtml, April 2005). The DAAC also includes a policy for data producers on quality control for data dissemination (e.g., metadata, defined parameters, consistency). The constraints on data producers are much more detailed than for data users.

Interviews

Interviewee statements on their understood rights, personal rewards, observed ownership and implicit patents/copyrights are summarized in Table 2. For all respondents rewards were essentially uniform: publication or acknowledgement; other rewards included personal satisfaction, scientific advancement, and salary. Their perceptions of rights, ownership, and patents and copyrights varied tremendously, especially among data users, though the data producers were more homogeneous in their ideas. In general, the interviewees did not claim many rights to their data production or data use. Notions of rights extended from none to first-use to as specified by the agreement, supervisor or cost. Data producers tend to have priority use rights for publication with their own data, and most data producers indicated a responsibility or requirement of data sharing. Data users expressed a right to use publicly funded data, and they saw their rights sometimes abused by data producers who were unwilling or slow to share. Notions of ownership ranged, but were effectively split 50/50 among either the funder or the researcher. Interviewees offered a number of potential patents and copyrights, from measuring devices and processes to algorithms and analysis methods.

DATA PRODUCERS

The FLUXNET/AmeriFlux community has been struggling with the issue of data sharing, rights and obligations of data users and data producers. The data producers, Paul

Person	Rights	Ownership	Patents/Copyrights
Producer	First-use	Data producer and public	Measuring device
Ilabas	First-use	Funder	Measuring device, process
Beide	None	Funder	Measuring device
Ambos	Right not to share	Inapplicable	Unsure
Deux	Unsure	Researcher unless otherwise stipulated	Depends on physical location of product development
Yong	If any, then absoute	Funder	Methods in the form of software
Utente	Only usufruct, no redistribution	Unsure	Measuring device, process, analysis, data
Sayoung	Vary depending on cost	Purchaser	Unsure
Bhoga	None to data; limited for analyses, must inform DP	Funder, university	Process, analysis, data
Polza	First-use	DP for data, DU for analysis	Nothing
Riyousha	Depends on agreement	Stipulated by funder	Process, new data
Kayttaa	Ownership to analysis and reformatting	Researcher and private investigator	New model
Bruk	Publication, not redistribution	Funder	Nothing, often explicitly stated in waivers
Fayda	Analysis and publication, but must give opportunity for co-authorship	Funder and researcher, proportion depends on funding proportion	Algorithm
Guna	Depends on supervisor	Researcher—based on intellectual input, funder is merely thanked	Algorithms, not methods
Gebruiker	Depends on agreement	Researcher, funder, collaborators in that order	Depends on country
Kutimo	Publish without offering co-authorship if data are not major part of analysis, distribute with acknowledgement	50% funder, 50% researcher and collaborators	Engineering products, but patents must be shared

Table 2. Summary of interviewee statements rights, ownership and patents/copyrights. Rewards were uniform for all interviewees: publication and/or acknowledgment; Guna added salary to the rewards as well. Data producers include Producer and Ilabas; data producers/data users include Beide, Ambos, and Deux; data users include Yong through Kutimo.

Producer[8] and Ian Ilabas, have seen publications that used their data, but when the data users never informed Producer or Ilabas. Still, Producer and Ilabas realize there is a "fine

[8] Pseudonyms used for confidentiality.

line" between who owns the data and whether or not a user needs to ask permission or offer co-authorship or even acknowledgement if the shared data only constitute a "small" percentage of the analysis (boundaries not clearly defined). Although the data producers did not act directly against those papers after they were published, they did implement low level sanctions against the authors. They reported they were much more critical in scrutiny of the offending authors during review of publications, grant proposals, and collaborations following the offense. In a less formal context, though perhaps of equal or even greater importance, they reported that data *mis*-users may be stigmatized at conferences, avoided in social settings, or may suffer a loss of reputation via discourse among data producers. Though it is seldom-done, data producers can "flood the community" with excessive or incorrect data that only the data producers themselves know is incorrect or correct as a pre-emptive defense; the data producers could notionally attack any paper that used the bad data. Ethically, the practice is questionable, but this practice might occur if a data producer feels that data users are not following fair use policies and that the monitoring and sanctioning systems are inadequate. Although the practice was mentioned, none of the interviewees claimed to have done so nor revealed any specific cases of this practice.

Monitoring is not centralized in terms of a unitary body, but occurs in the peer review process where highly effective community review of publications and conflict-resolution mechanisms from successful monitoring are resolved at the editorial stage. The FLUXNET community is highly dependent on the "honor system," and the data producers insist that they should always be asked for input out of "courtesy." There is no minimal recognition of the fair-use policy outside the FLUXNET community, but

organizers are hoping to be involved in a larger international treaty that would connect the parts of FLUXNET (e.g., AmeriFlux, OzFlux) and tie the fair-use practices to international treaties. Work on an international treaty is not a top priority, however, as the FLUXNET community is currently working on broadening the data-sharing community before integrating itself into international and federal policies.

The FLUXNET fair-use policy acts as appropriation rules and guides most of the data producers and data users, with the public as the final owner for federally funded research. Data producers wrote the fair-use policy for the data users. Data users had little input into the policy, so the policy was not a collective-choice arrangement. Ilabas explained, "Data producers enjoy the relationship between data users and data producers because the data users give interpretation and feedback to the data producers to increase understanding on the data produced." A data producer's responsibilities include giving modelers "first-look" or "first-use" of the data, defined as priority viewing before public access. The modelers must reciprocate by offering co-authorship on publications. The data producers are responsible for abiding by a time limit on how long they are allotted by their grants to use the data before they must transfer the data to the public domain (trade-secret law). In terms of access, data download sites can be password-protected (Digital Consumer Right to Know Act) so that the data are only accessible to a small cohort of users.

DATA PRODUCERS/DATA USERS

According to one data producer/data user, Mike Beide, few people actually make their data readily available, even if publicly supported, because of heavy competition for

publication. Beide points out that "shared data appear to be a finished product [to the data user], but in fact are quite raw with flaws and errors." Another data producer/data user, Aaron Ambos, feels "no obligation to share data," although he does try to share as much as possible when requested and expects others to do the same. Ambos feels free to "horde" data if he so chooses, unless he has signed an agreement with a journal or a funding source. Beide says that data sharing is guided by "personal responsibility," but the data and analyses are completely separate. The funder owns the data and analyses, but funding agencies do not keep careful accounts. For instance, the funder might request monthly data, but the researcher records and keeps the hourly data. Ambos believes that "the concept of data or analysis ownership is inapplicable in most situations, except in specific agreements with funders." His notion of inapplicable ownership is contradictory, however, with the idea that he can horde his data since he has a sense of personal ownership rights.

Beide described two cases of data sharing that he was involved in, one with a conflict over a dyad-level shared measuring device and one without regarding the use of federally-sourced remote sensing data. As the owner of the shared device, Beide expected the user to share her data obtained from the device, but the user refused. In this case, Beide had not initially specified clear boundaries, rules, nor made any collective-choice agreements with the user on data sharing. Conflict-resolution mechanisms were not set up, and conflicts had to be dealt with informally through personal communication among the parties and their respective superiors. In the case of conflict-free data sharing, Beide acquired data from NASA's DAAC, which shares data with modelers on a formal basis. There is a formal statement of acknowledgement that clearly defines boundaries,

and NASA expects peer review rules to govern the actions of the researchers and accepts feedback in collective-choice arrangements. A Circular out of the White House (similar to an Executive Order) governs the policy for data collected by or through the federal government. The Circular directs the government to have an open and free data sharing policy after an initial "check out" period whereby government officials may review the quality and accuracy of the data. An official at NASA Headquarters sees the content of the Circular as something of a guiding "spirit" that should extend and apply to data collected by a PI through a grant, as well. Some commercial data, however, cannot be freely shared. Nonetheless, there are situations where NASA purchases a bulk license so that the data can be used freely if the individual is a current and "legitimate" PI sponsored by NASA. There is no formal monitoring mechanism in place, but if a rule-breaker is caught by chance, then NASA invokes the legal system and the courts assign penalties appropriately based on the severity of the offense (graduated sanctions). The NASA official could not recall any specific cases of a court case, however. NASA's policies are recognized by Federal IPR agreements on data sharing. The success of the NASA data sharing, according to Beide, depends on the government payment of transaction costs so that conflicts over money are minimized. Essentially, the data are subsidized because the user does not have to pay for the development of sensors and satellites, but merely the cost to maintain the data once acquired from the sensors.

Another data producer/data user, Levia Deux, knows her rights as a user more clearly than as a producer. For instance, she has the right "to use data under the stipulation that [she] must keep the data producer informed of [her] work." Deux notes that "upfront conversations on rules and policies are wise" but rare—laying down some

basic understanding of ground rules without going through any legal or contractual venues can pave the way for conflict-free interactions. From her experience, discussions are more often carried out under initial friendly settings than under settings of miscommunication or conflict, however, where these conversations may be most beneficial. As a producer, Deux is unsure of her rights on ownership and distribution. She would like to share data given the beneficial reciprocity, but two disincentives force her to question the motives of the data requester: she feels unsure whether or not the data user will give her authorship even at her request, and she is even more afraid of people using her data to produce poor quality publications without her oversight. Deux wants to know the plans of the data users before she distributes her data, but notes that this demand conflicts with the fundamental scientific tenet of replication whereby anyone should be able to replicate the results of a previous study. But, replication is almost impossible if the same data are not available, especially when her data are essentially irreplicable due to high cost of production and time-dependency. Deux feels that she owns her data or analyses unless otherwise informed, particularly within grant stipulations. She notes that local funders (e.g., city, county, private) tend to want more ownership than do state or federal funding agencies. In addition, Deux has confronted legal issues over data ownership, and according to the lawyers of her university any "work" produced on university property is owned by her university (University of California Institutional Policy). The term "work" is undefined, and whether or not "work" refers to data production or data analysis is unclear. This policy becomes a gray area when off-site locations are used, especially when university resources or equipment are still used.

Deux described the effects of power hierarchy in conflict resolution. She shared her data with a senior researcher who produced a poor analysis of the data. Deux clearly owned her data and was able to monitor the data (mis)use, but felt unable to institute any kind of appropriation rules or even engage in collective-choice arrangements due to the power relationships. The only sanctions she could see were that although this senior researcher gave many lectures and seminars about his analysis of her data, he was never able to publish his poor analysis. Misuse in the form of poor quality due to lack of producer input was essentially self-regulating with regards to publication. In a different case, conflict arose when Deux had contributed to a paper and was supposed to be co-author, but later received a request from the journal that the paper was submitted to asking her to review the paper (because she was not listed as an author and did not try to be put back on). All the design principles seemed to be present in this situation except for monitoring, but she is not sure which principles broke down at either the individual or institutional levels that led to her exclusion from authorship unbeknownst to her. In a case of conflict-free advancement of science, Deux received data from a producer who had a lot of data, but did not necessarily possess an extensive set of analytical tools. She was analytically experienced, but did not have a good dataset. They collaborated and produced several publications that would have been impossible to produce if each had acted in isolation.

DATA USERS

Data users Chris Polza, Kim Kayttaa, and Ben Bruk have been inadvertently restricted from data access because data producers had difficulties or delays in publication. The

data producers had trouble benefiting from the priority use rights due to lengthy review processes, slow collaborations, or case-specific hold-ups. Because data sharing would not commence until the producers first published the data, these delays meant delays in the time when users could start analyzing the data. Polza, Kayttaa, and Bruk pointed out a conflict with publishing analyses using someone else's data. Journals often mandate that the researchers share the data used in an analysis, but this mandate frequently conflicts with prior arrangements between data users and data producers in which data users cannot redistribute or share the data themselves. If the data user has no redistribution rights, then the data user cannot publish. Data users must wait for data producers to publish the data first, otherwise they must request approval from the data producers to share the data with the journal. In this case, an outside entity (the journal) affects the rights and relationship between the data user and data producer.

The data users feel guided by fair-use policies in addition to the "unwritten understanding" that they should not publish using a data producer's data before the data producer herself publishes with that data. Data users struggle with their own ideas of ownership. "I feel that I own my data or analysis, but I realize that my point of view may conflict with other policies (e.g., fair-use, university, grant)," said Polza. Another data user, Gabe Gebruiker, felt reluctant to share ideas of analysis or methodology (rather than data) for fear of intellectual theft (patent law).

A few data users—Gebruiker, Frank Fayda, and Dan Kutimo—had ideas of relative ownership down to exact proportions or percents. Ownership in a proportional or "bundle of ownership rights" sense means claim or responsibility to one part or another in an analysis to these data users. For example, one breakdown by Gebruiker specified 50%

ownership in the funders depending on proportion of total funding, and the remaining 50% ownership in the researcher and collaborators. Another example included the ownership order of first the primary researcher, then the funder, and last the collaborators. Other specifications for ownership included "intellectual input," "ideas," "time," and "energy." Gebruiker noted that the benefit for including others in the ownership is that they can also share in some of the responsibility for publishing fees. In practice this might range from an actual percentage allotment for fees or a chain of approval for use of the analysis, to being wholly dismissed by funders and collaborators.

Another data user, Ron Utente, stated that his rights are specified in formal agreements at either the individual or institutional levels, but the rights never include the redistribution of someone else's data, and often money is involved in ensuring rights. At first, Utente was sure that the funder owns all data and analyses. But, then he pointed out that journals own published analyses and copyright data. In addition, he noted that the university has rights and the individual has rights. After thinking through these issues, Utente was left unsure; he pointed out that "data sharing rules are not codified in [his] university rules," nor has he "ever received a hard copy or email about these issues" (University of California Institutional Policy).

Personal relationships and personalities play a large role in the success of data sharing. One data user, Steve Sayoung, sees data producers as taking one of two stances: sharing data at-will depending on connections or personal relationships, or creating data for users who have absolute rights. Sayoung stated that data sharing success depends largely on the personalities of the researchers involved, in particular the specific rapport that one researcher or lab group has with another researcher or lab group. His sense of

ownership of data depends on money—Sayoung feels that if he pays for his data, then he owns it, though rights, protection and rewards are variable depending on the ease of acquisition and cost of data. Additionally, collective-choice arrangements may be made because everyone involved in the collaboration is in a slightly different field so that one party must trust the requests and actions in terms of data use and analysis quality of the other parties. On the other hand, because the research fields are often quite narrow, according to Kutimo, monitoring of published infractions can be effective under the general literature review of most scientific methods.

One data user, Lee Yong, compared his experiences with American agencies to Chinese or Canadian agencies. American agencies tend to draw clearly defined boundaries and explicitly state rules and expectations for data sharing, whereas "Chinese and Canadian governments tend to purchase data for analysis but bar publication of the data." While there is no central monitoring, Yong emphasizes the effectiveness of monitoring by American tax payers. Though he has not seen any conflict-resolution mechanisms and enforcement is patchy, he feels that international laws recognize the rights of data producers and data users in a "general human rights sense"— seizure of data or analyses is prohibited without due process and everyone has the right to own property alone as well as in association with others nor shall be arbitrarily deprived of property (Universal Declaration of Human Rights, 1948). Some government agencies may tend to overstep these bounds, however, as expressed by one data user, James Guna, who had his algorithms requested by the U.S. Department of Defense in a collaborative situation, though the Department did not have the explicit right to appropriate the code. Guna did not give up his algorithms.

Another data user, Ryan Riyousha, also shared two cases of international data sharing—one of which was successful and the other was not. In the successful case, Riyousha received data from another country, performed an analysis and sent the analysis back to the data producer. There were clearly defined boundaries in a licensing agreement, though appropriation rules were not as clearly defined on the international level and between academia and government. There were collective arrangements between the data producer and himself, but monitoring internationally of adherence to the arrangements and agreements is rather difficult and rests mainly on the "honor system." Conflict-resolution mechanisms follow international copyright law and their licensing agreement was recognized by international copyright treaties. The unsuccessful case involved the multiple purchases of rights in China and Taiwan. Researchers in Fudan, China generated new data and sold the rights to another Chinese company in Beijing, but then the Beijing company sold the rights to a company in Taiwan. Later, the researchers in Fudan wanted to use their original data under the agreed rights from the Beijing arrangement, but the Taiwan company claimed those rights. The Fudan researchers contested those claims in court. In this case, boundaries were not clearly defined and interpretations varied. The international copyright laws between Fudan and Taiwan differed so appropriation rules related to local conditions were problematic. There were no collective-choice arrangements because of the intermediary separation by the Beijing company. There was no monitoring in place, and the Fudan researchers almost succeeded in using the data outside of their rights except that they were caught by chance by one person in the Taiwan company who happened to read something about their work. Due to the contention and blurring of national and international laws between Taiwan and

mainland China, the conflict-resolution mechanism rested in the Chinese courts, which provided a political disadvantage to the company in Taiwan.

The final two cases of data sharing conflict come from a data user, Tim Bhoga, who did not fully understand his own rights and the rights of the data producer, who was senior to him.. First, Bhoga put the data producer on a paper as co-author without informing the data producer of that action. The data producer later found out about this co-authorship and was upset. Second, Bhoga and another student were under time-constraints to submit an abstract about an analysis with shared data. The data producer could not be informed in time, and, having learned from previous experience not to include a data producer as co-author without prior consent, Bhoga did not include the data producer as co-author. Bhoga immediately contacted the data producer the following day, but the data producer was still upset that the abstract was submitted without prior consent. In both of these cases, Bhoga felt that although boundaries between data users and data producers were clear at the institutional level, the rules at the individual level were not. There was no monitoring mechanism in case and no formal conflict-resolution mechanism at any level. Dyadic agreements should have been clear and collective, but they were not.

Discussion

How are Ostrom's design principles and the IPR questions (what are IPR, why produce IP, and who owns IP) tied to the cases discussed in the interviews? We analyzed which design principles were present or absent in data sharing cases with and without conflict. Additionally, we assessed the relative importance of each design principle for our cases.

Although we previously discussed IPR, the interviewees varied considerably in their perceptions of IPR. Further, we determined why they produced IP, and what their knowledge was of who owns IP.

Design Principles in Cases

We summarized Ostrom's design principles as applied to the data sharing cases (Figure 1 and Table 3). Success was defined as lack of conflict or irresolvable disagreement, and determined by the interviewees to be present or absent in their cases. "Mostly successful" cases were defined as resolvable conflicts or disagreements. The "mostly successful" category was created to encompass the somewhat subjective continuum between conflict and success (Steins et al. 2000). The subjectivity is linked to what a researcher considers a minor conflict versus a major conflict. Although many common property researchers have found monitoring (Table 1) to be one of the most important

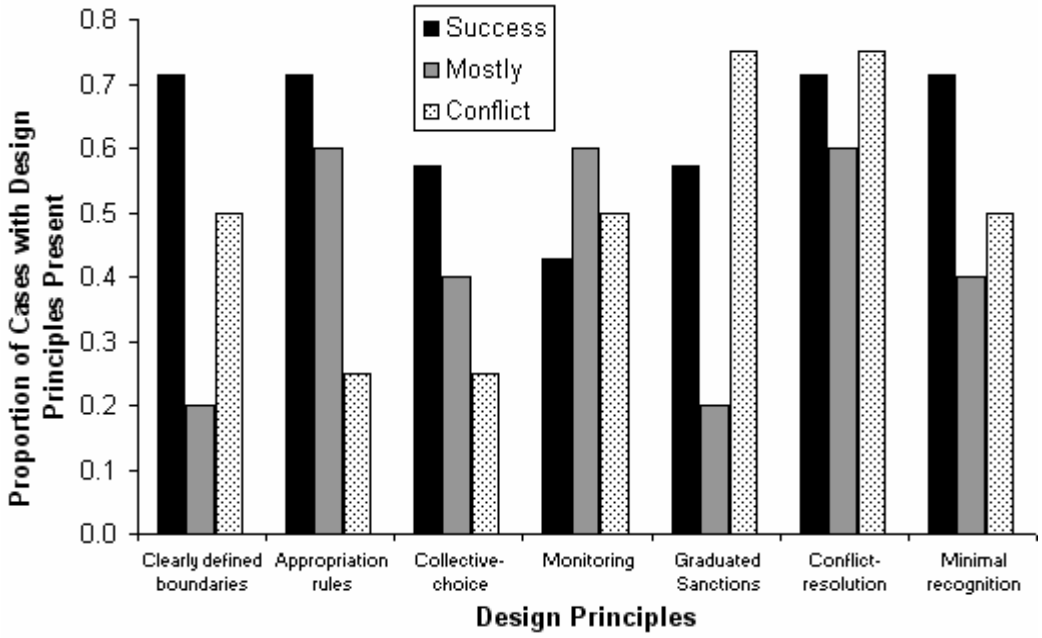

Figure 1. The proportion of design principles present in Success, Mostly Success, and Conflicting cases.

	Clearly defined boundaries	Appropriat-ion rules related to local conditions	Collective-choice arrange-ments	Monitor-ing	Graduated Sanctions	Conflict-resolution mechanisms	Minimal recog-nition of rights to organize	Conflict
Beide: NASA DAAC	√	√	√		√	√	√	No
Deux: data lead to publications	√	√	√	√	√	√		No
Riyousha: data for analysis	√		√			√	√	No
Polza: FLUXNET	√	√	√	√		√		No
Bruk: remote sensing	√						√	No
Fayda: remote sensing		√			√		√	No
Kutimo: international data		√		√	√	√	√	No
Ilabas: FLUXNET publications w/out prior consent		√	√	√		√		Some
Producer: FLUXNET publications w/out prior consent		√		√		√		Some
Bhoga: co-authorship	√						√	Some
Guna: DOD request		√		√	√	√	√	Some
Gebruiker: reluctance to share ideas			√					Some
DU6: China/Taiwan rights conflict					√	√	√	Yes
Beide: measuring device				√				Yes
Deux: bad analysis on her data	√			√	√	√		Yes
Deux: authorship exclusion	√	√	√		√	√	√	Yes

Table 3. Ostrom's design principles applied to 17 data sharing cases.

principles leading to successful property sharing, this design principle occurred least in the successful cases analyzed here within the intellectual/common property context. Monitoring was present in a higher percentage of the unsuccessful cases (50%) than in the successful ones (43%). It is possible that the lack of monitoring indicates the

presence of trust—not only in the other party's ability to follow rules or adhere to boundaries, but also to produce a product of high quality in the absence of any good mechanism for monitoring of quality since each party had a different area of expertise in the collaboration. It is also possible that the fact that shared data are not substractible is relevant. In general though, the successful cases were characterized by the presence of more design principles than did the mostly successful or conflict-laden cases. Attention to conflict also plays a role in the personal relationships that revolve around trust and communication when sharing data.

Clearly defined boundaries, appropriation rules related to local conditions, conflict-resolution mechanisms, and minimal recognition of rights to organize were strongly present in the successful cases, with collective-choice arrangements and graduated sanctions present in just over half of the cases. The cases that were mostly successful with a few scattered conflicts generally lacked clearly defined boundaries and graduated sanctions but were characterized by the strong presence of appropriation rules, monitoring, and conflict-resolution mechanisms. There were different perspectives on success and conflict within the FLUXNET data sharing community from both data producers and data users. One data user indicated that the FLUXNET community is a success, whereas the data producers in the FLUXNET community indicated that the relationship is mostly successful—the data user saw clearly defined boundaries, but the data producers did not. Given the start of any given data sharing relationship, we suggest that the presence of appropriation rules may play the strongest role in the development of a successful case. The rules might be more often followed if they are collectively-arranged, though our data do not show this trend.

The initial focus of beginning a data sharing relationship tends to be on the first three principles—clearly defined boundaries, appropriation rules, and collective-choice arrangements. No one on either side wants to admit up-front that there could be conflict, in which case a discussion of monitoring, sanctions, and conflict-resolution mechanisms would be warranted. Thus, unsuccessful cases tended to be characterized by the presence of graduated sanctions and conflict-resolution mechanisms, whereas appropriation rules and collective-choice arrangements were not. Without rules, which may or may not be the product of collective-choice arrangements, it is not surprising that conflict arises regardless of the sanctions in place. In these cases, there was not consensus on or even awareness of what the rules were within the community. That is, only one person in the relationship thought there was a rule. When "the rule" was unknowingly broken, the rule knower initiated sanctions to the surprise of the unsuspecting rule breaker. Nor were the definitions of "sanction" (and "success", "free-riding") uniform for both parties (Steins et al. 2000). Though the graduated sanctions and conflict-resolution mechanisms are strongly present in the unsuccessful cases, these two design principles reactive strategies for situations in which rules are predictably broken and subsequently dealt with, rather than a proactive strategy for developing rules with which a plan is developed to avoid conflict. It is not unlikely that conflict-resolution mechanisms should be present in cases with conflicts.

The case of authorship exclusion surprisingly contained all but one design principle, at least initially, exactly the same as the first success case in Table 3. Without monitoring, however, Deux could not identify which design principle(s) broke down in the relationship so emphasis should be made as to the timing and duration of design

principles. Perhaps the initial understanding of clearly defined boundaries and appropriation rules faded with time.

Success of data sharing often depended heavily contextual factors such as the "honor system," researcher personalities, and rapport between researchers. Additionally, timing appeared to be critical in relationship outcomes. Upfront conversations, early asking of permission, and establishment of common understanding can address the first three design principles and lead to successful data sharing even in the absence of the other design principles. The choice of whether or not to initiate these factors was influenced by the social network within which the actors were embedded (Steins et al. 2000). In this sense, informal agreements and the "honor system" are mechanisms that can promote the same goals as written contracts and licensing agreements. When money was involved the transfer of data, there tended to be explicitly written rules and regulations that addressed most, if not all, of the design principles. Whether or not the costs went to preventing conflict, the data rarely were involved in conflict over data sharing.

IPR of Interviewees

The interviewees initially had trouble applying their ideas of rights and IPR to data and analyses. Data producers were aware of how fast, cheap, and inconspicuous the internet has made dissemination of information and data. They were trying to find the critical balance between fluid data sharing and retention of rights to acknowledgement and authorship. On one hand, data producers did not want their data to be so difficult to

obtain that no one would analyze them, but on the other hand data users could easily forget where the data came from if the data were easy to acquire.

Most interviewees did not know the rules and laws of IP because their primary goal and interest was not interested in patenting or copyrighting their work. Many were confused about the point at which one can copyright data. One source of confusion was that up until 1976, publication was required for copyright protection, but the 1976 Copyright Act eliminated that requirement (Johnston 1982). Because copyright and data purchase were minimal, especially for FLUXNET, many of the rules and laws under acts such as "Consumer Access to Information Act of 2004" were inapplicable.

Even if the interviewees could have patented or copyrighted their work, they were unlikely to do so. Their interpretive rational choice for producing IP was motivated by publication or acknowledgement in addition to personal satisfaction, scientific advancement, and salary. In publish-or-perish academia, publications are a key to employment acquisition and promotion. Furthermore, publication can lead to the benefits of name recognition and prestige. Some researchers, however, were interested in a copyright for their work, but not for the intent of profit—a "copyleft" which is the application and protection of copyright law with the intent of free redistribution (Heffan 1997). In this case a copyright would be sought so that someone else with more private or profit-motivated interests could not seek the copyright.

Perceptions of data/analysis ownership differed among the interviewees. One principal investigator on a FLUXNET site initially found our framework of data producer and user definitions surprising since he thought of his field assistants as the data producers, with himself as only a manager of the project (Latour 1987 and; Boyle 2003

discuss the issue of who does science and how it relates to ownership). In general, however, because there were so many potential owners in scientific research, none of the interviewees knew for certain who owned what (Heller 1998; Heller and Eisenberg 1998). Conflicts with funding sources, sharing results and co-authorship are often due to misaligned perceptions of rights among the parties involved (Wolf 1996). Rules about ownership, data sharing, and co-authorship generally were not taught formally to the interviewees—they learned the rules through conversations, lab meetings (a functional explanation would suggest that social groups play operating roles in the larger system), or the "hard way" by learning from mistakes.

Some data users expressed interest in partial ownership, but it is difficult to objectively quantify the value of IP and thus the exact apportionment one would receive in partial ownership[9]. In addressing the question of partial ownership, Boyle (1996) tells a story of the apportionment of property rights in a conflict over a fox that was first pursued by one hunter and then killed by another. "The owner of the land may have the right to hunt some natural resource capable of movement but should not be deemed to own it until it is 'captured'," he states. In our case ownership is similarly complicated. The owner of the data may have the right to analyze data that are capable of being analyzed by many people, but the data should not be deemed owned until they are published. In terms of this point of view, ownership of data depends on who had access to them. But Boyle's example, based as it is in allocating total ownership to the second hunter, reflects neither existing property regimes that distribute partial usufructary rights

[9] A copyright apportionment doctrine was established in (1939). Sheldon v. Metro-Goldwyn Pictures, 106 F.2d 45 2d Cir, (1940). Sheldon v. Metro-Goldwyn Pictures, 309 U.S. 390. Judge Hand and Justice Hughes decided that the profits earned by the defendant were attributed to only a portion of the plaintiff's work, and they upheld the apportionment of twenty percent of the profits to the plaintiff.

among claimants nor the non-substractible nature of shared data (Fortmann 1985). In Boyle's example, the land owner, the first hunter and the second hunter could each have had a share in the slaughtered fox. In the case of shared data, it is similarly possible to assign specific rights to the producers and users, rights which might be subject to change over time.

Conclusion

We have shown that the intersection of common property theory and intellectual property theory provide insights into the practice of self organized governance of property rights in shared data in the form of remotely sensed data and FLUXNET data. Intellectual property theory and practice helped to identify the international, national and institutional legal frameworks and constraints in which the practices of individual data producers and users are embedded. However, for the most part, there was no clear effect in the property beliefs or practices of these actors possibly because, in contrast to scientists of biotechnology, ecological and bio-meteorological scientists generally do not form their own companies. The practices of peer-reviewed scholarly journals did constitute practical constraints on data sharing practices. Once these two sets of external constraints are accounted for, common property theory in the form of Ostrom's (1990) design principles provides insights into the property aspects of data-sharing practices. We note though, that the resource in our study, data, is not subtractable and that the communities of data producers are often scattered geographically. The two most important design principles in our case study were appropriation rules and collective-choice arrangements, which may be most applicable to IP and which are in support of our initial hypothesis:

successful data sharing involves rule making—either as explicitly written contracts, codes of conduct or mutual understanding.

It is important to note that the currency is publication or acknowledgement—the finite resource is not the data itself, but the publications. When data users bypass data producers' input, the data producers may feel shortchanged. When data producers do not share their data or restrict data redistribution rights between data users and journals, data users are prevented from producing publications and earning this academic currency. Future research should address the degree to which journal publication can be considered a substractible resource and how this affects governance of data sharing. In an age where data sharing has become increasingly important in the environmental sciences and other disciplines, it is crucial that we put existing theories of common property and IP to use to avoid conflicts and advance our disciplines.

Acknowledgments

We thank Greg Biging and Carmel Levitan for assistance with this project. This work was supported by NASA Headquarters under the Earth System Science Fellowship Grant NGT5-30473, and by the University of California at Berkeley.

References

Agarwal, B., 1997. Environmental action, gender equity and women's participation. Development and Change 28 (1), 1-44.

American Library Association, 2005. Open Access to Research. American Library Association.

American Psychological Association, 1992. Ethical principles of psychologists and code of conduct. American Psychologist 47, 1597-1611.

Baird, D., 1983. Common Law Intellectual Property and the Legacy of international News Service v. Associated Press. University of Chicago Law Review 50, 411, 413.

Baldocchi, D., Falge, E., Gu, L.H., Olson, R.J., Hollinger, D., Running, S.W., Anthoni, P.M., Bernhofer, C., Davis, K., Evans, R., Fuentes, J., Goldstein, A., Katul, G., Law, B.E., Lee, X.H., Malhi, Y., Meyers, T., Munger, W., Oechel, W., U, K.T.P., Pilegaard, K., Schmid, H.P., Valentini, R., Verma, S., Vesala, T., Wilson, K., Wofsy, S.C., 2001. FLUXNET: A new tool to study the temporal and spatial variability of ecosystem-scale carbon dioxide, water vapor, and energy flux densities. Bulletin of the American Meteorological Society 82 (11), 2415-2434.

Bayh-Dole Act, 1980. Patent and Trademark Act Amendments of 1980. PL 96-517.

Bollier, D., 2003. The missing vocabulary of the Digital Age: The Commons. The Common Property Resource Digest 65, 1-4.

Boyle, J., 1996. Shamans, Software, and Spleens: Law and the Construction of the Information Society. Harvard University Press, Cambridge, MA.

Boyle, J., 2003. The Second Enclosure Movement and the Construction of the Public Domain. Law & Contemp. Probs. 33.

Bradley, V., Agosta, J., Smith, G., Taub, S., Ashbaugh, J., Silver, J., Heaviland, M., 2001. The Robert Wood Johnson Foundation Self-Determination Initiative: Final Impact Assessment Report, The Human Services Research Institute, Cambridge, MA.

Buck, S.J., 1998. Global Commons: an Introduction. Island Press, Washington, D.C., 225 pp.

Council, N.R., 2000. Individual Behavior, Private Use, and Fair Use and the System for Copyright, The Digital Dilemma: Intellectual Property Rights in the Information Age. National Academy Press, Washington D.C.

Deck, W.R., DiRaimo, S., Epstein, M., Fritz, N., Maness, M., Matysek, P., Morelli, J., Stone, V., 2001. A Guide for Applying Information Technology in Law Enforcement, National Law Enforcement and Corrections Technology Center, Rockville, MD.

Drazen, J.A., 2002. Who owns the data in a clinical trial? Science and Engineering Ethics 8 (3), 407-411.

Fienberg, S.E., Martin, M.E., Straf, M.L., 1985. Sharing Research Data. Committee on National Statistics, National Research Council, 240 pp.

Fisher, W.W.I., 1999. The Growth of Intellectual Property: A History of the Ownership of Ideas in the United States. In: V. Ruprecht (Ed.), translated from Eigentum im internationalen Vergleich, pp. 265-291.

Fortmann, L., 1985. The tree tenure factor in agroforestry with particular reference to Africa. Agroforestry Systems 2 (4), 229-251.

Fortmann, L., 1988. Locality and Custom: Non-aboriginal Claims to Customary Usufructary Rights as a Source of Rural Protest. Institute of Governmental Studies, University of California, Berkeley, Berkeley, CA.

Frischmann, B.M., 2005. An economic theory of infrastructure and commons management. Minnesota Law Review 89, 217-1030.

Glisson, G.W., 1996. A Practitioner's Defense of the White Paper. Oregon Law Review 75, 277.

Goodman, K.W., 1996. Ethics, genomics, and information retrieval. Computers in Biology and Medicine 26 (3), 223-229.
Harper & Row Publishers, Inc. v. Nation Enterprises, 1985. U.S.
Heffan, I.V., 1997. Copyleft: Licensing collaborative works in the digital age. Stanford Law Review 49 (6), 1487-1521.
Heller, M.A., 1998. The tragedy of the anticommons: Property in the transition from Marx to markets. Harvard Law Review 111 (3), 621-688.
Heller, M.A., Eisenberg, R.S., 1998. Can Patents Deter Innovation? The Anticommons in Biomedical Research. Science 280, 698-701.
Hess, C., 2005. A resource guide for authors: Open access, copyright, and the Digital Commons. The Common Property Resource Digest 72, 1-8.
Hess, C., Ostrom, E., 2003. Ideas, artifacts, and facilities: Information as a common-pool resource. Law & Contemp. Probs. 66 (111).
Huberman, B.A., Lukose, R.M., 1997. Social dilemmas and Internet congestion. Science 5325, 535-537.
Hughes, J., 1988. The Philosophy of Intellectual Property. Georgetown Law Journal 77, 287, 296-314.
Johnston, D.F., 1982. The Copyright Handbook.
Key, J.R., Schweiger, A.J., 1998. Tools for atmospheric radiative transfer: Streamer and FluxNet. Computers & Geosciences 25 (5), 443-451.
Kollock, P., Smith, M., 1996. Managing the Virtual Commons: Cooperation and Conflict in Computer Communities. In: S.C. Herring (Ed.), Computer-Mediated Communication: Linguistic, Social and Cross-Cultural Perspectives.
Latour, B., 1987. Science in Action. Harvard University Press, Cambridge, Massachusetts.
Latour, B., 1995. The "Pédofil" of Boa Vista: A Photo-Philosophical Montage, Common Knowledge, pp. 145-187.
Lele, S., 2001. "Pixelising the Commons" and "Commonising the Pixel": Boon or bane? The Common Property Resource Digest 58, 1-3.
Lessig, L., 1999. Code and Other Laws of Cyberspace. Basic Books, New York, 297 pp.
Litman, J., 1990. The Public Domain. Emory Law Journal 965, 975.
Locke, J., 1990. Of Conquest. In: C.B. MacPherson (Ed.), Second Treatise of Civil Government. Hackett Publishing Company, Incorporated, pp. 124.
Machlup, F., 1983. Semantic Quirks in Studies of Information. In: F. Machlup and U. Mansfield (Eds.), The Study of Information: Interdisciplinary messages. John Wiley & Sons, Inc., New York.
May, C., 2000. A Global Political Economy of Intellectual Property Rights: The New Enclosures? Routledge, New York.
McCay, B.J., Acheson, J.M. (Eds.), 1987. The Question of the Commons: The Culture and Ecology of Communal Resources. The University of Arizona Press, Tucson, AZ.
Morrow, C.E., Hull, R.W., 1996. Donor-initiated common pool resource institutions: The case of the Yanesha Forestry Cooperative. World Development 24 (10), 1641-1657.
Noonan, D.S., 1998. Internet Decentralization, Feedback, and Self-Organization. In: J.A. Baden and D.S. Noonan (Eds.), Managing the Commons.

Ostrom, E., 1990. Governing the Commons: The Evolution of Institutions for Collective Action. Cambridge University Press, Cambridge.
Penner, J.E., 1996. The "bundle of rights" picture of property. UCLA Law Review 43 (3), 711-820.
Posey, D.A., Dutfield, G., Plenderleith, K., 1995. Collaborative research and intellectual property-rights. Biodiversity and Conservation 4 (8), 892-902.
Rai, A.K., 1999. Regulating scientific research: Intellectual property rights and the norms of science. Northwestern University Law Review 94 (1), 77-152.
Reichman, J.H., Samuelson, P., 1997. Intellectual property rights in data? Vanderbilt Law Review 51 (1), 49-166.
Rogers, D.J., Randolph, S.E., Snow, R.W., Hay, S.I., 2002. Satellite imagery in the study and forecast of malaria. Nature 415 (6872), 710-715.
Rose, C.M., 2002. Common property, regulatory property and environmental protection: Comparing community-based management to tradable environmental allowances. In: E. Ostrom, T. Dietz, N. Dolšak, P.C. Stern, S. Stonich and E.U. Weber (Eds.), The Drama of the Commons. National Academy Press, Washington, DC.
Sarker, A., Itoh, T., 2001. Design principles in long-enduring institutions of Japanese irrigation common-pool resources. Agricultural Water Management 48 (2), 89-102.
Schlager, E., Ostrom, E., 1992. Property-Rights Regimes and Natural Resources: A Conceptual Analysis. Land Econ. 249, 250.
Schroeder, R.A., 1997. "Re-claiming" land in the Gambia: Gendered property rights and environmental intervention. Annals of the Association of American Geographers 87 (3), 487-508.
Sekher, M., 2001. Organized participatory resource management: insights from community forestry practices in India. Forest Policy and Economics 3 (3-4), 137-154.
Sheldon v. Metro-Goldwyn Pictures, 1939. 106 F.2d 45 2d Cir.
Sheldon v. Metro-Goldwyn Pictures, 1940. 309 U.S. 390.
Singh, A., 1989. Digital change detection techniques using remotely-sensed data. International Journal of Remote Sensing 10 (6), 989-1003.
Smirnoff, G.I., 1996. Copyright on the Internet: A Critique of the White Paper's Recommendation for Updating the Copyright Act and how the Courts Are Already Filling in Its Most Important Shortcoming, Online Service Provider Liability. Cleveland State Law Review 44, 197.
Steins, N.A., Edwards, V.M., Röling, N., 2000. Re-designed principles for CPR theory. The Common Property Resource Digest 53, 1-5.
Universal Declaration of Human Rights, 1948. resolution 217 A (III).
U.S. Department of Commerce, T.F.-.-W.G.o.I.P.R., 1995. Intellectual Property and the National Information Infrastructure: The Report of the Working Group on Intellectual Property Rights.
van Wendel de Joode, R., 2004. Explaining the organization of open source communities with the CPR framework, International Association for the Study of Common Property, Oaxaca, Mexico.
Wolf, D., 1996. Situating feminist dilemmas in fieldwork. In: D. Wolf (Ed.), Feminist Dilemmas in Fieldwork. Westview, Boulder, pp. 1-55.

Yandle, T., 2003. The challenge of building successful stakeholder organizations: New Zealand's experience in developing a fisheries co-management regime. Marine Policy 27 (2), 179-192.

Part II

GIS and spatial analysis for environmental justice and wildlife

Chapter 5

Scales of Environmental Justice: Combining GIS and Spatial Analysis for Air Toxics in West Oakland, California

Abstract This paper examines the spatial point pattern of industrial toxic substances and the associated environmental justice implications in the San Francisco Bay Area, California, USA. Using a spatial analysis method called Ripley's K we assess environmental justice across multiple spatial scales, and we verify and quantify the West Oakland neighborhood as an environmental justice site as designated by the US Environmental Protection Agency. Further, we integrate the ISCST3 air dispersion model with Geographic Information Systems (GIS) to identify the number of people potentially affected by a particular facility, and engage the problem of non-point sources of diesel emissions with an analysis of the street network.

Introduction

Environmental Justice Theory

Environmental injustice has multiple meanings to different people, but can be thought of simply as occurring when a particular social group is disproportionately burdened with environmental hazards (Pellow 2000). Pellow defines environmental racism, an environmental justice issue, as the institutional rules, regulations, and policies of government or corporate decisions that deliberately target certain communities for least desirable land uses, resulting in the disproportionate exposure of toxic and hazardous

waste on communities. Environmental inequality addresses structural questions that focus on social inequality of power, resources and environmental burdens.

Environmental justice cases in California have focused recently on air pollution exposure from urban traffic (Houston et al. 2004), especially with regards to public schools (Morello-Frosch et al. 2002; Pastor et al. 2002), and public policy for health risk measurements (Dunsby 2004). Additionally, environmental justice has been addressed in California's water management (Haughton 1998), Toxic Releases Inventory (TRI; volume and location of emissions from facilities), and treatment, storage, and disposal facilities (TSDF), though the geographic focus has been primarily on Southern California and Los Angeles rather than the San Francisco Bay Area (Boer et al. 1997; Sadd et al. 1999; Morello-Frosch et al. 2001; Morello-Frosch et al. 2002). The US Environmental Protection Agency's (EPA) Air Toxics and Environmental Justice teams at the Region 9 Office recently focused their assessment of justice and equality on the health impacts of air toxics on a dense minority and low-income area in West Oakland, California in the San Francisco Bay Area through a sequence of events. Citizens suspected that their health was at risk from odorous releases from the many facilities in the area. Additionally, heavy diesel truck (vehicular) traffic was increasingly becoming a problem due to truck routes through their residential neighborhood (Pacific Institute and Coalition for West Oakland Revitalization 2003). The community of West Oakland mobilized (for mobilization on a transit issue, see Rodriguez 1999) and approached the US EPA for help.

A working relationship does not in itself push a community to the top of the US EPA list. Two additional factors made West Oakland a top priority: an unusually high

number of pollutant sources and a high density of minority and low-income people, all of which were matters of high public awareness in the region. On this base of perception, there was then need for valid empirical demonstration of congruent clustering of emissions and of minority residential populations. The agency needed to know the numbers of pollutant sources and the population structure in West Oakland before designating this area for priority attention.

We analyzed environmental justice in West Oakland across multiple scales with a point pattern analysis of spatial statistics new to environmental justice. Our objectives were to pinpoint statistically significant clusters of point source polluters and examine the surrounding demographics. Through Geographic Information Systems (GIS) we investigated non-point source pollution in addition to estimating the demographics affected by the most dangerous point-source polluter via a Gaussian plume model. The purpose of this research was to answer and quantify questions of scale in environmental justice.

The underlying processes that lead to environmental injustices can be political, economic, historical, and social. Politically, this could be lack of representation or participation, lack of lobbying power, greed among politicians, NIMBYism (not in my backyard), unequal power in the legal system and inadequate laws (Cole 1992), zoning (Maantay 2001), and inadequate regulations/enforcement/permitting (Levenstein and Wooding 1998; Mank 1999; Weinberg 1999). Economic processes include suburban sprawl (Ellis et al. 2002), widening income gaps (Krugman 2002), capitalism externalities (Levenstein and Wooding 1998), and market dynamics (Been 1994). Historical processes vary for different peoples, but these might include slavery, Jim Crow

laws[10], land ownership (Romm 2000), disenfranchisement, persecution, anti-immigrant laws, genocide, access to health care (US Commission on Civil Rights 2003), and immigrant work programs (Marentes 2004). Social processes include stereotypes (Bobo 2001), racism (Pulido 1996), language barriers, segregation, hegemony, social construction, affirmative inaction and mismatched attitudes (Blackwell et al. 2002).

Critics of environmental justice have cited methodological problems (Oakes et al. 1996; Yandle and Burton 1996; Friedman 2003), alternative causal interpretations such as market dynamics of capitalism (Been 1994), and misplaced priorities such as poverty over pollution (Foreman 1998). Further, it has been argued that potentially hazardous industries would provide compensation such as jobs for minorities and that increased wealth leads to increased health benefits (Tiebout 1956; Adler 1999; Simon 2000), but these arguments neglect the scale at which wealth and health benefits relate to the detrimentally affected local people. Facilities may not employ local residents nor pay an equitable wage (Pellow 2000). Further, even if facilities are not directly polluting, accidents can occur (Bolin et al. 2000).

Legislatively, environmental justice in the U.S. is addressed in a number of media. The 14th Amendment mandates equal protection under law, but intent must be shown to prove discrimination (such as clearly selective enforcement, unequal municipal services, or statements by government officials). Title VI of the Civil Rights Act prohibits discrimination by Federally funded programs, and the Supreme Court requires intent to be shown if a lawsuit is brought under Section 601, yet only disparate impact for

[10] Jim Crow laws were part of anti-African American legislation passed in the Southern states after the American Civil War. Examples include attendance in public schools and the use of facilities such as restaurants, theaters, hotels, cinemas and public baths. Trains and buses were segregated and interracial marriage was outlawed.

administrative complaints under Section 602 (Mank 1999; Weinberg 1999). Disparate impact may be evaluated through five steps (Mank 1999): 1) Identify the affected population, especially those in close proximity to the facility; 2) Determine the demographics of the affected population through mapping technology such as GIS; 3) Determine the universe(s) of facilities and total affected population(s), especially the cumulative pollution burden of neighboring facilities; 4) Conduct a disparate impact analysis both by examining the racial or ethnic composition within the affected population and by comparing that composition to unaffected populations in other relevant areas; 5) Determine the significance of the disparity through the use of standard statistical methods. We follow the steps outlined above in this research.

The U.S. Environmental Protection Agency (US EPA) historically has failed to enforce Title VI because of conflicts with the agency's primary goal to reduce pollution (Mank 1999). In 1994, President Clinton issued Executive Order 12898, which mandated all Federal agencies to address environmental justice in minority and low-income populations. Although the US EPA created an Office of Environmental Justice for guidance (U.S. Environmental Protection Agency 1992; U.S. Environmental Protection Agency 1998), the Office of Inspector General[11] released a review report stating that the US EPA had not been consistently implementing the intent of the Executive Order (Office of Inspector General 2004). Among the Office of Inspector General's findings were that the US EPA had recently de-emphasized minority and low-income populations in environmental justice, and that the methods of analysis, including the use of GIS, had

[11] The Office of Inspector General is an independent office within EPA that audits, evaluates, and investigates the EPA to promote economy and efficiency, and to prevent and detect fraud, waste, and abuse (http://www.epa.gov/oigearth).

been inconsistent. The US EPA must follow a methodology by which disparate impact can be assessed, and populations can be analyzed appropriately and consistently.

Spatial Analyses of Environmental Justice

In this paper we apply a point pattern statistical approach to environmental justice research that avoids pre-determined units of analysis to identify appropriate scales of analysis. A number of studies have integrated point pattern analysis into a GIS framework and have explored the value of this approach to epidemiology (Kingham et al. 1995; Gatrell and Bailey 1996) in the context of detecting clusters (Bhopal et al. 1992; Fotheringham and Zhan 1996; Gatrell et al. 1996). Our spatial point pattern analysis is based on Ripley's K-function (Ripley 1976), which has been broadly applied in ecological spatial patterns; examples include landscape dynamics of forest disease (Kelly and Meentemeyer 2002), distribution patterns of herbs (Kenkel 1993), desert shrubs (Prentice and Werger 1985; Skarpe 1991), and tropical forest trees (Sterner et al. 1986). O'Brien et al. (1999) used Ripley's K to assess the spatial and temporal distribution of canine cancers in Michigan. Barff (1987) analyzed the second-order point pattern of manufacturing plants in Ohio for economic and social justice.

Ripley's K examines the test statistic across various spatial scales and reveals the scale at which the pattern of events is operating most strongly. Furthermore, our analysis avoids the use of census tracts[12], which are politically defined and can change with time. Ripley's K addresses the distributive theory of equality in questioning whether or not

[12] A census tract, as defined by the U.S. Census Bureau, is a statistical subdivision of a county delineated by a local committee of census data users for the purpose of presenting data. Census tract boundaries normally follow visible features, but may follow governmental unit boundaries and other non-visible features. They are designed to be relatively homogeneous units with respect to population characteristics, economic status, and living conditions at the time of establishment, and average about 4,000 inhabitants.

certain communities are burdened with a disproportionate number of facilities. Not only does the statistic provide agencies such as the US EPA with sound backing of statistical significance and a link to equality and justice theory, but it also helps guide policies at the appropriate political-spatial scale—from international, national, and regional/state to county, city, and neighborhood.

Initial studies in environmental justice showed that emissions are concentrated in minority relative to predominantly white residential areas, with consequently differential health impacts among racial groups (United Church of Christ Commission on Racial Justice 1987; Bullard 1994). However, critics were quick to point out flaws in the analysis with emphasis on scale—results and conclusions can change depending on the range of space and time analyzed (Anderton et al. 1994; Friedman 2003). Maantay (2002) reported that there is a need to develop more accurate methods for determining the geographic extent of exposure and the characteristics of the affected populations, to use dispersion modeling and advanced proximity analysis, and neighborhood-scale analysis. Rhodes (2003) suggested the use of several different spatial measurement units with geographic problems and to be sensitive if or when the indications of environmental justice problems change. We implement the conclusions of these researchers here, with particular attention to varying spatial scale, neighborhood-level analysis and dispersion modeling.

The standard spatial scale of analysis for environmental justice with GIS in the US has been the census tract level (Bowen et al. 1995; Yandle and Burton 1996; Szasz and Meuser 2000; Cutter et al. 2002; Buzzelli et al. 2003). The focus on the census tract assumes that point sources and the population are distributed uniformly throughout the

census tracts, which are inconsistent in size and shape. Researchers have attempted to avoid the census tract level with proximity-based assessments of demographics within a certain radius of a given facility. The exact radius is often fitted, subjective, or arbitrary (Anderton et al. 1994), however, and should depend on air movement. Radius sizes have ranged from 0.5 km (Dunn and Kingham 1995; Dunn et al. 1995; Dunn et al. 2001), 0.8 km (Baden and Coursey 2002), and 1.6 km (Glickman and Hersh 1995; Bolin et al. 2000), to 4.0 km (Anderton et al. 1994); Pastor et al. (2004) examined a range of 0.8 km, 1.6 km, and 4 km buffers. Additionally, these authors employed a range of statistical tests, such as Chi-square, Cramer's V (Cramér 1999), raised incidence modeling (Diggle and Rowlingson 1994), and the Townsend index of deprivation (Townsend et al. 1988). Some authors were content with producing maps with no statistics.

Scholars have debated what the unit of analysis should be, from the "community" that is based on census block groups and travel time (Taquino et al. 2002) to raster-based (Mennis 2002) or multi-scalar analysis (Williams 1999). There has also been criticism that the choice of target predetermines the evaluation of social impact. We take a different path: scale becomes a variable rather than a pre-determined measure. We seek to identify the scales at which clusters, and congruence among them, are more and less likely to exist for different analytical purposes.

Methods

Data

The main demographic information (e.g. population density, race breakdown) was obtained from the US Census Bureau's 2000 survey at census tract, block group, and

block spatial scales. We used TRI for 1999 (to compare to the 2000 Census data) for the point pattern analysis[13]. The annual TRI records the volume and location of self-reported releases from private sector and federal facilities. All industries that meet the following criteria have mandatory reporting: (a) the production facility's primary Standard Industrial Classification is manufacturing; (b) the facility has 10 or more full-time employees; and (c) the facility manufactures or processes over 25,000 pounds of at least one of the over 600 TRI chemicals, or uses more than 10,000 pounds of at least one TRI chemical (U.S. General Accounting Office 1991; U.S. General Accounting Office 1991; U.S. Environmental Protection Agency 1997). Specifically, TRI chemicals in West Oakland included: chlorine, chromium, nitrate compounds, and zinc compounds, though the carcinogen acetaldehyde is perhaps the most harmful. Data are provided for each release medium, including air, water, underground injection, land, and off-site transfers. A critical methodological issue is the accuracy of the locations of point-source hazards found in US EPA data sets (e.g., Stockwell et al. 1993; Glickman and Hersh 1995; Scott et al. 1997). But, the US EPA TRI data offers the most comprehensive measures of industrially released hazardous emissions in the United States, particularly after we checked for locational validity by geocoding each TRI location to its correct street address (Krieg 1998b; Daniels and Friedman 1999; Mitchell et al. 1999; Bolin et al. 2000). Addresses used in geocoding were verified as the facility address rather than the office address.

[13] Additional data reviewed for West Oakland, but not used in the point pattern analysis: US EPA Region 9 Air Division's Air Quality System (formerly named the Aeromatic Information Retrieval System or AIRS); National Pollutant Discharge System (NPDS); sources listed under the Resource Conservation and Recovery Act (RCRA); and a yellow pages listing for gasoline stations.

The BAAQMD health risk screening was based on the US EPA's Industrial Source Complex Short Term (ISCST3) air dispersion model (U.S. Environmental Protection Agency 1995; U.S. Environmental Protection Agency 1999), and those risks were estimated in accordance with procedures adopted by Cal/EPA's Office of Environmental Health Hazard Assessment (OEHHA) for the Air Toxics Hot Spots Program. The ISCST3 model has been validated successfully for a number of pollutants in a variety of locations (e.g., Kumar et al. 1999; Lorber et al. 2000; Elbir 2002; Mazzeo and Venegas 2004). Dispersion is a term that describes advection (horizontal movement) and diffusion (mixing) of gases. Air dispersion models can range from simple models that require minor computation to complex three-dimensional models that require extensive data and computation, the type of which depends on the scale of the problem and the input data available. Chakraborty and Armstrong (1995) detail the methodology by which to determine demographic composition of a population affected by the release of toxic substances. They describe the Geographic Plume Analysis approach that takes a dispersion model, which outputs a dispersal "footprint", and superimposes it on a demographic database. We follow this approach here.

The data were processed in a GIS database containing air pollutant source data (U.S. Environmental Protection Agency 1997) for US EPA Region 9 (Arizona, California, Nevada and the Pacific Islands) and detailed demographic information for West Oakland from the 2000 US Census (U.S. Bureau of the Census 2000). We integrated the database with ESRI's *ArcGIS* 8.1 and *S-Plus* 6.0. The main statistical processing of point pattern analyses relied on *S-Plus* 6.0, and analyses and map

production on the *ArcMap* component of *ArcGIS* 8.1. The data were projected into Albers Equal Area with the North American Datum 1983 to preserve area measurements.

Analysis

Clusters of point source polluters were identified through point pattern analysis that combined intensity distributions and Ripley's K. Intensity is defined as the mean number of points per unit area; intensity distributions reveal first-order properties of a spatial point process and variation through space to assess the spatial dependence between points. First-order properties of a spatial point process describe how the mean number of points per unit area (the intensity) varies through space. For a stationary process, the intensity is assumed to be constant over the bounded region of interest. We initially followed a weighted edge correction (Ripley 1977), though Lancaster and Downes (2004) specify that edge correction is not necessary for length-scale assessment of clusters. Intensity distributions show *where* clusters are occurring, Ripley's K reveals *statistical significance* of those apparent clusters.

Ripley's K is a second-order (variance of distances) function for spatial point pattern and is used to detect spatial randomness (Ripley 1976). A spatial point pattern is a collection of points irregularly located within a bounded region of space (e.g. pollutant sources within a county). The data set may consist of locations only, or it may be a marked point process, with data values associated with each location (e.g. longitude/latitude with associated emissions). The analysis is termed "second-order" because of its focus on the variance of the test statistic across a series of progressively larger areas—the size of the step is set to reveal the inter-event distances at which

clustering, if present, is strongest. By examining the test statistic at various spatial scales (e.g. region, county, city), the scale at which the pattern of events (points) is operating most strongly (highest statistical significance and confidence) can be determined. Ripley's K examines the null hypothesis of Complete Spatial Randomness (CSR) for a mapped spatial point pattern. CSR is defined by the following criteria: a) the intensity of the point pattern does not vary over the bounded sampling region, and the pattern follows a homogeneous Poisson distribution; b) there are no interactions among the points. Ripley's K can reject the null hypothesis that the spatial pattern of points is random.

After the data were analyzed by the Ripley's K method, a plot of count $K(h)$ versus distance h revealed deviations as expected under CSR. The deviation was tested for statistical significance. One test employed the calculation of constant approximate confidence intervals around CSR (Getis and Franklin 1987; Szwagrzyk and Czerwczak 1993). Another test used Monte Carlo methods to determine statistical significance of the results by determining the amount of variation to be expected in sample statistics from computer-generated data (e.g., Manly 1991). In the context of spatial pattern analysis, Monte Carlo methods simulate randomly generated plots of the same dimensions of the observed plot thus creating confidence intervals from the highest and lowest values of $K(h)$ (Haase 1995). We plot $((K(h)/\pi)^{0.5} - h)$ or simply $(L(h) - h)$ against h to show the deviation of $K(h)$ from CSR. If the deviation of the sample statistic from zero expectation is positive and above the upper limit of the confidence interval, then a clumped distribution can be assumed, while negative deviation indicates a regular pattern, otherwise the null hypothesis of CSR cannot be rejected (Haase 1995).

Our GIS analysis followed the point pattern analysis with an examination of the communities and pollutant sources in the proximity of identified clusters of point source polluters. We determined race and income distributions in addition to the presence or absence of environmental goods (e.g, parks). With the BAAQMD health risk screening based on the US EPA's ISCST3 air dispersion model, we evaluated in the West Oakland cluster the potential exposure by the facility Red Star Yeast (LaSaffre Yeast Corp.), which the US EPA determined posed the greatest health risk due to carcinogenic emissions of acetaldehyde (personal communication Grow 2001). LaSaffre Yeast, which operates in over 180 countries, ranked 8th of all SF Bay Area facilities for cancer health risks, and 2nd in Oakland for air pollution health risks (Greenaction.org 2003). Finally, we assessed mobile source pollution with an examination of the road network and travel routes within and around the neighborhood.

Results

First- and Second-Order Spatial Analysis

An initial examination of point sources in the US EPA's Region 9 in California shows clusters unsurprisingly in the major population centers of the San Francisco Bay Area and Los Angeles. With the question of West Oakland in mind, we first analyzed all TRI sources from 1999 in the San Francisco Bay Area cluster, which includes the counties of Alameda, Contra Costa, Marin, San Mateo and San Francisco (Figure 1a).

An intensity distribution revealed multiple peaks, with the two largest clusters located in the East Bay (Figure 1b). Our Ripley's K test found that the two major clusters were statistically significant whereby the deviation of the sample statistic from zero

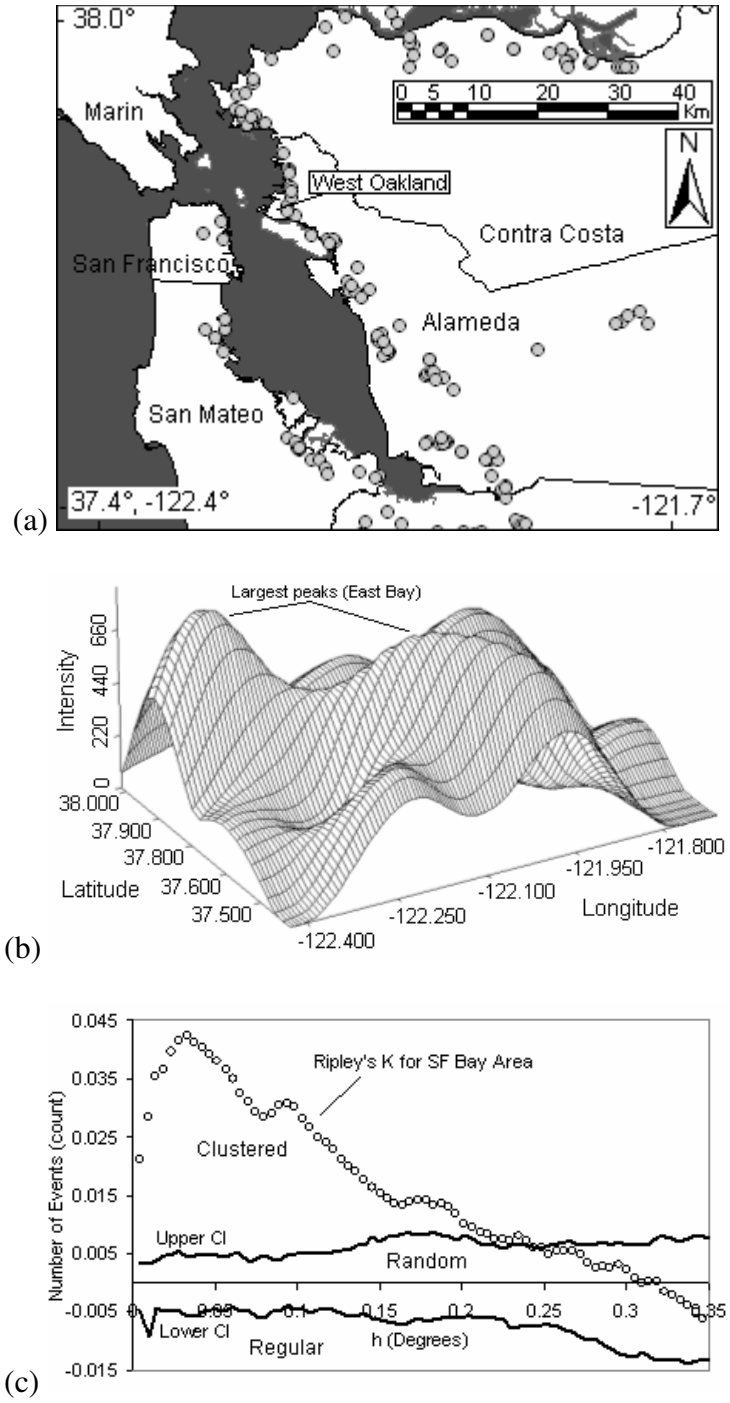

Figure 1. (a) TRI (1999) facilities in the San Francisco (SF) Bay Area. (b) Intensity distribution for TRI (1999) sources in the SF Bay Area of points per grid cell in longitude by latitude. (c) Ripley's K test for TRI (1999) facilities in the SF Bay Area. The distribution above the upper confidence interval indicates clustering at the scales of degrees. The distribution between the confidence intervals indicates a random spatial pattern. Below the lower confidence interval would indicate a regular spatial pattern. The y-axis represents the deviation of the sample statistic from CSR; the units are in transformed count numbers. The x-axis represents distance (units are in degrees).

expectation was positive and above the confidence interval (Figure 1c). The distribution of Ripley's K above the upper confidence interval indicates clustering, between the confidence intervals indicates random spatial pattern, and below the lower confidence interval indicates a regularly distributed pattern. The y-axis represents the deviation of the sample statistic from CSR; the units are in count numbers, but have been transformed as per Haase (1995). The x-axis represents distance (units are in degrees of longitude and latitude here), and the distance shows the extent of the clustering.

Second, we examined the East Bay (Alameda County) TRI clusters specifically, again with the intensity distribution and Ripley's K (Figures 2a, b, and c). The intensity distribution shows the evident positioning of facilities along the west side, but cannot distinguish clearly individual clusters within that swell of facilities. We were able to distinguish the individual clusters within that swell with the Ripley's K plot as evidenced by the three peaks in the clustered area of the plot (Figure 2a). Because the US EPA was interested in validating the identification of West Oakland as an environmental justice site, we examined in depth the City of Oakland cluster (Figure 3a). The intensity distribution illustrates the two clusters of facilities, but cannot determine if those peaks are statistically significant clusters (Figure 3b). The Ripley's K plot shows that there is still statistically significant clustering occurring, though the data have become limited at this small of a spatial scale so this is the smallest scale at which we can examine with Ripley's K (Figure 3c).

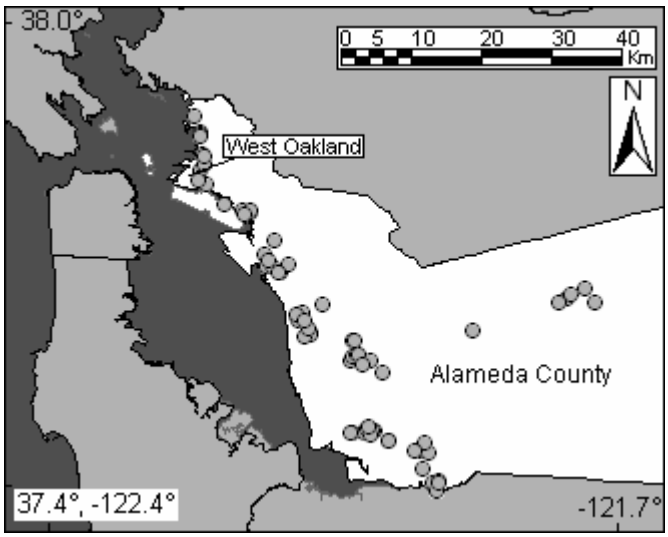

(a)

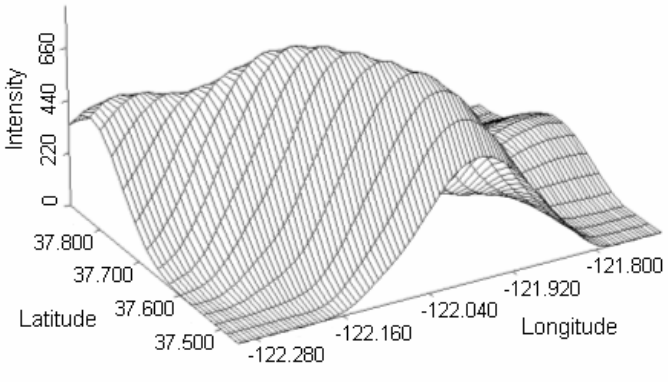

(b)

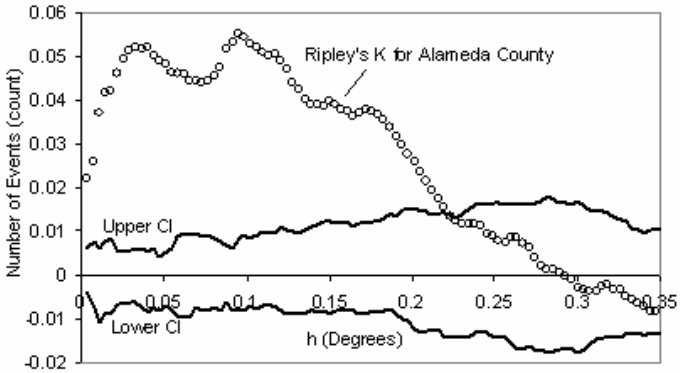

(c)

Figure 2. (a) TRI (1999) facilities in Alameda County. (b) Intensity distribution for TRI (1999) facilities in Alameda County. (c) Ripley's K test for TRI (1999) facilities in Alameda County.

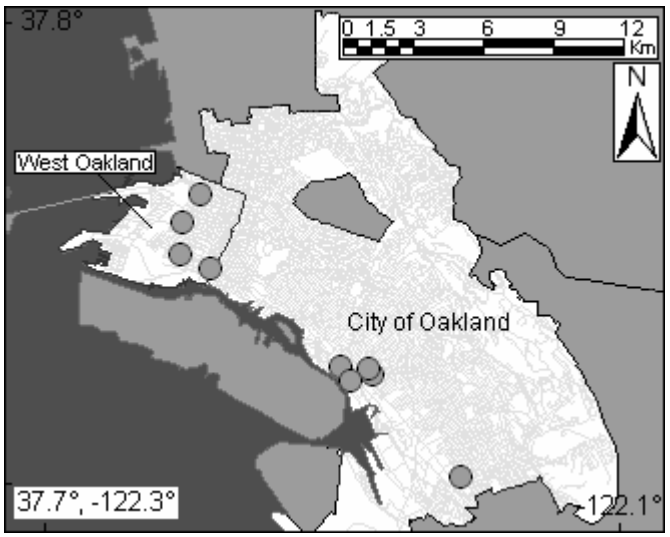

(a)

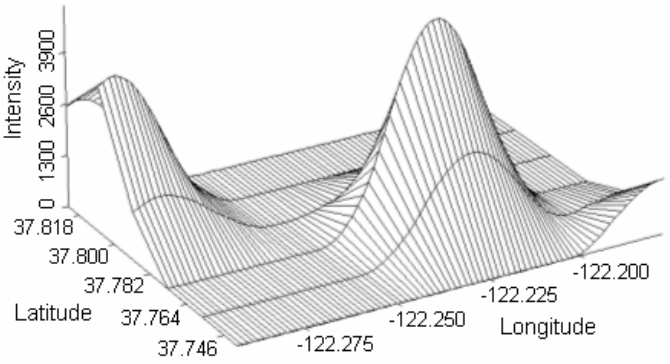

(b)

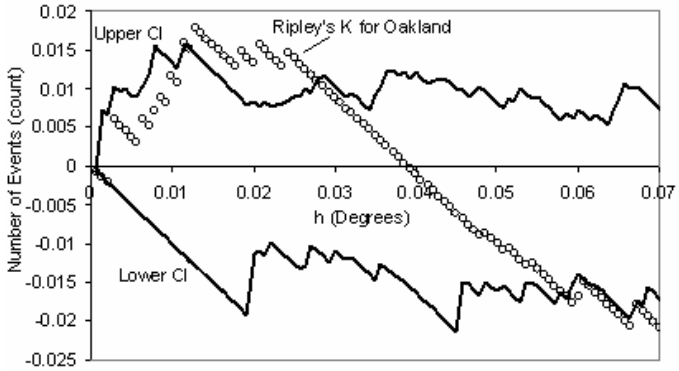

(c)

Figure 3. (a) TRI (1999) facilities in the City of Oakland. (b) Intensity distribution for TRI (1999) facilities in the City of Oakland. (c) Ripley's K test for TRI (1999) facilities in the City of Oakland.

GIS Analysis for West Oakland

After determining the presence, scale, and location of clusters, the next step in an environmental justice framework is to examine the communities within the extent of those clusters. Using the US Census Bureau 2000 survey, we analyzed the block level data (a block is roughly equal to a city block) for the cluster at West Oakland. The greatest density of West Oakland residents is situated in the center and along the eastern freeway border of the area; the western industrial port is largely uninhabited. We created a broad race distribution map based on the racial majority for each block (Figure 4). This map shows that the majority of the West Oakland community is African American. In West Oakland, African Americans (Black) comprise 65% of the population, the rest of the population is made up of Caucasians (White; 9%), Latinos (Hispanic; 7%), Asians (9%), and "Other" (racial mixes, Native Americans/American Indians, Hawaiian; 10%). The median household income per year is roughly $20-25,000US, which is lower than that of the surrounding areas (Figure 5). There are 14 schools in West Oakland, half of which are within 600 m of a TRI facility. There are some parks (an environmental good),

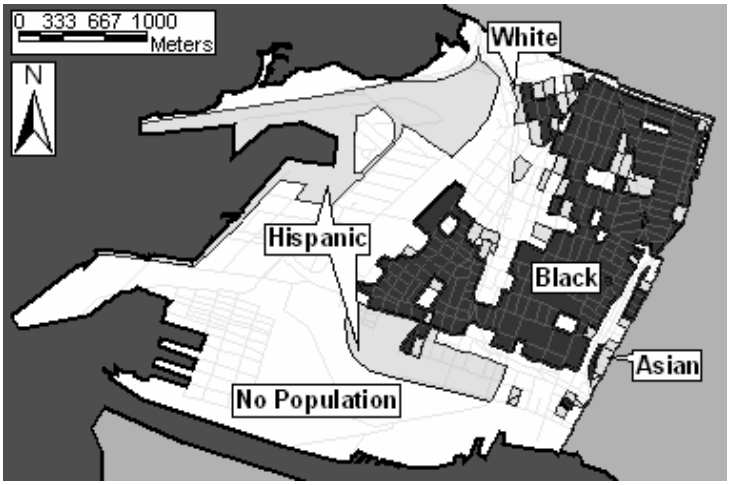

Figure 4. Broad race distribution map based on racial majority for each block in West Oakland.

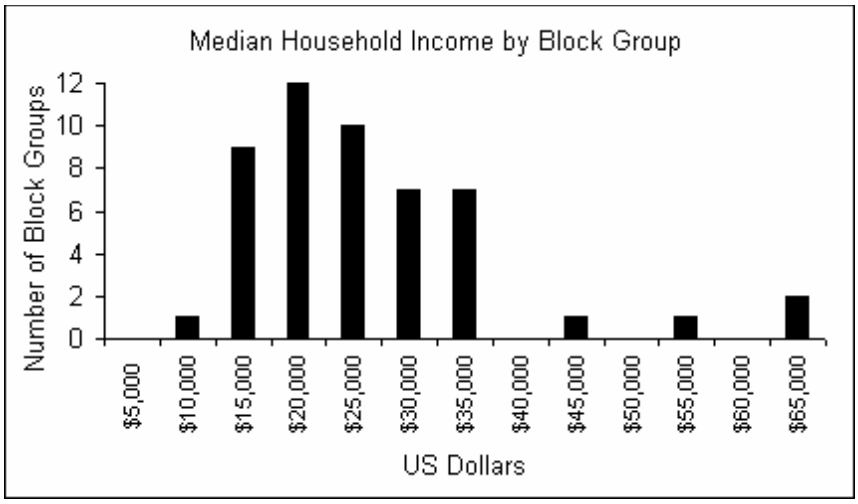

Figure 5. Median household income by block group (frequency) in US Dollars.

but the newest one is rarely used as it is adjacent to the freeway and a Superfund site[14]. There are no hospitals in West Oakland.

We split air pollutant sources into stationary (e.g. factories) and mobile (e.g. vehicles) sources. Stationary sources are scattered throughout West Oakland, but they are not equal to each other in their relative health threat to the community. Now, from a TRI database with thousands of facilities the US EPA can focus on the facilities that pose the greatest health threats—in the case of West Oakland, the carcinogenic emissions of acetaldehyde by Red Star Yeast. We integrated the BAAQMD air modeling analysis of Red Star Yeast's emissions into the GIS (Figures 6a and b). We overlaid the ISCST3 air dispersion model on top of the block level population layer in order to determine the number of people potentially affected by Red Star Yeast (Figure 6c). The resulting estimate of 5,628 people is derived from the maximum extent of the BAAQMD model, including the whole of those blocks cut by the model, but the number of people who live

[14] A Superfund site is any land in the US that has been contaminated by hazardous waste and identified by the EPA as a candidate for cleanup because it poses a risk to human health and/or the environment (http://www.epa.gov/superfund/).

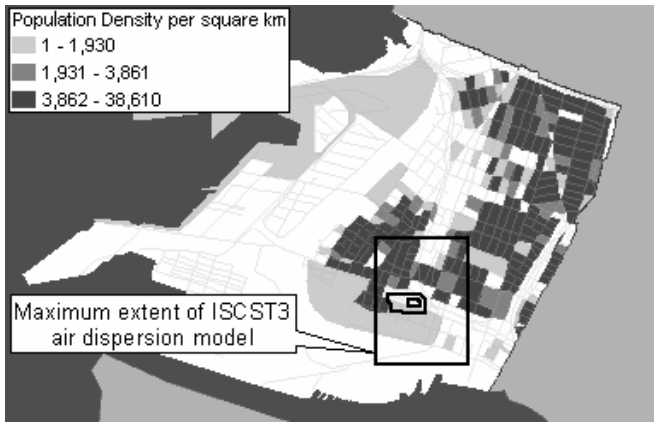

(a)

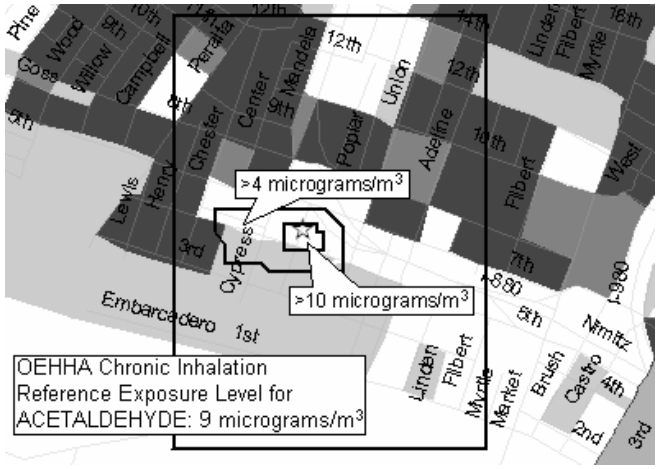

(b)

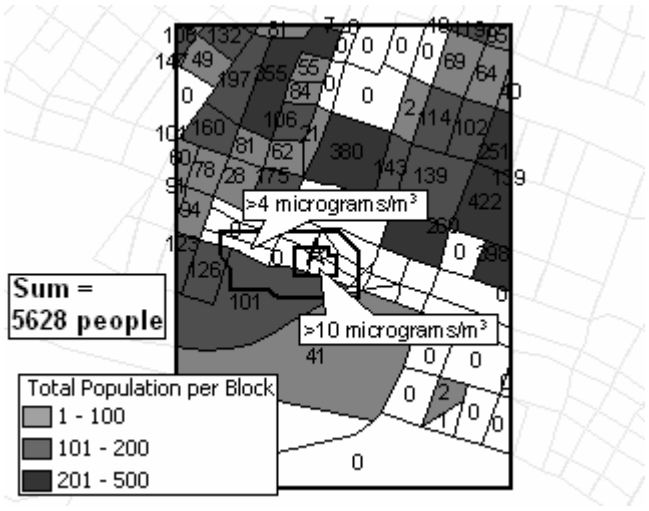

(c)

Figures 6. (a) and (b) Extent of Red Star Yeast emissions based on BAAQMD's Health Risk Screening Analysis on population density per square mile. (c) Total number of people potentially affected by Red Star Yeast emissions.

within the high-concentration areas is under 268. Furthermore, the air dispersion model is drawn in much more detail closer to the facility, whereas uncertainty leads to a generalized rough rectangle for the maximum bounds. The highest concentrations of acetaldehyde emitted from the facility effect those populations living closest to Red Star Yeast, and the associated health effects are subject to the assumptions of the model. Here, we found the estimated number of people potentially exposed to Red Star Yeast's emissions based on the block level demographic information within the boundaries of the ISCST3 model.

The mobile source in West Oakland is primarily from heavy diesel truck traffic through the community to the Port of Oakland. Chemicals in diesel pollution may cause cancer, harm the reproductive system and aggravate asthma (Morgan et al. 1997; Kagawa 2002). The Pacific Institute and Coalition for West Oakland Revitalization (2003) offered a number of ideas to alleviate these problems. With GIS we assess two of their recommendations: install traffic barriers on prohibited streets, and create a designated truck route not through the neighborhood. As communicated by the US EPA, the truck drivers indicated that there are only a few gasoline (petrol) stations near the port and those stations are unavoidably in the middle of the densely populated neighborhoods (personal communication Grow 2001). We mapped the population density, road network, port terminals, and all gasoline stations (15) within a 2.4-km (1.5-mile) radius of the center of West Oakland along with the major terminals (Figure 7). Based on the two recommendations and Figure 7, we found an alternative driving route around the high population density. The roads currently used—which cut through the community—are crossed off with X's, and the alternative route is highlighted. In sum, the key results

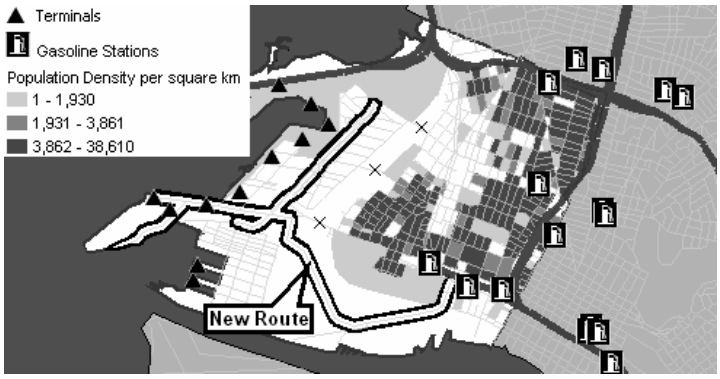

Figure 7. Road network, port terminals, gasoline stations, and an alternative driving route around the high population density.

here are: 1) detection of the cause of the problem—the three roads that run into the community; and 2) recommendation of a solution to the problem—an alternative route around the community. Without site familiarity, the US EPA would have little sense of road spacing and gasoline station locations. The GIS can provide a clear picture to the arguments posed by the residents and truckers on transit routes and gasoline stations.

Discussion

We used Ripley's K combined with GIS to identify not only statistically significant areas of clusters, but also the scales at which those clusters exist. This research focused on narrowing down the extensive region- and state-wide datasets into local neighborhoods that can be applied with local remedies. It is not unusual that a hierarchy of politics and economics exists across spatial scales for environmental justice (Simmons 2004). At the local level, new issues emerge that may not otherwise be evident at larger scales, such as the road network and transportation problem. Corrective justice, which is the notion that polluters should be punished and held responsible for cleanups and should compensate or repair communities damaged by historic pollution, can be implemented at the local level

(Lazarus 1993). But, intermediate scales of clusters were also seen in, for example, the clustering of facilities in the East Bay relative to the San Francisco Bay Area as a whole. We focused on West Oakland not only as a directly applicable problem, but also as a means to raise and answer broader questions and purposes to be applied generally.

As the spatial scale becomes smaller we necessarily lose the amount of data points to work with and the analysis and interpretation of the intensity distributions and Ripley's K plots likewise changes. At the scale of the San Francisco Bay Area, clustering is most dominant in the East Bay, though geography influences clustering and edge effects as well (water and topography constrain potential sites at this scale that play less of a role at other sites and scales). The intensity distribution can show where clumping occurs, but the largest peaks are likely the most important clusters because the peaks are based on a scale relative to one another. At the scale of Alameda County, the intensity distribution reveals little about individual clustering, as it seems that the point sources are evenly spread along the water (large peak on the west side). The Ripley's K plot, however, is more informative at the county scale where geography and edge effects are minimized. Three clear peaks in the plot point to three areas of clusters all within the broad cluster along the water. Analysis of one of those three peaks—the City of Oakland—shows two areas where facilities are located. The intensity distribution shows a cluster where West Oakland is defined, and another more intense peak (the facilities are clustered closer together) further south. The Ripley's K plot is not as clear at this scale because the data have become so sparse relative to the larger scales.

As with other EPA hazard data, there are recognized limitations to the TRI data. In addition to not providing human exposure information, the data are restricted to large

manufacturing facilities and exclude releases from smaller firms, landfills and abandoned industrial sites, hazardous waste facilities, and power plants (Bolin et al. 2000). Pastor et al. (2004) report that it is difficult to make time series or longitudinal comparisons in TRI emission reporting due to periodic changes in the reporting requirements, but this paper focuses primarily on issues of spatial scale. Further epidemiological work is still needed.

The literature on GIS and spatial analysis for environmental justice has focused on census tracts or proximity-based assessments within variable radii from facilities. Critics have argued the need to assess environmental justice across different spatial scales; additionally, dispersion modeling and neighborhood-scale analysis has been called for (e.g., Maantay 2002). Further, no clear consensus on appropriate spatial statistics has emerged, because each statistic addresses different types of questions. We add to the environmental justice literature a method that: 1) avoids census tracts and radii-based proximity assessments; 2) assesses environmental justice across large and small spatial scales; 3) integrates a well-developed air dispersion model with demographic data; and 4) includes a measure of statistical significance for cluster evaluation.

The Office of Inspector General criticized the US EPA's de-emphasis of minority and low-income populations in addressing Executive Order 12898. While the criticism is certainly justified, the US EPA must grapple with changing political power and administrative changes that lead to these shifts in emphasis. The method we present here approaches the issue of environmental justice without starting with race or income, since such a starting point might lead to bias in data interpretation. In other words, our results showed that clusters of polluters are statistically pinpointed first, and then the surrounding demographics are examined next rather than the other way around.

Unfortunately, minorities and low-income populations are often coupled with these clusters nonetheless, hence the rationale behind the environmental justice movement, though certainly many minorities and poor people live in clean environments.

This analysis also ties into "disparate impact" as was discussed on Section 602 in Title VI of the Civil Rights Act. Disparate impact is now connected to communities living within statistically significant clusters, or a disparate number, of TRI facilities relative to other communities. The US EPA can apply these results to implement policies, but based on what notions of justice or equality? Theories of justice (Wenz 1988; Miller 1999; Rawls 1999) range from utilitarian (greatest good for greatest number), libertarian (greatest individual benefits without harm), communitarian (community over individual), and egalitarian (greatest benefit to least advantaged—maximize the minimum). Theories of equality (Sharder-Frechette 2002) include distributive justice (equal apportionment of social benefits and burdens), participative justice (equal rights to self-determination in societal decision-making), and procedural justice (equal distribution of enforcement, monitoring and other processes).

Some theories of justice and equality simply are insufficient to base policies on. A utilitarian approach, for instance, might justify disproportionate environmental burdens if society as a whole is better off economically due to production, but Lejano et al. (2002) has already found that there is no justice in this approach, at least for air quality policies in Southern California. Procedural justice has been argued as insufficient in the environmental justice in California and the Southwestern US to advance environmental equality (Pulido 1994). Although the State of California's EPA has emphasized participative justice in environmental justice policies (California Environmental

Protection Agency 2003), this may be more difficult to apply at a federal level for the US EPA. Other theories of justice and equality need to be reinforced through policies. The egalitarian approach is lacking because West Oakland, considered as the least advantaged in terms of income, exposure to pollution and access to environmental goods, is not realizing the greatest benefits. The US EPA must implement distributive justice because these social burdens are not equally apportioned.

Areas like West Oakland may be obvious areas for targeting environmental justice research due to the high amounts of pollution coupled with high minority concentrations, and the communities mobilized to solve their local injustice found there. For future inquiry, however, other communities may be less mobilized and empowered or the clustering of pollutant sources may be less obvious than those studied here. Although the spatial data analysis techniques were used to verify existing environmental justice areas, these methods can be used to identify new areas for study relatively quickly and efficiently. The creation of potential environmental injustice areas may be proactively avoided if the US EPA has an efficient data monitoring strategy whereby clusters of possible polluters would trigger a statistical alarm. Certainly, not every cluster would necessarily be an environmental justice site, but this would at least provide a mechanism for the US EPA to focus their efforts for further research. Additionally, if the air dispersion model can be applied to many facilities simultaneously, then a possible aggregate impact could be assessed. It is important that the US EPA continue to use GIS and spatial data analysis to approach these issues and expedite the process to the enforcement stage.

Following the completion of this analysis (but before publication), the US EPA applied our results in combination with community members, activist groups[15], and Federal, State and local agencies to apply pressure on Red Star Yeast to significantly restrict emissions or face sanctions and be shut down. Further, BAAQMD did not renew Red Star Yeast's air emissions permit. Subsequently, Red Star Yeast announced that they would close their facility in West Oakland due to "market conditions" and "challenging California environmental conditions." From an environmental justice standpoint for the community, the closure was a victory that came from activism, science, and involvement with government agencies.

Acknowledgements

We wish to thank Greg Biging, Catherine Brown, Nicole Buffa, Louise Fortmann, Richard Grow, Dave Guiliano, John Kennedy, and Dara O'Rourke for assistance and support for this project. We are grateful for the anonymous reviewers who provided invaluable comments and suggestions. Preliminary results were presented at the American Public Health Association conference 2003, and won the 1st place award in the Environment section. This work was supported by NASA Headquarters under the Earth System Science Fellowship Grant NGT5-30473, and by the US EPA Region 9, Air Division funding for summer internships.

[15] The activist groups included: Chester Street block Club Association, Citizens for West Oakland Revitalization, Environmental Science Institute, Greenaction for Health and Environmental Justice, Pacific Institute, and Youth Empowerment Center.

References

Adler, J.H. 1999. There's no justice in EPA's environmental justice policy. Corporate Environmental Strategy. 6:183-189.

Anderton, D.L., A.B. Anderson, J.M. Oakes and M.R. Fraser 1994. Environmental Equity: The Demographics of Dumping. Demography. 31:229-248.

Baden, B.M. and D.L. Coursey 2002. The locality of waste sites within the city of Chicago: a demographic, social, and economic analysis. Resource and Energy Economics. 24:53-93.

Barff, R.A. 1987. Industrial clustering and the organization of production: A point pattern analysis of manufacturing in Cincinnati, Ohio. Annals of the Association of American Geographers. 77:89-103.

Been, V. 1994. Locally Undesirable Land Uses in minority neighborhoods: Disproportionate siting or market dynamics? Yale Law Journal. 103:1383-1421.

Bhopal, R.S., P. Diggle and B. Rowlingson 1992. Pinpointing clusters of apparently sporadic cases of Legionnaires' disease. British Medical Journal. 304:1022-1027.

Blackwell, A., S. Kwoh and M. Pastor 2002. A Changing America. *In* Searching for the Uncommon Common Ground - New Dimensions of Race in America Eds. A. Blackwell, S. Kwoh and M. Pastor. Norton, New York, pp. 21-26.

Bobo, L. 2001. Racial Atttitudes and Relations at the Close of the Twentieth Century. *In* America Becoming - Racial Trends and their Consequences Eds. N. Smelser, W.J. Wilson and F. Mitchell. National Research Council, Washington, D.C., pp. 264-301.

Boer, J.T., M. Pastor, J.L. Sadd and L.D. Snyder 1997. Is there environmental racism? The demographics of hazardous waste in Los Angeles County. Social Science Quarterly. 78:793-810.

Bolin, B., E. Matranga, E.J. Hackett, E.K. Sadalla, K.D. Pijawka, D. Brewer and D. Sicotte 2000. Environmental equity in a sunbelt city: the spatial distribution of toxic hazards in Phoenix, Arizona. Environmental Hazards. 2:11-24.

Bowen, W.M., M.J. Salling, K.E. Haynes and E.J. Cyran 1995. Toward Environmental Justice: Spatial equity in Ohio and Cleveland. Annals of the Association of American Geographers. 85:641-663.

Bullard, R. 1994. Environmental Justice for all: It's the right thing to do. Journal of Environmental Law and Litigation. 281

Buzzelli, M., M. Jerrett, R. Burnett and N. Finklestein 2003. Spatiotemporal perspectives on air pollution and environmental justice in Hamilton, Canada, 1985-1996. Annals of the Association of American Geographers. 93:557-573.

California Environmental Protection Agency 2003. Final Report of the Advisory Committee on Environmental Justice to the Cal/EPA Interagency Working Group on Environmental Justice. California Environmental Protection Agency, Sacramento, CA, pp. 13-35.

Chakraborty, J. and M.P. Armstrong 1995. Using geographic plume analysis to assess community vulnerability to hazardous accidents. Computers, Environment and Urban Systems. 19:341-356.

Cole, L. 1992. Empowerment as the key to environmental protection: The need for environmental poverty law. Ecology Law Quarterly. 19:634-683.

Cramér, H. 1999. Mathematical Methods of Statistics. Princeton University Press.
Cutter, S.L., M.S. Scott and A.A. Hill 2002. Spatial variability in toxicity indicators used to rank chemical risks. American Journal of Public Health. 92:420-421.
Daniels, G. and S. Friedman 1999. Spatial inequity and the distribution of industrial toxic releases: evidence for the 1990 TRI. Social Science Quarterly. 80:244-262.
Diggle, P. and B. Rowlingson 1994. A conditional approach to point process modelling of elevated risk. Journal of the Royal Statistical Society. Series A 157:433-440.
Dunn, C.E. and S.P. Kingham 1995. Modelling air quality and the effects on health in a GIS framework. *In* Innovations in GIS 3 Ed. D. Parker. Taylor & Francis, London, pp. 205-213.
Dunn, C.E., S.P. Kingham, B. Rowlingson, R.S. Bhopal, S. Cockings, C.J.W. Foy, S.D. Acquilla, J. Halpin, P. Diggle and D. Walker 2001. Analysing spatially referenced public health data: a comparison of three methodological approaches. Health & Place. 7:1-12.
Dunn, C.E., J. Woodhouse, R.S. Bhopal and S.D. Acquilla 1995. Asthma and factory emissions in northern England: addressing public concern by combining geographical and epidemiological methods. Journal of Epidemiology and Community Health. 49:395-400.
Dunsby, J. 2004. Measuring environmental health risks: The negotiation of a public right-to-know law. Science, Technology & Human Values. 29:269-290.
Elbir, T. 2002. Application of an ISCST3 model for predicting urban air pollution in the Izmir metropolitan area. International Journal of Environment and Pollution. 18:498-507.
Ellis, J., C. Mason, B. Shamasunder and C. Garzón 2002. Brownfields Neighborhood Revitalization. *In* Second National People of Color Environmental Leadership Summit - Summit II. Urban Habitat, Oakland, CA, pp. 1-12.
Foreman, C. 1998. The Promise and Peril of Environmental Justice. Brookings Institution Press, Washington, D.C. 1-33 pp.
Fotheringham, A.S. and F. Zhan 1996. A comparison of three exploratory methods for cluster detection in point patterns. Geographical Analysis. 28:200-218.
Friedman, D. 2003. The Environmental Racism Hoax. American Enterprise Institute.
Gatrell, A.C. and T.C. Bailey 1996. Interactive spatial data analysis in medical geography. Social Science and Medicine. 42:843-855.
Gatrell, A.C., T.C. Bailey, P.J. Diggle and B.S. Rowlingson 1996. Spatial point pattern analysis and its application in geographical epidemiology. Transactions of the Institute of British Geographers. 21:256-274.
Getis, A. and J. Franklin 1987. Second-order neighborhood analysis of mapped point patterns. Ecology. 68:473-477.
Glickman, T. and R. Hersh 1995. Evaluating environmental equity: the impacts of industrial hazards on selected social groups in Allegheny County Pennsylvania. Resources for the Future, Washington, DC.
Greenaction.org 2003. Action Alert. Greenaction.org.
Grow, R. 2001. Air Grants and Program Integration Office, San Francisco, CA.
Haase, P. 1995. Spatial pattern analysis in ecology based on Ripley's *K*-function: Introduction and methods of edge correction. Journal of Vegetation Science. 6:575-582.

Haughton, G. 1998. Geographical equity and regional resource management: water management in southern California. Environment and Planning B: Planning & Design. 25:279-298.

Houston, D., J. Wu, P. Ong and A. Winer 2004. Structural disparities of urban traffic in Southern California: Implications for vehicle-related air pollution exposure in minority and high-poverty neighborhoods. Journal of Urban Affairs. 26:565-592.

Kagawa, J. 2002. Health effects of diesel exhaust emissions - a mixture of air pollutants of worldwide concern. Toxicology. 181:349-353.

Kelly, M. and R.K. Meentemeyer 2002. Landscape dynamics of the spread of sudden oak death. Photogrammetric Engineering and Remote Sensing. 68:1001-1009.

Kenkel, N.C. 1993. Modeling Markovian dependence in populations of *Aralia nudicaulis*. Ecology. 74:1700-1706.

Kingham, S.P., A.C. Gatrell and B. Rowlingson 1995. Testing for clustering of health events within a Geographical Information System framework. Environment and Planning A. 27:809-821.

Krieg, E. 1998b. Methodological considerations in the study of toxic waste hazards. The Social Science Journal. 35:191-201.

Krugman, P. 2002. For Richer. *In* The New York Times, Sunday Magazine, p. 62.

Kumar, A., N.K. Bellam and A. Sud 1999. Performance of an industrial source complex model: Predicting long-term concentrations in an urban area. Environmental Progress. 18:93-100.

Lancaster, J. and B.J. Downes 2004. Spatial point pattern analysis of available and exploited resources. Ecography. 27:94-102.

Lazarus, R. 1993. Pursuing environmental justice: the distributional effects of environmental protection. Northwestern University Law Review. 87:787-857.

Lejano, R.P., B. Piazza and D. Houston 2002. Rationality as social justice and the spatial-distributional analysis of risk. Environment and Planning C: Government and Policy. 20:871-888.

Levenstein, C. and J. Wooding 1998. Dying for a Living - Workers, Production, and the Environment. *In* The Struggle for Ecological Democracy: Environmental Justice Movements in the United States Ed. D. Faber. The Guilford Press, New York, pp. 60-81.

Lorber, M., A. Eschenroeder and R. Robinson 2000. Testing the USA EPA's ISCST-Version 3 model on dioxins: a comparison of predicted and observed air and soil concentrations. Atmospheric Environment. 34:3995-4010.

Maantay, J. 2001. Zoning, equity, and public health. American Journal of Public Health. 91:1033-1041.

Maantay, J. 2002. Mapping environmental injustices: Pitfalls and potential of geographic information systems in assessing environmental health and equity. Environmental Health Perspectives. 110:161-171.

Mank, B. 1999. Title VI. *In* The Law of Environmental Justice Ed. M. Gerrard. American Bar Association, pp. 23-67.

Manly, B.F.J. 1991. Randomization and Monte Carlo Methods in Biology. Chapman and Hall, London and New York.

Marentes, C. 2004. Farm Workers Fight against Environmental Racism and Neo-liberalism. Synthesis/Regeneration 33.

Mazzeo, N.A. and L.E. Venegas 2004. Some aspects of air pollution in Buenos Aires city. International Journal of Environment and Pollution. 22:365-378.

Mennis, J. 2002. Using Geographic Information Systems to create and analyze statistical surfaces of population and risk for Environmental Justice analysis. Social Science Quarterly. 83:281-297.

Miller, D. 1999. Social Justice and Environmental Goods. *In* Fairness and Futurity - Essays on Environmental Sustainability and Social Justice Ed. A. Dobson. Oxford University Press, Oxford, pp. 151-172.

Mitchell, J., D. Thomas and S. Cutter 1999. Dumping in Dixie revisited: the evolution of environmental inequality in South Carolina. Social Science Quarterly. 80:229-243.

Morello-Frosch, R., M. Pastor, C. Porras and J. Sadd 2002a. Environmental justice and regional inequality in southern California: Implications for future research. Environmental Health Perspectives. 110:149-154.

Morello-Frosch, R., M. Pastor and J. Sadd 2001. Environmental justice and Southern California's "riskscape" - The distribution of air toxics exposures and health risks among diverse communities. Urban Affairs Review. 36:551-578.

Morello-Frosch, R., M. Pastor and J. Sadd 2002b. Integrating environmental justice and the precautionary principle in research and policy making: The case of ambient air toxics exposures and health risks among schoolchildren in Los Angeles. Annals of the American Academy of Political and Social Science. 584:47-68.

Morgan, W.K.C., R.B. Reger and D.M. Tucker 1997. Health effects of diesel emissions. Annals of Occupational Hygiene. 41:643-658.

Oakes, J.M., D.L. Anderton and A. Anderson 1996. A longitudinal analysis of environmental equity in communities with hazardous facilities. Social Science Research. 25:125-148.

O'Brien, D.J., J.B. Kaneene, A. Getis, J.W. Lloyd, M.R. Rip and R.W. Leader 1999. Spatial and temporal distribution of selected canine cancers in Michigan, USA, 1964-1994. Preventive Veterinary Medicine. 42:1-15.

Office of Inspector General 2004. EPA Needs to Consistently Implement the Intent of the Executive Order on Environmental Justice. Office of Inspector General, Washington, D.C.

Pacific Institute and Coalition for West Oakland Revitalization 2003. Clearing the Air: Reducing Diesel Pollution in West Oakland. Pacific Institute, Oakland, CA, pp. 1-16.

Pastor, M., J.L. Sadd and R. Morello-Frosch 2002. Who's minding the kids? Pollution, public schools, and environmental justice in Los Angeles. Social Science Quarterly. 83:263-280.

Pastor, M., J.L. Sadd and R. Morello-Frosch 2004. Waiting to inhale: The demographics of toxic air release facilities in 21st-century California. Social Science Quarterly. 85:420-440.

Pellow, D.N. 2000. Environmental inequality formation: Toward a theory of Environmental Justice. American Behavioral Scientist. 43:581-601.

Prentice, I.C. and M.J.A. Werger 1985. Clump spacing in a desert dwarf shrub community. Vegetatio. 63:133-139.

Pulido, L. 1994. Restructuring and the contraction and expansion of environmental rights in the United States. Environment and Planning A. 26:915-936.

Pulido, L. 1996. A critical review of the methodology of environmental racism research. Antipode. 28:142-159.

Rawls, J. 1999. Justice as Reciprocity. *In* John Rawls - Collected Papers Ed. S. Freeman. Harvard University Press, Cambridge, pp. 190-224.

Rhodes, E.L. 2003. The Measurement of Environmental Injustice: Some Rules for Engagement. *In* Environmental Justice in America - A New Paradigm. Indiana University Press, Bloomington, pp. 118-136.

Ripley, B.D. 1976. The second-order analysis of stationary processes. Journal of Applied Problems. 13:255-266.

Ripley, B.D. 1977. Modelling Spatial Patterns. Journal of the Royal Statistical Society. Series B 39:172-192.

Rodriguez, J.A. 1999. Rapid transit and community power: West Oakland residents confront BART. Antipode. 31:212-228.

Romm, J. 2000. The Coincidental Order of Environmental Justice. *In* Justice and Natural Resources Eds. K.M. Mutz, G.C. Bryner and D.S. Kenney. Island Press, Washington, DC.

Sadd, J.L., M. Pastor, J.T. Boer and L.D. Snyder 1999. "Every breath you take ...": The demograhics of toxic releases in southern California. Economic Development Quarterly. 13:107-123.

Scott, M., S. Cutter, C. Menzel, M. Ji and D. Wagner 1997. Spatial accuracy of the EPA's environmental hazards databases and their use in environmental equity analysis. Applied Geographic Studies. 1:45-61.

Sharder-Frechette, K. 2002. Distributive Justice, Participative Justice, and the Principle of Prima Facie Political Equality. *In* Environmental Justice: Creating Equality, Reclaiming Democracy. Oxford University Press, Oxford, pp. 23-34.

Simmons, C.S. 2004. The political economy of land conflict in the Eastern Brazilian Amazon. Annals of the Association of American Geographers. 94:183-206.

Simon, T.W. 2000. In defense of risk assessment: A reply to the environmental justice movement's critique. Human and Ecological Risk Assessment. 6:555-560.

Skarpe, C. 1991. Spatial patterns and dynamics of woody vegetation in an arid savanna. Journal of Vegetation Science. 2:565-572.

Sterner, R.W., C.A. Ribic and G.E. Schatz 1986. Testing for life historical changes in spatial patterns of four tropical tree species. Journal of Ecology. 74:621-633.

Stockwell, J., J. Sorensen, J. Eckert and E. Carreras 1993. The US EPA geographic information system for mapping environmental releases of toxic release inventory (TRI) chemicals. Risk Analysis. 13:155-164.

Szasz, A. and M. Meuser 2000. Unintended, inexorable: The production of environmental inequalities in Santa Clara County, California. American Behavioral Scientist. 43:602-632.

Szwagrzyk, J. and M. Czerwczak 1993. Spatial patterns of trees in natural forests of East-Central Europe. Journal of Vegetation Science. 4:469-476.

Taquino, M., D. Parisi and D.A. Gill 2002. Units of analysis and the Environmental Justice hypothesis: The case of industrial hog farms. Social Science Quarterly. 83:298-316.

Tiebout, C.M. 1956. A pure theory of local expenditures. Journal of Political Economy. 64:416-424.
Townsend, P., P. Phillimore and A. Beattie 1988. Health and deprivation: Inequality and the North, Routledge, London.
U.S. Bureau of the Census 2000. Statistical Abstract of the United States: 2000. U.S. Department of Commerce, Washington, DC.
U.S. Environmental Protection Agency 1992. Environmental equity - reducing risk for all communities. U.S. Environmental Protection Agency, Washington, DC.
U.S. Environmental Protection Agency 1995. Draft users guide for the industrial source complex (ISC3) dispersion models (Revised). User Instructions, Vol. I. Office of Air Quality Planning and Standards, Research Triangle Park, NC.
U.S. Environmental Protection Agency 1997. Toxic release inventory relative risk-based environmental indicators methodology. U.S. Environmental Protection Agency, Washington, DC.
U.S. Environmental Protection Agency 1998. Interim Guidance for Investigating Title VI Administrative Complaints Challenging Permits. U.S. Environmental Protection Agency, Washington, DC.
U.S. Environmental Protection Agency 1999. Appendum: users guide for the industrial source complex (ISC3) dispersion models, User Instructions. Office of Air Quality Planning and Standards, Research Triangle Park, NC.
U.S. General Accounting Office 1991a. Toxic chemicals: EPA's toxic release inventory is useful but can be improved. Government Printing Office, Washington, DC, pp. 19-121.
U.S. General Accounting Office 1991b. Toxic chemicals: EPA's toxic release inventory program: more comprehensive data and better public outreach needed. Government Printing Office, Washington, DC, pp. 91-75.
United Church of Christ Commission on Racial Justice 1987. Toxic Wastes and Race in the United States. United Church of Christ, New York, NY.
US Commission on Civil Rights 2003. A Quiet Crisis: Federal Funding and Unmet Needs in Indian Country. US Commission on Civil Rights, Washington, D.C., pp. 1-139.
Weinberg, P. 1999. Equal Protection. *In* The Law of Environmental Justice Ed. M. Gerrard. American Bar Association, pp. 3-22.
Wenz, P. 1988. Principles of Justice. *In* Environmental Justice Ed. P. Wenz. State University Press of New York, New York, pp. 22-36.
Williams, R.W. 1999. Environmental injustice in America and its politics of scale. Political Geography. 18:49-73.
Yandle, T. and D. Burton 1996. Reexamining environmental justice: a statistical analysis of historical hazardous waste landfill siting in metropolitan Texas. Social Science Quarterly. 77:477-492.

Chapter 6

Use of GIS and Spatial Analysis to Assess Wildlife Management Measures: A Burrowing Owl Example

Abstract Assessing the effectiveness of conservation management for burrowing owls (*Athene cunicularia*) is challenging because accurate and consistent data that combine large scales of space and time are necessary for reliable analyses. Following management to maintain low vegetation height at nest burrow sites, we observed the spatial pattern of burrowing owls over two years at NASA Ames Research Center before, during, and after conducting this management approach. We integrated spatial metrics that included nearest neighbor distances, first-order intensity distributions, and second-order Ripley's K analysis into a geographic information system (GIS) to assess cluster change over the two year period. We identified the scale and timing of clusters and determined that they matched the scale and timing of our conservation management actions. Thus, we conclude that our management approach was effective, at least on a short time scale, and that applying GIS and Ripley's K were appropriate for this species.

Introduction

The burrowing owl, a grassland species, is unique in that it is the only owl species that lives in underground burrows and is often active in broad daylight. It is ranked second to the barn owl as the most economically beneficial in North America because it eats many insects and rodents near agricultural areas, and is relatively tolerant of non-threatening

human activity (Campbell et al. 1990). Diet consists primarily of Orthoptera (e.g., crickets, katydids, grasshoppers), beetles and rodents (Green et al. 1993; Plumpton and Lutz 1993; York et al. 2002). The yearly life cycle in Northern California consists of owls pairing up and laying eggs in Spring (February – May), and breeding in Summer (May – September). In Fall and Winter, adults and chicks disperse and some may migrate (September – January). The burrowing owl ranges throughout Canada, the U.S., and Mexico. A comprehensive burrowing owl bibliography can be found at: http://uwadmnweb.uwyo.edu/fish_wild/buow/index.html.

In 1972, the burrowing owl was included on the U.S. Audubon Blue List, which records North American bird species undergoing population or range reductions (Tate 1986). The U.S. Department of Interior has since designated the burrowing owl as vulnerable (U.S. Department of Interior 1992), and the U.S. Fish and Wildlife Service listed the burrowing owl as a national priority species in the Birds of Conservation Concern (U.S. Fish and Wildlife Service 2002). Many states, including California, consider the burrowing owl a special status species (James and Espie 1997).

Internationally, Mexico and Canada are signatories to the 1918 Migratory Bird Treaty Act, which protects burrowing owls, their nests, and their eggs in Mexico, but not in Canada because the treaty does not include Strigiformes. Additionally, in Mexico the burrowing owl was listed as a federally threatened (amenazada) species in 1994 (Diario Oficial de la Federación 1994). In Canada, the Committee on the Status of Endangered Species classified the burrowing owl as threatened in 1979 (Wedgwood 1978), but changed its designation to endangered in 1995 (Wellicome and Haug 1995). Clayton and Schmutz (1999) predicted that burrowing owls in Canada may face extinction due to

irreversible changes to ecosystem processes in the Great Plains. Burrowing owls in northern California, where our study site is located, have been studied and observed since the 1960s and have recently been managed to avoid further population decreases (Thomsen 1971; Burrowing Owl Consortium Mitigation Committee 1993; Trulio 1995; Trulio 1997).

Orth and Kennedy (2001) used GIS and spatial analysis to analyze if nest-site selection in Colorado was altered by a decrease in the availability of preferred foraging habitat. They used circles with radii of 1000 and 2500 m centered on prairie dog towns to assess the landscape characteristics within the average home range of male burrowing owls and immediate foraging habitat (Haug and Oliphant 1990). While most bird species nest as solitary pairs for purposes of concealment or territoriality, many birds have been observed to nest colonially in close association with each other (Horn 1968; Lack 1968; Krebs 1971; Hoogland and Sherman 1976). Active owl burrows tend to be located in areas with more than one burrow, and in areas of foraging habitat such as open fields with sparse and low height vegetation (Plumpton and Lutz 1993; Uhmann et al. 2001; Belthoff and King 2002). Nest clustering may be due to a clustered food source, limited suitable nesting habitat, and/or reduced predation risk due to owls alerting each other to predators (Coulombe 1971; Green and Anthony 1989; Desmond et al. 1995). Smith and Belthoff (2001) found that artificial burrow systems placed together as clusters was effective in a study of nest dimensions.

Researchers have found that habitat size and continuity play an important role in nest distribution patterns (Todd 2001). Desmond et al. (1995) analyzed the spatial patterns of burrowing owls in Nebraskan prairie dog towns. Using the *T*-square index

(Diggle et al. 1976) to compare the square of the distance from a random point to the nearest burrow and the distance from that burrow to its nearest neighbor (Ludwig and Reynolds 1988), Desmond et al. found that nests were located randomly in small prairie dog towns (<35 ha^{-1}) and clumped in large prairie dog towns (≥ 35 ha^{-1}), though clumping was not due to burrow or space availability. They calculated average nearest neighbor distances of 125.0 m for the clusters, and 105.1 m for the random patterns. As the size of prairie dog towns increased, burrowing owls occurred in higher numbers but lower densities (Desmond and Savidge 1996), although they point out there may be a time lag in owl response to changes in active burrow densities (Desmond et al. 2000).

It is well-known that burrowing owls prefer short grass habitat, under approximately 15 cm in height (Trulio 1997). For example, Uhmann et al. (2001) developed a habitat suitability index for burrowing owls in eastern Canada and recommended a management approach to maintain low vegetation height at all nest burrow sites. To provide burrowing owl habitat at our study site, NASA Ames Research Center followed standard management recommendations by mowing large tracts of grassland for short-grass conservations areas (~53 ha in sum). We assessed the effectiveness of this management approach to attract burrowing owl nests by integrating cluster detection in a GIS with a spatial analysis metric called Ripley's K (Ripley 1976). We also used nearest neighbor distances to determine if the spatial pattern of active burrows shifted with the management practice. Ripley's K, a statistical method to detect spatial patterns such as clusters, has been widely applied in epidemiology and ecology. Examples include cancer clusters detection (O'Brien et al. 1999), pollution clusters in environmental justice (Fisher et al. in press), landscape dynamics of forest disease (Kelly

and Meentemeyer 2002), and distribution patterns of herbs (Kenkel 1993), desert shrubs (Prentice and Werger 1985; Skarpe 1991), and tropical forest trees (Sterner et al. 1986). This method has not been applied previously to colonially-nesting birds. The overall objective of this study is to evaluate GIS and Ripley's K as methods to detect change in owl nest clustering.

Methods

Study Site

We observed burrowing owls in 2003 and 2004 at the NASA Ames Research Center, located Sunnyvale, California, approximately 56 km (35 miles) south of San Francisco (37° 23'N, -122° 4'W). The study site was a combination of large areas of open, non-native grassland habitat in a matrix of urban and industrial development. The Mediterranean climate of the region was characterized by wet winters and dry summers. Rainfall in 2003 and 2004 averaged from 5 – 8 cm (November through March) and 0 – 2 cm (April through October) and temperatures ranged from 4 – 12° C in the winter to 10 – 26° C in the summer. The site was adjacent to the San Francisco Bay and consequently received some wind and moisture influence from the Bay. Land use and land cover, as determined through the GIS, included coastal salt marsh (0.18 km^2), coyote brush scrub (0.23 km^2), disturbed areas (0.02 km^2), ditches (0.30 km^2), fresh and brackish water marsh (1.06 km^2), non-native grassland (17.44 km^2), seasonal salt marsh and transition (1.69 km^2), and weed dominated areas (0.56 km^2). The total area of the site including built structures was 7 km^2.

Field Techniques

All suitable burrowing owl habitats (fields, mounds, landscaping, and embankments) were visually examined between April and June each year by researchers performing diurnal surveys walking along transects 5 – 15 m apart, as dictated by vegetation height and density. During walk-through transect surveys, observers looked for owls that flushed when approached and/or burrows that showed evidence of owl activity such as whitewash, pellets, feathers, bedding material, prey item remains, or nest decoration. Any burrow that contained evidence of owl activity was marked with a flag or stake and received further observations to determine whether a nest was active or inactive. Active nests were identified by an owl pair. If, after three to four observations we did not see an owl pair at a potential nest site, we did not count it as a nest. During the breeding season, from 1 April to 31 July, we observed each potential owl nest for 30 minutes every week. During the rest of the year, owl locations were observed only 2 times per month. Variation due to uneven visibility of owls was minimized by two years of prior observation and experience by field biologists at our site; error around counts was relatively stable at ±1 – 3 owls.

We used binoculars (10 X 50) and spotting scopes (15 – 45 X 60 zoom) mounted on tripods or window mounts to locate new owls and resight previously banded owls. All active nests were numbered. Universal Transverse Mercator coordinates (NAD83) were recorded with a Global Positioning System (GPS) unit for every nest that was assigned a number. To correct for GPS positional accuracy and for coordinate error in points that we could not access with our unit (to avoid owl disturbances, for example) we corrected

for each individual point within the GIS using a high resolution aerial photograph of our site.

In 2003, we cut the grass by hand in areas approximately 8 m in diameter around active burrows; there was no large-scale mowing. In 2004, NASA mowed 54 ha of owl habitat (8% of the total site area) with a mechanical flail mower, first during the period from 28 April to 14 May and again 7 – 29 July. Our primary focus here is to determine if a significant difference in spatial clustering of nests before versus after the large-scale mowing. To account for temporal effects on spatial change: 1) we compared nest clustering in August 2003 (before any large-scale mowing) and nest clustering in August 2004 (after the large-scale mowing)—keeping season/month constant; 2) we compared nest clustering in April 2004 (before any large-scale mowing) and nest clustering in August 2004 (after the large-scale mowing) for mowed and non-mowed areas.

Spatial Analysis

We calculated nearest neighbor distances to assess adjacency of immediate neighboring burrows to one another. The nearest neighbor index compares the average distance of the nearest other point (nest) with a spatially random expected distance based on area size and number of points. The empirical average nearest neighbor distance is divided by the expected random distance (the nearest neighbor index).

We identified clusters of burrows through point pattern analysis that combined intensity distributions and Ripley's K-function (Ripley 1976). Intensity is defined as the mean number of points (nests) per unit area; intensity distributions reveal first-order properties of a spatial point process and variation through space to assess the spatial

dependence between points. First-order properties of a spatial point process describe how the mean number of points per unit area (the intensity) varies through space. For a stationary process, the intensity is assumed to be constant over the bounded region of interest. Intensity distributions show where potential clusters are occurring, and Ripley's K reveals statistical significance of those apparent clusters. Grid size for intensity was set to normalize the maximum count per grid cell at 0.5 to match an approximate Gaussian spatial distribution.

Ripley's K is a second-order (covariance of distances) function for spatial point pattern and is used to detect spatial randomness (Ripley 1976). A spatial point pattern is a collection of points irregularly located within a bounded region of space (e.g. burrows within a field site). The data set may consist of locations only, or it may be a marked point process, with data values associated with each location (e.g. longitude/latitude with number of burrowing owls). The analysis is termed "second-order" because of its focus on the variance of the test statistic across a series of progressively larger areas—the size of the step is set to reveal the interevent distances at which clustering, if present, is strongest. By examining the test statistic at various spatial scales (e.g. region, county, city), the scale at which the pattern of events (points) is operating most strongly (highest statistical significance and confidence) can be determined. We initially followed a weighted edge correction (Ripley 1977), though Lancaster and Downes (2004) specify that edge correction is not necessary for length-scale assessment of clusters.

Ripley's K examines the null hypothesis of Complete Spatial Randomness (CSR) for a mapped spatial point pattern. CSR is defined by the following criteria: a) the intensity of the point pattern does not vary over the bounded sampling region, and the

pattern follows a homogeneous Poisson distribution; b) there are no interactions among the points. Ripley's K can reject the null hypothesis that the spatial pattern of points is random. Certainly, little in nature at large scales is perfectly uniform so that 100% CSR would be highly unlikely. Thus, Ripley's K identifies scales of clusters and indirectly identifies the possible causes to those clusters, i.e., fish "cluster" across a landscape at the scale of a lake rather than a forest.

After the data were analyzed by the Ripley's K method, a plot of count $K(h)$ versus distance h revealed deviations as expected under CSR (Ripley 1976). The deviation was tested for statistical significance. One test employed the calculation of constant approximate confidence intervals around CSR (Getis and Franklin 1987; Szwagrzyk and Czerwczak 1993). Another test used Monte Carlo methods to determine statistical significance of the results by determining the amount of variation to be expected in sample statistics from computer-generated data (e.g., Diggle 1983; Manly 1991; Cressie 1993). In the context of spatial pattern analysis, Monte Carlo methods simulate randomly generated plots of the same dimensions of the observed plot thus creating confidence intervals from the highest and lowest values of $K(h)$ (Haase 1995). We conducted 1000-run Monte Carlo simulations to provide confidence intervals around the data. We plot $(K(h)/\pi)^{0.5} - h$ or simply $L(h) - h$ against h to show the deviation of $K(h)$ from CSR. If the deviation of the sample statistic from zero expectation is positive and above the upper limit of the confidence interval, then a clumped distribution can be assumed, while negative deviation indicates a regular pattern, otherwise the null hypothesis of CSR (between the confidence intervals) cannot be rejected (Haase 1995).

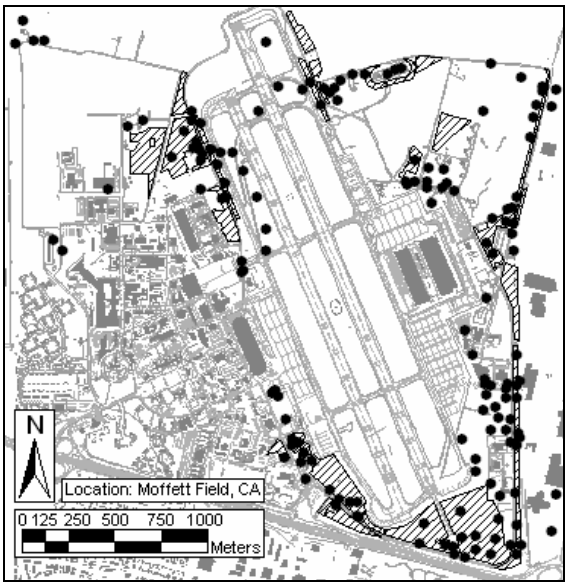

Figure 1. Distribution of all burrowing owls (filled black circles) observed from 1998-2004 at NASA Ames Research Center, California. Polygons with diagonal striping indicate mowed areas. Gray lines and polygons represent buildings and paint lines.

We processed the data in a GIS with ESRI's *ArcGIS* 8.1 and *S-Plus* 6.0. Nearest neighbor distances were calculated with *CrimeStat* 2.0 (Ned Levine & Associates). The main statistical processing of point pattern analyses relied on *S-Plus* 6.0, and analyses and map production on the *ArcMap* component of *ArcGIS* 8.1. The data were projected into Universal Transverse Mercator Zone 10N with the North American Datum 1983. We used Microsoft's *Excel* for general data processing.

Results

As a general indication of possible burrows at NASA Ames Research Center, we show all burrowing owl observations from 1998-2004 in Figure 1. The gray lines and polygons represent paint lines (indicating roads) and buildings. Typically, the owls have been spread out along the buffered perimeter of the site and around inactive runways where

Figure 2. Number of burrowing owls sited per month for 2003 and 2004. The durations of the two mows in 2004 are indicated in between the two sets of vertical lines; the first mow was from 28 April – 14 May, and the second mow was from 7 – 29 July.

there is open grassy vegetation away from people and buildings. The site is visibly fragmented, with large buildings preventing owl access to all tracts of land at our site. Due to the incomplete randomness allowable for owls to move everywhere on the site, clustering larger than 25 ha is impossible to detect. Because of the relatively low numbers of owls at our site, however, clustering at these scales would be unlikely, regardless. Additionally, because we are comparing time periods, any limitations due to space are factored out. The polygons with diagonal striping indicate the mowed areas in 2004 (pictured here are the boundaries of the second mowing event, though the first mow was in approximately the same locations). Corridors between mowed areas were generally continuous, although some corridors were interrupted.

In both 2003 and 2004, a clear seasonal pattern is exhibited with an increase in burrowing owls due largely to the breeding season and the presence of adults and young in the summer months 1 April – 31 August (Figure 2). Numbers leveled off to a baseline of approximately 20 burrowing owls throughout the rest of the year (1 Sept – 30 March) for both years. During this period, the young have dispersed, birds are, in general, more

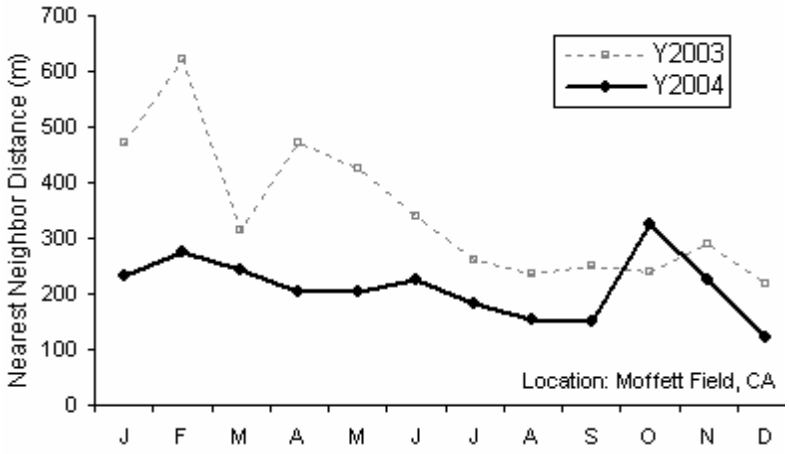

Figure 3. Mean nearest neighbor distances by month for 2003 and 2004.

difficult to find than in the summer, and our observation effort was approximately half that of the breeding season. The time periods of the two mowing events in 2004 are indicated in between the two sets of vertical lines. The first mowing event was from 28 April – 14 May, and the second mowing event was from 7 – 29 July. The summer counts in 2004 were larger than in 2003, but in particular a large and early peak in 2004 occurs directly after the first large-scale mowing.

Nearest neighbor distances did not follow the seasonal pattern as in Figure 2, but showed a decreasing trend whereby nearest neighbors became closer into the summer season for both years (Figure 3). The high values at the beginning of 2003 and in October and November 2004 correspond to the dips in the time series of Figure 1 when we observed the fewest burrowing owls for each year. Our nearest neighbor values for 2004 (211.4 m average) were roughly double that of Desmond et al. (1995), but over a larger area; our minimum value (121.5 m) correspond to the maximum values of Desmond et al. Desmond et al. report their nearest neighbor values on a yearly basis, whereas we report monthly values for a finer temporal assessment of spatial change.

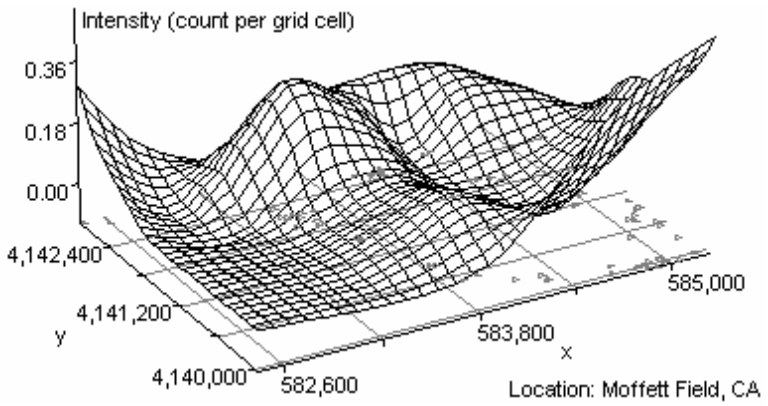

Figure 4. First-order intensity distribution for all active burrows during 2004. The distribution is draped over the burrow locations.

We draped the first-order intensity distribution on all active burrows during 2004 (Figure 4). The largest peaks (trough-to-trough) appear to be on the order of 600 m, which is misleading because those peaks included multiple clusters operating on smaller scales. The second-order Ripley's K analysis revealed the exact statistically significant scales of the spatial clusters.

The Ripley's K plot (Figure 5) was analyzed specifically for two time comparisons: 1) the month before the first mow (April 2004) and after the second mow (August 2004), and 2) August 2003 versus August 2004. The plot shows that in April 2004 the burrowing owls were generally randomly distributed throughout the area. In August 2004, however, clustering with a peak of 100 – 120 m (1 – 1.4 ha) became strongly evident and statistically significant. The Ripley's K plot for August 2003 shows that burrowing owls were randomly distributed except for a small peak at the scale of 160 m; clustering in April 2003 was similar to that in August 2003. The mowed conservation areas were on average 1.8 ha. The minimum statistically significant (above the upper confidence interval) part of the Ripley's K plot for August (h = 45 m) was 0.20 ha, which

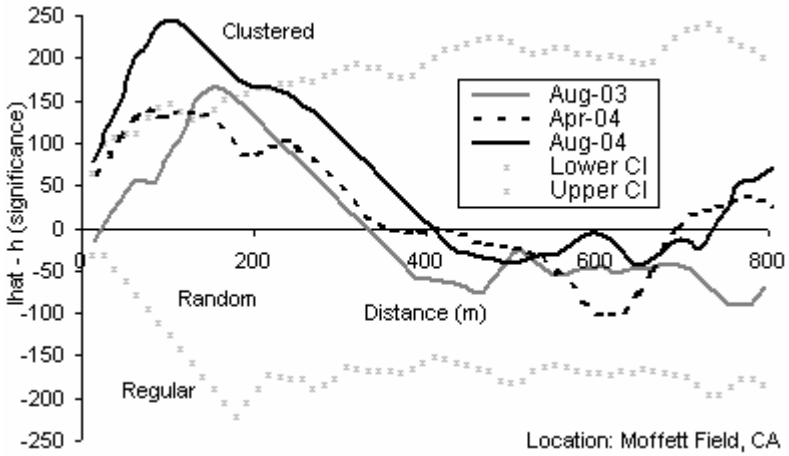

Figure 5. Ripley's K plot for August 2003, April 2004 and August 2004. The distribution of Ripley's K above the upper confidence interval indicates clustering, between the confidence intervals indicates random spatial pattern, and below the lower confidence interval indicates a regularly distributed pattern. The y-axis represents the deviation of the sample statistic from CSR; the units are in count numbers, but have been transformed as per Haase (1995). The x-axis represents distance (units are in meters here), and the distance shows the extent of the clustering.

corresponds with the minimum conservation area of 0.23 ha. Likewise, the maximum was 4.4 ha (210 m), which corresponds to our larger (but not largest) conservation areas (4.2, 4.6 and 4.7 ha).

We took the difference of the Ripley's K plot and the upper confidence interval for each month in 2004 to present a three-dimensional spatial-temporal picture of cluster change over time (Figure 6). Throughout the first half of the year, very little statistically significant spatial clustering occurred. After the second mowing (July) the strong clustering became apparent, and clustering remained throughout the rest of the year.

Discussion

This spatial analysis is effective in assessing the extent to which owl nests are clustered, and showed differential clustering and interannual differences in 2003 versus 2004. A

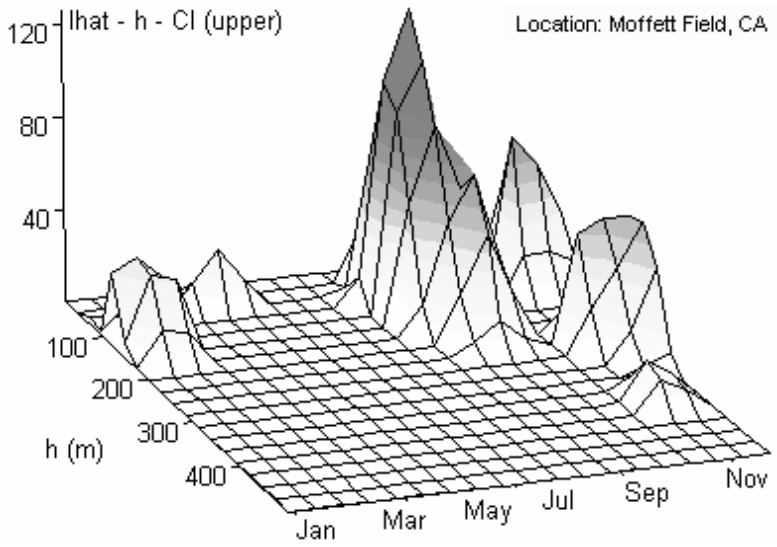

Figure 6. Cluster change over time based on the difference of the Ripley's K plot and the upper confidence interval for each month.

simple count of the number of burrowing owls within the areas per month might seem feasible, but this count is correlated with the total number of burrowing owls observed over the entire study site. Thus, an apparent rise in the number of owls within the areas may simply be an artifact of a rise in total owls at the study site. Also, owls in mowed versus pre-mowed areas may be the reason as a percent, however, the number of owls within the mowed areas remains higher post-management (39% in August 2004) than the pre-management value of 20% (April 2004).

To factor out the influence of seasonality, we compared Ripley's K for August 2003 against August 2004. In August 2003, the owls were randomly distributed as they were earlier that year in April, but significant clustering appeared in 2004. What had caused the owls to become clustered from season to season and from year to year? The smallest conservation area was 0.23 ha and the larger conservation areas were 4.2, 4.6 and 4.7 ha. The minimum significant area from the Ripley's K plot in August was 0.20 ha and the maximum was 4.4 ha: the statistically significant clustering in the Ripley's K

plot corresponds directly with the conservation areas from the mows. Thus, if one were to expect the scale of the burrow clusters to approach the scale of the mowed conservation areas (assuming that these areas promoted movement and habitability), then this is precisely what the data suggest.

There may be a maximum scale of clustering possible, however. For instance, the maximum clustering from the Ripley's K analysis corresponds to our second, third, and fourth largest conservation areas (4.7, 4.6, and 4.2 ha). Our largest area, however, was 10.3 ha, which was not significant in the Ripley's K plot. Although that area is not homogenous, the hypothetical question arises that if we studied a uniform, perfectly managed area greater than 10 ha, would burrowing owls spatially pattern themselves randomly or regularly throughout, or would they restrict themselves to smaller clusters of 4.5 ha or otherwise? We will continue to monitor to address this question.

Another possible explanation for the observed spatial pattern is that post-fledgling broods would create a superficial clumping behavior not explained by movement patterns. The assumption is that the broods stay close to their home. From a spatial statistics standpoint, an increase in local production that remained local would be evident in the nearest neighbor statistic—one would expect a drop based on the assumption. It is important to notice that the spatial patterns of nearest neighbors (Figure 3) and of cluster scale (Figure 6) over time do not follow the seasonal count pattern of Figure 2. Additionally, if clumping were due to dispersing young near natal burrows, then we would expect the same pattern in August 2003 and 2004, but this is not the case.

While the results suggest movement into and habitability of the conservation areas, the exact characteristics of the areas that make them so appealing is more difficult

to determine. In addition to the uniformly shorter grass over large areas, debris piles were moved and coyote bushes and other "weeds" were removed. Prey density, which was not quantified, may have been inconsistent in space and time. Additionally, NASA Ames employees were alerted to proceed with caution around the areas so perhaps the reduced disturbance was a major contributing factor to the appeal. This work was not designed to analyze the factors that may have made mowed sites more attractive to birds.

GIS and spatial analysis are useful tools in assessing environmental management practices and allow testing of alternative hypotheses. Not only can we create maps to visualize the data, but we can also derive meaningful interpretations of the spatial and temporal patterns. To reliably determine if mowing is important in promoting clustering, we need to examine seasonality over more years and determine if large mowed areas have a long-term effect on nest clustering. We need to track the diffusion of birds from the study area, and assess the spatial pattern of dispersion on even larger scales. These data will be valuable in guiding NASA Ames and other land managers in the protection and management of burrowing owls and other wildlife on their lands. Previous research has shown that a management approach to maintain low vegetation height at nest burrow sites is recommended (Plumpton and Lutz 1993; Uhmann et al. 2001; Belthoff and King 2002). Management decisions, however, must be coupled with tools for assessing the efficacy of these decisions. GIS can be used in future analyses to assess the effect of different habitat management approaches on owl distribution and population change.

Acknowledgements

We thank C. Alderete, T. Anderson, S. Clubb, C. Johnson, J. H. Lee, C. Levitan, and E. Watkins for help and assistance with this research. This work was supported by NASA Headquarters under the Earth System Science Fellowship Grant NGT5-30473, by NASA Ames Research Center funding for summer internships, and by a contract from NASA Ames Research Center and administered by PAI Corporation.

References

Belthoff, J.R. and R.A. King 2002. Nest-site characteristics of Burrowing Owls (*Athene cunicularia*) in the Snake River Birds of Prey National Conservation Area, Idaho, and applications to artificial burrow installation. Western North American Naturalist. 62:112-119.

Burrowing Owl Consortium Mitigation Committee 1993. Burrowing owl survey protocol and mitigation guidelines. Tech. Rep. Burrowing Owl Consortium, Alviso, California.

Campbell, R.W., N.K. Dawe, I. McTaggart-Cowan, J.M. Cooper, G.W. Kaiser and M. McNall 1990. The Birds of British Columbia: Diurnal Birds of Prey through Woodpeckers. Royal British Columbia Museum, Victoria, B.C.

Clayton, K.M. and J.K. Schmutz 1999. Is the decline of Burrowing Owls (*Speotyto cunicularia*) in prairie Canada linked to changes in Great Plains ecosystems? Bird Conservation International. 9:163-185.

Coulombe, H.N. 1971. Behavior and population ecology of the Burrowing Owl, *Speotyto cunicularia*, in the Imperial Valley of California. Condor. 73:162-176.

Cressie, N. 1993. Statistics for Spatial Data (Revised Edition). Wiley, New York.

Desmond, M.J. and J.A. Savidge 1996. Factors influencing burrowing owl (*Speotyto cunicularia*) nest densities and numbers in western Nebraska. American Midland Naturalist. 136:143-148.

Desmond, M.J., J.A. Savidge and K.M. Eskridge 2000. Correlations between burrowing owl and black-tailed prairie dog declines: A 7 year analysis. Journal of Wildlife Management. 64:1067-1075.

Desmond, M.J., J.A. Savidge and T.F. Seibert 1995. Spatial patterns of Burrowing Owl (*Speotyto-cunicularia*) nests within Black-Tailed Prairie Dog (*Cynomys-ludovicianus*) towns. Canadian Journal of Zoology. 73:1375-1379.

Diario Oficial de la Federación 1994. Especies y subespecies de flora y fauna silvestres terrestres y acuáticas en peligro de extinción, amenazadas, raras y las sujetas a protección especial. Norma Oficial Mexicana, México, D.F.

Diggle, P.J. 1983. Statistical analysis of spatial point patterns. Academic Press, New York.

Diggle, P.J., J. Besag and J.T. Gleaves 1976. Statistical analysis of spatial point patterns by means of distance methods. Biometrics. 32:659-667.
Fisher, J.B., M. Kelly and J. Romm in press. Scales of environmental justice: Combining GIS and spatial analysis for air toxics in West Oakland, California. Health & Place
Getis, A. and J. Franklin 1987. Second-order neighborhood analysis of mapped point patterns. Ecology. 68:473-477.
Green, G. and R. Anthony 1989. Nesting success and habitat relationships of Burrowing Owls in the Columbia Basin, Oregon. Condor. 91:347-354.
Green, G.A., R.E. Fitzner, R.G. Anthony and L.E. Rogers 1993. Comparative diets of burrowing owls in Oregon and Washington. Northwest Science. 67:88-93.
Haase, P. 1995. Spatial pattern analysis in ecology based on Ripley's *K*-function: Introduction and methods of edge correction. Journal of Vegetation Science. 6:575-582.
Haug, E.A. and L.W. Oliphant 1990. Movements, activity patterns, and habitat use of burrowing owls in Saskatchewan. Journal of Wildlife Management. 54
Hoogland, J.L. and P.W. Sherman 1976. Advantages and disadvantages of bank swallow (*Riparia riparia*) coloniality. Ecological Monographs. 46:33-58.
Horn, H.S. 1968. The adaptive significance of colonial nesting in the brewer's blackbird (*Euphagus cyanocephalus*). Ecology. 49:682-694.
James, P.C. and R.H.M. Espie 1997. Current status of the Burrowing Owl in North America: an agency survey. *In* The Burrowing Owl, its biology and management including the proceedings of the first international Burrowing Owl symposium Eds. J.L. Lincer and K. Steenhof. Journal of Raptor Research, pp. 3-5.
Kelly, M. and R.K. Meentemeyer 2002. Landscape dynamics of the spread of sudden oak death. Photogrammetric Engineering and Remote Sensing. 68:1001-1009.
Kenkel, N.C. 1993. Modeling Markovian dependence in populations of *Aralia nudicaulis*. Ecology. 74:1700-1706.
Krebs, J.R. 1971. Territory and breeding density in the great tit, *Parus major* L. Ecology. 52:2-22.
Lack, D. 1968. Ecological adaptations for breeding in birds. Western Printing Services, London, U.K.
Lancaster, J. and B.J. Downes 2004. Spatial point pattern analysis of available and exploited resources. Ecography. 27:94-102.
Ludwig, J.A. and J.F. Reynolds 1988. Statistical ecology. John Wiley & Sons, New York, USA.
Manly, B.F.J. 1991. Randomization and Monte Carlo Methods in Biology. Chapman and Hall, London and New York.
O'Brien, D.J., J.B. Kaneene, A. Getis, J.W. Lloyd, M.R. Rip and R.W. Leader 1999. Spatial and temporal distribution of selected canine cancers in Michigan, USA, 1964-1994. Preventive Veterinary Medicine. 42:1-15.
Orth, P.B. and P.L. Kennedy 2001. Do land-use patterns influence nest-site selection by burrowing owls (*Athene cunicularia hypugaea*) in northeastern Colorado? Canadian Journal of Zoology. 79:1038-1045.
Plumpton, D.L. and R.S. Lutz 1993a. Nesting habitat use by burrowing owls in Colorado. Journal of Raptor Research. 27:175-179.

Plumpton, D.L. and R.S. Lutz 1993b. Prey selection and food-habits of burrowing owls in Colorado. Great Basin Naturalist. 53:299-304.
Prentice, I.C. and M.J.A. Werger 1985. Clump spacing in a desert dwarf shrub community. Vegetatio. 63:133-139.
Ripley, B.D. 1976. The second-order analysis of stationary processes. Journal of Applied Problems. 13:255-266.
Ripley, B.D. 1977. Modelling Spatial Patterns. Journal of the Royal Statistical Society. Series B 39:172-192.
Skarpe, C. 1991. Spatial patterns and dynamics of woody vegetation in an arid savanna. Journal of Vegetation Science. 2:565-572.
Smith, B.W. and J.R. Belthoff 2001. Effects of nest dimensions on use of artificial burrow systems by burrowing owls. Journal of Wildlife Management. 65:318-326.
Sterner, R.W., C.A. Ribic and G.E. Schatz 1986. Testing for life historical changes in spatial patterns of four tropical tree species. Journal of Ecology. 74:621-633.
Szwagrzyk, J. and M. Czerwczak 1993. Spatial patterns of trees in natural forests of East-Central Europe. Journal of Vegetation Science. 4:469-476.
Tate, J., Jr. 1986. The blue list for 1986. American Birds. 40:227-236.
Thomsen, L. 1971. Behavior and ecology of burrowing owls on Oakland Municipal Airport. Condor. 73:177-192.
Todd, L.D. 2001. Dispersal patterns and post-fledging mortality of juvenile Burrowing Owls in Saskatchewan. Journal of Raptor Research. 35:282-287.
Trulio, L.A. 1995. Passive Relocation - A method to preserve burrowing owls on disturbed sites. Journal of Field Ornithology. 66:99-106.
Trulio, L.A. 1997. Burrowing owl demography and habitat use at two urban sites in Santa Clara County, California. *In* The Burrowing Owl, its biology and management including the proceedings of the first international Burrowing Owl symposium Eds. J.L. Lincer and K. Steenhof. Journal of Raptor Research, pp. 84-89.
U.S. Department of Interior 1992. Endangered and threatened wildlife and plants; animal candidate review for listing, proposed rule: Part VIII.
U.S. Fish and Wildlife Service 2002. Birds of Conservation Concern 2002. U.S. Fish and Wildlife Service, Division Migratory Bird Management, Arlington, VA.
Uhmann, T.V., N.C. Kenkel and R.K. Baydack 2001. Development of a habitat suitability index model for Burrowing Owls in the eastern Canadian prairies. Journal of Raptor Research. 35:378-384.
Wedgwood, J.A. 1978. The status of the Burrowing Owl in Canada. Canadian Wildlife Service, Ottawa, ON, Canada.
Wellicome, T.I. and E.A. Haug 1995. Second update of status report on the Burrowing Owl *Speotyto cunicularia*. Committee on the Status of Endangered Wildlife in Canada, Ottawa, Ontario, Canada.
York, M.M., D.K. Rosenberg and K.K. Sturm 2002. Diet and food-niche breadth of Burrowing Owls (*Athene cunicularia*) in the Imperial Valley, California. Western North American Naturalist. 62:280-287.

Appendix A

Instructions for Building Sap Flow Sensors[16]

Materials

Thermocouples and Heaters

- 18G drawing-up needle
- Polymide Tubing
- Solder
- Flux fluid
- 3 mm clear heat-shrink tube
- Scalpel
- Teflon Tape
- Multi-meter
- Evercoat 105685 Mold Release
- West System 105 Epoxy Resin, 205 Hardner

Thermocouples

- 36G PFA Teflon constantan wire
- 36G Grade 1 enamelled copper wire
- 18G drawing-up needle
- 20G constantan extension wire
- Extension copper wires
- Silicone Heat Transfer Compound

Heaters

- 7.5 amp wire
- NiCr A+ 36G, 0.127mm dia, 85.3 ohm/meter heater wire
- Fishing line
- Drill
- Weight, pipe

[16] Based on instructions by Steve Burgess.

Manufacture of Thermocouple Probes (2 TC's per probe)

1. Melt the plastic base off the needles.
2. File the needle tip, clean it out with a drill bit, then seal the distal end with solder (use a touch of corrosive flux fluid to get the solder to stick).
3. Cut a 10 cm length of 36G constantan wire and two 10 cm lengths of enameled copper wire.
4. Strip 1.7 cm of the constantan wire, and 2 mm of the copper wires.
5. Thread the three wires through a micro-capillary/polymide tubing, stripped ends first, so that the constantan and one of the copper wires protrudes through by 1.7 cm, and the other copper wire protrudes through by 2 mm.
6. Solder this second copper wire to the base of the stripped portion of the constantan (minimal amount of solder so that you can slide everything back through the micro-capillary). Solder the first copper wire to the tip of the constantan. The 2 junctions should now be spaced 1.5 cm apart.
7. Pull the wires just back inside the micro-capillary. Strip the protruding 5 cm ends of all three wires. With a multi-meter set at 200 Ω, check to make sure the difference between the constantan and each copper wire differs by ~0.5 Ω (i.e., 2.5 and 2.0). Add a dab of super glue at this base of the micro-capillary so that the wires are fixed in place.
8. Cut a 15 cm length of extension grade 20G constantan wire (which comes as a twin conductor so the copper wire must be stripped off), and two 15 cm copper wires (White and Black or Yellow/Green and Red). Strip the ends and solder the ends.
9. Wrap the 5 cm stripped protruding end of the constantan from the micro-capillary around the tip of the extension constantan, solder together and wrap in Teflon tape. Wrap the longer protruding copper wire around the White copper extension wire tip, solder and wrap. Wrap the shorter protruding copper wire around the Black copper wire tip, solder and wrap. Yellow/Green and Red together can substitute for White and Black together so that you end up with equal parts Black-White and equal parts Yellow/Green-Red.
10. With a 1 mL syringe + 25G 5/8 needle, inject Unick Silicone Heat Transfer Compound into the micro-capillary tip so that both TC junctions are covered.
11. Place micro-capillary in needle, slide 10 cm of heat-shrink tube over the extension wires and heat-shrink into place.
12. Apply Mold Release to lube the mold, wait 0.5-1 hour.
13. Mix epoxy resin and hardener (4:1 ratio) in plastic container.
14. Stick needles into the mold, fill the mold with the epoxy/hardener mix (a syringe works well). Dry overnight. 5 cc's of mix = 4 probes.

Manufacture of Heater probes

1. Attach a narrow weight to 3 feet of fishing line, knot the other end of the line and insert into drill. Fix drill to clamp with line facing down. Spray lubricant on line. Position weight loosely in small pipe.
2. Tape end of heater wire to base of drill. Start the drill, slowly coiling the heater wire tightly around the fishing line. Each section of coil should measure 25 mm in length and contain 5 cm of non-coiled wire on each side of each coil.
3. When finished filling the line with coils, move to work bench and remove coil. Thread one loose end through the coil, and place the loop around a fixed nail. Tighten the loop and stretch out the coil to measure 50 mm. Remove from nail and slide into polymide tubing.
4. Strip the ends of the heater coil, and wrap around stripped ends of speaker wire. Solder into place, and wrap with Teflon tape.
5. Check resistance with multi-meter. Readings should be between 14 – 19 ohms.
6. Melt the plastic base off the needles.
7. File the needle tip, clean it out with a drill bit, then seal the distal end with solder (use a touch of corrosive flux fluid to get the solder to stick).
8. Slide polymide tubing into needle.
9. Apply Mold Release to lube the mold, wait 0.5-1 hour.
10. Mix epoxy resin and hardener (4:1 ratio) in plastic container.
11. Stick needles into the mold, fill the mold with the epoxy/hardener mix (a syringe works well). Dry overnight. 5 cc's of mix = 4 probes.

Manufacture of leads

1. Cut 4 core shielded wires into required lengths (from plant to multiplexer/datalogger).
2. Strip 200 mm of sheath from one end and 100 mm from the other. Do not cut through braided shield.
3. At both ends, separate the 4 conductor wires and unwrap the shielding strands from around the conductors. Twist the shield wires together with silver from heater leads to form a conductor.
4. Place 3 mm of heat-shrink over the twisted shield wire, leaving 10 mm tip exposed, and shrink to place. Tin the end with solder.
5. Strip the ends of the 4 conductor wires and tin.
6. Cut ample heat shrink (extra big pieces) and place over leads.
7. Connect the TC and heater probes to the leads as follows:
    a. Black to Black, White to White, Red to Red, Yellow/Green to Yellow.
    b. The ends of the 2 TC constantan wires are twisted together and then both are connected to the 1 constantan wire on the lead.
    c. Connect 1 end of the heater probe to the Blue wire, and the other end to the twisted wire.
8. Heat-shrink all exposed soldered ends.

Heater Relay Pictures

Front

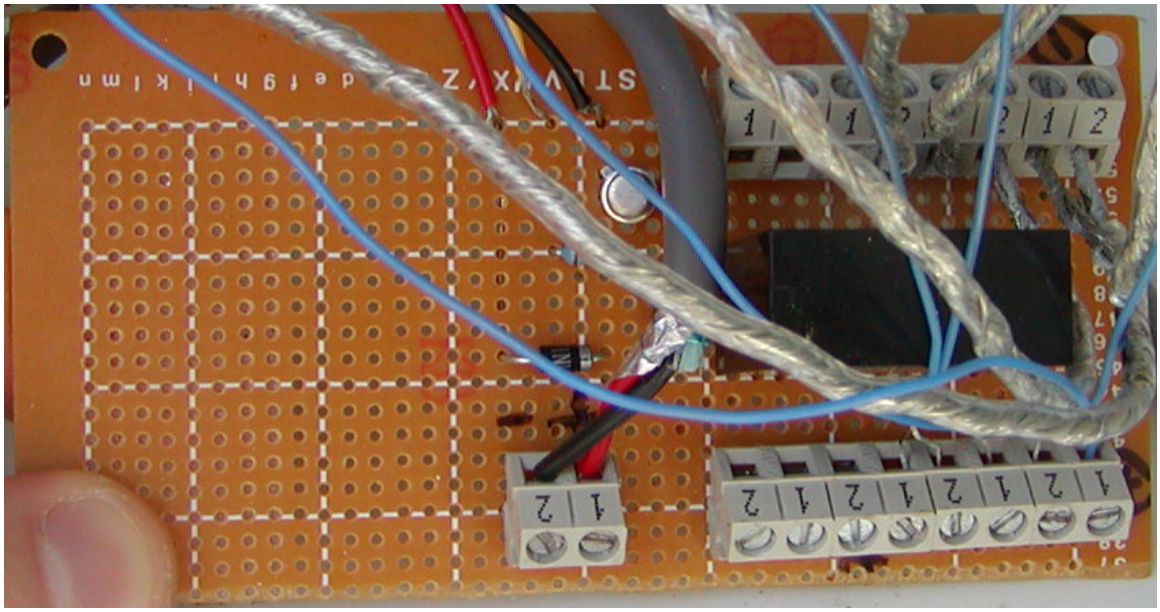

Back

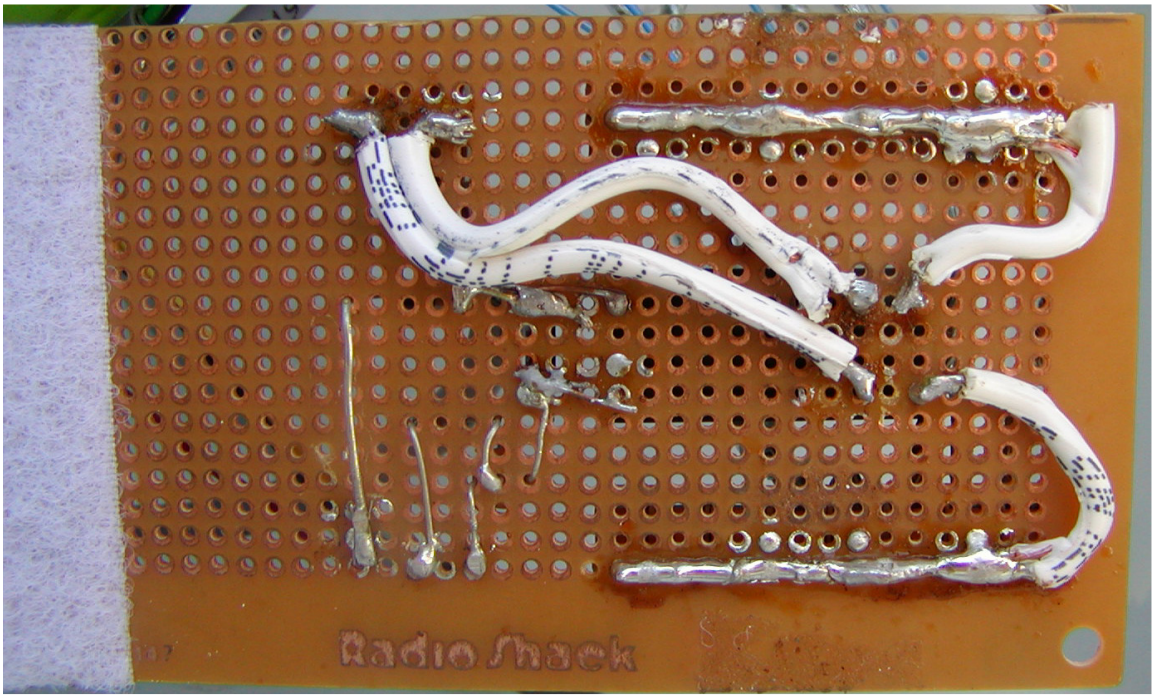

Datalogger and Multiplexer Wiring

Sapflow wiring for Campbell datalogger CR10X & MUX AM416

MUX	***Datalogger***	***Wire***
RES	C1	Green1
CLK	C2	White1
GND	G	Black2
12V	12V	Red2

PTEMP	***Destination***	***Wire***
Clear	GND (MUX)	
Black	E1 (datalogger)	Black1
Red	1H1 (datalogger)	Red1

MUX	***Datalogger***	***Wire***
COM H1	2H	Green2
COM L1	2L	White2
COM H2	3H	Red3
COM L2	3L	Black3

Jumper Sets (on MUX)
(3 blue copper wires)
1: 1L1--1L2--2L1--2L2
2: 3L1--3L2--4L1--4L2
3: 5L1--5L2--6L1--6L2
4: 7L1--7L2--8L1--8L2
5: 9L1--9L2--10L1--10L2
6: 11L1--11L2--12L1--12L2
7: 13L1--13L2--14L1--14L2
8: 15L1--15L2--16L1--16L2

Reset datalogger
*, A, A, A, A, A
98765

Sensors (on MUX)

Sensor Set #1		Sensor Set #5	
1H1	green	9H1	green
1L1	constantan	9L1	constantan
1H2	red	9H2	red
2H1	white	10H1	white
2H2	black	10H2	black

Sensor Set #2		Sensor Set #6	
3H1	green	11H1	green
3L1	constantan	11L1	constantan
3H2	red	11H2	red
4H1	white	12H1	white
4H2	black	12H2	black

Sensor Set #3		Sensor Set #7	
5H1	green	13H1	green
5L1	constantan	13L1	constantan
5H2	red	13H2	red
6H1	white	14H1	white
6H2	black	14H2	black

Sensor Set #4		Sensor Set #8	
7H1	green	15H1	green
7L1	constantan	15L1	constantan
7H2	red	15H2	red
8H1	white	16H1	white
8H2	black	16H2	black

HEATER

Destination	***Wire***
SW12V (datalogger)	Red4
G (datalogger)	Black4
C3 (datalogger)	Yellow
Red (battery)	Red5
Black (battery)	Black5

Photograph

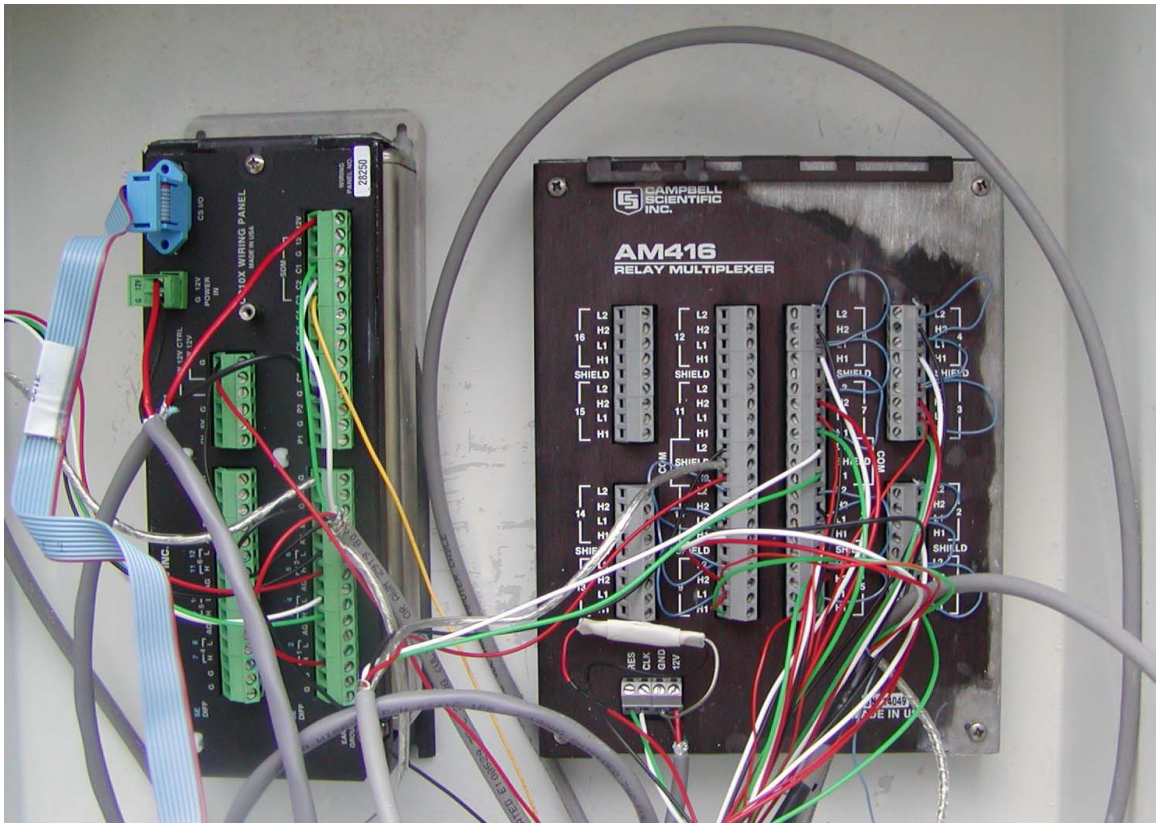
CAMPBELL SCIENTIFIC INC.
AM416
RELAY MULTIPLEXER
SHIELD
COM
AES
CLK
GND
12V

Appendix B

Datalogger Code for Sap Flow Measurement

```
;{CR10X}
; Josh Fisher & Vanessa Schmidt's Sap Flow program
; jfisher@nature.berkeley.edu, www.cnr.berkeley.edu/~jfisher
; Designed to measure an initial temperature among 10 TC's in 5 probes,
; Send out a 6 second heat pulse,
; Wait 60s then measure the temperature for 40 seconds and take an avg.

;{CR10X}
*Table 1 Program
  01: 1800      Execution Interval (seconds)

; Check the battery!
1:  Batt Voltage (P10)
 1: 1        Loc [ Batt_Volt ]

; Shortcut loves us!
2:  If time is (P92)
 1: 0        Minutes (Seconds --) into a
 2: 1440     Interval (same units as above)
 3: 30       Then Do

     3:  Signature (P19)
      1: 2        Loc [ Prog_Sig  ]

4:  End (P95)

; Reset the HRdivisor!
5:  Z=X*F (P37)
 1: 77       X Loc [ HRdivisor ]
 2: 0        F
 3: 77       Z Loc [ HRdivisor ]

; Check the pannel temp!
6:  Temp (107) (P11)
 1: 1        Reps
 2: 1        SE Channel
 3: 1        Excite all reps w/E1
 4: 3        Loc [ PTemp_C   ]
 5: 1        Mult
 6: 0        Offset


; Reset the multiplexor!
7:  Do (P86)
 1: 41       Set Port 1 High

; Begin the multiplexor loop!
8:  Beginning of Loop (P87)
 1: 0        Delay
```

```
 2: 10       Loop Count

; Step the loop ahead after the loop finishes!
     9:  Step Loop Index (P90)
      1: 2        Step

; Start the multiplexor!
     10:  Do (P86)
      1: 72       Pulse Port 2

; Delay so the mux can catch a breath!
     11:  Excitation with Delay (P22)
      1: 1        Ex Channel
      2: 0        Delay W/Ex (units = 0.01 sec)
      3: 1        Delay After Ex (units = 0.01 sec)
      4: 0        mV Excitation

; Measure the TC 10 times for the even differential channels!
     12:  Beginning of Loop (P87)
      1: 0        Delay
      2: 10       Loop Count

          13:  Thermocouple Temp (DIFF) (P14)
           1: 1        Reps
           2: 1        2.5 mV Slow Range
           3: 2        DIFF Channel
           4: 1        Type T (Copper-Constantan)
           5: 3        Ref Temp (Deg. C) Loc [ PTemp_C   ]
           6: 65    -- Loc [ tempiT_1  ]
           7: 1        Mult
           8: 0        Offset

     14:  End (P95)

; Average the initial 10 TC measurements!
     15:  Spatial Average (P51)
      1: 10       Swath
      2: 65       First Loc [ tempiT_1  ]
      3: 44    -- Avg Loc [ ainitT_1  ]

; Do it again (but for the even odd channels)!
     16:  Beginning of Loop (P87)
      1: 0        Delay
      2: 10       Loop Count

          17:  Thermocouple Temp (DIFF) (P14)
           1: 1        Reps
           2: 1        2.5 mV Slow Range
           3: 3        DIFF Channel
           4: 1        Type T (Copper-Constantan)
           5: 3        Ref Temp (Deg. C) Loc [ PTemp_C   ]
           6: 65    -- Loc [ tempiT_1  ]
           7: 1        Mult
           8: 0        Offset

     18:  End (P95)
```

```
     19:  Spatial Average (P51)
      1: 10       Swath
      2: 65       First Loc [ tempiT_1  ]
      3: 45    -- Avg Loc [ ainitT_2  ]

20:  End (P95)

; Turn off the multiplexor!
21:  Do (P86)
 1: 51       Set Port 1 Low


; Do the heater!
22:  Do (P86)
 1: 43       Set Port 3 High

23:  Excitation with Delay (P22)
 1: 1        Ex Channel
 2: 0        Delay W/Ex (units = 0.01 sec)
 3: 600      Delay After Ex (units = 0.01 sec)
 4: 0        mV Excitation

24:  Do (P86)
 1: 53       Set Port 3 Low



; Start a timer to let the heat travel!
25:  Timer (P26)
 1: 0000     Reset Timer

26:  Beginning of Loop (P87)
 1: 0        Delay
 2: 0        Loop Count ; Zero loops = infinite looping (until exit
loop @ 100s command)

     27:  Timer (P26)
      1: 76       Loc [ timer     ]

     28:  IF (X<=>F) (P89)
      1: 76       X Loc [ timer     ]
      2: 3        >=
      3: 60       F
      4: 30       Then Do

          29:  IF (X<=>F) (P89)
           1: 76       X Loc [ timer     ]
           2: 3        >=
           3: 100      F
           4: 31       Exit Loop if True

; Measure the temperatures between 60-100s!
          30:  Do (P86)
           1: 41       Set Port 1 High

          31:  Beginning of Loop (P87)
           1: 0        Delay
```

```
           2: 10       Loop Count

               32:  Step Loop Index (P90)
                1: 2        Step

               33:  Do (P86)
                1: 72       Pulse Port 2

               34:  Excitation with Delay (P22)
                1: 1        Ex Channel
                2: 0        Delay W/Ex (units = 0.01 sec)
                3: 1        Delay After Ex (units = 0.01 sec)
                4: 0        mV Excitation

               35:  Thermocouple Temp (DIFF) (P14)
                1: 2        Reps
                2: 1        2.5 mV Slow Range
                3: 2        DIFF Channel
                4: 1        Type T (Copper-Constantan)
                5: 3        Ref Temp Loc [ PTemp_C   ]
                6: 24    -- Loc [ postT_1   ]
                7: 1.0      Mult
                8: 0.0      Offset

           36:  End (P95)

; The HRdivisor is how many times each sensor takes a measurement
during the 40s!
           37:  Z=Z+1 (P32)
            1: 77       Z Loc [ HRdivisor ]

     38:  End (P95)



; DISABLE MUX

39:  Do (P86)
 1: 51       Set Port 1 Low


; Output data
40:  If time is (P92)
 1: 0        Minutes (Seconds --) into a
 2: 30       Interval (same units as above)
 3: 10       Set Output Flag High (Flag 0)

41:  Set Active Storage Area (P80)^30133
 1: 1        Final Storage Area 1
 2: 100      Array ID


42:  Real Time (P77)^26495
 1: 1221     Year,Day,Hour/Minute,Seconds (midnight = 2400)
```

```
; Battery voltage, panel Temp, avg initial temp, and avg post-heat temp
43:  Average (P71)^15633
 1: 1        Reps
 2: 1        Loc [ Batt_Volt ]

44:  Average (P71)^19815
 1: 1        Reps
 2: 3        Loc [ PTemp_C   ]

45:  Average (P71)^24723
 1: 20       Reps
 2: 44       Loc [ ainitT_1  ]

46:  Average (P71)^7966
 1: 20       Reps
 2: 24       Loc [ postT_1   ]


47:  End (P95)



*Table 2 Program
  01: 10.0000   Execution Interval (seconds)


*Table 3 Subroutines

End Program

-Input Locations-
1 Batt_Volt 1 1 1
2 Prog_Sig  1 0 1
3 PTemp_C   1 4 1
4 initT_1   1 0 0
5 initT_2   1 0 0
6 initT_3   1 0 0
7 initT_4   1 0 0
8 initT_5   1 0 0
9 initT_6   1 0 0
10 initT_7   1 0 0
11 initT_8   1 0 0
12 initT_9   1 0 0
13 initT_10  1 0 0
14 initT_11  1 0 0
15 initT_12  1 0 0
16 initT_13  1 0 0
17 initT_14  1 0 0
18 initT_15  1 0 0
19 initT_16  1 0 0
20 initT_17  1 0 0
21 initT_18  1 0 0
22 initT_19  1 0 0
23 initT_20  1 0 0
24 postT_1   5 1 1
25 postT_2   17 1 1
26 postT_3   1 1 0
27 postT_4   1 1 0
28 postT_5   1 1 0
29 postT_6   1 1 0
30 postT_7   1 1 0
31 postT_8   1 1 0
32 postT_9   1 1 0
```

```
33 postT_10  1 1 0
34 postT_11  1 1 0
35 postT_12  1 1 0
36 postT_13  1 1 0
37 postT_14  1 1 0
38 postT_15  1 1 0
39 postT_16  1 1 0
40 postT_17  1 1 0
41 postT_18  1 1 0
42 postT_19  1 1 0
43 postT_20  1 1 0
44 ainitT_1  1 1 1
45 ainitT_2  1 1 1
46 ainitT_3  1 1 0
47 ainitT_4  1 1 0
48 ainitT_5  1 1 0
49 ainitT_6  1 1 0
50 ainitT_7  1 1 0
51 ainitT_8  1 1 0
52 ainitT_9  1 1 0
53 ainitT_10 1 1 0
54 ainitT_11 1 1 0
55 ainitT_12 1 1 0
56 ainitT_13 1 1 0
57 ainitT_14 1 1 0
58 ainitT_15 1 1 0
59 ainitT_16 1 1 0
60 ainitT_17 1 1 0
61 ainitT_18 1 1 0
62 ainitT_19 1 1 0
63 ainitT_20 1 1 0
64 preT      1 0 0
65 tempiT_1  5 2 2
66 tempiT_2  1 2 0
67 tempiT_3  1 2 0
68 tempiT_4  1 2 0
69 tempiT_5  1 2 0
70 tempiT_6  1 2 0
71 tempiT_7  1 2 0
72 tempiT_8  1 2 0
73 tempiT_9  1 2 0
74 tempiT_10 1 2 0
75 tempiT_11 1 0 0
76 timer     1 2 1
77 HRdivisor 1 1 2
78 postSumT1 1 0 0
79 postToT1  5 0 0
80 postToT2  9 0 0
81 postToT3  9 0 0
82 postToT4  9 0 0
83 postToT5  9 0 0
84 postToT6  9 0 0
85 postToT7  9 0 0
86 postToT8  9 0 0
87 postToT9  9 0 0
88 postToT10 9 0 0
89 postToT11 9 0 0
90 postToT12 9 0 0
91 postToT13 9 0 0
92 postToT14 9 0 0
93 postToT15 9 0 0
94 postToT16 9 0 0
95 postToT17 9 0 0
96 postToT18 9 0 0
97 postToT19 9 0 0
98 postToT20 17 0 0
99 _________ 1 0 0
-Program Security-
0000
0000
0000
```

```
-Mode 4-
-Final Storage Area 2-
0
-CR10X ID-
0
-CR10X Power Up-
3
-CR10X Compile Setting-
3
-CR10X RS-232 Setting-
-1
-DLD File Labels-
0
-Final Storage Labels-
0,100,30133
1,Year_RTM,26495
1,Day_RTM
1,Hour_Minute_RTM
1,Seconds_RTM
2,Batt_Volt_AVG~1,15633
3,PTemp_C_AVG~3,19815
4,ainitT_1_AVG~44,24723
4,ainitT_2_AVG~45
4,ainitT_3_AVG~46
4,ainitT_4_AVG~47
4,ainitT_5_AVG~48
4,ainitT_6_AVG~49
4,ainitT_7_AVG~50
4,ainitT_8_AVG~51
4,ainitT_9_AVG~52
4,ainitT_10_AVG~53
4,ainitT_11_AVG~54
4,ainitT_12_AVG~55
4,ainitT_13_AVG~56
4,ainitT_14_AVG~57
4,ainitT_15_AVG~58
4,ainitT_16_AVG~59
4,ainitT_17_AVG~60
4,ainitT_18_AVG~61
4,ainitT_19_AVG~62
4,ainitT_20_AVG~63
5,postT_1_AVG~24,7966
5,postT_2_AVG~25
5,postT_3_AVG~26
5,postT_4_AVG~27
5,postT_5_AVG~28
5,postT_6_AVG~29
5,postT_7_AVG~30
5,postT_8_AVG~31
5,postT_9_AVG~32
5,postT_10_AVG~33
5,postT_11_AVG~34
5,postT_12_AVG~35
5,postT_13_AVG~36

5,postT_14_AVG~37
5,postT_15_AVG~38
5,postT_16_AVG~39
5,postT_17_AVG~40
5,postT_18_AVG~41
5,postT_19_AVG~42
5,postT_20_AVG~43
```

Appendix C

Equations for Processing and Calculation of Sap Flow Data[17]

Calculation of heat pulse velocity with heat ratio method

$V_h = (k/x)\ ln(v_1/v_2)*3600$ cm/hr

k: thermal diffusivity of wood; 0.0025 $cm^2 \cdot s^{-1}$
x: distance between heater and (either) temperature probe; 0.6 cm
v_1: upstream probe
v_2: downstream probe

Correction for probe misalignment

$x_2 = (4*k*t*ln(v_1/v_2)+x_1^2)^{0.5}$

x_1: assumed to be correctly spaced; 0.6 cm
t: time following heat pulse; 80 s

$V_h = ((4*k*ln(v_1/v_2)-(x_2^2-x_1^2))/(2*t*(x_1-x_2))*3600 = 0$ cm/hr

- Switch x_1 and x_2 to re-calculate V_h, then take the average of the 2 V_h's

Correction for wounding

$V_c = b*V_h+c*V_h^2+d*V_h^3$

a, b, and c: wound widths; 1.9, 2.0, 2.1 mm

$V_c = B*V_h = 1.96*V_h$ cm/hr

B: based on linear model; 1.93 for 0.6 cm spacing

- "For oak trees, the wound space was estimated to be at least an annulus as wide as a large blue oak vessel if one were broken by the probes, the largest being 0.4 mm. Therefore, the needle sensor diameter of 1.275 mm plus double the annulus width gives an oak wound diameter of 2.075 mm." (Kiang, 2002)

[17] Based on Burgess (2001) and Ph.D. theses by Kiang (2002) and Kurpius (2001)

Calculation of sap velocity from heat pulse velocity

$V_s = (V_c*\rho_b*(c_w+m_c*c_s)/(\rho_s*c_s) = 1.52*V_c$ cm/hr

ρ_b: basic density of wood (dry weight/green volume); 1530 $kg \cdot m^{-3}$
- Panshin & deZeeuw (1980)

c_w: specific heat capacity of the wood matrix; 1200 $J \cdot kg^{-1} \cdot C^{-1}$ at 20ºC
- Burgess et al. (2001), Becker & Edwards (1999)

c_s: specific heat capacity of sap (or water); 4182 $J \cdot kg^{-1} \cdot C^{-1}$ at 20ºC
- Lide (1992)

m_c: water content of sapwood; 0.7 m^3/m^3

ρ_s: density of water; 996 $kg \cdot m^{-3}$
- Mills (1999)

Integration of sap velocity to tree sap flow

$F_{tree} = (1-\gamma)*integral\ from\ r_{in}\ to\ r_{out}\ (V_s*r*dr*d\theta)$ $cm^3 \cdot hr^{-1}$

γ: fraction of sapwood area covered by ray cells; 0.21
r: radial distance from the center of the tree bole; cm
r_{in}: inner radial limit, sapwood-heartwood boundary; cm
- = tree radius – sapwood thickness = radius – 0.21*radius

r_{out}: outer radial limit of sapwood = tree radius; cm
θ: angle around the tree bole; radians

Processing steps

1. Set to zero when zero sap flow (no divide by zero)
2. Calculate sap flow or velocity
3. Eliminate data spikes (standard deviation threshold equation or alternative)
4. Delete data during heater failures (examine 1-day maximums)

Appendix D

MATLAB Code for Evapotranspiration Model with Remote Sensing Data

```
function ETmodel
%LAST MODIFIED: May 8, 2006
clear all

imax=180;
jmax=360;

%based on the middle of each month
daynum=[15 46 74 105 135 166 196 227 258 288 319 349];

for y=1986:1994,
   year=num2str(y)
   year2dig=y-1900;

   if year2dig==94, mmax=8; else mmax=12; end
   %reading in all the data and storing it into a 3D array
   for m=1:mmax,
      if m<10,
         Taname=['raw/cru5_temp_mean_1d_',num2str(year),'0',num2str(m),'.asc'];
         NDVIname=['raw/fasir_ndvi413_1d_',num2str(year),'0',num2str(m),'.asc'];
         Rnname=['raw/srb_ntf_av_1d_',num2str(year),'0',num2str(m),'00.asc'];
         eaname=['raw/cru5_vapor_pres_1d_',num2str(year),'0',num2str(m),'.asc'];
         ch1aname=['raw/avhrrpf.ch1.1ntegl.',num2str(year2dig),'0',num2str(m),'01.txt'];
         ch1bname=['raw/avhrrpf.ch1.1ntegl.',num2str(year2dig),'0',num2str(m),'11.txt'];
         ch1cname=['raw/avhrrpf.ch1.1ntegl.',num2str(year2dig),'0',num2str(m),'21.txt'];
         ch2aname=['raw/avhrrpf.ch2.1ntegl.',num2str(year2dig),'0',num2str(m),'01.txt'];
         ch2bname=['raw/avhrrpf.ch2.1ntegl.',num2str(year2dig),'0',num2str(m),'11.txt'];
         ch2cname=['raw/avhrrpf.ch2.1ntegl.',num2str(year2dig),'0',num2str(m),'21.txt'];
         Ta(:,:,m)=load(Taname);
         NDVI(:,:,m)=load(NDVIname);
         Rn(:,:,m)=load(Rnname);
         ea(:,:,m)=load(eaname);
         ch1a(:,:,m)=load(ch1aname);
         ch1b(:,:,m)=load(ch1bname);
         ch1c(:,:,m)=load(ch1cname);
         ch2a(:,:,m)=load(ch2aname);
         ch2b(:,:,m)=load(ch2bname);
         ch2c(:,:,m)=load(ch2cname);
         ch1avg(:,:,m)=((ch1a(:,:,m)+ch1b(:,:,m)+ch1c(:,:,m))/3 - 10) *.002;
% averages channel one and scales
         ch2avg(:,:,m)=((ch2a(:,:,m)+ch2b(:,:,m)+ch2c(:,:,m))/3 - 10) *.002;
      else
         Taname=['raw/cru5_temp_mean_1d_',num2str(year),num2str(m),'.asc'];
         NDVIname=['raw/fasir_ndvi413_1d_',num2str(year),num2str(m),'.asc'];
```

```
        Rnname=['raw/srb_ntf_av_1d_',num2str(year),num2str(m),'00.asc'];
        eaname=['raw/cru5_vapor_pres_1d_',num2str(year),num2str(m),'.asc'];
        ch1aname=['raw/avhrrpf.ch1.1ntegl.',num2str(year2dig),num2str(m),'01.txt'];
        ch1bname=['raw/avhrrpf.ch1.1ntegl.',num2str(year2dig),num2str(m),'11.txt'];
        ch1cname=['raw/avhrrpf.ch1.1ntegl.',num2str(year2dig),num2str(m),'21.txt'];
        ch2aname=['raw/avhrrpf.ch2.1ntegl.',num2str(year2dig),num2str(m),'01.txt'];
        ch2bname=['raw/avhrrpf.ch2.1ntegl.',num2str(year2dig),num2str(m),'11.txt'];
        ch2cname=['raw/avhrrpf.ch2.1ntegl.',num2str(year2dig),num2str(m),'21.txt'];
        Ta(:,:,m)=load(Taname);
        NDVI(:,:,m)=load(NDVIname);
        Rn(:,:,m)=load(Rnname);
        ea(:,:,m)=load(eaname);
        ch1a(:,:,m)=load(ch1aname);
        ch1b(:,:,m)=load(ch1bname);
        ch1c(:,:,m)=load(ch1cname);
        ch2a(:,:,m)=load(ch2aname);
        ch2b(:,:,m)=load(ch2bname);
        ch2c(:,:,m)=load(ch2cname);
        ch1avg(:,:,m)=((ch1a(:,:,m)+ch1b(:,:,m)+ch1c(:,:,m))/3 - 10) *.002;
% averages channel one and scales
        ch2avg(:,:,m)=((ch2a(:,:,m)+ch2b(:,:,m)+ch2c(:,:,m))/3 - 10) *.002;
      end

   for i=1:imax,
      lat(i)=abs(1.0056*i-91.006);
      %lat(i)=45; % TEMP
      for j=1:jmax,
         for m=1:mmax,
            SAVI0(i,j,m)=1.5*(ch2avg(i,j,m)-ch1avg(i,j,m))/(ch2avg(i,j,m)+ch1avg(i,j,m)+0.5);
            NDVI0(i,j,m)=NDVI(i,j,m);
         end
         SAVImax(i,j)=max(SAVI0(i,j,:));
         SAVImin(i,j)=min(SAVI0(i,j,:));
         NDVImax(i,j)=max(NDVI0(i,j,:));
         NDVImin(i,j)=min(NDVI0(i,j,:));
         for m=1:mmax,
            if SAVImax(i,j)==0,
               SAVI(i,j,m)=0;
            else
               SAVI(i,j,m)=0.95*(SAVI0(i,j,m)-SAVImin(i,j,:))/(SAVImax(i,j,:)-SAVImin(i,j,:));
            end
            for m=1:mmax,
               if NDVImax(i,j)==0,
                  NDVI1(i,j,m)=0;
               else
                  if NDVImax(i,j)==NDVImin(i,j),
                     NDVI1(i,j,m)=0;
                  else
                     NDVI1(i,j,m)=(NDVI(i,j,m)-NDVImin(i,j,:))/(NDVImax(i,j,:)-NDVImin(i,j,:));
                  end
               end
            end
         end
```

```
%calculates daylength and caps it at 0 and 24
        for m=1:mmax,
           daylength(i,j,m) = (((exp(7.42 + 0.045 * lat(i)) / 3600)*(sin((daynum(m)-79)*0.01721))+12));
           if daylength(i,j,m) > 24, daylength(i,j,m)=24; end
           if daylength(i,j,m) <= 0, daylength(i,j,m)=0; end

           es(i,j,m)=.61121 * exp(17.502*Ta(i,j,m)/(Ta(i,j,m)+240.97));
           VPD(i,j,m)=es(i,j,m)-.1*ea(i,j,m);
           RH(i,j,m)=min(1,max(0,.1*ea(i,j,m)/es(i,j,m)));

           growthopt(i,j,m)=SAVI(i,j,m)*Ta(i,j,m)*RH(i,j,m)^VPD(i,j,m);
        end
           growthoptmax(i,j)=max(growthopt(i,j,:));
        for m=1:mmax,
           if growthopt(i,j,m)==growthoptmax(i,j), Topt(i,j)=Ta(i,j,m); end       %Topt=Ta
        end
        for m=1:mmax,
           if daylength(i,j,m)==0,
              RnDay(i,j,m)=0;
           else
              RnDay(i,j,m)=Rn(i,j,m)*24/daylength(i,j,m);
              RnDaymm(i,j,m)=RnDay(i,j,m)*daylength(i,j,m)*0.0000004*3600*30;
           end;

           if Topt(i,j)==0,
              fT(i,j,m)= 0;
           else
              fT(i,j,m)=exp(-(((Ta(i,j,m)-Topt(i,j))/(Topt(i,j)))^2));
           end
           s(i,j,m)=17.502*240.97/((Ta(i,j,m)+240.97)^2);
           EFeq(i,j,m)=s(i,j,m)/(s(i,j,m)+.066);
           fSM(i,j,m)=RH(i,j,m)^VPD(i,j,m);
           fc(i,j,m)=NDVI1(i,j,m);
           if fc(i,j,m)==0,
              fg(i,j,m)=0;
           else
              fg(i,j,m)=(1.3/fc(i,j,m))*(SAVI(i,j,m));
           end
           LEs(i,j,m)=(1-
fc(i,j,m))*fSM(i,j,m)*1.26*EFeq(i,j,m)*RnDay(i,j,m)*daylength(i,j,m)*0.0000004*3600*30;
           if LEs(i,j,m)==0,
              tr(i,j,m)=9999;
           else
              tr(i,j,m) = ((4/(2*LEs(i,j,m)/30))^2);
           end
           if tr(i,j,m)<1, tr(i,j,m)=1; end
           nw(i,j,m)=30/tr(i,j,m);

           LEswet(i,j,m)=(1-fc(i,j,m))*RnDay(i,j,m)*daylength(i,j,m)*0.0000004*3600*30;
           LEcwet(i,j,m)=fc(i,j,m)*RnDay(i,j,m)*daylength(i,j,m)*0.0000004*3600*30;
           LEi(i,j,m)=LEswet(i,j,m)+LEcwet(i,j,m);
          LEc(i,j,m)=fc(i,j,m)*fg(i,j,m)*fT(i,j,m)*1.26*EFeq(i,j,m)*RnDay(i,j,m)*daylength(i,j,m)*0.0000
004*3600*30;
          LE(i,j,m) = nw(i,j,m)*LEi(i,j,m)/30 + (30-nw(i,j,m))*((LEc(i,j,m)/30) + (LEs(i,j,m)/30));
           LEnoi(i,j,m) = LEc(i,j,m)+LEs(i,j,m);
```

```
        %               %turn neg values to -999 for purpose of future plots
        if NDVI(i,j,m)<0, LE(i,j,m)=-999; LEnoi(i,j,m)=-999; RnDaymm(i,j,m)=-999; end
        %               if LE(i,j,m)<0, LE(i,j,m)=-999; end
        %               if LEc(i,j,m)<0, LEc(i,j,m)=-999; end
        %               if LEs(i,j,m)<0, LEs(i,j,m)=-999; end
        %               if LEi(i,j,m)<0, LEi(i,j,m)=-999; end

        LEall(i,j,m,y-1985)=LE(i,j,m);
        end
    end

%calculation for row averages
    for m=1:mmax
       LEforavg=[];
       for j=1:jmax
          if LE(i,j,m)>=0, LEforavg=[LEforavg LE(i,j,m)]; end
       end
       if size(LEforavg)==0, LElatmavg(i,m)=0; else LElatmavg(i,m)=mean(LEforavg); end
       end
 end

 %write out variables
 for m=1:mmax,
    if m<10,
       fullPath=['output/','LEc_',num2str(year),'_0',num2str(m),'.txt'];
       varName=LEc(:,:,m);
       str1 = sprintf ('save %s varName -ascii', fullPath);
       eval (str1);
       fullPath=['output/','LEs_',num2str(year),'_0',num2str(m),'.txt'];
       varName=LEs(:,:,m);
       str1 = sprintf ('save %s varName -ascii', fullPath);
       eval (str1);
       fullPath=['output/','LEi_',num2str(year),'_0',num2str(m),'.txt'];
       varName=LEi(:,:,m);
       str1 = sprintf ('save %s varName -ascii', fullPath);
       eval (str1);
       fullPath=['output/','LE_',num2str(year),'_0',num2str(m),'.txt'];
       varName=LE(:,:,m);
       str1 = sprintf ('save %s varName -ascii', fullPath);
       eval (str1);
       fullPath=['output/','LElatmavg_',num2str(year),'_0',num2str(m),'.txt'];
       varName=LElatmavg(:,m);
       str1 = sprintf ('save %s varName -ascii', fullPath);
       eval (str1);
       fullPath=['output/','RnDaymm_',num2str(year),'_0',num2str(m),'.txt'];
       varName=RnDaymm(:,:,m);
       str1 = sprintf ('save %s varName -ascii', fullPath);
       eval (str1);
       fullPath=['output/','LEnoi_',num2str(year),'_0',num2str(m),'.txt'];
       varName=LEnoi(:,:,m);
       str1 = sprintf ('save %s varName -ascii', fullPath);
       eval (str1);

    else
       fullPath=['output/','LEc_',num2str(year),'_',num2str(m),'.txt'];
       varName=LEc(:,:,m);
```

```
            str1 = sprintf ('save %s varName -ascii', fullPath);
            eval (str1);
            fullPath=['output/','LEs_',num2str(year),'_',num2str(m),'.txt'];
            varName=LEs(:,:,m);
            str1 = sprintf ('save %s varName -ascii', fullPath);
            eval (str1);
            fullPath=['output/','LEi_',num2str(year),'_',num2str(m),'.txt'];
            varName=LEi(:,:,m);
            str1 = sprintf ('save %s varName -ascii', fullPath);
            eval (str1);
            fullPath=['output/','LE_',num2str(year),'_',num2str(m),'.txt'];
            varName=LE(:,:,m);
            str1 = sprintf ('save %s varName -ascii', fullPath);
            eval (str1);
            fullPath=['output/','LElatmavg_',num2str(year),'_',num2str(m),'.txt'];
            varName=LElatmavg(:,m);
            str1 = sprintf ('save %s varName -ascii', fullPath);
            eval (str1);
            fullPath=['output/','RnDaymm_',num2str(year),'_',num2str(m),'.txt'];
            varName=RnDaymm(:,:,m);
            str1 = sprintf ('save %s varName -ascii', fullPath);
            eval (str1);
            fullPath=['output/','LEnoi_',num2str(year),'_',num2str(m),'.txt'];
            varName=LEnoi(:,:,m);
            str1 = sprintf ('save %s varName -ascii', fullPath);
            eval (str1);

        end
    end
end

%calculate year averages for each pixel and subtract year to year changes
for i=1:imax,
    for j=1:jmax,
        for k=1:9,
            LEyravg(i,j,k)=mean(LEall(i,j,:,k));
            LEyrsum(i,j,k)=sum(LEall(i,j,:,k));
            %LElatysum(i,k)=mean(LEyrsum(i,:,k));

            if k>1, LEyr2yr(i,j,k-1)=LEyravg(i,j,k)-LEyravg(i,j,k-1); end

        end
    end
end

for i=i:imax,
    for k=1:9,
        LElatysum(i,k)=sum(LElatmavg(i,:));
    end
end

%write out year averages and changes and lat sums
for k=1:9,
    fullPath=['output/','LEyravg_',num2str(k+1985),'.txt'];
    varName=LEyravg(:,:,k);
    str1 = sprintf ('save %s varName -ascii', fullPath);
```

```
   eval (str1);
   fullPath=['output/','LEyrsum_',num2str(k+1985),'.txt'];
   varName=LEyrsum(:,:,k);
   str1 = sprintf ('save %s varName -ascii', fullPath);
   eval (str1);
   fullPath=['output/','LElatyavg_',num2str(k+1985),'.txt'];
   varName=LElatysum(:,k);
   str1 = sprintf ('save %s varName -ascii', fullPath);
   eval (str1);
   if k<9,
      fullPath=['output/','LEyr2yr_',num2str(k+1985),'.txt'];
      varName=LEyr2yr(:,:,k);
      str1 = sprintf ('save %s varName -ascii', fullPath);
      eval (str1);
   end
end

%subtract one month from the next
for k=1:9,
   if k==9, mmax=8; else mmax=12; end
   for m=1:mmax,
      for i=1:imax,
         for j=1:jmax,

            if m<12,
               LEmo2mo(i,j,m,k)=LEall(i,j,m+1,k)-LEall(i,j,m,k);
            else
               if k==9,
                  LEmo2mo(i,j,m,k)=0;
               else
                  LEmo2mo(i,j,m,k)=LEall(i,j,1,k+1)-LEall(i,j,m,k);
               end
            end
         end
      end
   end
end

%write out LEmo2mo
for k=1:9,
      if k==9, mmax=8; else mmax=12; end
   for m=1:mmax,
      if m<10,
         fullPath=['output/','LEmo2mo_',num2str(k+1985),'_0',num2str(m),'.txt'];
         varName=LEmo2mo(:,:,m,k);
         str1 = sprintf ('save %s varName -ascii', fullPath);
         eval (str1);
      else
         fullPath=['output/','LEmo2mo_',num2str(k+1985),'_',num2str(m),'.txt'];
         varName=LEmo2mo(:,:,m,k);
         str1 = sprintf ('save %s varName -ascii', fullPath);
         eval (str1);
      end
   end
end
```